



National Library  
of Canada

Acquisitions and  
Bibliographic Services Branch

395 Wellington Street  
Ottawa, Ontario  
K1A 0N4

Bibliothèque nationale  
du Canada

Direction des acquisitions et  
des services bibliographiques

395, rue Wellington  
Ottawa (Ontario)  
K1A 0N4

*Your file - Votre référence*

*Our file - Notre référence*

## NOTICE

The quality of this microform is heavily dependent upon the quality of the original thesis submitted for microfilming. Every effort has been made to ensure the highest quality of reproduction possible.

If pages are missing, contact the university which granted the degree.

Some pages may have indistinct print especially if the original pages were typed with a poor typewriter ribbon or if the university sent us an inferior photocopy.

Reproduction in full or in part of this microform is governed by the Canadian Copyright Act, R.S.C. 1970, c. C-30, and subsequent amendments.

## AVIS

La qualité de cette microforme dépend grandement de la qualité de la thèse soumise au microfilmage. Nous avons tout fait pour assurer une qualité supérieure de reproduction.

S'il manque des pages, veuillez communiquer avec l'université qui a conféré le grade.

La qualité d'impression de certaines pages peut laisser à désirer, surtout si les pages originales ont été dactylographiées à l'aide d'un ruban usé ou si l'université nous a fait parvenir une photocopie de qualité inférieure.

La reproduction, même partielle, de cette microforme est soumise à la Loi canadienne sur le droit d'auteur, SRC 1970, c. C-30, et ses amendements subséquents.

Canada

**Feasibility Investigations on Thermocontrolled Tank for  
On-board Storage of Gaseous Fuels in Vehicles**

**Manoj Tummala**

**A Thesis  
in  
The Department  
of  
Mechanical Engineering**

**Presented in Partial Fulfillment of the Requirements  
for the Degree of Doctor of Philosophy at  
Concordia University  
Montreal, Quebec, Canada**

**June, 1994**

**© Manoj Tummala, 1994**



National Library  
of Canada

Acquisitions and  
Bibliographic Services Branch

395 Wellington Street  
Ottawa, Ontario  
K1A 0N4

Bibliothèque nationale  
du Canada

Direction des acquisitions et  
des services bibliographiques

395, rue Wellington  
Ottawa (Ontario)  
K1A 0N4

*Your file    Votre référence*

*Our file    Notre référence*

THE AUTHOR HAS GRANTED AN  
IRREVOCABLE NON-EXCLUSIVE  
LICENCE ALLOWING THE NATIONAL  
LIBRARY OF CANADA TO  
REPRODUCE, LOAN, DISTRIBUTE OR  
SELL COPIES OF HIS/HER THESIS BY  
ANY MEANS AND IN ANY FORM OR  
FORMAT, MAKING THIS THESIS  
AVAILABLE TO INTERESTED  
PERSONS.

L'AUTEUR A ACCORDE UNE LICENCE  
IRREVOCABLE ET NON EXCLUSIVE  
PERMETTANT A LA BIBLIOTHEQUE  
NATIONALE DU CANADA DE  
REPRODUIRE, PRETER, DISTRIBUER  
OU VENDRE DES COPIES DE SA  
THESE DE QUELQUE MANIERE ET  
SOUS QUELQUE FORME QUE CE SOIT  
POUR METTRE DES EXEMPLAIRES DE  
CETTE THESE A LA DISPOSITION DES  
PERSONNE INTERESSEES.

THE AUTHOR RETAINS OWNERSHIP  
OF THE COPYRIGHT IN HIS/HER  
THESIS. NEITHER THE THESIS NOR  
SUBSTANTIAL EXTRACTS FROM IT  
MAY BE PRINTED OR OTHERWISE  
REPRODUCED WITHOUT HIS/HER  
PERMISSION.

L'AUTEUR CONSERVE LA PROPRIETE  
DU DROIT D'AUTEUR QUI PROTEGE  
SA THESE. NI LA THESE NI DES  
EXTRAITS SUBSTANTIELS DE CELLE-  
CI NE DOIVENT ETRE IMPRIMES OU  
AUTREMENT REPRODUITS SANS SON  
AUTORISATION.

ISBN 0-315-97683-7

Canada

## ABSTRACT

### **Feasibility Investigations on Thermocontrolled Tank for On-board Storage of Gaseous Fuels in Vehicles**

Manoj Tummala, Ph.D.  
Concordia University, 1994

The use of alternative gaseous fuels, such as natural gas and hydrogen in vehicles, is limited by the difficulties with on-board storage and conditioning. These problems become even more difficult when supplying the gas for direct injection into the cylinder of an engine. To increase the operational range of a vehicle equipped with direct gas injection system and eliminate the possible problems associated with the high pressure cryogenic pumps, a concept called *thermocontrolled tank* has been investigated. In this process, liquid gaseous fuel will be supplied to an insulated vessel where the gas temperature and pressure are limited by the heat transfer to the tank. To control the rapid build-up of the pressure, both, insulation and preheating of the gas will be used, by utilizing engine exhaust gases. This will overcome some of the major drawbacks of such a system, namely, maintaining the necessary pressure required for direct injection and increasing the utilizable portion of the tank gas content.

Based on this concept, two prototype tanks have been manufactured and tested in the laboratory. The test results showed that the liquid gaseous fuel can be brought from atmospheric pressure to the high pressure required for direct

injection in a reasonable time and that the pressure increase can be to some extent limited by an appropriate insulation. A mathematical model for the heat transfer process in the tank has been developed and computer simulation has been performed. It was observed that the experimental data reasonably match the simulation results.

To find the optimum design of a composite vessel that could be used as a thermocontrolled tank in a vehicle, different aspects of storage such as the gas mass to vessel weight ratio, the gas mass to vessel volume ratio and the initial operational temperature have been investigated. The thermocontrolled tank design has been optimized for both natural gas and hydrogen using the theory of non-linear multi-objective optimization. The thermodynamic properties of these two gaseous fuels inside the thermocontrolled tank have been simulated to find out how long the vehicle can operate after each fill-up. The performance of a thermocontrolled tank installed in a vehicle has been optimized for different vehicles based on operating schedule. Finally, the storage of *Hythane*, a mixture of natural gas and hydrogen, has been investigated which could bring a significant reduction in pollutants, as compared with natural gas and an increase in the range, as compared with hydrogen. Conclusions have been drawn from the tests, from computer simulation and from optimization results to demonstrate the potential improvement in the storage and the utilization of gaseous fuels by the proposed thermocontrolled tank system.

**This thesis is dedicated to the memories of my mother:**

**Late PARVATHAVARDHANAMBA**

## ACKNOWLEDGEMENTS

The author would like to express his greatest gratitude to his supervisors Dr. T. Krepec and Dr. A.K.W. Ahmed for their constant encouragement and support throughout the course of this investigation. Thanks are extended to Dr. R.V. Dukkipati for his help and advice in the early stages of this work.

Thanks are directed to Dr. S. Lin for his invaluable advice and several of the author's friends and colleagues for their valuable discussions and suggestions. Special thanks go to the technical staff of the machine shop in the Faculty of Engineering and Computer Science for the manufacturing of several parts required for building the prototypes.

Most of all, the author wishes to express his gratitude to his wife, Lakshmi, and son, Saketh, for their encouragement and understanding.

Finally, thanks go to the Natural Sciences and Engineering Research Council Canada (NSERC), Mines and Energy Resources Canada and FCAR for their financial support, without which the present work would not have been possible. Also, the interest and support of Bendix Avelex Inc. is very much appreciated.

## TABLE OF CONTENTS

	<b>List of Figures</b>	xii
	<b>Nomenclature</b>	xviii
<b>1</b>	<b>Introduction</b>	<b>1</b>
1.1	General	1
1.2	Alternative Fuels Considered for Storage	9
1.2.1	Natural Gas	9
1.2.2	Hydrogen	12
1.3	Gaseous Fuel Storage Systems - Literature Review	17
1.3.1	Natural Gas Storage Systems	17
1.3.2	Hydrogen Storage Systems	22
<b>2</b>	<b>Concept Definition, Objectives and Methodology</b>	<b>28</b>
2.1	Thermocontrolled Tank: Concept Presentation	28
2.2	Proposed Gas Supply System for the Thermocontrolled Tank	32
2.3	Objectives of the Investigation	40
2.4	Thesis Outline and Methodology	41

<b>3</b>	<b>Mathematical Model and Simulation of Thermocontrolled Tank</b>	<b>43</b>
3.1	Mathematical Model for the Tank without a Heat Exchanger	43
3.2	PVT Relation for Real Gases	45
3.3	Mathematical Model for the Tank with a Heat Exchanger	46
3.4	Simulation Results	49
3.4.1	Simulation with Nitrogen	50
3.4.2	Simulation with Natural Gas	52
3.4.3	Simulation with Hydrogen	53
<b>4</b>	<b>Experimental Evaluation and Validation of the Mathematical Model</b>	<b>55</b>
4.1	Thermocontrolled Tank Prototypes	55
4.1.1	Steel Tank with Insulation and Preheating	56
4.1.2	The High Pressure Composite Tank	60
4.2	Testing of Prototypes and Discussion of Results	61
4.2.1	Testing of the Steel Vessel	61
4.2.2	Testing of the Composite Tank	73
4.3	Validation of the Mathematical Model	76
<b>5</b>	<b>Optimization of Thermocontrolled Vessel Design</b>	<b>78</b>
5.1	Preliminaries	78
5.2	Guidelines for Vessel Optimization	80

5.3	Design Parameter Sensitivity Study	82
5.3.1	Initial Operational Temperature	82
5.3.2	Gas Mass to Vessel Mass Ratio	83
5.3.3	Gas Mass to Tank Volume Ratio	87
5.4	Multiple Objective Optimization	92
5.4.1	Formulation of the Problem	92
5.4.2	Solution Method	95
5.5	Conclusions	100
<b>6</b>	<b>Thermocontrolled Tank Applications Consideration</b>	<b>102</b>
6.1	Preliminaries	102
6.2	Thermocontrolled Tank Considerations for a Bus	102
6.3	Thermocontrolled Tank Considerations for a Car	107
6.4	Practical Aspects of Thermocontrolled Tank Use	111
<b>7</b>	<b>Simulation of Gaseous Fuel Properties in a Thermocontrolled Tank During Vehicle Operation</b>	<b>112</b>
7.1	Preliminaries	112
7.2	Mathematical Model for Thermocontrolled Tank Installed in a Vehicle	112
7.3	Simulation of Gaseous Fuel Properties during Bus Operation	113
7.3.1	Simulation of Hydrogen Properties	116
7.3.2	Simulation of Natural Gas Properties	119

7.4	Simulation of Gaseous Fuel Properties during Car Operation	123
7.4.1	Simulation of Hydrogen Properties	125
7.4.2	Simulation of Natural Gas Properties	130
7.5	Conclusions	134
<b>8</b>	<b>Optimization of On-Board Gas Storage Systems</b>	<b>136</b>
8.1	Preliminaries	136
8.2	Design Objectives and Variables	136
8.3	Optimization of the Storage System for a Car	139
8.3.1	Design Parameter Sensitivity Study	139
8.3.1.1	Initial Waiting Time	139
8.3.1.2	Parking Time	142
8.3.1.3	Safe Pressure Ratio	142
8.3.1.4	Range	147
8.3.2	Formulation of the Problem	147
8.3.3	Solution Method	151
8.4	Optimization of the Storage System for a Bus	153
8.4.1	Design Parameter Sensitivity Study	153
8.4.1.1	Initial Waiting Time	153
8.4.1.2	Parking Time	153
8.4.1.3	Safe Pressure Ratio	158

	8.4.1.4	Range	158
	8.4.2	Solution Method	163
<b>9</b>		<b>Natural Gas-Hydrogen Mixtures for Vehicles</b>	<b>166</b>
	9.1	Preliminaries	166
	9.2	Simulation of the Mixture Properties in Thermocontrolled Tank during Vehicle Operation	169
	9.2.1	Natural Gas-Hydrogen Mixture for Bus Operation	169
	9.2.2	Natural Gas-Hydrogen Mixture for Car Operation	171
<b>10</b>		<b>Summary, Conclusions and Recommendations</b>	<b>173</b>
		<b>References</b>	<b>178</b>
		<b>Appendices</b>	<b>A1</b>
	A	Properties of Different Fuels Used in Vehicles	A2
	B	Technical Details and Calibration Curves	A4

## LIST OF FIGURES

Fig. 1.1a	Volumetric energy of different fuels	4
Fig. 1.1b	Mass energy of different fuels	4
Fig. 1.2	Methods of achieving fuel/air mixtures in internal combustion engines	6
Fig. 1.3a	Energy concentration of natural gas	11
Fig. 1.3b	Specific volume of natural gas	11
Fig. 1.4a	Energy concentration of hydrogen	14
Fig. 1.4b	Specific volume of hydrogen	14
Fig. 1.5	Comparison of current and future hydrogen storage systems	27
Fig. 2.1	Schematic of the thermocontrolled tank	30
Fig. 2.2	Hydrogen gas supply system for direct injection in diesel engine equipped with thermocontrolled tank	33
Fig. 2.3	Temperature-specific volume (T-v) graph for hydrogen with storage points marked	34
Fig. 3.1	Schematic of the heat transfer process in a thermocontrolled tank	47
Fig. 3.2	Simulation results of temperature-time history for nitrogen	51
Fig. 3.3	Simulation results of temperature-time history for natural gas	52
Fig. 3.4	Simulation results of temperature-time history for hydrogen	54
Fig. 4.1a	Design of steel thermocontrolled tank	57

Fig. 4.1b	Design of the heat exchanger	58
Fig. 4.2	Design of insulation jacket for the steel tank	59
Fig. 4.3	Schematic of the test set-up for steel tank evaluation	62
Fig. 4.4	Pictorial view of the test set-up of steel tank for evaporation test	64
Fig. 4.5	Temperature and pressure records from the test on the uninsulated steel vessel	65
Fig. 4.6	Temperature and pressure records from the test on the insulated steel vessel	67
Fig. 4.7	Results from the tests conducted to investigate the peaks in pressure and temperature	69
Fig. 4.8	Temperature and pressure records from the test on the insulated steel vessel with additional heating through the heat exchanger	72
Fig. 4.9	Schematic of the test set-up for the composite vessel evaluation	74
Fig. 4.10	Temperature and pressure records from the test on the composite high pressure vessel	75
Fig. 4.11	Experimental and simulation results for insulated steel tank	76
Fig. 5.1	Effect of design variables on initial operational temperature for natural gas	84
Fig. 5.2	Effect of design variables on initial operational temperature for hydrogen	85
Fig. 5.3	Schematic of the pressure vessel	86
Fig. 5.4	Variation of gas mass to vessel mass ratio with design variables for natural gas	88

Fig. 5.5	Variation of gas mass to vessel mass ratio with design variables for hydrogen	89
Fig. 5.6	Variation of gas mass to vessel volume ratio with design variables for natural gas	90
Fig. 5.7	Variation of gas to vessel volume ratio with design variables for hydrogen	91
Fig. 5.8	Variation of global objective criterion vs pressure for natural gas	96
Fig. 5.9	Variation of global objective criterion vs pressure for hydrogen	96
Fig. 5.10	Flow chart of the optimization process	98
Fig. 5.11	Iteration history of design variables during optimization for hydrogen	99
Fig. 6.1	Bus with a battery of thermocontrolled tanks installed on the roof	104
Fig. 6.2	Proposed gas storage and supply system for a bus	107
Fig. 6.3	Installation of thermocontrolled tanks in the trunk of a car	108
Fig. 6.4	Proposed gas storage and supply system for a car	110
Fig. 7.1	Bus operational schedule for gaseous fuel use	115
Fig. 7.2	Case Bus H1: Bus starts operation just after the pressure in the tank reaches 100 bar	117
Fig. 7.3	Case Bus H2: Bus starts operation just before the pressure in the tank reaches 500 bar	118
Fig. 7.4	Case Bus N1: Bus starts operation just after the pressure in the tank reaches 100 bar	120

Fig. 7.5	Case Bus N2: Bus starts operation just before the pressure in the tank reaches 500 bar	121
Fig. 7.6	Car operational schedule for natural gas and hydrogen	124
Fig. 7.7	Case Car H1: Car starts operation just after the pressure in the tank reaches 100 bar; it runs continuously until the pressure drops to 100 bar	126
Fig. 7.8	Case Car H2: The tank of the car is charged with 25% more gas, assuming that it will start operation immediately after refuelling	127
Fig. 7.9	Case Car H3: Car starts its operation at the beginning of the week-schedule with a short commuting trip	128
Fig. 7.10	Case Car N1: Car starts operation just after the pressure in the tank reaches 100 bar; it runs continuously until the pressure drops to 100 bar	131
Fig. 7.11	Case Car N2: Car starts its operation at the beginning of the week-schedule with frequent commuting trips	132
Fig. 8.1	Variation of initial waiting time with the change in variables for hydrogen car	140
Fig. 8.2	Variation of initial waiting time with the design variables for natural gas	141
Fig. 8.3	Variation of parking time with the design variables for hydrogen car	143
Fig. 8.4	Variation of parking time with the design variables for natural gas car	144
Fig. 8.5	Sensitivity of safe pressure ratio with design variables for hydrogen car	145
Fig. 8.6	Variation of safe pressure ratio with the design variables for natural gas car	146

Fig. 8.7	Sensitivity of the range with design variables for hydrogen car	148
Fig. 8.8	Variation of the range for natural gas car with the design variables	149
Fig. 8.9	Progress of optimization for hydrogen car	152
Fig. 8.10	Progress of optimization for natural gas car	152
Fig. 8.11	Variation of initial waiting time with the change in variables for hydrogen bus	154
Fig. 8.12	Variation of initial waiting time with the change in variables for natural gas bus	155
Fig. 8.13	Variation of parking time of hydrogen bus with the change in variables	156
Fig. 8.14	Variation of parking time of natural gas bus with the change in variables	157
Fig. 8.15	Sensitivity of safe pressure ratio to design variables for hydrogen bus	159
Fig. 8.16	Sensitivity of safe pressure ratio to design variables for natural gas bus	160
Fig. 8.17	Variation of range with the change in design variables for hydrogen bus	161
Fig. 8.18	Variation of range with the change in design variables for natural gas bus	162
Fig. 8.19	Convergence of design variables during optimization for hydrogen bus	164
Fig. 8.20	Convergence of design variables during optimization for natural gas bus	164

Fig. 9.1	Specific volume of natural gas, hydrogen and the mixture at 200 K	167
Fig. 9.2	Range covered by natural gas and natural gas-hydrogen mixture vehicles	168
Fig. 9.3	Simulation of the mixture properties inside thermocontrolled tank during the bus operation	170
Fig. 9.4	Simulation of the mixture properties inside thermocontrolled tank during the car operation	172
Fig. B.1	Calibration curve for OMEGA thermocouple	A4
Fig. B.2	Calibration curve for RTD thermocouple	A4
Fig. B.3	Calibration curve for OMEGA pressure transducer	A5
Fig. B.4	Calibration curve for VALIDYNE pressure transducer	A5

## NOMENCLATURE

$A$	Current output from the amplifier of the thermocouple/pressure transducer
$c_{ex}$	Specific heat of exhaust gas
$c_g$	Specific heat of the gas
$c_h$	Specific heat of the heat exchanger pipe
$c_p$	Constant-pressure specific heat
$c_t$	Specific heat of the tank material
$c_t^l, c_t^u$	Lower and upper bounds on the specific heat of material
$c_v$	Constant-volume specific heat
$CH_4$	Natural gas (Methane)
CNG	Compressed natural gas
$d_1$	Inside diameter of the vessel
$d_2$	Outside diameter of the vessel
$d_1^l, d_1^u$	Lower and upper bounds on inside diameter
$F(X)$	Global objective criterion
$g(X)$	Inequality constraint on the design variables
$GH_2$	Gaseous hydrogen
$GVV(X)$	Normalized gas mass to vessel volume ratio
$GVVMAX$	Maximum value of $GVV(X)$

GVVMIN	Minimum value of GVV(X)
$h(X)$	Equality constraint
$H_2$	Hydrogen
IWT(X)	Initial waiting time of the vehicle
L	Length of the vessel
$LH_2$	Liquefied hydrogen
LHV	Lower heat value of the fuel
$LN_2$	Liquefied nitrogen
LNG	Liquefied natural gas
$m_{ex}$	Mass of exhaust gas present inside the heat exchanger
$\dot{m}_{ex}$	Mass flow rate of the exhaust gas
$m_g$	Mass of gas inside the tank
$m_{gi}$	Initial mass of gaseous fuel in the tank after fill-up
$m_{gi}^l, m_{gi}^u$	Lower and upper bounds on the initial mass of the gaseous fuel filled into the tank
$\dot{m}_g$	Fuel consumption of the engine
$\dot{m}_g^l, \dot{m}_g^u$	Lower and upper bounds on the fuel consumption
$m_h$	Mass of the heat exchanger pipe with fins
$m_t$	Mass of the tank

$N_2$	Nitrogen
$P$	Pressure of gas inside the tank
$P_a$	Ambient pressure
$P^l, P^u$	Lower and upper bounds on the pressure of gas
$PT(X)$	Parking time of the vehicle
$q_{ex}$	Heat added from exhaust gases to the gaseous fuel
$q_{ex}^l, q_{ex}^u$	Lower and upper bounds on the heat added from engine exhaust gases
$r_p$	Penalty parameter
$R$	Gas constant
$RAN(X)$	Range covered by the vehicle in each fill-up
$R_{exh}$	Thermal resistance between the exhaust gas stream and the heat exchanger pipe
$R_{gt}$	Thermal resistance between the tank and the gaseous fuel
$R_{g/t}$	Gas mass to vessel mass ratio
$R_{g/t}MAX$	Maximum value of $R_{g/t}(X)$
$R_{g/t}MIN$	Minimum value of $R_{g/t}(X)$
$R_{hg}$	Thermal resistance between the heat exchanger pipe and gaseous fuel
$R_{m/v}$	Gas mass to tank volume ratio
$R_{ta}$	Thermal resistance between the tank and atmosphere

$S$	Hoop stress of the tank material
$S^l, S^u$	Lower and upper bounds on the stress of material
$SPR(X)$	Safe pressure ratio
$t$	Thickness of the tank wall
$T$	Temperature of the system used in calibration of the thermocouples
$T_a$	Ambient temperature
$T_{ex}$	Temperature of exhaust gas inside the heat exchanger
$T_{exi}$	Temperature of exhaust gas entering the heat exchanger
$T_g$	Temperature of gas inside the tank
$T_h$	Temperature of the heat exchanger wall
$T_{io}$	Initial operational temperature
$TIO(X)$	Normalized initial operational temperature
$TIOMAX$	Maximum value of $TIO(X)$
$TIOMIN$	Minimum value of $TIO(X)$
$T_t$	Temperature of the tank wall
$v_g$	Specific volume of gas
$VO$	Voltage output from the amplifier of the thermocouple/pressure transducer
$V_c$	Volume of the material
$V_i$	Tank inside volume
$V_i^l, V_i^u$	Lower and upper bounds on the inside volume of the tank

$V_o$	Tank outside volume
$W_1, W_2, W_3$	Weighting factor for the design objectives
$X$	Design variable vector
$X_1$	Initial feasible starting point
$Z(X)$	Objective function

### **Greek Symbols**

$\Delta E$	Energy released by the tank walls
$\Delta T$	Temperature change
$\Delta u$	Internal energy change
$\phi(X)$	Pseudo-objective function
$\rho$	Density of the tank material
$\tau$	Time after completing the filling process

### **Subscripts**

a	Ambient
c	Composite
ex	Exhaust gas
exh	Exhaust gas stream and the heat exchanger pipe
exi	Exhaust gas entering the heat exchanger

<b>g</b>	Gas
<b>gi</b>	Initial gas
<b>g/t</b>	Gas mass to vessel mass
<b>gt</b>	Gaseous fuel and tank
<b>h</b>	Heat exchanger wall
<b>hg</b>	Heat exchanger pipe and gaseous fuel
<b>i</b>	Inside
<b>io</b>	Initial operational
<b>m/v</b>	Gas mass to vessel volume
<b>o</b>	Outside
<b>p</b>	Penalty
<b>t</b>	Tank
<b>ta</b>	Tank and atmosphere

### **Superscripts**

<b>l</b>	Lower bound on the design variable
<b>u</b>	Upper bound on the design variable

# CHAPTER 1

## INTRODUCTION

### 1.1 General

During the past century, vehicles of all kinds have gained an important place in human life. They provide almost unlimited mobility, ensure comprehensive supply of all goods required for daily life, and thus guarantee what in the broadest sense of the word is called *standard of living*.

The development of an extensive traffic system such as we have today was only possible because of the discovery and exploitation of sufficient energy resources. The development of liquid hydrocarbons on the basis of crude oil constituted a prerequisite for all types of road traffic where - apart from a few exceptions - only such energy media are utilized which are not dependent on electric power supply lines.

Our present day transportation system is inconceivable without the widespread availability of liquid hydrocarbons. But the fossil resources are finite and the environmental changes due to the release of the carbonaceous combustion products give us cause to think about them. Despite all controversies as to how much crude oil is left on our planet, all scientists agree that crude oil deposits are limited and according to the most optimistic estimates, the beginning of their

exhaustion will come approximately in the year 2040 [1\*]. At the same time, fears over the continuity of imported oil supply that first emerged during the early 1970s and resurfaced during the Gulf war in 1990, have led to increased calls for **domestic fuel sources**.

Automotive emissions contribute heavily to the current air pollution problems in urban areas throughout the world. Unburned hydrocarbons (HC), oxides of nitrogen and sulphur, carbon monoxide (CO) and dioxide, carbon particulates and additional unregulated pollutants foul the air, creating a threat to both local health and planetary ecology. The quality of air we breathe has degraded steadily with the advent of the use of hydrocarbon fuels for transportation. Ground level ozone, a cancer-causing component in urban smog, is becoming a major national problem. Carbon dioxide levels have increased from 315 parts per million (ppm) thirty years ago to 348 ppm today [2], contributing to the emerging *Greenhouse Effect*.

Environmental concerns have been reflected in federal regulations like the *Clean Air Act*, as well as the legislations that have been already passed in California, Colorado and Texas [3]. These regulations call for clean air initiatives that include a plan for phased introduction of **clean fuelled vehicles**, which reduce pollution levels.

---

\* Numbers in the parenthesis indicate references at the end

With the two demands, for the availability of domestic fuel sources and for cleaner vehicles, a large number of alternative fuels, in either liquid or gaseous form, are being considered with increasing interest [4,5]. The prominent alternative fuels that emerged as the replacement for gasoline are electrical energy, alcohols: methanol and ethanol, gaseous fuels: natural gas, propane and hydrogen. Some of these fuels have already been used in internal combustion engines, especially with spark ignition, to power commercial vehicles [6-9].

The large scale implementation of the gaseous fuel vehicles is hindered mainly by the problems associated with the on-board storage and conditioning. Fig. 1.1 shows the energy densities of different alternative fuels in comparison to commonly used gasoline and diesel [10]. It can be seen from the figures, that although mass energy density is high, the volumetric energy density of natural gas or hydrogen is very low and hence large tank volume is required to store the same amount of energy as compared to gasoline. The weight and size of the cylinders limit the operational range of the vehicles. An answer to this inefficient storage is the use of cryogenic tanks in which the gas is stored in the liquid phase. However, to maintain the low temperature in a cryogenic tank, an expensive insulation of the tank is required.

Performance of a spark ignition engine supplied with gas as fuel through the intake manifold, is inferior to that supplied with gasoline. While satisfactory efficiency can be obtained, there is a power penalty due to the high specific volume

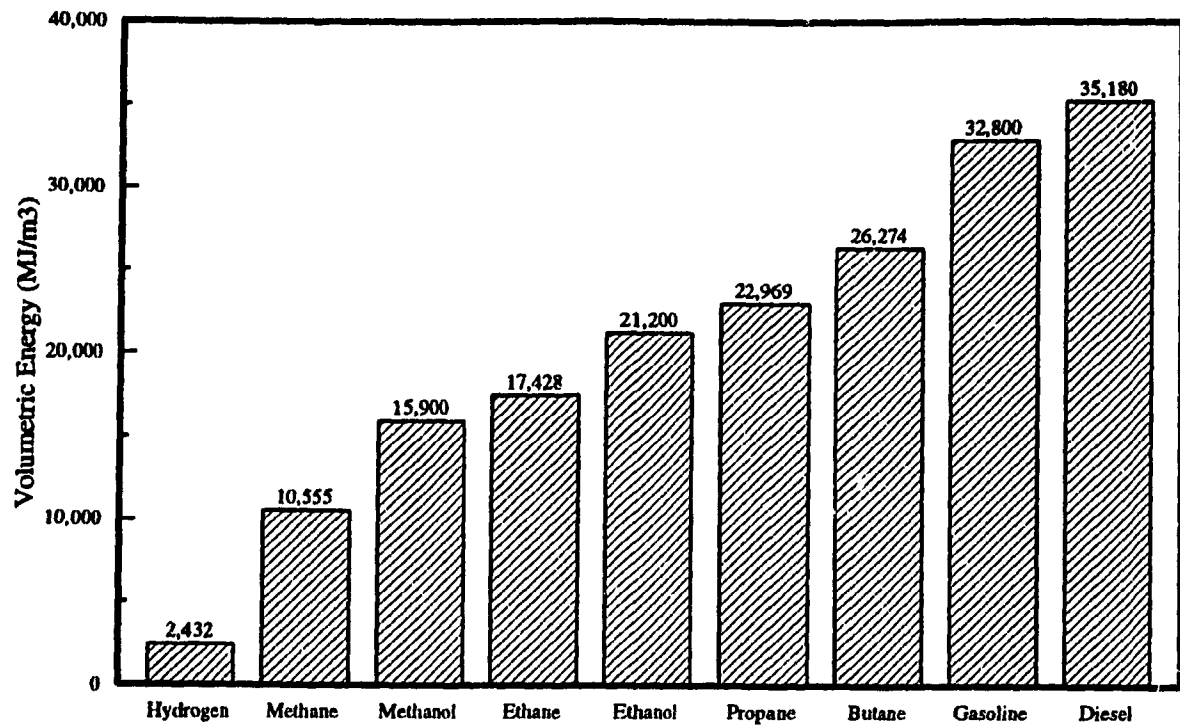


Fig. 1.1a Volumetric Energy of Different Fuels

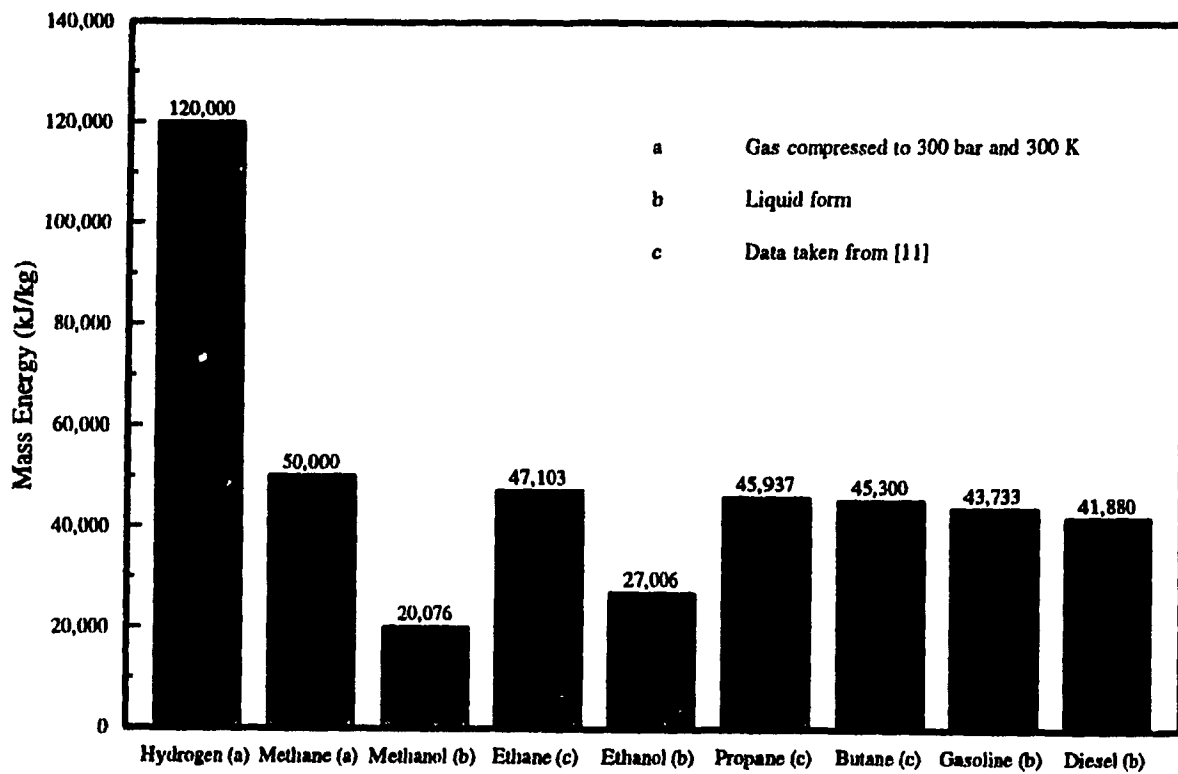
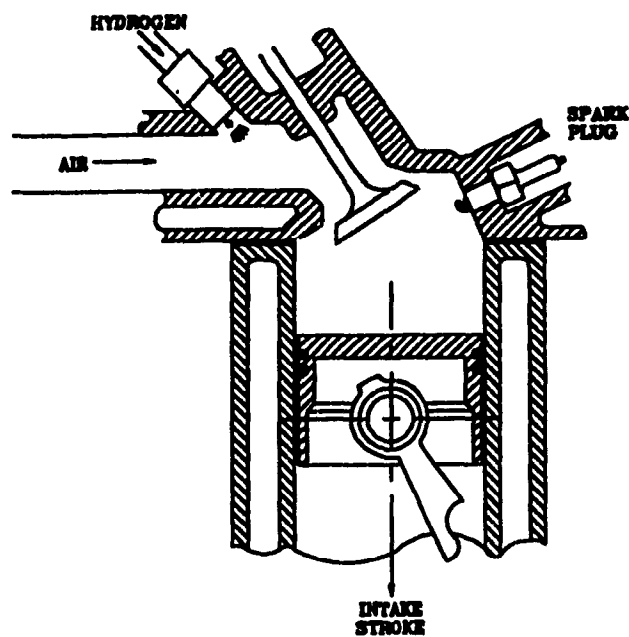


Fig. 1.1b Mass Energy of Different Fuels

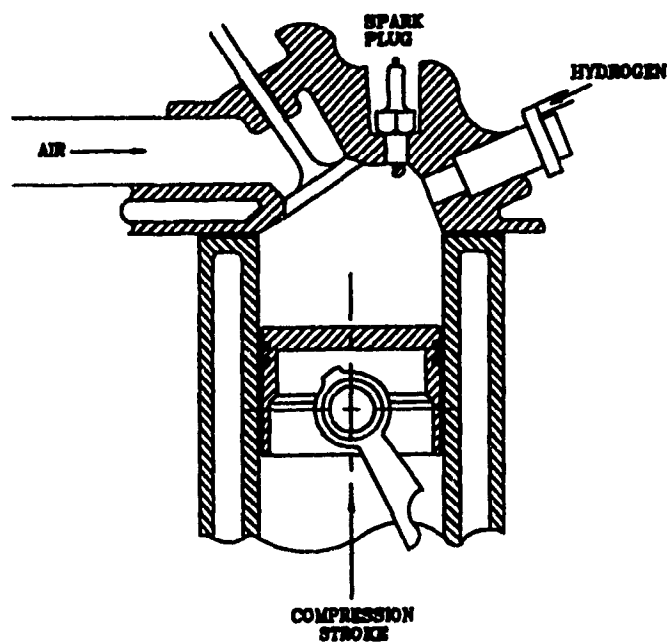
of gaseous fuel in the intake manifold. This, in turn reduces the amount of air available for combustion. The engine power in the case of natural gas is being further reduced by the slow combustion process, due to lower velocity of flame propagation in the mixture of air and natural gas as compared with gasoline mixtures (refer to Appendix A for the properties of different fuels). An improvement in efficiency through the increase of the compression ratio is also limited in the case of manifold injection (Fig. 1.2a), as compared to direct injection (Fig. 1.2b) by the knock phenomenon.

In the case of gas fuelled diesel engines, called *dual fuel diesel engines*, the gaseous fuel is introduced together with air through the intake manifold and the regular diesel fuel is injected to provide ignition only in small quantities by a conventional diesel injection system. However, as in the spark ignition engines, the power of the engine is also reduced, due to the presence of gaseous fuel inside the intake manifold where it replaces some of the air. The thermal efficiency of such an engine is also affected by the limitation in engine compression ratio to avoid the knock.

The engines supplied with hydrogen through the intake manifold are also plagued by the backfiring phenomenon of the air-hydrogen mixture which is caused by the pre-ignition of the mixture following the opening of the intake valve. This is due to the low heat requirement for hydrogen air mixture to auto-ignite and also to the high speed of flame propagation in air-hydrogen mixtures.



a) Manifold Injection



b) Direct Injection

Fig. 1.2 Methods of Achieving Fuel/Air Mixtures in Internal Combustion Engines

Taking all the above factors into account, direct injection of gaseous fuel (Fig. 1.2b) would be the best solution to the efficient extraction of energy from this type of fuel. This conclusion stems from the following observations:

1. There is no limitation in the engine compression ratio regarding the knock phenomenon due to the direct gas injection controlling the combustion process.
2. There is no power penalty and no back firing possibility related to the presence of the gaseous fuel in the intake manifold.
3. There is a potential of preheating the gaseous fuel before injection, by using the waste energy of the exhaust gases in order to improve the thermal efficiency of the engine. The gas preheating might also improve the ignition ability of the gaseous fuels. Preheating of liquid hydrocarbon fuels might be however limited because it could lead to the fuel cocking which would result in contamination of the injectors with carbon deposits.

In direct injection, the gaseous fuel must be delivered into the combustion chamber under high pressure above 100 bar to overcome the gas pressure inside the cylinder. This imposes a restriction on the utilization of the rest of the fuel remaining in the tank. For example, if the initial pressure in the tank is 200 bar, then only about 60% of the fuel could be utilized. If the initial pressure is increased to 500 bar, the utilizable portion of fuel could be increased to approximately 84%. To create the high initial gas pressure, it is estimated [12] that

an energy equivalent of approximately 5.5% of the lower heating value (LHV) of the gas would be required. Because of all these problems, the present gaseous fuel vehicle technology is limited to manifold injection. The objective of this study is to carry out a thorough feasibility investigation on a novel storage and supply system for gaseous fuels, natural gas and hydrogen, for vehicles with the direct gas injection system. Analytical models validated through laboratory experiments have been used to propose optimal gas storage system for a given vehicle. In the following subsections, a literature survey is presented on alternative fuels and storage systems in order to develop the scope and methodology of the present investigation outlined in chapter 2.

## **1.2 Alternative Fuels Considered for Storage**

A large number of alternative fuels in either liquid or gaseous form are being considered with increasing interest. Some alternative gaseous fuels such as hydrogen, natural gas and propane have already been used in internal combustion engines, especially with spark ignition, to power commercial vehicles. The most promising alternative fuels are natural gas, for its low cost and availability and hydrogen, for its almost pollution free combustion.

### **1.2.1 Natural Gas**

Natural gas is available in large quantities throughout the world. It is a mixture of several different gases. The primary constituent is methane ( $\text{CH}_4$ ), which typically makes up 85-99% of the total volume, depending on the source. The other constituents include other hydrocarbons; inert gases such as nitrogen and helium as well as carbon dioxide and also traces of hydrogen sulphide and water.

Natural gas under normal conditions mixes readily with air, and is an excellent fuel for Otto-cycle (spark ignition) engines. Unlike liquid hydrocarbon fuels, it does not need to vaporize before it will burn - thus, cold engine starting is easier (especially at low temperatures) and cold start enrichment is required to a lesser degree. It is an important factor, since cold-start enrichment is a major

source of HC and CO emissions in gasoline fuelled vehicles.

Natural gas has a higher ignition temperature, and therefore is more resistant to self-ignition which results in good antiknock properties. Natural gas can be used with engine compression ratios as high as 12:1 (compared to 8:1-10:1 for gasoline) reaching [13] significantly higher efficiencies than are possible with gasoline.

Because of its higher activation energy needs, the laminar flame speed of natural gas-air mixtures is lower than that of other hydrocarbons. This effect is most significant under lean burning conditions. The low flame front speed of natural gas mixture results in a longer duration of combustion, impairing thermal efficiency, unless the spark timing is advanced to start the combustion process earlier. The need for advanced ignition timing can be offset to some extent by the use of higher compression ratios and more compact, highly turbulent combustion chambers.

Natural gas remains in the gaseous phase under atmospheric conditions and liquefies at 111 K and 2 bar. Natural gas may be stored on-board a vehicle in any one of the following ways:

1. As a compressed gas in high pressure cylinders
2. As a cryogenic liquid in cryogenic containers
3. As adsorbents in carbon skeletal networks.

Fig. 1.3 shows the volumetric energy and specific volume of natural gas at different pressures and temperatures [43]. The volumetric energy content of liquid

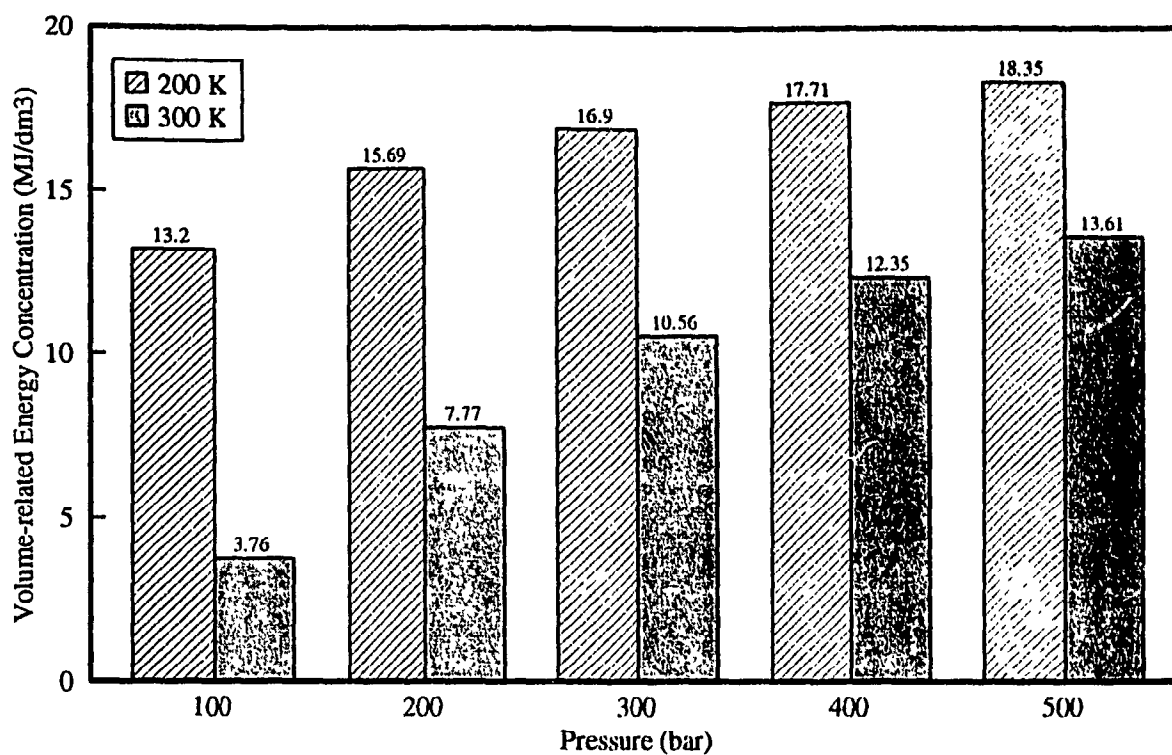


Fig. 1.3a Energy Concentration of Natural Gas

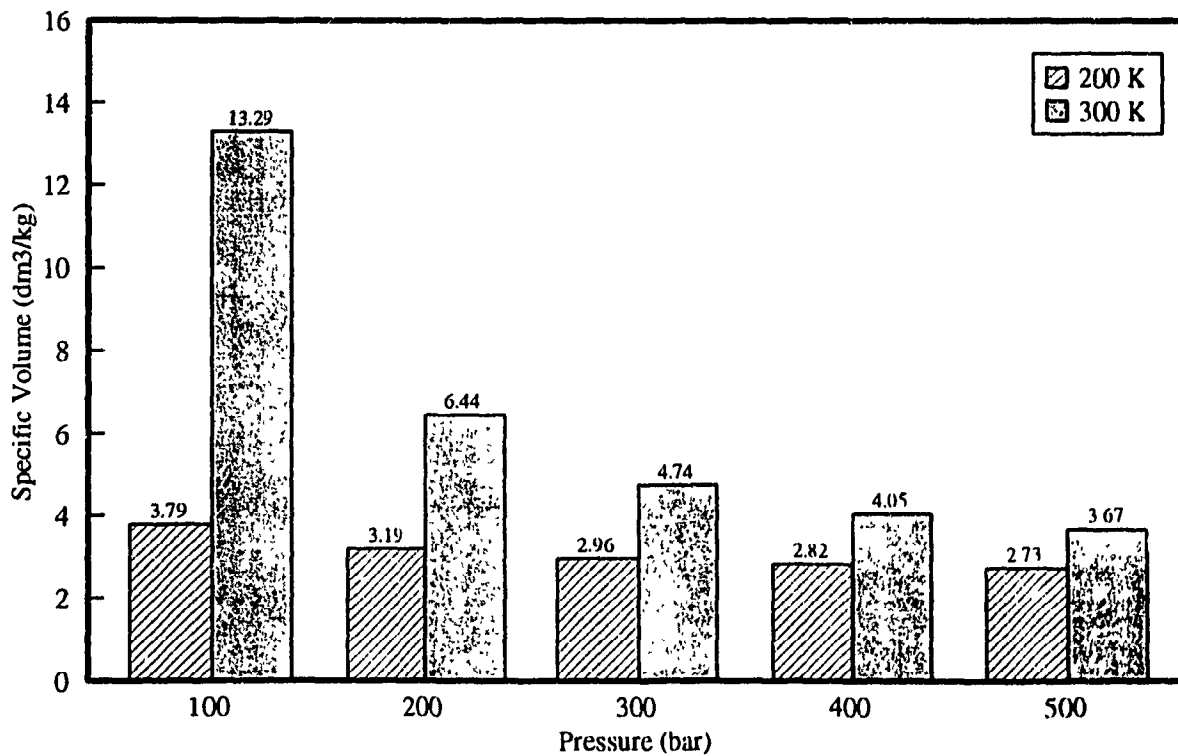


Fig. 1.3b Specific Volume of Natural Gas

methane is three times greater than that of methane gas at 200 bar and 300 K. At a low temperature of 200 K and 200 bar pressure, the energy content becomes double that of the gas at 300 K and 200 bar, which means that more energy can be stored at low temperatures.

Natural gas is stored in vehicles mainly as compressed natural gas, with the exception of ship-tankers and railway car-tankers which transport natural gas in liquefied form. Therefore, generally high pressure cylinders are used as tanks in passenger cars, buses or trucks fuelled with natural gas.

### 1.2.2 Hydrogen

Hydrogen is considered a very attractive alternative fuel for two important reasons. It is the least polluting fuel that can be used in an internal combustion engine, where the only pollutant to the environment may be limited  $\text{NO}_x$  emissions. It is potentially available anywhere there is water and energy. It can be produced by using any energy source such as solar, nuclear, hydro, geothermal, etc. The prospect of a clean, widely available transportation fuel has motivated much of the research on hydrogen.

Hydrogen remains in a gaseous state under atmospheric conditions and liquefies at 20 K and 2 bar. The possible ways of storing hydrogen on board a vehicle are:

1. As compressed gas in ultra-high pressure vessels
2. As a liquid in cryogenic containers
3. As a gas bound with certain metals, called *metal hydrides*.

An appealingly simple way to store hydrogen on board a vehicle is as compressed gas, in high-pressure vessels. Fig. 1.4 shows the volumetric energy and specific volume of hydrogen at different pressures and temperatures [43]. At 200 bar and 300 K, hydrogen occupies approximately 11 times higher volume than natural gas and thus requires a much higher storage pressure to represent the corresponding energy density. For example, 1.5 kg of compressed gaseous hydrogen ( $\text{GH}_2$ ) occupying  $0.1 \text{ m}^3$  at 298 K and 200 bar will provide an operating range of 100 km, in comparison to 14.85 km/litre for gasoline. To increase the range and to make volumetric requirement more manageable, the pressure should be increased. Light weight carbon-wrapped aluminium cylinders capable of storing hydrogen safely at high pressure, used in aerospace applications, would be very expensive for vehicular use. Less expensive Kevlar-wrapped cylinders are weaker per unit of weight, and thus would be heavier at high storage pressures [8, 9]. For example, at 690 bar, a carbon/aluminium storage vessel providing a 420 km range in a vehicle would be about three times heavier and nine times larger than the gasoline tank providing the same range in the comparable gasoline vehicle [10]. Due to its very high specific volume, hydrogen is stored in vehicles generally in the liquid phase, i.e., in cryogenic tanks at 20 K or in metal hydrides which

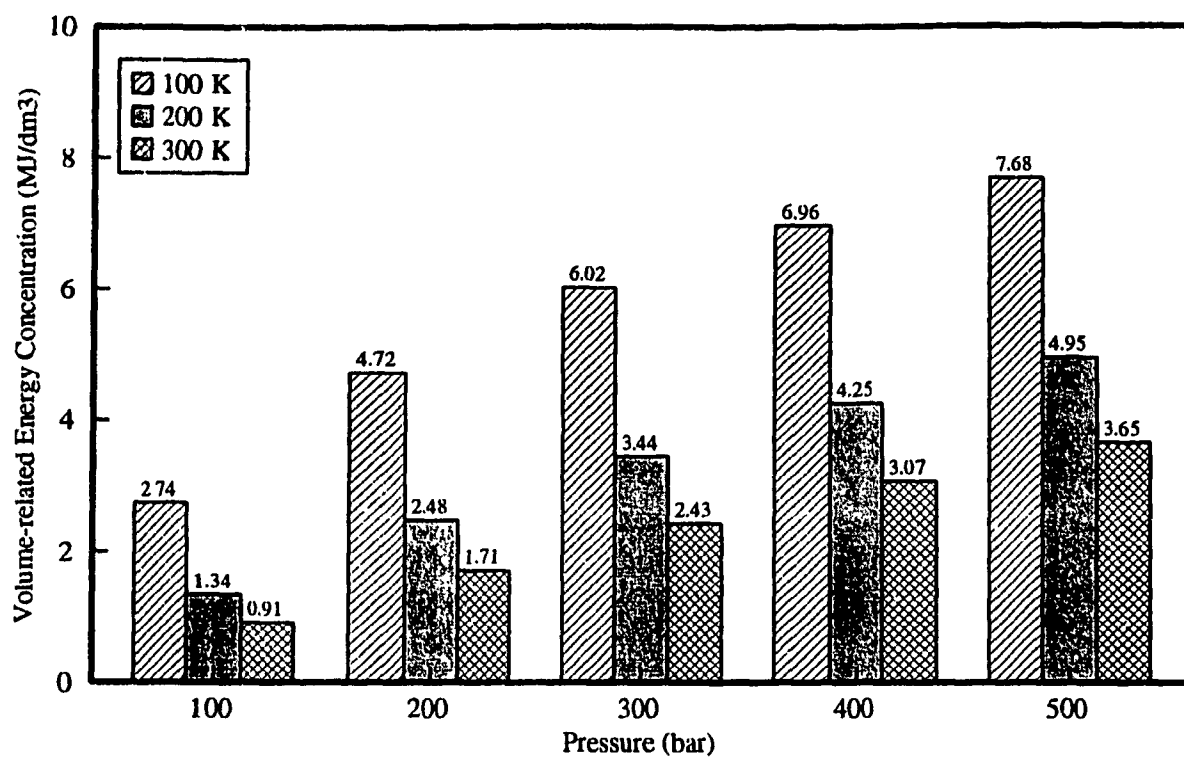


Fig. 1.4a Energy Concentration of Hydrogen

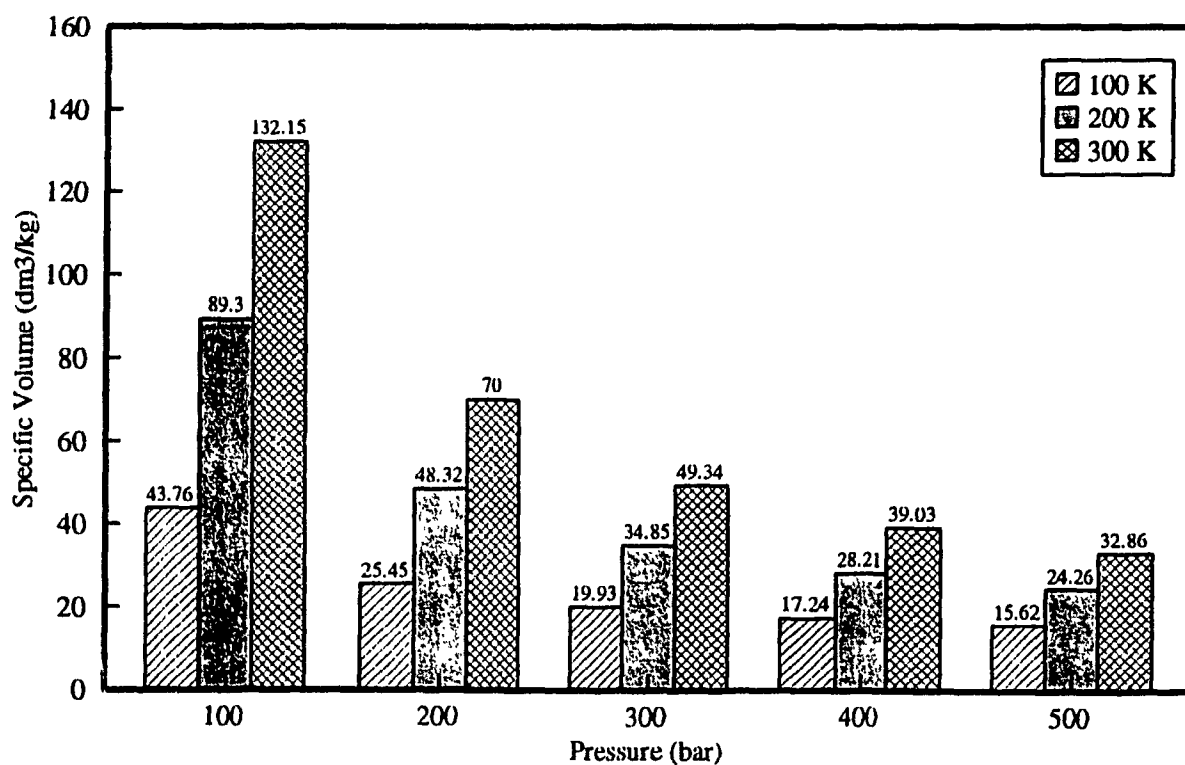


Fig. 1.4b Specific Volume of Hydrogen

however, are much heavier than the cryogenic tanks.

Liquid hydrogen ( $\text{LH}_2$ ) has an energy density of  $10\,000\text{ MJ/m}^3$ , as compared to  $33\,000\text{ MJ/m}^3$  for gasoline, a ratio of about 3.3 to 1. Liquid hydrogen is stored in double-walled, super-insulated vessels designed to minimize the heat transfer and the rate at which  $\text{LH}_2$  boils off. Hydrogen is drawn from either the liquid or gas phase and delivered to the engine. If hydrogen is taken from the liquid phase, it should be compressed using cryogenic pumps, in order to create the high pressure required for direct injection. A significant advantage of using  $\text{LH}_2$  is that these systems are much lighter and more compact than compressed gaseous systems providing an equal range, because of the higher volumetric energy density. Liquid hydrogen is not significantly heavier than gasoline on an equal energy basis; it is, however, much bulkier. The main obstacles to widespread use of  $\text{LH}_2$  vehicles are the size of storage system, the higher cost of liquid hydrogen and cryogenic technology, the evaporation losses of  $\text{LH}_2$  and the problems associated with the reliability and maintenance of cryogenic pumps as well as the safety.

*Metal hydrides* represent the storage of hydrogen in the form of a decomposable chemical compound. There are a number of metals like iron, magnesium, nickel, manganese and titanium, that will react directly with gaseous hydrogen to form a metal hydride. Vehicular hydride storage systems are usually long thin hollow cylinders, tightly bundled and pressurized with hydrogen to about 34 bar. When the vessel is charged, a good deal of heat is released and must be

transported out of the container, typically by cooling water. During gas discharge, the reaction is reversed and heat is required. With most hydrides, the exhaust heat from the engine would be used to release hydrogen from the metal. The main disadvantage of hydrides is their low mass energy density. Most hydrides suitable for automotive application contain only 0.5 to 2.0% hydrogen by weight. The low mass energy density of most hydrides means that hydride vehicles are much heavier and less fuel efficient than comparable gasoline or  $\text{LH}_2$  vehicles, and are limited by the weight of storage system to about 100 km range.

### 1.3 Gaseous Fuel Storage Systems - Literature Review

#### 1.3.1 Natural Gas Storage Systems

More than 40 years of natural gas vehicle (NGV) use have demonstrated the safety of CNG as a vehicular fuel, and have produced a significant technology base. Renewed interest in NGVs in the last few years has promoted considerable research and development activity, with consequent improvements in storage, injection, emissions and efficiency. In the following paragraphs, the results of the research in natural gas storage are presented.

During 1980, Beech Aircraft has outfitted a vehicle with a 49 kg (108 lb), 0.0685 m<sup>3</sup> (18.1 gallon) nominal capacity, double-walled cylindrical cryogenic storage vessel [14, 15]. The full tank weighs 77.7 kg (171.3 lb), which compares with a *standard* 66.7 kg (147 lb) full gasoline tank, and occupies 0.123 m<sup>3</sup> (123 litres). The full tank can sit unused for a week before it is necessary to vent the boil-off gas.

During 1982, the Aerospace Corporation [16] has simulated for the U.S. Department of Energy an LNG vehicle that was 38% more efficient and only 11.8 kg (26 lb) heavier than a comparable gasoline car with the same 563.3 km (350 mile) range.

In 1983, Ford demonstrated an LNG vehicle [17], which has 0.06814 m<sup>3</sup> (18 U.S. gallon) LNG tank and adds about 36.3 kg (80 lb) to the weight of the vehicle.

The no-venting period is 8 days.

In 1983, Golovoy et al from Ford Motor Co. published an analysis of several options for natural gas storage in vehicles [12]. The following three gas pressure levels were proposed for the tank of a vehicle having operational range of 160 km and a fuel consumption of 0.0127 m<sup>3</sup> (12.7 litres<sup>\*\*</sup>) of gasoline per 100 km.

Tank pressure in bar (PSIG)	21 (300)	69 (1000)	165 (2400)
Tank volume in m <sup>3</sup> (l)	0.23 (232)	0.17 (170)	0.06 (62)
Tank weight in kg	186	65	52
Tank cost in US \$	1300	800	750

They also proposed home refuelling with gas using a small compressor driven by an electric motor. The electrical energy required to compress natural gas to the needed 165 bar (2400 PSIG) amounted to 5.5% of the gas lower heating value (LHV), approximately.

In 1986, Duncan et al from Hamilton, Ontario, demonstrated the conversion of 6 city-buses to operate on natural gas [18]. The on-board gas storage system was composed initially of 7 cylinders made of fibre wound aluminum skin, pressurized to 207 bar (3000 PSIG), which provided the buses with an operational range of 375 km. Finally, 5 cylinders of size 0.33 x 1.83 m (13 x 72 in.), plus 2 cylinders of size 0.38 x 1.83 m (15 x 72 in.), were recommended, which were to

---

<sup>\*\*</sup>Figures in parenthesis are the actual numbers given in the original work. They have been converted to SI system of units for the purpose of uniformity.

provide the buses with an operation range goal of 460 km. The natural gas distribution and refuelling was assured by Union Gas in Ontario, which used a 149 kW (200 hp), 34 m<sup>3</sup>/hr (20 SCFM) compressor to fill up the tanks of the bus. Testing of the bus on a 130 km circuit showed the fuel consumption at the level of 40.5 kg/100 km.

In 1986, Noon from Perth, Australia, unveiled a bus conversion to run on natural gas, initially using 11 Baber steel cylinders with 0.06 m<sup>3</sup> (60 l) volume each [19]. The cost of this storage system was A\$ 9,500 and the bus operational range was about 300 km. Finally, fiber wound aluminium cylinders were used: 7 cylinders with 0.119 m<sup>3</sup> (119 l) each, plus 1 cylinder with 0.079 m<sup>3</sup> (79 l) at a total cost of A\$ 10,800. This was to provide the bus with an operational range of 400 km.

In 1988, Krepec et al at Concordia University, Montreal, Canada, proposed a semi-cryogenic tank for natural gas storage containing CNG at a much lower than ambient temperature of 200 K [20], however, higher than the temperature of the liquid phase, which is approximately 110 K. Such a semicryogenic tank must be well insulated and should use the waste heat of the engine exhaust gases to increase the gas pressure to the level required for direct natural gas injection. The proposed semicryogenic tank would store the natural gas with energy density twice as high as in pressurized cylinders at 200 bar pressure and ambient temperature, and only 1.5 times lower than in a cryogenic tank.

A New Orion Bus fuelled by CNG was unveiled [21] in 1989. It was prompted by the new emission regulations scheduled to come into effect in Canada and the United States in 1995. Fifty buses have been ordered for transit systems in Toronto, Mississauga & Hamilton, Ontario. The natural gas storage system consists of 3 long 0.33 x 6 m (13" x 20') Alusuisse cylinders, with a total capacity of 1.23 m<sup>3</sup> (1230 l). At 200 bar, they hold about 200 kg of natural gas and provide the bus with an estimated operational range of 500 km. The cylinders are installed on the roof of the bus.

In 1989, a dual fuel diesel highway-tractor fuelled by natural gas, was made operational in British Columbia, Canada [22]. It has four 0.096 m<sup>3</sup> (96 l) Alcoa aluminium composite cylinders mounted in place of the one fuel diesel tank and two 0.118 m<sup>3</sup> (118 l) cylinders mounted just behind the cab. Total volume for natural gas storage at 200 bar was 0.6 m<sup>3</sup> (612 l) which contained 102 kg of natural gas. Using this gas charge plus diesel fuel injected for ignition, the tractor had a 350 km operational range.

Since 1989, Powertech Laboratories in British Columbia, Canada are performing research in high pressure cylinders for natural gas [23]. According to the information released, in the last few years several manufacturers introduced the aluminium cylinders wrapped in resin-coated glass fibre. The main concern with these cylinders is their behaviour in a fire situation as they soften at 200°C. There are also new designs of entirely composite cylinders, with no metal inner liner,

which are presently under investigation.

In 1989, Davies from University of Saskatchewan and Sulatisky from Saskatchewan Research Council, published information about a CNG fuelled agriculture tractor [24]. Cylinders with natural gas compressed to 200 bar were stored on three tractors in the following manner:

-The first tractor had six  $0.12 \text{ m}^3$  (119 l) gas cylinders (three on each side of the tractor). The cylinders were made of an aluminium alloy liner hoop-wrapped with glass fibre reinforced plastic (FRP). The total mass of natural gas stored was 119 kg.

-The second tractor was equipped with 11 steel cylinders, with  $0.07 \text{ m}^3$  (70 l) volume each. They were saddle mounted between the front and rear tractor wheels on both sides of the tractor. The total mass of natural gas stored was 128 kg.

-The third tractor had seven  $0.14 \text{ m}^3$  (138 l) gas cylinders made of a steel liner with FRP hoop-wrapping. Four were mounted vertically at the front of the tractor, while the other 3 were installed horizontally at the top of the cabin. Total mass of CNG stored was 161 kg.

Presently, CNG is used to a much greater extent than LNG as vehicular fuel. CNG storage cylinders are built to rigorous quality standards established by U.S. Department of Transportation regulations. These regulations require tests-to-destruction of several cylinders in each batch of 200 produced [25]. The tests

include hydrostatic burst tests (with a minimum acceptable burst pressure at least 2.5 times the rated service pressure), thermal cycling and fatigue tests and immersion in fire to test the operation of the pressure relief devices. Each individual cylinder is hydrostatically tested initially and at periodic intervals thereafter to a pressure well in excess of the service pressure. Studies conducted in the late 1970s were unable to identify a single instance of a CNG cylinder failing due to collision damage, either in the U.S. or in Italy (where more than 300 000 NGVs have been used) [26]. This stands in sharp contrast to the record of collision resulting in fuel leakage and fires in gasoline vehicles.

Methane can also be stored in carbon skeletal networks, called *adsorbents*. This form of storage, although not yet commercially viable, has a great potential to lower the cost and volume of on-board storing of natural gas, and makes low pressure compression of gas at home more viable [13].

### 1.3.2 Hydrogen Storage Systems

In 1980, Peschka from the DFVLR Institute in West Germany, together with the BMW car manufacturing company, developed a cryogenic tank for a hydrogen fuelled passenger car. This tank was next used for supplying hydrogen to the manifold injected engine at a pressure of 15 bar using a plunger type pump for liquid hydrogen [27]. It was also recommended by Peschka, that in further

development, the  $\text{LH}_2$  pump should be placed outside the cryogenic tank to reduce the heat release in the tank. Peschka also carried out a study, showing the weight and size of different storage systems for 1 kg of hydrogen stored. According to Peschka, the latest improvements in the design of cryogenic tanks, will lead to a tank of capacity  $0.13 \text{ m}^3$  (130 l) weighing only 30 kg and having a boil-off rate reduced to 1% of the tank content per 24 hours. Therefore, he considers the cryogenic tank as the best solution for hydrogen storage in vehicles.

In 1982, Furuhashi and other investigators from Musashi Institute in Japan, manufactured a cryogenic tank for a car equipped with a diesel engine with direct hydrogen injection [28]. It was well insulated so that the liquid hydrogen inside the tank would boil off at the rate of less than 2% per 24 hours. To be able to bring hydrogen to the engine at the high pressure of 60 bar, a liquid hydrogen pump was used which was immersed in the liquid hydrogen at the bottom of the tank and driven by an electric motor. This tank was later improved and applied to a truck. The  $\text{LH}_2$  pump was also modified so that it could be driven by evaporating hydrogen under pressure, released from the tank.

In 1982, Buchner et al at Daimler-Benz in West Germany tried to develop a hydrogen storage system using metal hydrides [29]. They concentrated first on low temperature TiFe hydride tanks and later used high temperature light Mg alloy based hydrides. The low temperature hydrides have a reversible hydrogen storage capacity of up to 2% by weight; this gives an energy density of 2.38 MJ/kg. The

weight of the hydride tank is about 15% of the storage unit weight at pressures up to 15 bar and 25% at pressures up to 50 bar. As a result, the energy density of the storage unit drops to values between 1.8 and 1.98 MJ/kg, i.e., 17 to 20 times lower than in a comparable gasoline tank. The hydrogen released from the hydride tanks was supplied to the intake manifold of a spark ignition engine under low pressure. In case of MgNi hydrides, a high temperature of 400° C is required to release hydrogen, which was obtained using the heat of engine exhaust gases. However, during the engine starting and warming-up periods, the exhaust gas heat was not available. Also, in case of less than 100% pure hydrogen, the metal hydrides became contaminated and the hydrogen release process was not reversible, which reduced the tank storage capacity, after some time in service.

In 1986, Daimler-Benz started to pay more attention to other hydrogen storage systems. Feucht et al [31] compared the existing gas storage tanks and tabulated the results as shown below. It was stated that the composite containers for 300 bar pressure are commercially available.

	Specific Wt. (kg/kg H <sub>2</sub> )	Specific Wt. (kg/l gasoline)	Sp. Vol. (l/kg H <sub>2</sub> )	Sp. Volume (l/l gasoline)
GH <sub>2</sub> Storage tank (Steel cylinder 200 bar)	100	27	80	22

GH <sub>2</sub> Storage tank (Composite tank 300 bar)	30	8	62	17
LH <sub>2</sub> Storage tank	7	2	36	10
Metal Hydride Storage tank	95	26	40	11

In 1988, Krepec et al proposed a thermocontrolled tank for hydrogen storage which contains hydrogen as gas, however at much lower than ambient temperature of 100 K to 200 K, to increase the gas content in the tank [30, 59]. For this reason, the tank has to be insulated and also heated by the engine exhaust gases to extract more gas from the tank for the cases when the thermocontrolled tank is supplying the direct gas injection system for which a higher pressure is required. The storage capacity of such a tank would be 2.47 times higher than GH<sub>2</sub> compressed to 300 bar at ambient temperature and only 1.42 times lower than LH<sub>2</sub> in the cryogenic tank.

In 1989, Deluchi at the University of California published a broad study concerning all aspects of hydrogen use in vehicles, including costs [32]. This study recommended the use of composite wrapped aluminium cylinders, already used for aerospace application at up to 690 bar gas pressure, for storage of compressed hydrogen in vehicles. Deluchi has also confirmed the disadvantages of hydrogen

storage in hydride tanks. Regarding liquid hydrogen storage, he has provided necessary data for comparison between the vehicles with cryogenic tanks which have already been developed.

In the recent work for the US Department of Energy (DOE), Hynek et al [33] compared the present and future hydrogen storage technologies from the perspective of fuel cell powered vehicles. Fig. 1.5 shows the volumetric density vs gravimetric density for different kinds of storage. They concluded that carbon adsorption is the only developing technology likely to meet the goals of the DOE Hydrogen Plan for smaller fuel cell powered vehicles.

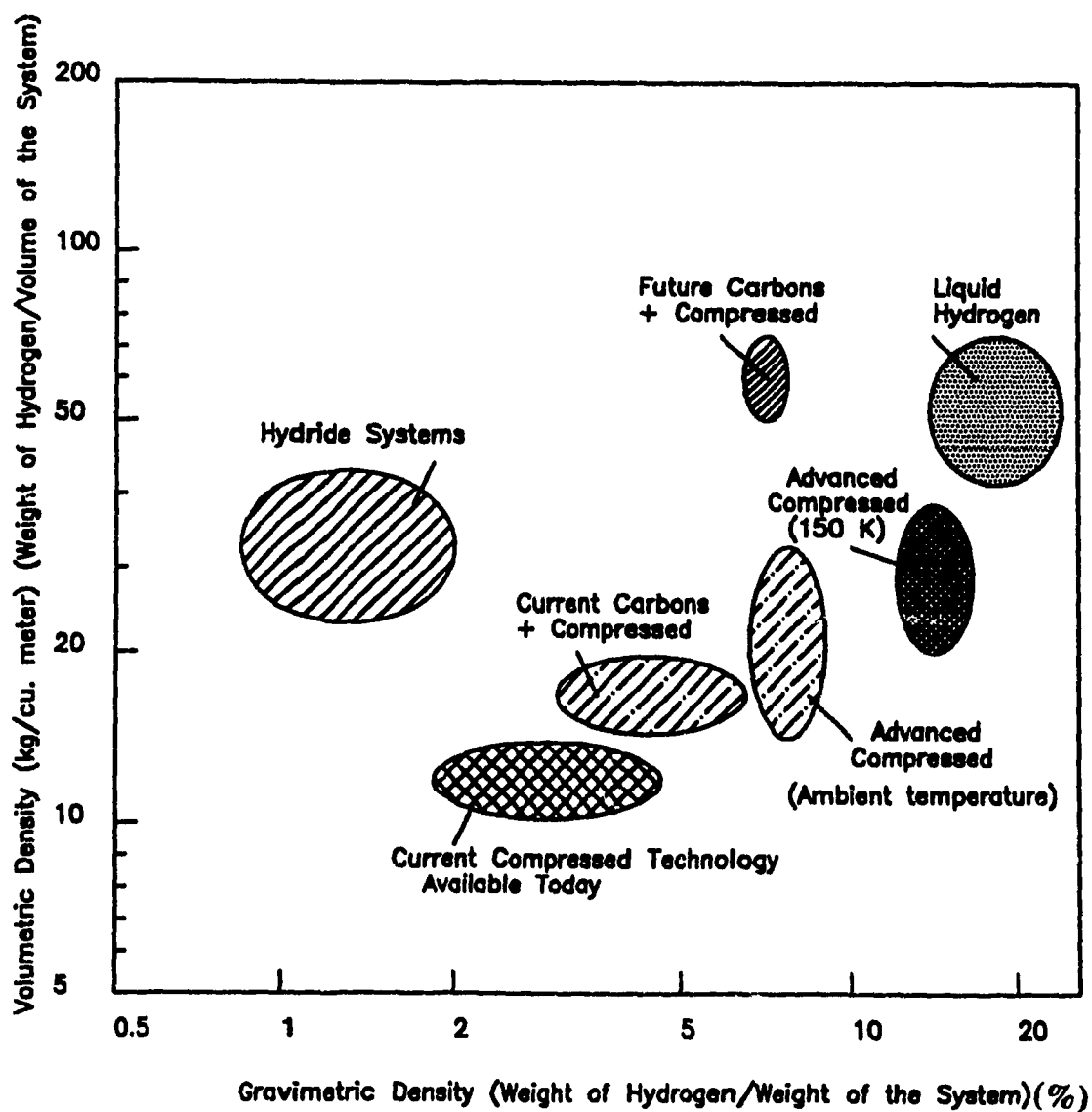


Fig. 1.5 Comparison of Current and Future Hydrogen Storage Systems [33]

## **CHAPTER 2**

### **CONCEPT DEFINITION, OBJECTIVES AND METHODOLOGY**

#### **2.1 Thermocontrolled Tank: Concept Presentation**

Based on the literature survey presented, it is quite clear that although gaseous fuel is an attractive alternative to gasoline, there is a major limitation due to problems associated with on-board storage. This study is aimed at a concept of on-board storage for gaseous fuels which allows for increased fuel tank capacity and high pressure without the use of any special pump or compressor, thus making possible direct gas injection into the cylinder of an engine, and increased operating range per fill. The study considers the concept of thermocontrolled tank which has the potential to satisfy the above requirements.

The gas pressure in the thermocontrolled tank would be initially created by introducing liquefied gaseous fuel into the vessel, which is at room temperature. Because of the heat transfer from the vessel wall and next from the ambient, the liquid fuel will evaporate and become high pressure gas. However, the much lower than ambient temperature of the gas would still be preserved by appropriate insulation to maintain the low density of gas in the tank. The gas pressure should then be maintained at a level higher than 100 bar during the operation of the vehicle, by heating the fuel in the tank using exhaust gases from the engine. The heating process would be controlled using the microprocessor technology. The

schematic of the proposed thermocontrolled tank system is presented in Fig. 2.1. It is not difficult to foresee that with rising energy prices, concern about environment and decreasing costs for electronic controls, such a system could become feasible for large vehicle fleets in the not-too-distant future.

The thermocontrolled tank has been selected for this investigation because of several advantages it provides when compared to other types of storage systems. Some of these advantages are listed as follows:

1. There is no need for advanced cryostorage systems and costly vacuum jacketed insulating systems, which means that it is less expensive and suitable for automotive use.
2. There is no need for cryogenic pumps to create the high pressure required for direct gas injection of the fuel into the combustion chamber. This means that the problems in manufacturing and maintenance of the cryogenic pumps can be avoided.
3. In the case of compressed gas storage system for the supply of the fuel for direct injection, only a maximum of 70% of the tank content can be used. In the case of thermocontrolled tank, by utilizing the engine exhaust gases to heat the fuel in the tank, the residual fuel content can be reduced to 15%, which means that 15% more of the fuel can be used and hence the range of the vehicle will be increased.
4. The amount of gas stored in a thermocontrolled tank will be 2.5 times

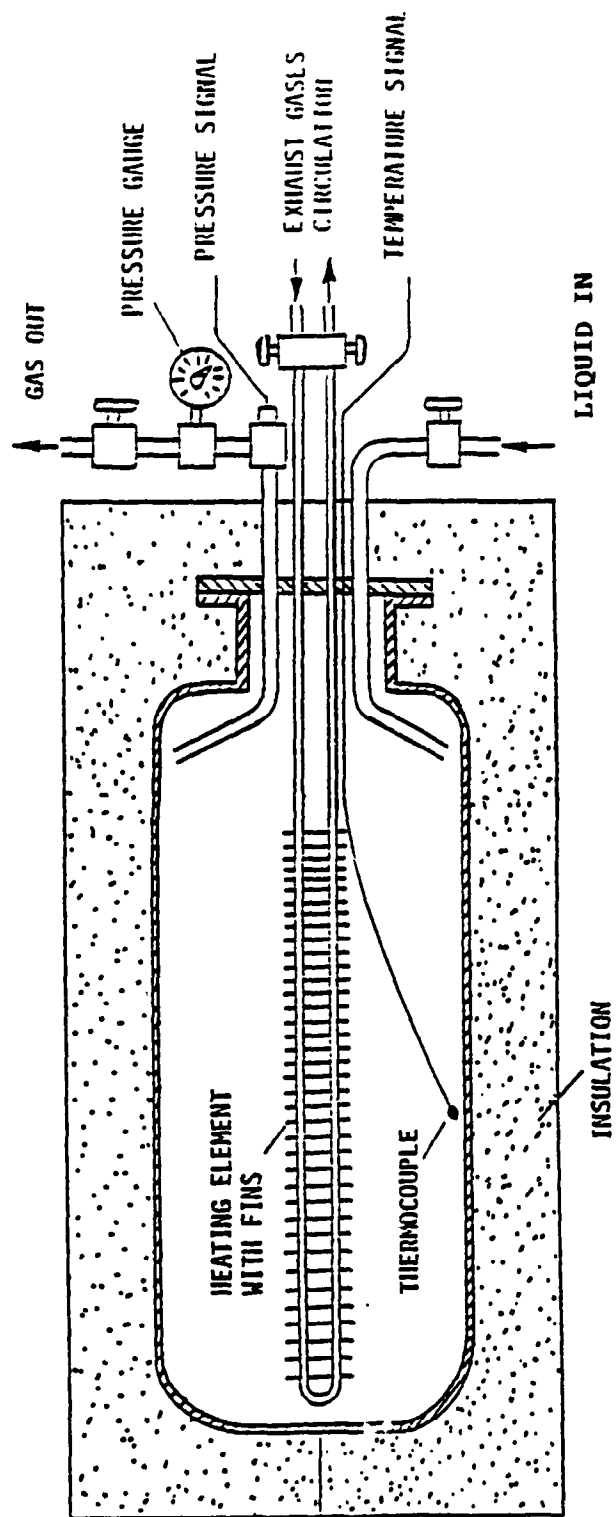


Fig. 2.1 Schematic of the thermocontrolled tank

higher than that stored in regular pressurized cylinders, hence the number of refuellings required for a given range will be significantly reduced.

5. The thermocontrolled tanks allow the gas to be injected directly into the cylinder. In the case of hydrogen, the heat content of the mixture is increased by 20% as compared with that of gasoline and by 41% as compared with the externally formed hydrogen mixture.

On the other hand, a thermocontrolled tank will require additional components such as a heat exchanger and a microprocessor based controller. Although the storage capacity of the thermocontrolled tank will be significantly less than that of an equivalent cryogenic tank, it appears to be a practical alternative for general vehicle applications.

## 2.2 Proposed Gas Supply System for the Thermocontrolled Tank

A system for direct injection of hydrogen into the cylinder of an internal combustion engine has been developed and tested at Concordia University [34]. The thermocontrolled tank, integrated with the direct injection system for hydrogen gas, is shown in Fig. 2.2. The hydrogen gas is stored in a high pressure thermocontrolled tank insulated and fitted with a heat exchanger through which hot exhaust gases could be circulated to heat hydrogen in the tank. This tank is also fitted with a pressure regulator. The gas from the tank flows at the required pressure to the preheater where it is heated before entering the gas accumulator. There, the gas properties are measured and a signal is sent to the computer to control the heat transfer rate from the exhaust gases to the hydrogen. The preheated gas is then injected through a solenoid operated injector (interfaced with a metering valve) to the engine cylinder.

The thermocontrolled tank concept can be explained using a T-v graph shown in Fig. 2.3. Point 1 on the graph shows the state of hydrogen in a cryogenic tank under atmospheric pressure and at 20 K. Point 2 shows the state of compressed hydrogen gas as it is stored in the pressurized cylinder under 300 bar pressure and at atmospheric temperature. It can be seen that in the same tank volume, 3.5 times more hydrogen fuel can be stored in the cryogenic tank than in pressurized cylinders. Point 3 shows the state of hydrogen in the proposed



thermocontrolled tank at 300 bar and at 200 K. The amount of gas stored will be 1.41 times higher than in regular pressurized cylinders, and 2.48 times lower than in a cryogenic tank. However, the gas will be already under a high pressure, as required for direct injection and there is no need to compress it using special pumps.

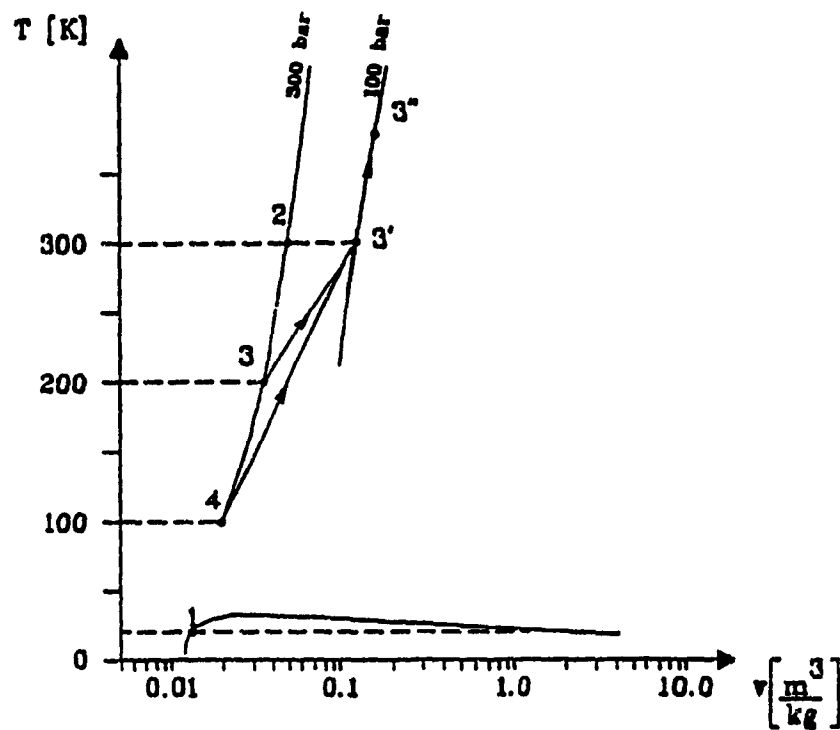


Fig. 2.3 Temperature-specific volume ( $T$ - $v$ ) graph for hydrogen with storage points marked

The capacity of the proposed thermocontrolled tank for hydrogen storage can be further improved at the properties shown at point 4. Then the hydrogen fuel would be stored at 300 bar pressure and 100 K temperature which would provide gas storage capacity 2.47 times higher than it is for pressurized cylinders at ambient temperature and only 1.42 times lower when compared with the cryogenic tank. With the above data an estimation of the specific weight and volume of a thermocontrolled tank for large vehicles (truck or bus) has been done and given below:

for 200 K:	specific weight	-	25 kg/kg of stored $\text{GH}_2$
	volume	-	0.088 $\text{m}^3$ /kg of stored $\text{GH}_2$
for 100 K:	specific weight	-	15 kg/kg of stored $\text{GH}_2$
	volume	-	0.05 $\text{m}^3$ /kg of stored $\text{GH}_2$

It can be seen, by comparison with the data given in [31], that the specific weight data for a thermocontrolled tank are the closest to those for the cryogenic tank. However, the specific volume is quite large, particularly for 200 K. It could be reduced by using more effective (but also more expensive) MLI (multilayer) insulation; this would not be justified for large vehicles, which usually have less restriction on space availability. The specific values could become more advantageous for the thermocontrolled tank when gas preheating would be considered to extract more gas from cylinder for high pressure injection. It must also be mentioned that the task to insulate the tank at 200 or 100 K temperature

is easier than at 20 K required for liquid hydrogen in a cryogenic tank. This is due not only to the higher absolute temperature of hydrogen in the tank and consequently, to the lower heat transfer from the surroundings, but also to the fact that liquid nitrogen at 77 K is widely available and remains inexpensive as a byproduct of liquid oxygen which is produced in huge quantities by the industry. Liquid nitrogen can be helpful in maintaining the low temperature for the proposed hydrogen-gas storage, if required.

The operation of the thermocontrolled tank system can be better explained when describing the possible scenario of hydrogen refuelling, storing and supplying to an engine. It was first assumed that the minimum pressure required for direct injection of hydrogen into the engine is 100 bar. It was also assumed that the refuelling station can provide the tank with both liquefied and compressed hydrogen, the first at 20 K, the second at ambient temperature.

At *refuelling*, when the  $\text{LH}_2$  will be first introduced in the tank, the heat transfer from the tank's walls to the cold hydrogen will cause evaporation of a portion of the  $\text{LH}_2$ . This phenomenon is observed during refuelling of cryogenic tanks where 10-25% of  $\text{LH}_2$  is usually evaporated [32]. In case of the thermocontrolled tank, the portion of vaporized hydrogen will be greater than in the cryogenic tank due to the higher internal energy stored in the tank walls. This change in the hydrogen phase is anticipated as a factor providing the required temperature and pressure increase inside the tank. After the scheduled portion of

$\text{LH}_2$  is introduced in the tank, some  $\text{GH}_2$  could be added, if required to increase the gas pressure over 100 bar so that the vehicle could operate immediately. It is to be noted that in the case of large mass to volume ratio containers (old type cylinders) and when the tank is warm, even the total hydrogen charge inserted as  $\text{LH}_2$  might not bring the final tank temperature to the required low level. Then, a longer filling process of the tank with  $\text{LH}_2$  would be required with the evaporated hydrogen being evacuated to a special container at the refuelling station. A similar situation would occur when the vehicle comes for refuelling with the tank filled with some residual gas under pressure. To allow the refuelling, the gas from the tank should be first released into a container at the refuelling station until the pressure in the tank drops, allowing for subsequent charging with  $\text{LH}_2$ .

During *vehicle operation* if the fuel consumption is low or during parking, the pressure in the tank might increase slowly due to the heat transfer through the insulation; however, there will be no fuel loss as in the case of the regular cryogenic tank, as long as the pressure does not exceed 300 bar approximately. If the fuel consumption is high, causing a pressure drop in the tank not compensated by the heat transfer through the insulation, it would be necessary to heat the tank using exhaust gases in order to maintain the pressure. This will finally lead to a situation where the hydrogen preheating in the tank becomes necessary in order to extract the maximum amount of gas from the tank at the required 100 bar pressure and at higher than ambient temperature, as shown at 3" in Fig. 2.3.

In a *stationary vehicle*, when the gas remains in the thermocontrolled tank at 100 K and 300 bar, the heat transfer to the tank can be assumed at the same rate as in a cryogenic tank (calculated from 2% boiling-off daily). Then it would require 15 days to raise the pressure in the tank by 10% i.e., from 300 to 330 bar; for the tank at 200 K this process would require over 30 days. To keep the pressure in the tank constant for a longer time, only 0.8% of the tank gas content should be released daily, i.e., 2.5 times less than in the case of liquid hydrogen in a cryogenic tank. The following factors affect the heat transfer rate differently in the case of the thermocontrolled tank in comparison to that of a cryogenic tank;

1. The gas temperature in the thermocontrolled tank is 100 K or 200 K, not 20 K, so the heat transfer to the tank would be smaller than in a cryogenic tank.
2. The thermocontrolled tank has more connections for instrumentation and for hot gases circulation which would increase the heat transfer to the tank.
3. The thermocontrolled tank does not include a  $\text{LH}_2$  pump which will not contribute to the increased heat transfer as in the case of a cryogenic tank.

The proposed concept aims particularly at hydrogen injection systems requiring high injection pressure, because more gas can be extracted from the tank by preheating when the gas pressure in the tank drops below the injection pressure level. It was calculated that in the pressurized cylinders used for  $\text{GH}_2$  without preheating, the amount of hydrogen delivered to the engine from one refuelling

would be 3.5 times less (for the pressure drop from 300 to 100 bar), as compared with thermocontrolled tank having the same volume, 100 K initial storing temperature, and the maximum preheating temperature of 400 K.

It is clear from the above description that the proposed system requires an electronic control to operate efficiently. There is some similarity in the operation of the proposed thermocontrolled tank and in the heating of the  $\text{Mg}_2\text{Ni}$  hydride tanks by exhaust gases, as proposed by Daimler Benz [29].

### **2.3 Objectives of the Investigation**

The purpose of the proposed research is to investigate the feasibility of a well functioning and effective gaseous fuel storage system which would enable the internal combustion engine, equipped with direct gas injection system to operate with high efficiency, specific power and would give the vehicle an acceptable operating range. The different stages in this investigation are:

1. Mathematical model formulation, simulation and validation.
2. Design, manufacturing and testing of the prototypes to get the experimental data required for validation of the mathematical model.
3. Optimization of the storage vessel design for natural gas and hydrogen.
4. Simulation of the thermodynamic properties for gaseous fuels inside the thermocontrolled tank during the vehicle running, considered for a car and for a bus.
5. Optimization of the on-board storage conditions of the thermocontrolled tank for both the vehicles.
6. Investigation of the on-board storage conditions and simulation of the performance of the thermocontrolled tank filled with a blend of natural gas-hydrogen. Such a blend has the potential to significantly reduce the pollutants in the engine exhaust gases, and would still be not more expensive than the liquid hydrocarbon fuels (regarding energy content).

## **2.4 Thesis Outline and Methodology**

Two types of thermocontrolled tanks have been used in the investigation. The first vessel, a 316 stainless steel tank is equipped with a heat exchanger and covered with insulation. The second vessel is a composite high pressure vessel not equipped with heat exchanger and not covered with any insulation. These pressure vessels were tested with liquid nitrogen to get the required experimental data to validate the mathematical models. Liquid nitrogen was used for all the tests since it is readily available at Concordia University and is relatively safe and easy to handle, without affecting the university atmosphere. The thermocontrolled tank was assumed as a lumped parameter heat capacity system in the development of the mathematical model. This model, validated with the experimental data, was used for the optimization of the storage conditions of different gaseous fuels.

Chapter 3 presents the mathematical model for a thermocontrolled tank. The model has been used for simulation and the results are also presented in this chapter.

Chapter 4 contains a description of the thermocontrolled tank prototypes, the experimental setup and the test procedure. The results from the testing of steel vessel and composite vessel are presented in this chapter. The test results are also compared with the simulation results and conclusions have been drawn.

The design of a thermocontrolled vessel has been optimized in chapter 5.

Different aspects of gas storage are investigated and the results of multivariable optimization are presented.

In chapter 6, the adaptation of thermocontrolled tank to a car and a bus has been discussed. Also the practical aspects of using thermocontrolled tank are presented.

Chapter 7 outlines the simulation results of the thermodynamic properties of gaseous fuels in a thermocontrolled tank installed in a car and a bus. The mathematical model developed for this case is also discussed here

Optimization results of the on-board storage conditions of natural gas and hydrogen in a thermocontrolled tank for a car and a bus have been presented in chapter 8.

In chapter 9, the thermodynamic properties of natural gas/hydrogen mixture stored in a thermocontrolled tank installed in a car and a bus have been simulated.

Finally, in chapter 10, conclusions have been drawn from the present study and recommendations have been made for the effective storage of gaseous fuels in vehicles with direct gas injection.

# CHAPTER 3

## MATHEMATICAL MODEL AND SIMULATION

### OF THERMOCONTROLLED TANK

#### 3.1 Mathematical Model for the Tank without a Heat Exchanger

When the thermocontrolled tank is filled up with the liquid fuel and closed, the liquid absorbs heat from the vessel wall first, before the heat transfer from the ambient starts. Heat will be transferred from the inside surface of the tank wall to the liquid by free convection, causing the liquid to boil-off. When the atmospheric heat transfer starts to take place, the heat from the ambient will be transferred to the outside surface of the tank wall by free convection. Some of this heat will be absorbed by the tank wall, increasing its temperature,  $T_t$ . The rest will be conducted through the tank walls and finally will flow to the gaseous fuel by free convection. The resistances to the transfer of heat are the resistance between the gaseous fuel and the wall,  $R_{gt}$  and the resistance between the tank and the ambient,  $R_{ta}$ . The gas was assumed well stirred and at uniform temperature,  $T_g$ . Assuming a lumped heat capacity system [36], the differential equations governing the thermocontrolled tank can be written as:

$$m_g c_g \frac{dT_g}{d\tau} = \left( \frac{T_t - T_g}{R_{gt}} \right) \quad (3.1)$$

$$m_t c_t \frac{dT_t}{d\tau} = \left( \frac{T_g - T_t}{R_{gt}} \right) + \left( \frac{T_a - T_t}{R_{ta}} \right) \quad (3.2)$$

where  $T_a$  is the ambient temperature,  $m_g$  and  $m_t$  are the mass of the gaseous fuel and the mass of the tank, respectively,  $c_g$  and  $c_t$  are the specific heats of the gaseous fuel and the tank, respectively, and  $\tau$  is the time after completing the filling process.

### 3.2 PVT Relation for Real Gases

Ideal gas behaviour is not followed when a gas is subjected to pressures in excess of its critical pressure and maintained at cryogenic temperatures. Such gases are referred to as *real gases*. Since the alternative fuels will be stored in the thermocontrolled tank at such a combination of a low temperature and a high pressure, the ideal gas equation cannot be used to correlate P, V and T. However, it would be convenient to have analytical expressions for the relationships among these three properties. The accuracy of these PVT relations varies with the type of gas and the range of the properties under consideration. From the literature survey on PVT relationships for real gases [37-41], the following two correlations have been found appropriate for the simulation to follow.

1. Redlich-Kwong Equation [37]
2. The new equation of state as proposed by Wilsak and Thodos [41].

The applicability and accuracy of these two relations to natural gas and hydrogen within the operating limits of P, V and T for the thermocontrolled tank have been tested. It was found that in the case of natural gas, Redlich-Kwong equation deviates more from the actual values, particularly in the 125-200 K temperature range, which would be the normal operating range for a thermocontrolled tank. On the other hand, the new equation of state proposed by Wilsak and Thodos [41] closely follows the actual values for methane in that range

of temperature. In the case of hydrogen, the new equation of state deviates more from the actual values in the high pressure region than does the Redlich-Kwong equation [37]. Hence, the new equation of state proposed by Wilsak and Thodos was selected for the simulation for natural gas and Redlich-Kwong equation for hydrogen.

### **3.3 Mathematical Model for the Tank with a Heat Exchanger**

In this case, the thermocontrolled tank was assumed to be fitted with a heat exchanger to circulate hot exhaust gases from the engine. Heat will be transferred from the exhaust gas stream to the inside wall surface of the heat exchanger pipe by forced convection, followed by radial flow through the pipe wall through conduction (refer Fig. 3.1). During transients, some heat will be absorbed by the heat exchanger material, increasing its temperature. Heat then will be transferred by free convection from the exchanger outside pipe wall to the surrounding gaseous fuel. The gas was assumed to be at a uniform temperature. Some heat will be absorbed by the gaseous fuel, increasing its temperature. Heat also will be transferred from the gaseous fuel to the inside surface of the tank wall by free convection. Some of this heat will be absorbed by the tank wall, increasing its temperature. The rest will be conducted through the tank metal wall and the surrounding insulation and finally rejected to the atmosphere by free convection.

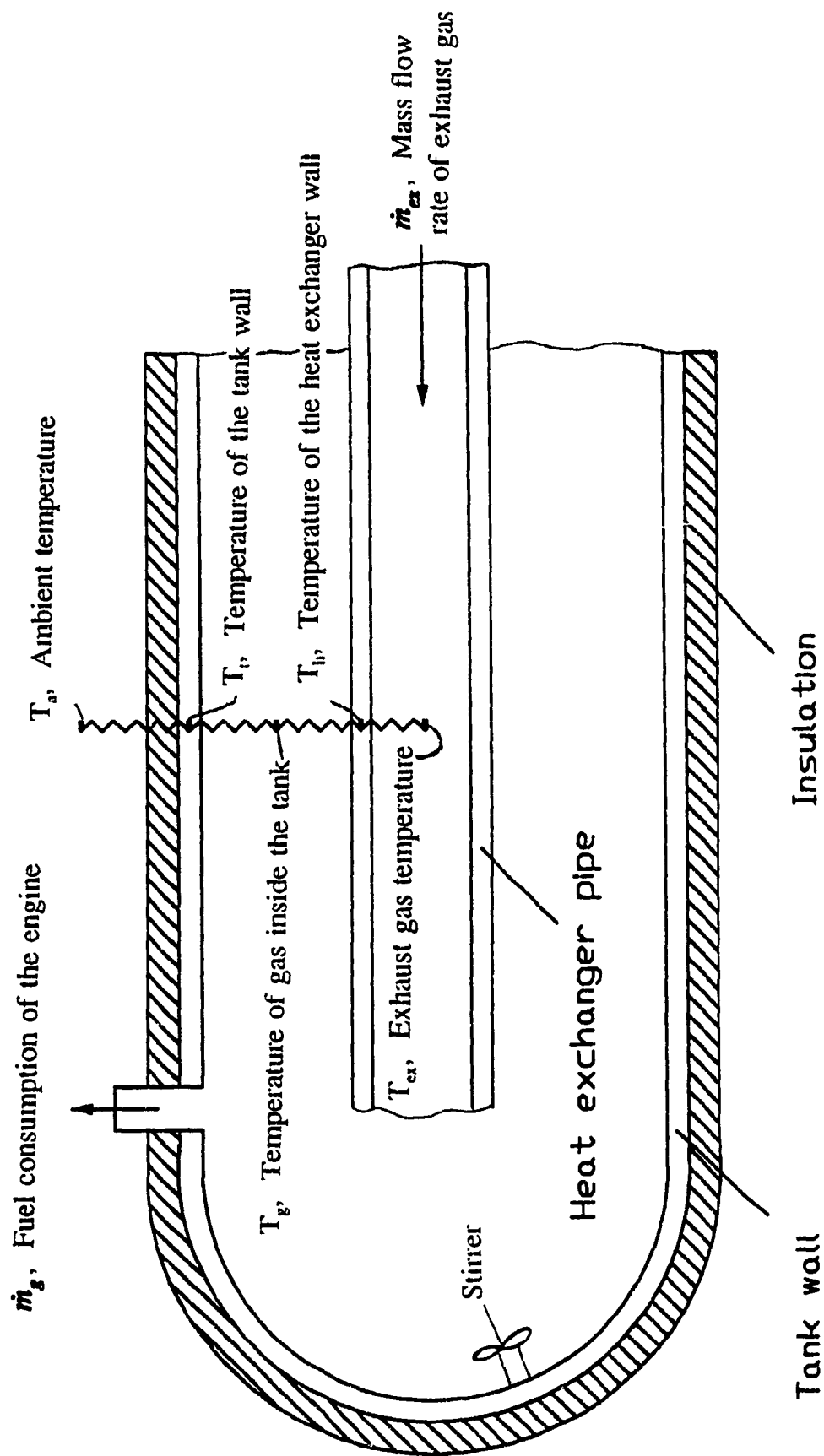


Fig. 3.1 Schematic of the heat transfer process in a thermocontrolled tank

The energy balance on the exhaust gas gives:

$$m_{ex} c_{ex} \frac{dT_{ex}}{d\tau} = \dot{m}_{ex} c_{ex} (T_{exi} - T_{ex}) - \left( \frac{T_{ex} - T_h}{R_{exh}} \right) \quad (3.3)$$

It was assumed that there is negligible pressure drop in the heat exchanger pipe, as compared to the throttling in the valves. Therefore, assuming constant mass flow throughout the pipe, the mass of exhaust gases in the cylindrical volume can be given by

$$m_{ex} = \frac{P_a V_{ex}}{RT_{ex}} \quad (3.4)$$

Neglecting the axial conduction in the heat exchanger pipe, since the pipe is thin and the dominant temperature gradient will be in the radial direction, the energy accumulated in the heat exchanger pipe can be given by:

$$m_h c_h \frac{dT_h}{d\tau} = \left( \frac{T_{ex} - T_h}{R_{exh}} \right) + \left( \frac{T_g - T_h}{R_{hg}} \right) \quad (3.5)$$

The energy balance on the gaseous fuel must consider the heat transferred to it from the heat exchanger pipe wall and the heat transferred from the gaseous

fuel to the tank walls.

$$m_g c_g \frac{dT_g}{d\tau} = \left( \frac{T_h - T_g}{R_{hg}} \right) + \left( \frac{T_t - T_g}{R_{gt}} \right) \quad (3.6)$$

Assuming that the tank wall temperature is uniform, the energy accumulated in the tank wall can be given by:

$$m_t c_t \frac{dT_t}{d\tau} = \left( \frac{T_g - T_t}{R_{gt}} \right) + \left( \frac{T_a - T_t}{R_{ta}} \right) \quad (3.7)$$

Solving the equations (3.3), (3.5), (3.6) and (3.7) will give the variation in the temperature of the gaseous fuel with respect to time.

### 3.4 Simulation Results

Separate simulations were carried out for nitrogen, natural gas and hydrogen. In each case, the effect of insulation is examined on the gas temperature. The mathematical model which was developed in the earlier section was simulated on a digital computer using fourth order Runge-Kutta method. The results are presented in the following subsection.

### 3.4.1 Simulation with Nitrogen

The composite vessel considered has a net internal volume of  $0.009 \text{ m}^3$  and weighs 15 kg. It is a cylinder of 0.63 m long and 0.2 m outside diameter with a wall thickness of 0.0254 m. For the composite vessel filled with 4.9 kg liquid nitrogen, the temperature variation inside the tank versus time is shown in Fig. 3.2. If the composite vessel is completely isolated from the atmosphere, the internal energy stored in the walls of the tank will bring the liquid gaseous fuel to a certain temperature. This temperature is called *Initial Operational Temperature*. The heavier the tank, as compared with the mass of inserted gas, the higher will be the initial operational temperature of the thermocontrolled tank. However, this temperature will result also in the initial operational pressure of the gas in the tank and will dictate the amount of liquefied fuel that can be inserted. The simulation has been repeated to calculate the initial operational temperature in the case of nitrogen and the results are also presented in Fig. 3.2 along with the data for perfect insulation. The results obtained for the perfectly insulated tank indicate that the initial operational temperature for nitrogen gas at 850 bar would be 240 K and the time required to reach this temperature would be about 4 hrs.

In the next case, the composite pressure vessel was assumed to be covered with 76.2 mm thick foam glass insulation, whose properties are given in chapter 4. The results were also presented in Fig. 3.2 as partial insulation. The difference

between the results of an uninsulated vessel and insulated vessel is that, the time required to reach the steady state temperature in the case of an insulated vessel is longer because of the presence of the insulation resistance.

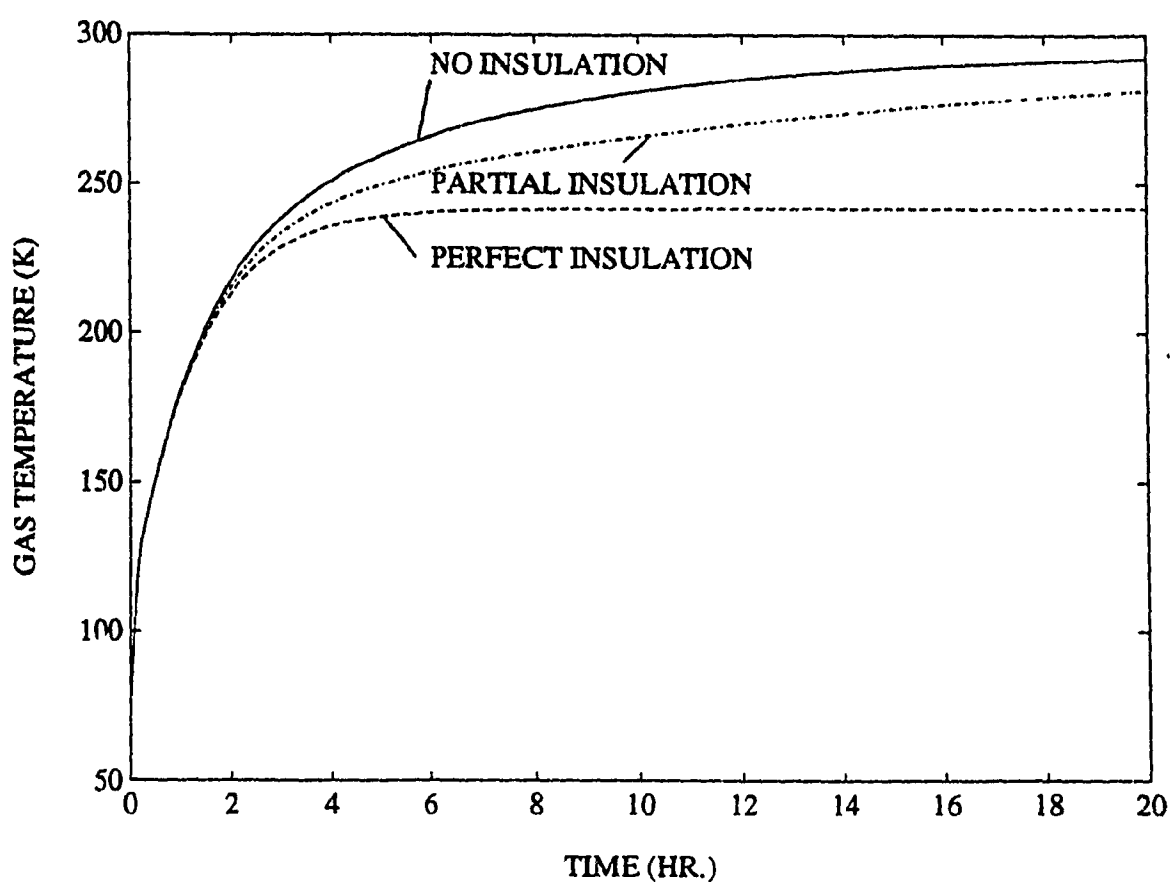


Fig. 3.2 Simulation results of temperature-time history for nitrogen

### 3.4.2 Simulation with Natural Gas

The simulation procedure developed for nitrogen, has been repeated for liquid natural gas. The results obtained are shown in Fig. 3.3. In this case, the tank was assumed to be filled-up with 3 kg of natural gas, to obtain the maximum pressure of 850 bar. Also, fully insulated and partly insulated tank cases were simulated for the same amount of gas as shown in Fig. 3.3.

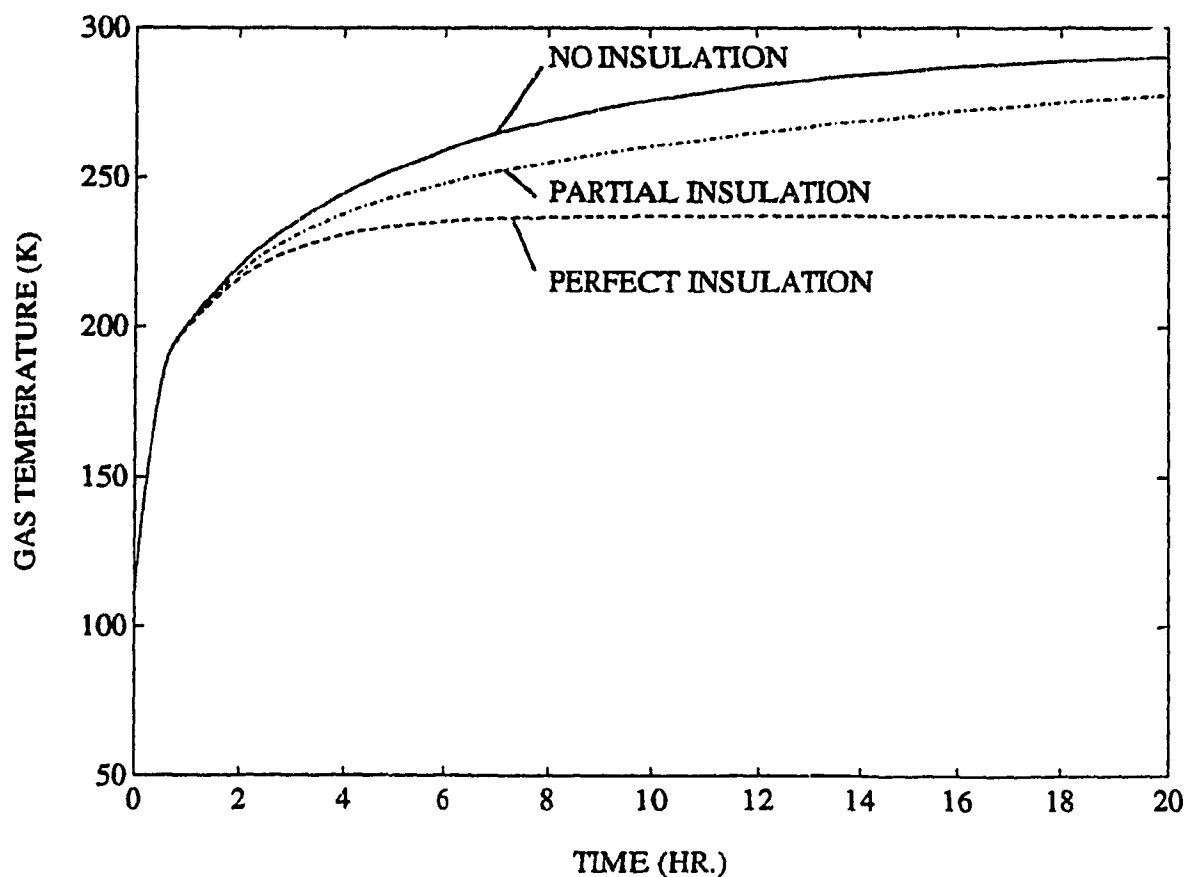


Fig. 3.3 Simulation results of temperature-time history for natural gas

The results obtained for an ideally insulated tank indicate that the initial operational temperature for natural gas at 850 bar would be 230 K and the time for reaching this temperature is about 6 hr. For an uninsulated tank, the gas temperature does not stabilize before 20 hr, as it approaches the ambient temperature. The simulation results are showing the potential of using an uninsulated tank in vehicles which would become operational in a relatively short time after tank refuelling.

### **3.4.3 Simulation with Hydrogen**

In this case, the tank was assumed to be filled-up with 0.4 kg of hydrogen, to obtain the maximum pressure of 850 bar. Also, fully insulated and partly insulated tanks were simulated for the same mass of hydrogen. The simulation results for hydrogen are shown in Fig. 3.4. The results indicate that the amount of liquid hydrogen required to create 850 bar pressure is only 13% of the amount of liquid natural gas for the same volume container. The results obtained also indicate that the initial operational temperature of hydrogen is 220 K at 850 bar and the time for reaching this temperature is about 6 hr.

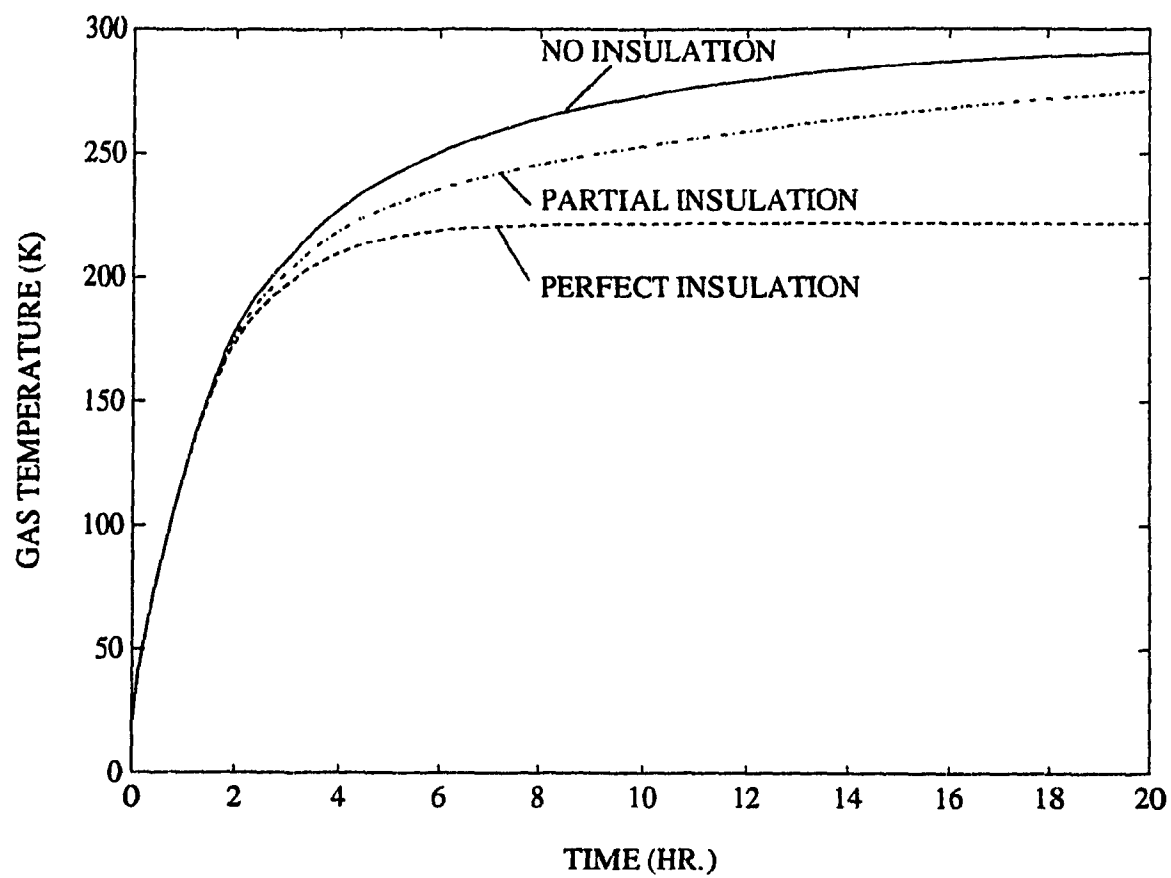


Fig. 3.4 Simulation results of temperature-time history for hydrogen

## CHAPTER 4

### EXPERIMENTAL EVALUATION AND VALIDATION OF THE MATHEMATICAL MODEL

Two types of tanks, capable of creating the high gas pressure required for direct injection into the cylinder of a diesel engine have been manufactured [42]. Both types of tanks will be filled with liquefied gas which will evaporate and increase the pressure because of the heat transfer into the tank and due to the consequent temperature increase. The maximum pressure increase will be determined by the ambient temperature level, volume of the container, insulating material and by the mass of the gas in the tank. During the operation of the vehicle, gas pressure will be maintained at the required level for direct injection by preheating the gas content in the tank, using heat transfer from the engine exhaust gases circulating in the heat exchanger located inside the tank or by controlling the heat transfer through the tank walls by means of insulation resistance. Experiments were carried out in the laboratory for both tanks using liquid nitrogen, for the reasons explained earlier. The following sections present the details of the tank design, experimental procedure and results.

#### 4.1 Thermocontrolled Tank Prototypes

- The first type, called *steel tank*, was designed for a maximum pressure of

250 bar. It can be insulated and will use the heat exchanger for circulating exhaust gases.

- The second type, called *high pressure composite tank*, was designed for a maximum gas pressure of 1000 bar.

The details of these two types of tanks are as follows:

#### **4.1.1 Steel Tank with Insulation and Preheating**

To make a prototype of a thermocontrolled steel tank, the following design was selected and is described below. The tank was based on a standard steel cylinder of size 0.1524 m diameter and 1.3 m length and made of 316 stainless steel material. To incorporate the heat exchanger, as well as a thermocouple and a pressure transducer, the upper part of the cylinder has been cut-off and a flange has been welded. The design of the steel pressure vessel is shown in Fig. 4.1a. A cover has been installed using bolts which will allow removal of the cover, as required, for inspection and exchange of the components inside the tank. The heat exchanger for exhaust gas circulation with several fins was also added along with the cover to increase the heat transfer rate to the gas (Fig. 4.1b).

The tank insulation, made of Cellular Glass was purchased from Pittsburgh Corning Corporation. This material has a density of 136.2 kg/cubic meter, compressive strength of 690 kPa and thermal conductivity of 0.027 W/m-K. It is

hard and fire resistant, therefore, it can be accepted as an insulating material for automotive tank. The design of the insulation jacket is shown in Fig. 4.2. It is shaped in such a manner that the heavy tank can be laid on one half of the insulation and covered by the second half. A cylindrical plug is used to fill up the space over the cover and to insulate the piping and instrumentation connections. The thermocontrolled steel tank prototype is quite heavy. However, it is easier to modify and to dismantle than a composite tank and, therefore it was used for the testing of the heat transfer rate from engine exhaust gases to the gas stored in the tank.

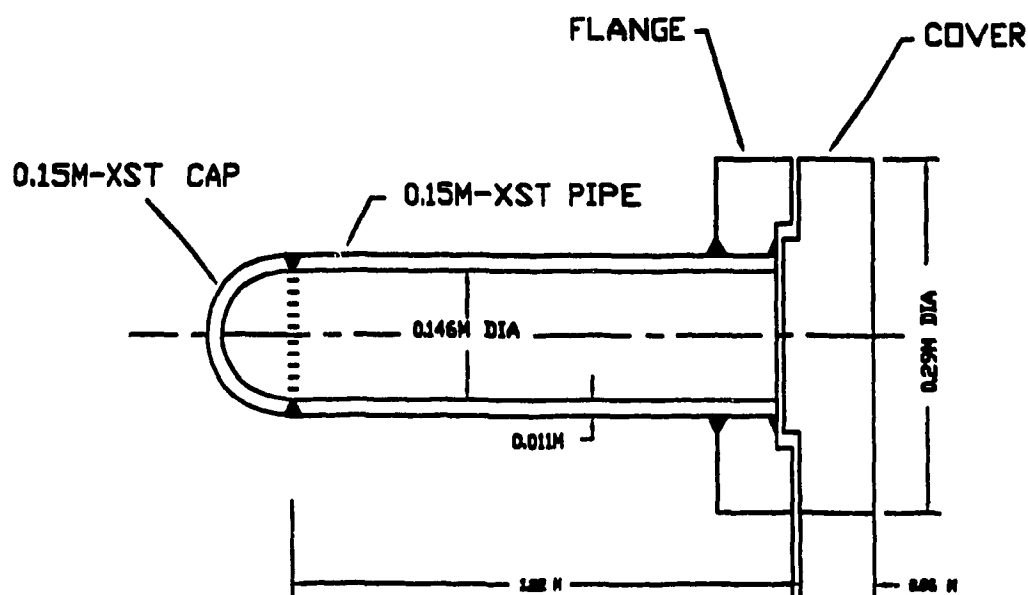


Fig. 4.1a Design of steel thermocontrolled tank

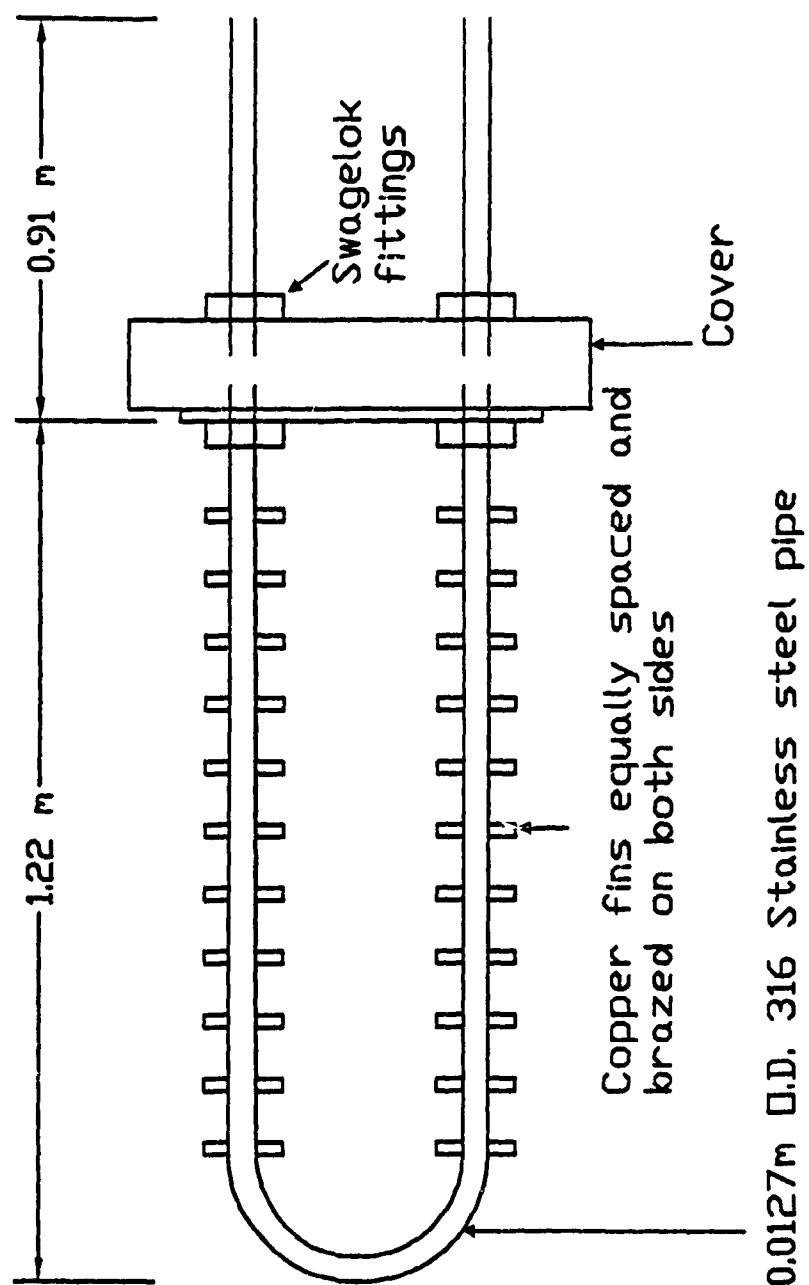


Fig. 4.1b Design of the heat exchanger

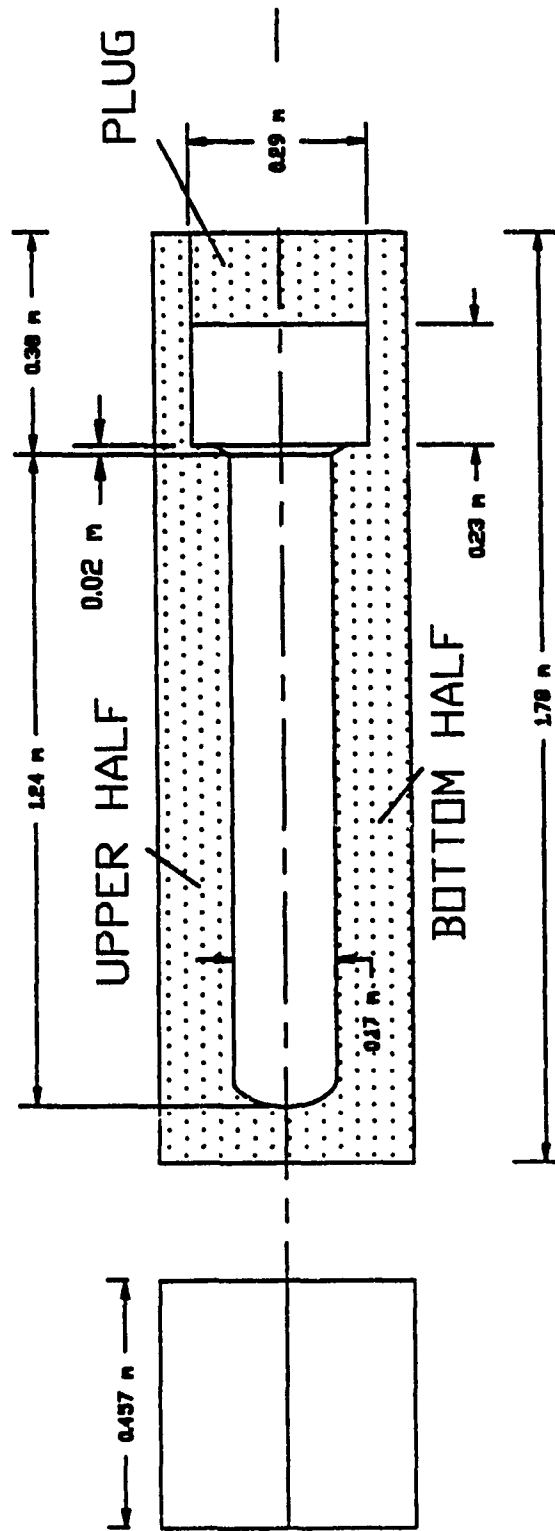


Fig. 4.2 Design of insulation jacket for the steel tank

#### 4.1.2 The High Pressure Composite Tank

This smaller composite tank has been built for a much higher gas pressure. It was decided to use a commercially available composite tank made for 310 bar pressure. The commercial tank was then reinforced with high strength kevlar filament winding. A tank was purchased from Structural Composite Inc., California. That vessel is a glass-fiber reinforced aluminium-lined fireman's air supply tank. The choice of commercially available vessels, which could be reinforced further using the filament winder available at Concordia University Composite Materials Laboratory was limited. The material used for overwinding was type 969 (aerospace grade) 4560 denier kevlar roving consisting of 4 x 768 filament yarns of 12  $\mu\text{m}$  diameter fiber with 3620 MPa minimum tensile strength. The resin system used was Ciba Geigy Araldite LY 556 with HY 917 hardener and DY 70 accelerator. The core vessel (SCI-ALT-295) size is 0.183 m diameter x 0.56 m long with 0.009  $\text{m}^3$  internal volume weighing 8.3 kg [42].

## **4.2 Testing of Prototypes and Discussion of Results**

The following subsections present the test procedure for each vessel and the corresponding experimental results.

### **4.2.1 Testing of the Steel Vessel**

The schematic of the test setup for the steel vessel is shown in Fig. 4.3. The vessel was mounted horizontally on a weight bridge with a wooden support to measure the amount of the fuel filled into the tank. The vessel was connected to a compressed nitrogen bottle through a cryogenic tank, which contains the liquid nitrogen. Liquid nitrogen was used for all the tests, because of its ready availability at Concordia University and safe handling in the university atmosphere. The heat exchanger was connected to a heavy duty air heater, which was used to heat the cryogenic gas in the second part of the experiments. A piezo electric type pressure transducer, made by Omega Instruments, model no. PX 305-10 KG1 and a thermocouple, also made by Omega Instruments, model no. CPSS-18G-12 were installed in the cover of the tank to measure the pressure and temperature of the cryogenic gas inside the tank. An IBM XT microcomputer equipped with IBM data acquisition peripherals was used for reading the measured variables. A distribution panel was used for making input/output signal connections. Additional

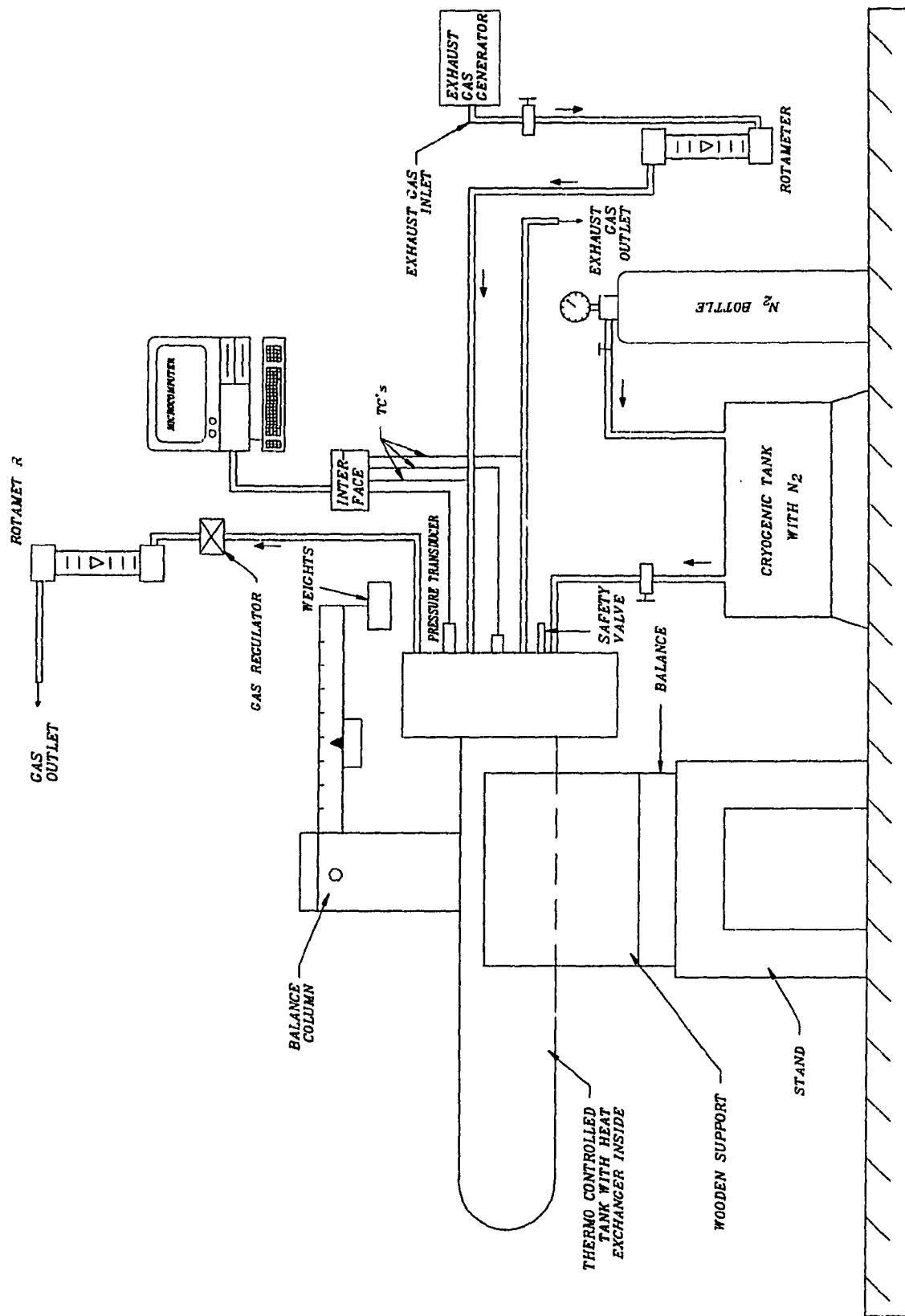


Fig 4.3 Schematic of the test set-up for steel tank evaluation

electrical circuits were built for conditioning and amplification of the input signals.

A pictorial view of the test set-up for the steel tank is shown in Fig. 4.4.

When nitrogen gas from the high pressure bottle was released, it forced the liquefied nitrogen into the steel tank. The liquefied nitrogen, after reaching the steel tank was boiled-off and changed into vapour very fast. It became evident that the filling-up process was too slow; the gas pressure inside the steel tank increased so fast that it did not allow the required amount of liquefied nitrogen to reach the tank before the reverse process of evacuating the gas back to the cryogenic tank started, as a result of higher pressure in the steel tank. There was no possibility of further pressurizing the cryogenic tank, which was designed for a maximum pressure of 1.5 bar. To overcome this problem, the liquefied gas filling pipeline and the vapour evacuating pipe were modified for a larger flow area, which allowed for the fill-up of the tank with enough gas, before the closing of the valve and the start of the pressurization of the vessel.

The first test was carried out for the uninsulated steel vessel by filling it up with 3.7 kg of liquid nitrogen ( $\text{LN}_2$ ). The time taken to fill up the tank was approximately 1 min. The gas pressure and temperature records (Fig. 4.5a) showed peaks of unknown origin immediately after the closing of the valves. To investigate the reason for the peaks in temperature and pressure, the test was repeated with different amounts of liquid nitrogen. But in all the tests, the same phenomenon was observed. The test results for 4.2 kg  $\text{LN}_2$  are also shown in Fig.



Fig. 4.4 Pictorial view of the test set-up of steel tank for evaporation test

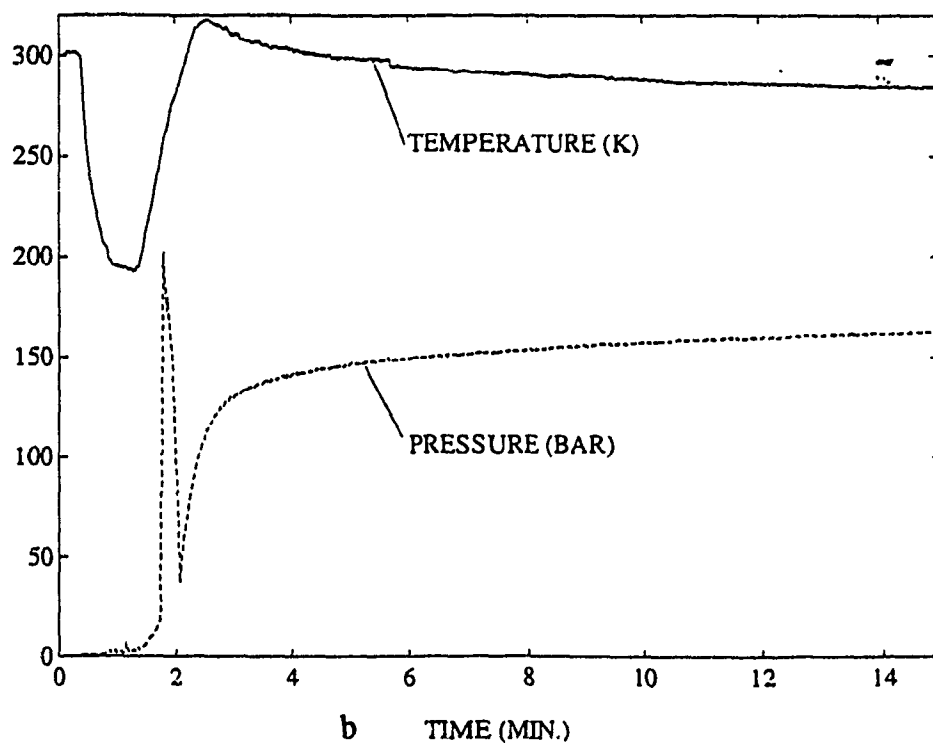
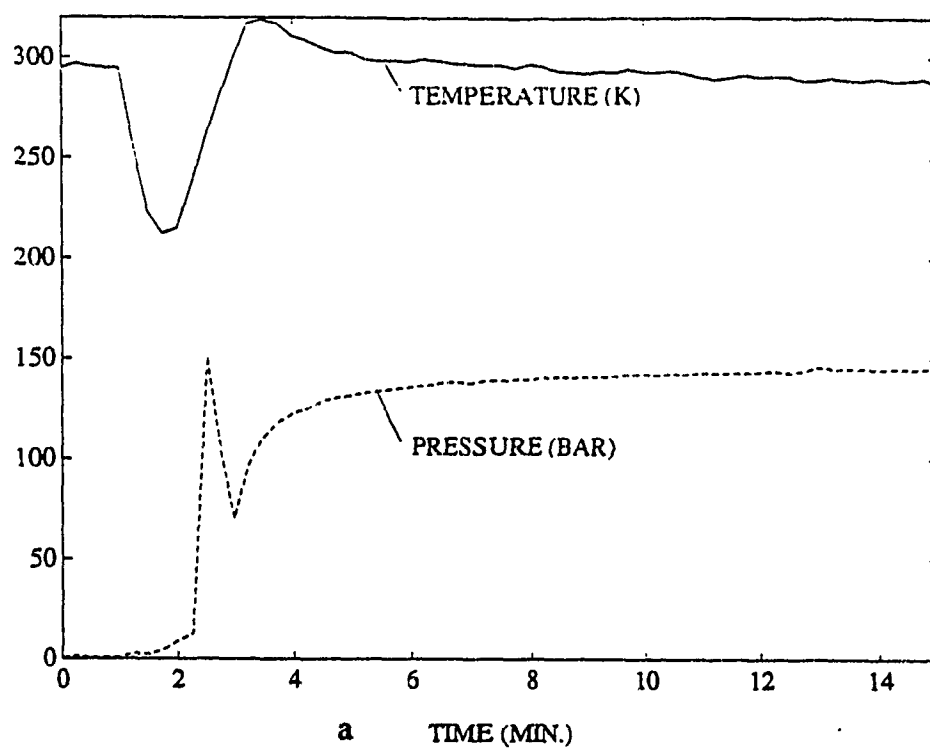


Fig. 4.5 Temperature and pressure records from the test on the uninsulated steel vessel

## 4.5b.

In the second stage of tests, the steel pressure vessel was covered with the insulation, and tested for 4.5 kg and 3.6 kg of liquid nitrogen. The test results are presented in Fig. 4.6a and 4.6b, respectively, for the two cases. It was observed that the rate of pressure build-up in the initial period was the same when compared with an uninsulated tank for the same mass of  $\text{LN}_2$ . This is because the  $\text{LN}_2$  first absorbs the heat from the vessel walls, before the heat transfer from the ambient starts to take place. Peaks of unknown origin were also noted in the temperature and pressure records.

It was decided to change the pressure transducer and the thermocouple to investigate the reason for the peaks in the pressure and temperature records. A diaphragm type pressure transducer, made by Valdyne, model no. DP22 was installed in place of the Omega piezoelectric pressure transducer. Similarly resistance temperature detector (RTD), made by Intempco Controls Ltd., model no. RH22-D3-2505-O-T-O-8 was installed in place of the Omega thermocouple. The test was repeated again with a mass of 3.7 kg of liquid nitrogen. The test results are presented in Fig. 4.7a. This time there was no peak observed in the pressure record. The reason for this observation is as follows. Since there was not enough space for directly installing the Validyne pressure transducer on the cover of the steel tank, an L - shaped steel pipe was used to connect the pressure transducer to the tank. In doing so, a distance of about 0.3 m resulted between the pressure

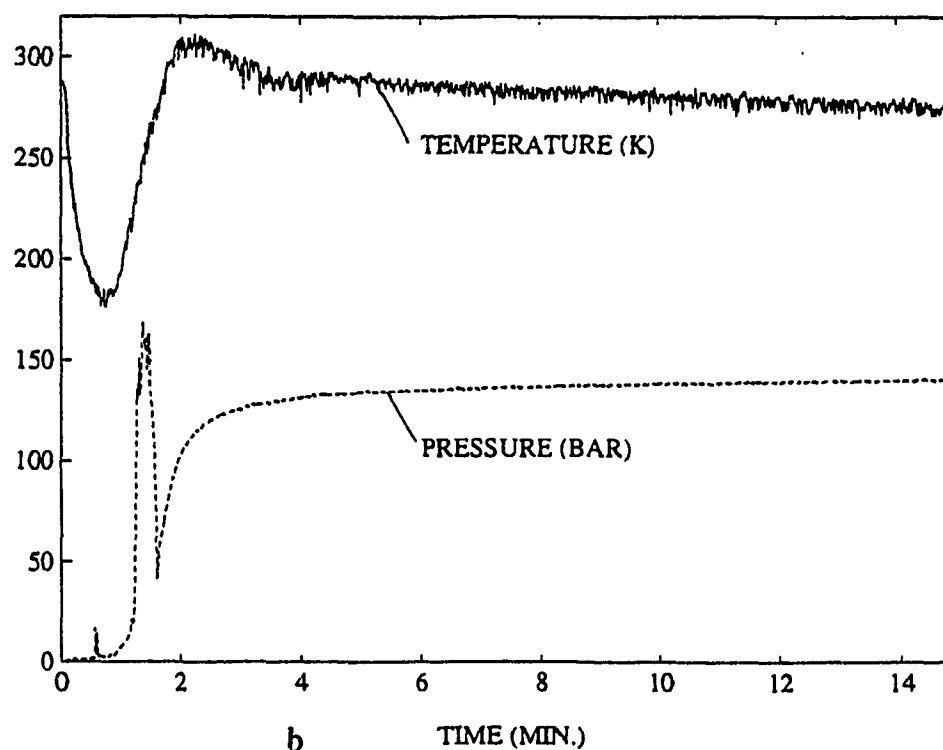
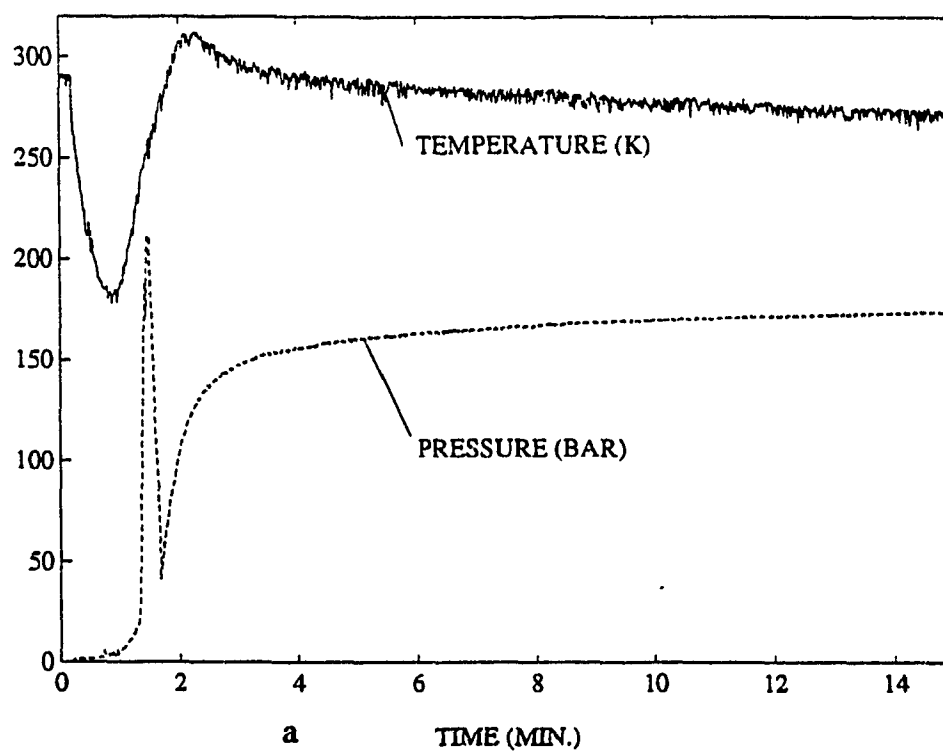
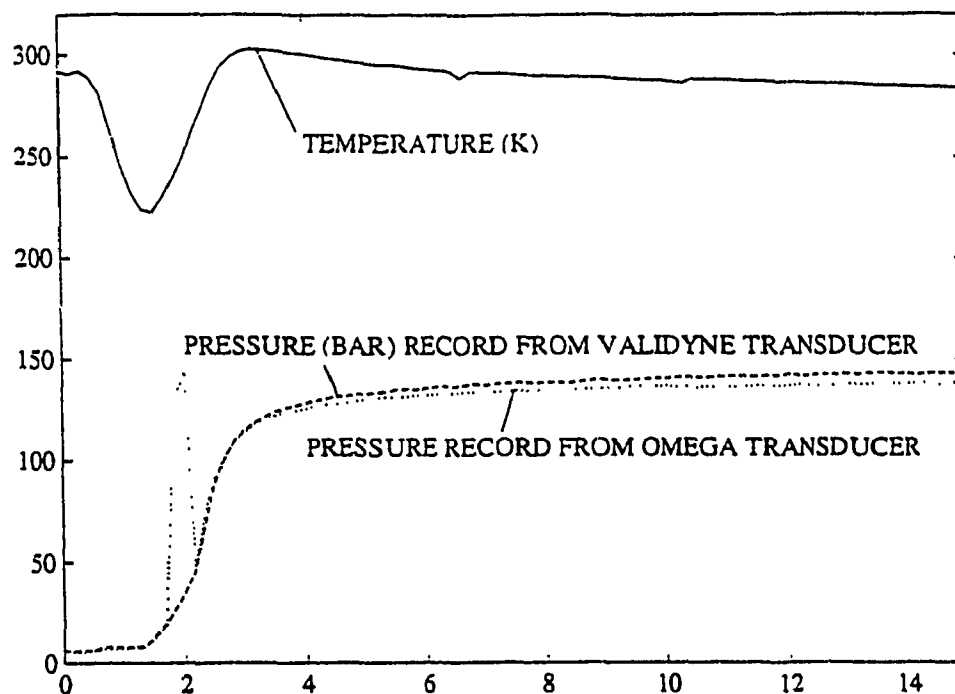


Fig. 4.6 Temperature and pressure records from the test on the insulated steel vessel

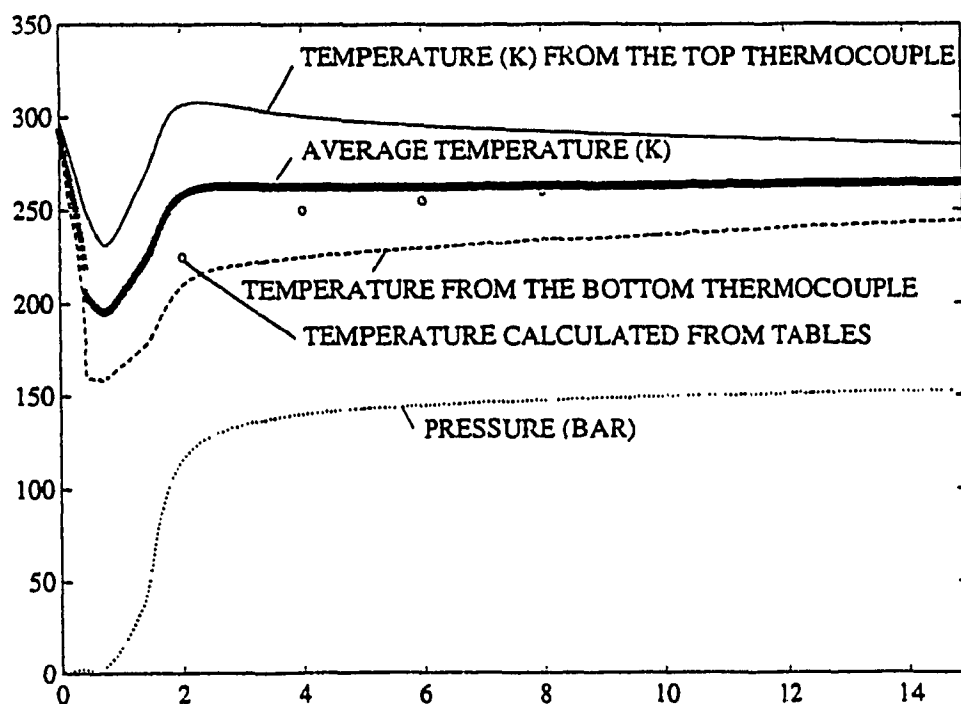
transducer and the fitting on the steel tank. Because of this, the liquid nitrogen did not enter the pressure transducer and affect the readings. On the other hand, the Omega pressure transducer, which is much smaller in diameter, was directly installed on the cover at the bottom of the steel tank. When the tank was filled with liquid nitrogen, the liquid was entering the Omega pressure transducer. The piezo-electric transducer which was not designed for such a low temperature range was not showing the exact pressure reading until the  $LN_2$  evaporated completely. When there is no liquid present inside the transducer, it was functioning normally. This phenomenon was also confirmed by the Omega instruments engineer.

The temperature reading from the RTD thermocouple did show a peak immediately after closing the valves. To further investigate the peak in the temperature, it was decided to install another thermocouple at the bottom of the tank. Hence the old Omega thermocouple was installed at the bottom of the tank and the test was repeated with a mass of 3.9 kg  $LN_2$ . During this test, it was observed that the temperature at the bottom of the tank was much lower when compared with the top as shown in Fig. 4.7b. This indicates that the liquefied gas first absorbs the heat from the bottom part of the tank wall and lowers its temperature. When the liquid boils-off taking the heat from the bottom of the tank, the gas goes into the top half of the tank, because of its low density compared with the liquid.

As it can be noticed from the graph (Fig. 4.7b), there is a temperature



a TIME (MIN.)



b TIME (MIN.)

Fig 4.7

Results from the tests conducted to investigate the peaks in pressure and temperature

difference of about 80 K between the top and bottom of the tank in the initial period. This difference decreases with time, which means that the temperature becomes uniform. This also indicates that the presence of a stirrer would help to maintain a uniform temperature inside the tank. Also, knowing the pressure inside the tank, the mass of  $\text{LN}_2$  and the volume of the vessel, the temperature of  $\text{LN}_2$  inside the tank was calculated from the tables [43] and the corresponding points are shown in Fig. 4.7b. The calculated temperature closely matches with the average temperature, as measured by the two thermocouples.

In the final phase of tests with the steel vessel, the effect of additional heat transfer from the heat exchanger was tested. The shop air was heated by passing it through a heavy duty heater before starting the experiment. After reaching the steady state temperature, the hot air was allowed to pass through the heat exchanger fitted inside the steel tank. Then the steel pressure vessel was filled with 3.7 kg  $\text{LN}_2$ . In this test, 2 more thermocouples were used to measure the temperature of incoming and outgoing hot air. The experimental results are presented in Fig. 4.8.

In this case, the heat transfer to nitrogen is from two sources: from the walls of the steel vessel and from the walls of the heat exchanger. Knowing the inlet and outlet hot air temperatures and the mass flow rate of hot air, the heat transfer from the hot air to nitrogen gas was calculated. It was observed that the heat transfer to nitrogen from hot air is very small compared to the heat transfer to

nitrogen from the steel vessel because of the following reasons. The higher mass and a higher specific heat of the steel vessel result in a higher internal energy stored in the vessel walls. In vehicles, light weight composite material will be used for thermocontrolled tanks and will have less internal energy stored in the walls. Also, the mass flow rate of hot air allowed to pass through the heat exchanger during the experiment was only 10 kg/hr. In the case of a vehicle, the mass flow rate of exhaust gases will be much higher, which will result in high heat transfer rates from the exhaust gas to the fuel inside the tank.

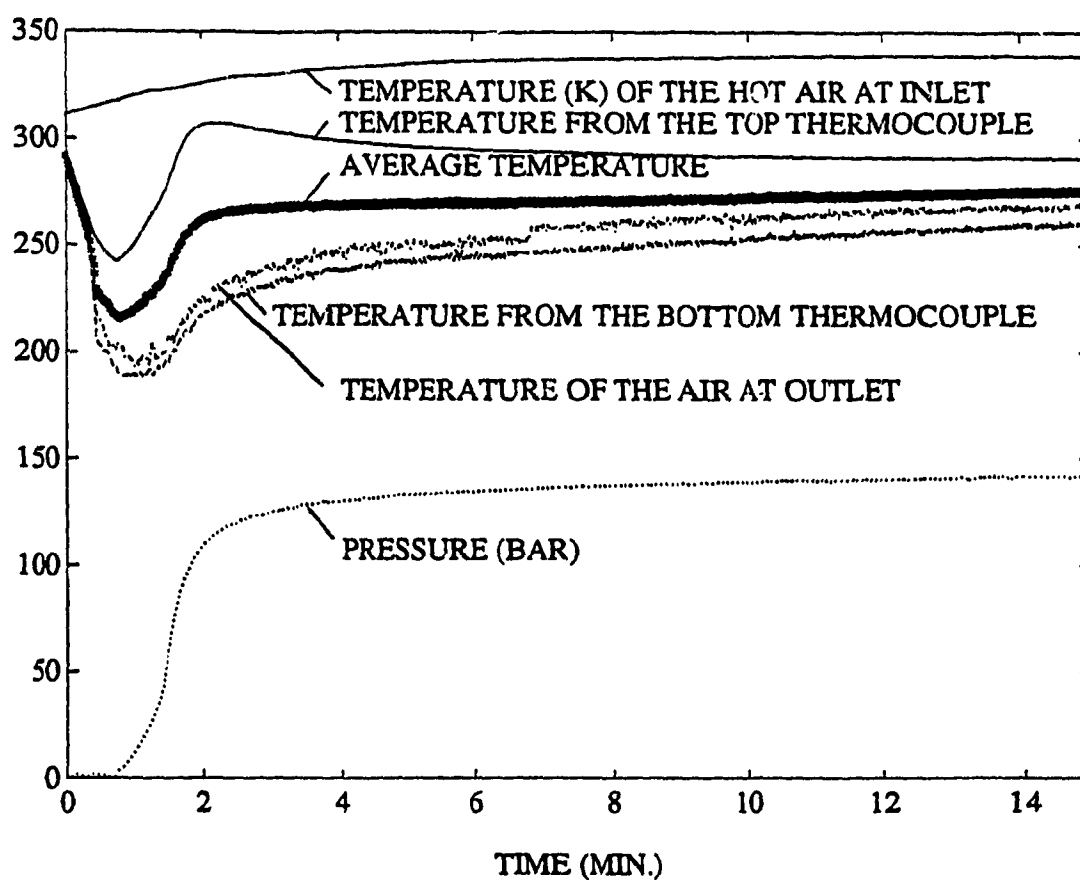


Fig. 4.8 Temperature and pressure records from the test on the insulated steel vessel with additional heating through the heat exchanger

#### 4.2.2 Testing of the Composite Tank

The prototype of the composite tank has been tested in a similar manner as that of steel tank with  $\text{LN}_2$  to obtain experimental data required for the validation of the mathematical model. The schematic of the test setup is shown in Fig. 4.9.

The tank was tested by introducing 4.9 kg of liquid nitrogen which was allowed to evaporate and attain an ambient temperature which would result in a pressure of 850 bar. Based on the pressure record, the gas temperature history in the tank has been calculated from the tables [43], and is presented in Fig. 4.10. When liquid nitrogen was supplied to the vessel, the latter kept at the ambient temperature, heat transfer starts immediately from the vessel walls to the liquid, resulting in a fast boil-off process which produces a temperature gradient across the wall of the vessel. It then takes some time, before the temperature of the outside wall surface drops to the level allowing for more intense heat transfer from the ambient to the wall of the tank.

It was observed that the initial pressure buildup was lower in the case of composite vessel, as compared with the steel vessel. This is because the composite vessel, having a smaller mass than the steel vessel, will have less internal energy stored in it. Also, the time taken to reach the steady state temperature and pressure was longer with the composite vessel, as compared with the steel vessel. This is because the thermal conductivity of the composite material is smaller than that of steel.

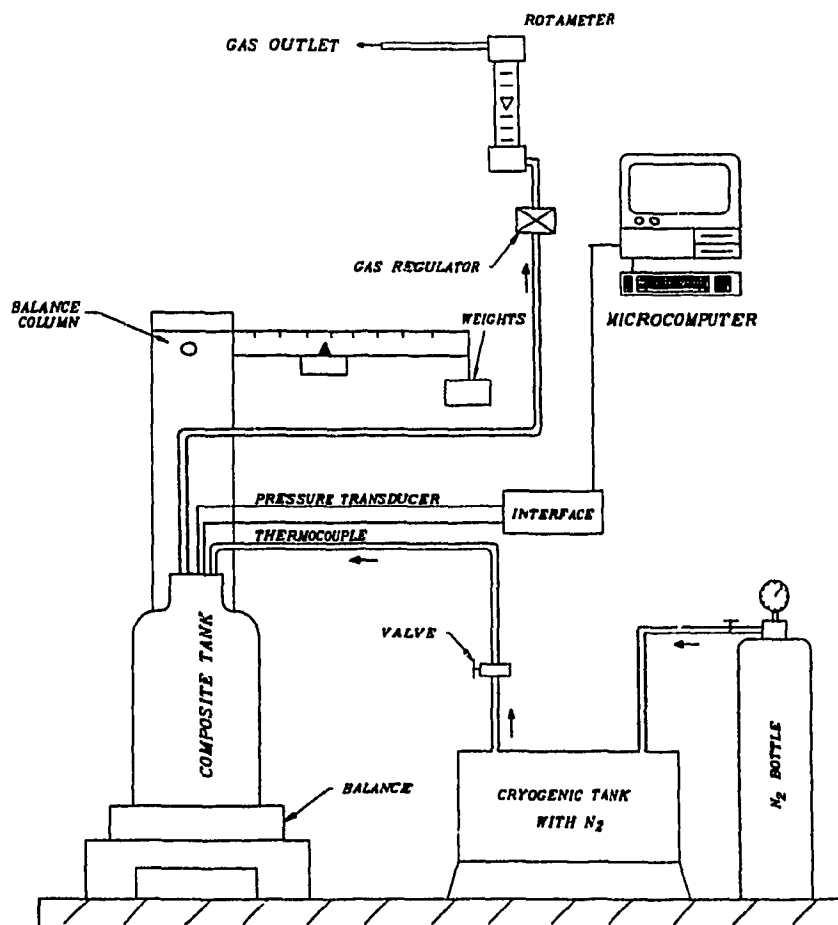


Fig. 4.9 Schematic of the test set-up for the composite vessel evaluation

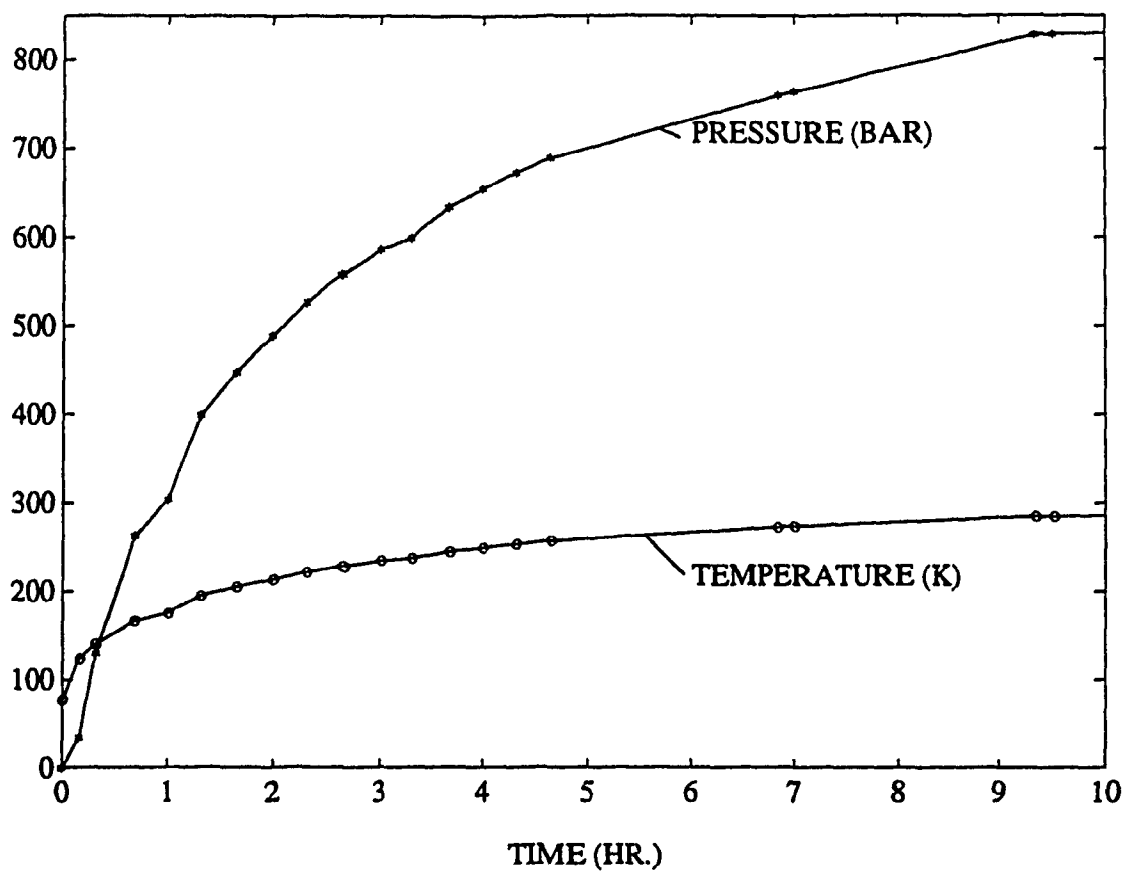


Fig. 4.10 Temperature and pressure records from the test on the composite high pressure vessel

### 4.3 Validation of the Mathematical Model

The mathematical model which was developed and simulated in Chapter 3 has been validated with the experimental data in this section. Fig. 4.11 shows the experimental and simulation results for the insulated steel tank filled with 3.9 kg  $\text{LN}_2$ . In this figure, it can be seen that the simulation results for the temperature closely match the average temperature inside the tank after the initial transient period is completed.

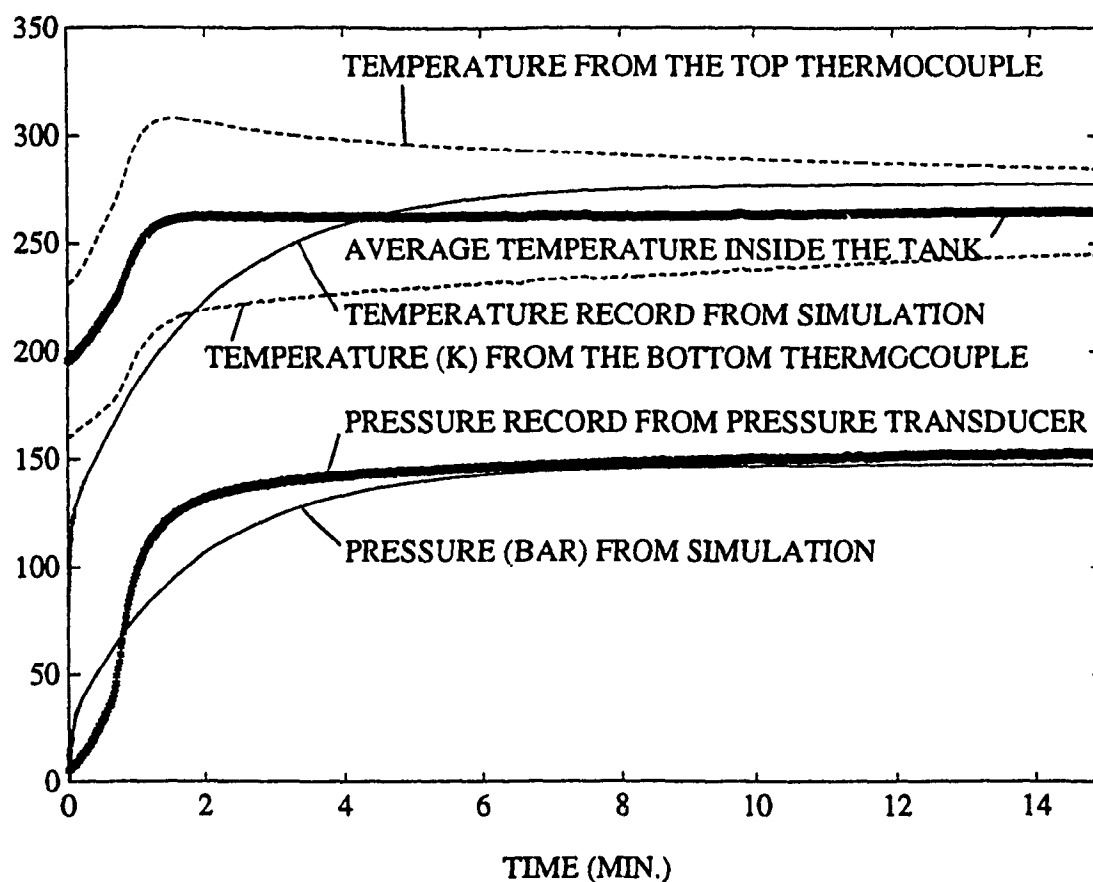


Fig. 4.11 Experimental and Simulation results for insulated steel tank

The difference in the experimental and simulated temperature record is due to the following phenomenon. During the tank filling, when the liquid comes in contact with the tank which is at the room temperature, the liquid starts to boil-off immediately because of the large temperature difference. The boiled-off gas should then escape out to avoid the pressure build-up and to allow more liquid to come in. The longer the filling process, the more liquid will change to gas in the tank. In the mathematical model and simulation, the initial filling process was not considered. If the time taken to fillup the tank is reduced, which can be done by properly designed refuelling stations, the difference in the temperature records in Fig. 4.11 will be minimum. Also the figure indicates that a stirrer would help to maintain the temperature inside the tank at an uniform level which will be close to the analytically predicted values.

## CHAPTER 5

### OPTIMIZATION OF THERMOCONTROLLED VESSEL DESIGN

#### 5.1 Preliminaries

For the development of a product, two approaches can be taken. In the first approach, the physical processes occurring in the product are described mathematically, in order to find its optimum design by calculation. In the second approach, the product is developed empirically. In practice, one will always move between these two procedures. How close one will follow each procedure depends on the product itself, and on the complexity of the physical processes to be described mathematically. Of course, the calculations can never totally replace the experiments, but they can assist and reduce the number of tests. One of the valuable tools used to improve the design is the *numerical optimization technique*. It offers the advantage of reducing the development costs, reducing the product development time and provides the ability to analyze the product without having to fabricate the parts. The evaluation of several design alternatives can be performed inexpensively in a relatively short amount of time.

Present alternative fuel storage systems in vehicles are, to some extent standardised for operation with compressed gaseous fuels. For example, there is a steel pressure vessel of diameter 0.3 m (12 in.) currently being used in natural gas vehicles for the gas storage at 200 bar (3000 PSI). Substitution of a liquid

alternative fuel for the compressed gas will result in unconventional storage conditions and a cryogenic tank has to be designed. The development of advanced composite materials has simplified the on-board gaseous storage systems. The performance factor (burst pressure.internal volume/weight) for advanced composite tank design can reach nine times that of steel tanks and almost six times that of aluminium tanks [33]. Hence it was decided to use a composite vessel as the thermocontrolled tank in vehicles. To find out the optimum values of the design parameters, gas storage pressure, tank material stresses and specific heat and also the internal diameter of the pressure vessel, the following three important design objectives have been identified and investigated.

1. To minimize the initial operational temperature of the gas inside the storage vessel. By keeping the initial operational temperature minimum, higher energy can be stored in the vessel.
2. To maximize the gas mass to the vessel weight ratio.
3. To maximize the gas mass to the vessel outside volume ratio.

## 5.2 Guidelines for Vessel Optimization

It should be decided at the beginning, which values of the design parameters better suit the use of hydrogen as gaseous fuel and which should be rather proposed for natural gas. Following are the statements which can be made to justify these decisions:

Hydrogen is more difficult to store than natural gas, i.e., using the same vessel and the same storing conditions, the energy density for a hydrogen unit will be approximately 4 times lower than that for natural gas, despite higher specific energy per unit mass. Hydrogen is also a more expensive fuel; the hydrogen energy costs approximately four times that for natural gas. Hydrogen, however, is a lesser pollutant than natural gas. These statements can lead to the following guidelines:

The material used for the vessel to store hydrogen should be stronger than that for natural gas, to keep the volume of the tank in the range acceptable for vehicular use. Consequently, the gas pressure would be higher and the tank would become more expensive. However, society should be willing to pay for a more expensive tank because less polluting engine exhaust gases would be the end result.

According to these guidelines, the following lower and upper boundaries have been established [44,45] for the design variables used in the optimization procedure.

For natural gas:

Tank Diameter, mm	100-400
Gas Pressure, bar	100-600
Material Stresses, MPa	80-320
Material Specific Heat, kJ/kg-K	0.6-1.1

For hydrogen:

Tank Diameter, mm	100-300
Gas Pressure, bar	200-800
Material Stresses, MPa	150-450
Material Specific Heat, kJ/kg-K	0.6-1.1

### 5.3 Design Parameter Sensitivity Study

Prior to optimization of the model, a detailed parametric study was carried out to obtain an indepth understanding of the system behaviour. Influence of system parameters on important design objectives such as: initial operational temperature, gas mass to vessel weight ratio and gas mass to vessel volume ratio are examined in this section.

#### 5.3.1 Initial Operational Temperature

*Initial operational temperature* is the final equilibrium temperature of the gas and the tank if the tank is assumed as perfectly insulated. In this case, the energy released by the tank walls is equal to the energy absorbed by the fuel to attain the initial operational temperature. The energy released by the tank walls can be given by:

$$\Delta E_t = m_t c_t \Delta T \quad (5.1)$$

where  $\Delta T = T_a - T_{io}$

The internal energy,  $\Delta u_g$  required for a particular gaseous fuel to attain the initial operating temperature has been calculated from the tables [43]. A graph is then plotted for  $T_{io}$  vs  $\Delta E_t$  and  $T_{io}$  vs  $\Delta u_g$ . From the intersection of these two plots, the initial operational temperature which the gaseous fuel will reach because of the heat

transfer from the tank walls has been found.

The effect of each important design variable on this temperature was examined by varying one parameter at a time in the simulation model while keeping other design variables fixed at their nominal values. Figs. 5.1 and 5.2 present the results for natural gas and hydrogen, respectively. It can be seen that the diameter has very little effect on the initial operational temperature. Increasing the gas pressure increases the weight of the tank and hence more internal energy is stored in it; this increases the initial operational temperature of the gas. The results also show that by using higher strength materials (higher hoop stress), the weight of the tank decreases and allows the initial operational temperature to be maintained at the lowest value. With tank materials having a low specific heat, the initial operational temperature will be also lower. An expression for the initial operational temperature was created from the data obtained by linear multi-variable regression analysis. In the case of hydrogen, it is given by:

$$T_{io} = 1.569361 \times 10^{-6} P - 1.111766 \times 10^{-7} S + 1.859925 \times 10^{-1} c_1 \quad (5.2)$$

### 5.3.2 Gas Mass to Vessel Mass Ratio

Specific volume of a gas,  $v_g$  at any given pressure and temperature can be found from the tables. Knowing the inside volume of the tank,  $V_i$ , the mass of the gas can be calculated as:

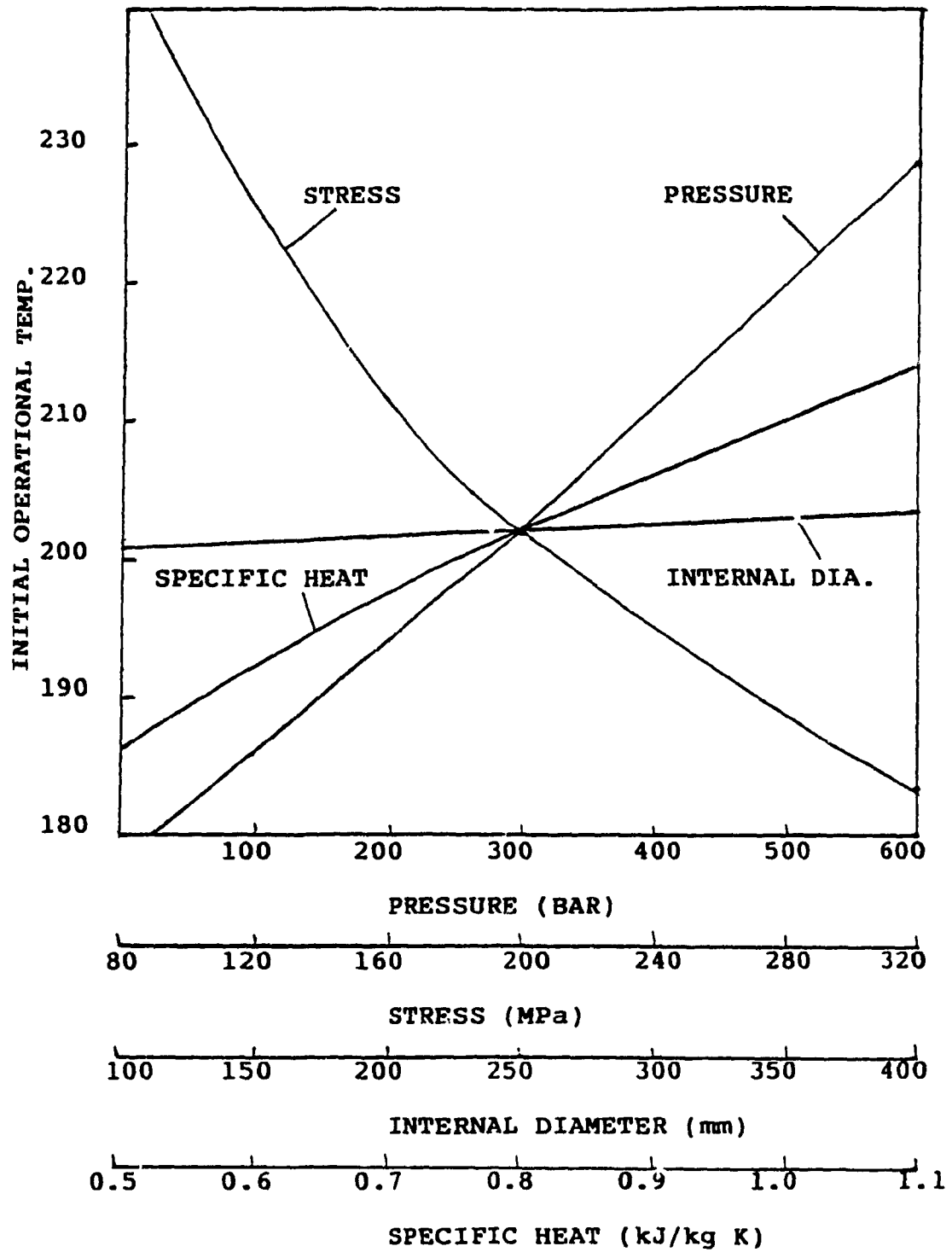


Fig. 5.1 Effect of Design Variables on Initial Operational Temperature for Natural Gas

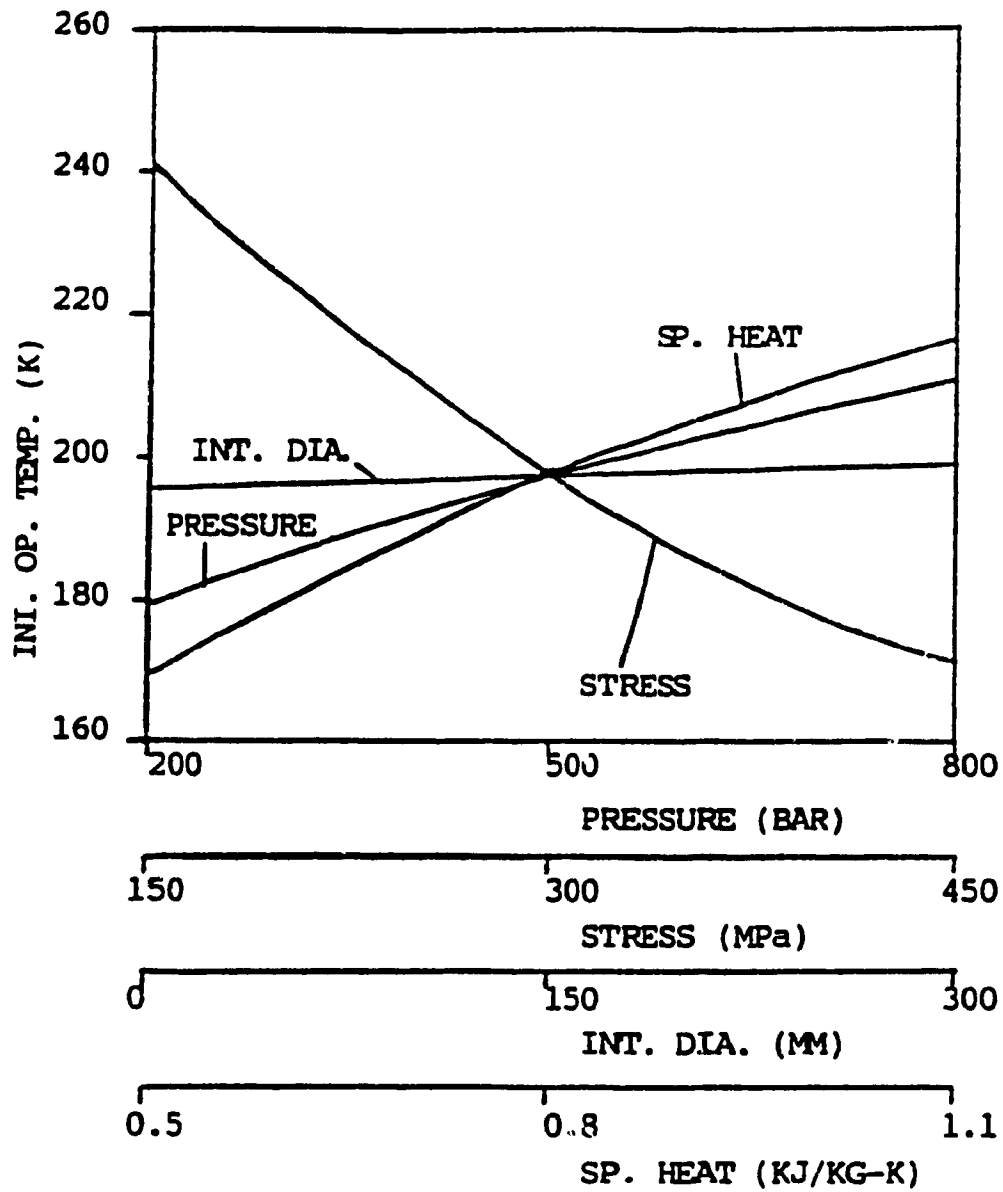


Fig. 5.2 Effect of Design Variables on Initial Operational Temperature for Hydrogen

$$m_g = V_i/v_g \quad [\text{kg}] \quad (5.3)$$

For a particular tank pressure and stress of the material, the thickness of the tank wall (see Fig. 5.3) can be calculated [46] as:

$$t = Pd_1/2S \quad [\text{m}] \quad (5.4)$$

The volume of the tank material,  $V_c$  can be calculated by the equation:

$$V_c = \frac{\pi}{4}[(d_1+2t)^2 - d_1^2] L \quad [\text{m}^3] \quad (5.5)$$

The corresponding weight of the tank can then be expressed as:

$$m_t = \frac{\pi}{4}[(d_1+2t)^2 - d_1^2] L \rho \quad [\text{kg}] \quad (5.6)$$

The gas mass to vessel mass ratio can then be simply expressed as:

$$R_{g/t} = m_g/m_t \quad (5.7)$$

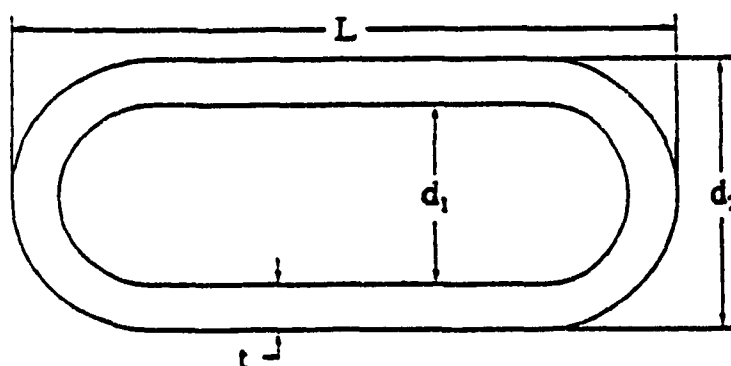


Fig. 5.3 Schematic of the Pressure Vessel

Figs. 5.4 and 5.5 show the effect of design variables on the gas to vessel mass ratio for natural gas and hydrogen, respectively. This ratio has again very weak dependence on the diameter. It was found that decreasing the storage pressure, decreases the weight of the tank and hence the ratio increases. Highly stressed materials decrease the weight of the tank and hence the ratio will be higher.

### 5.3.3 Gas Mass to Tank Volume Ratio

The tank outside volume,  $V_o$  can be calculated as:

$$V_o = \pi d_o^2 L / 4 \quad [\text{m}^3] \quad (5.8)$$

Then, the gas mass to tank volume ratio,  $R_{m/v}$  is given by:

$$R_{m/v} = m_g / V_o \quad [\text{Kg/m}^3] \quad (5.9)$$

The effect of design variables on the gas mass to tank volume ratio for natural gas and hydrogen are presented in Figs. 5.6 and 5.7, respectively. It can be seen again that the diameter has very weak effect on the ratio. At higher pressures, more gas can be stored and hence the ratio will be maximum at high pressures. The results also show that the ratio will increase at higher stresses.

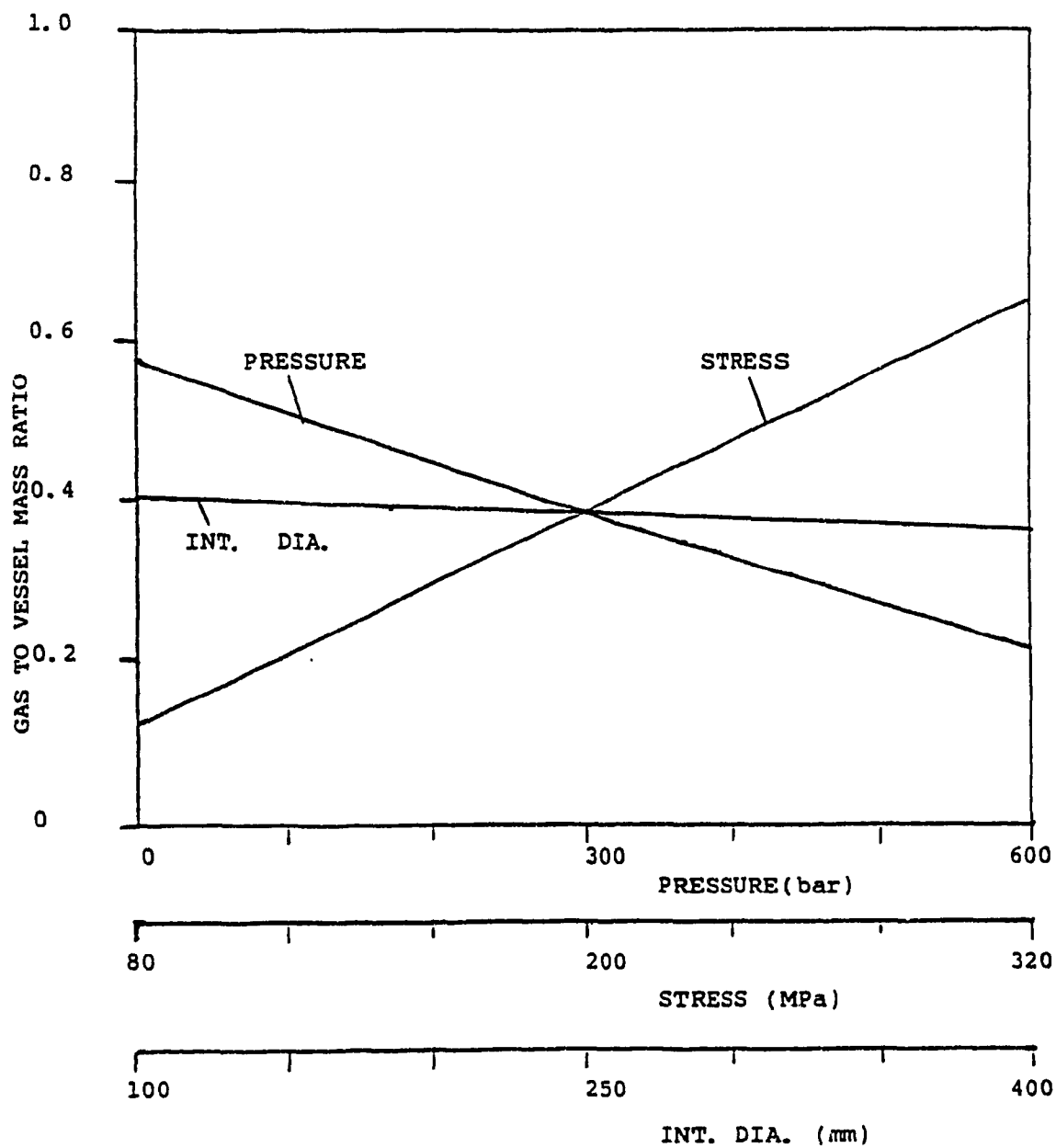


Fig. 5.4 Variation of Gas Mass to Vessel Mass Ratio with Design Variables for Natural Gas

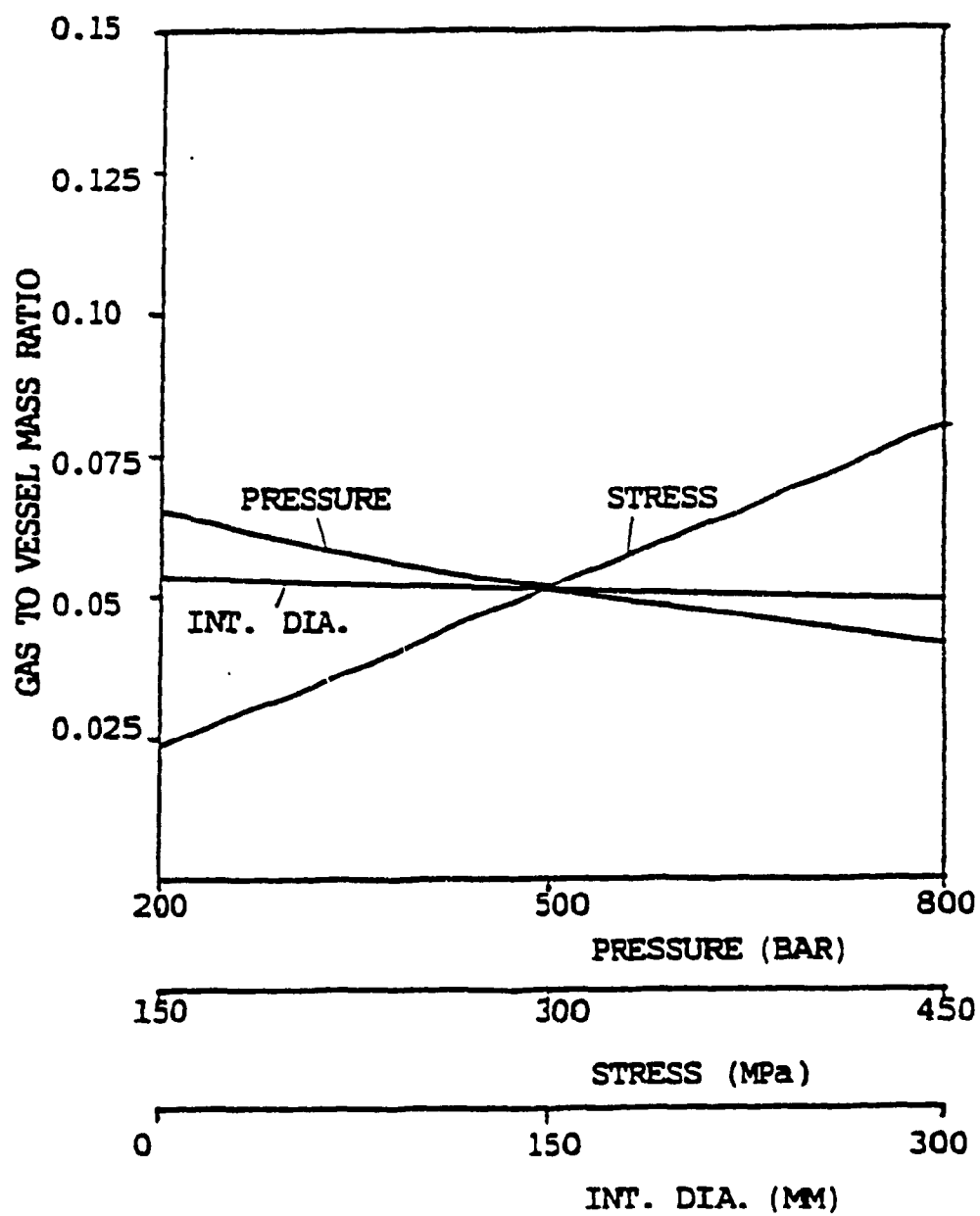


Fig. 5.5 Variation of Gas Mass to Vessel Mass Ratio with Design Variables for Hydrogen

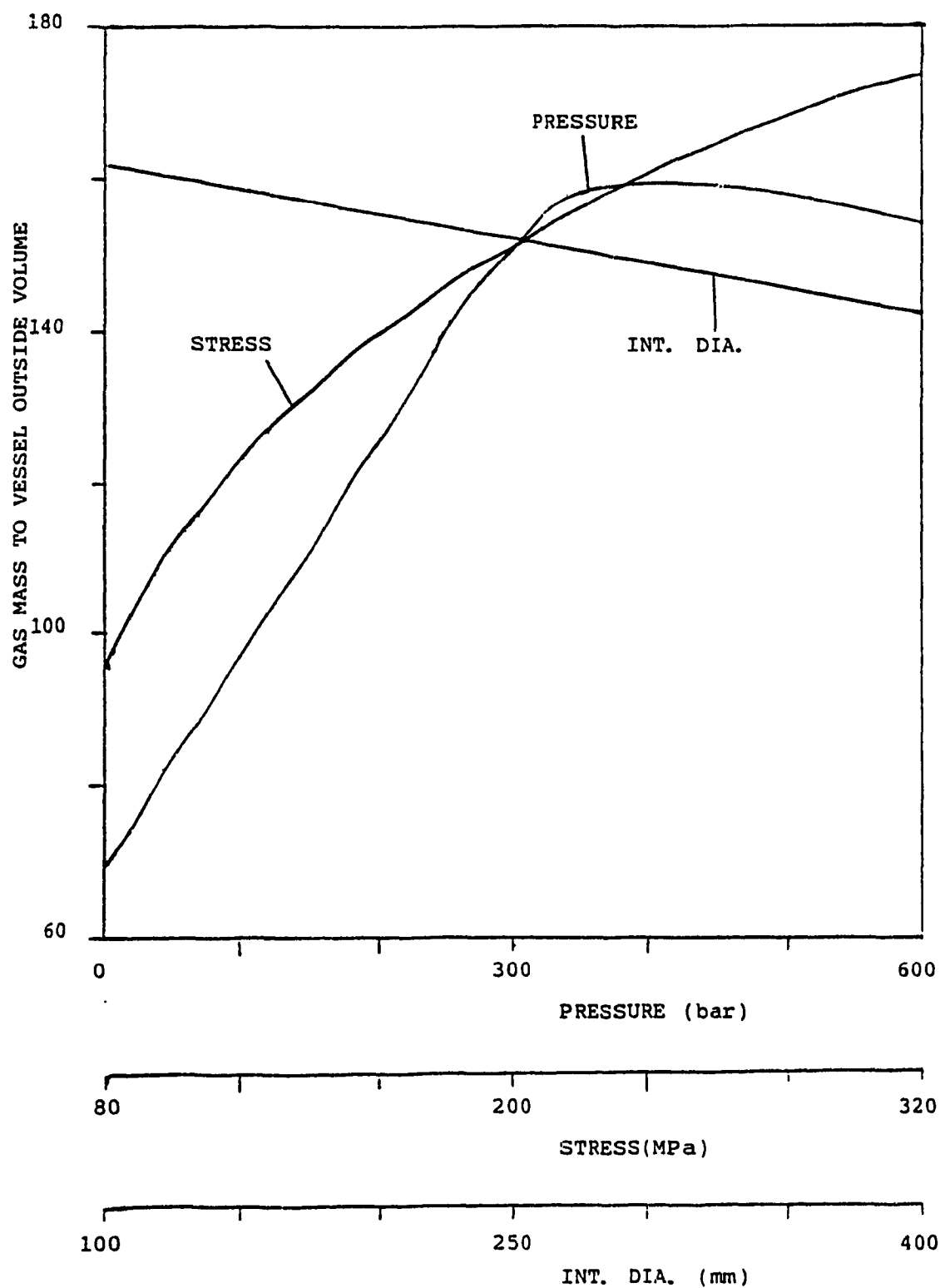


Fig. 5.6 Variation of Gas Mass to Vessel Volume Ratio with Design Variables for Natural Gas

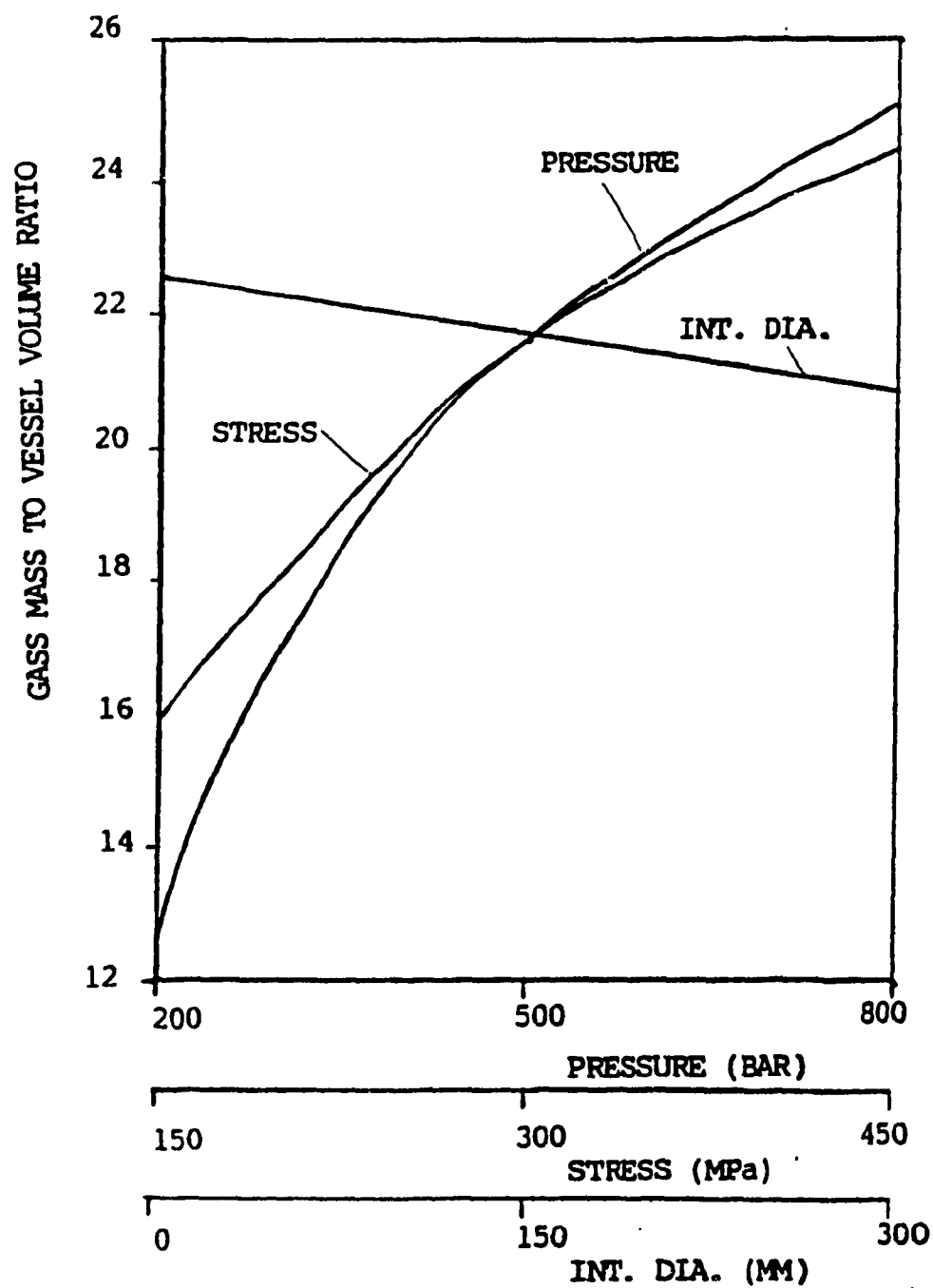


Fig. 5.7 Variation of Mass Gas to Vessel Volume Ratio with Design Variables for Hydrogen

## 5.4 Multiple Objective Optimization

The multicriteria optimization techniques are important in the design of complex engineering systems whose quality depends generally on a number of different and often conflicting criterion functions which cannot be combined into a single design criterion. Several methods have been proposed by applied mathematicians during the last several years for the solution of multicriteria optimization problems. *Global optimization criterion method* [47] is one of the methods to solve multicriteria optimization problems. In this method, an optimal vector can be found by minimizing some global criterion such as the sum of the squares of the relative deviation of the criteria from the feasible ideal points. Thus,  $X^*$  is the solution of the problem:

$$\text{Minimize } F(X) = \sum_{i=1}^k \left[ \frac{F_i(X_i^*) - F_i(X)}{F_i(X_i^*)} \right]^p ; p \geq 1 \quad (5.10)$$

$$\text{subject to } g_j(X) \leq 0, j = 1, 2, \dots, m \quad (5.11)$$

### 5.4.1 Formulation of the Problem

Having defined and investigated the three objectives, it was required to

normalize the initial operational temperature and gas to vessel volume ratio to make them non-dimensional. The initial operational temperature was divided by the boiling temperature of the fuel and the new ratio is denoted by TIO(X). Similarly, the gas mass to vessel volume ratio was multiplied by critical specific volume of the fuel and the new ratio is denoted by GVV(X). Now, the multi-objective constrained non-linear optimization problem can be formulated as:

$$\text{Minimize } Z(X) = [\text{TIO}(X), -R_{gh}(X), -\text{GVV}(X)] \quad (5.12)$$

subject to the following side constraints:

$$P^l \leq P \leq P^u \quad (5.13)$$

$$d_1^l \leq d_1 \leq d_1^u \quad (5.14)$$

$$S^l \leq S \leq S^u \quad (5.15)$$

$$c_t^l \leq c_t \leq c_t^u \quad (5.16)$$

It is desired to simultaneously minimize the first objective and maximize the other two objectives. The constraints (5.13)-(5.16) are the lower and upper bounds on the design variables.

The insight gained from examining the effect of design variables on each objective function can be used along with monotonicity analysis [48] to greatly simplify the problem. First, it was found that the internal diameter has very little effect on all the three objectives. Therefore the internal diameter of the cylinder was selected as 0.25 m for both the fuels, because these values closely match with the vessel diameters that are currently being used in alternative fuelled vehicles.

Since the  $TIO(X)$ ,  $-R_{g/t}(X)$  and  $-GVV(X)$  ratios are not commensurate, some scaling of these objectives and subjective input from the designers are required before an optimum design is found [49]. One simple method to deal with this is to find out the maximum and minimum limits on these three ratios. The maximum limits are denoted as  $TIOMAX$ ,  $R_{g/t}MAX$ , and  $GVVMAX$ , respectively, and the corresponding minimum limits are  $TIOMIN$ ,  $R_{g/t}MIN$ , and  $GVVMIN$ . A global criterion function was then defined as:

$$F(X) = \left[ \frac{TIO(X) - TIOMIN}{TIOMAX - TIOMIN} \right]^2 + \left[ \frac{R_{g/t}(X) - R_{g/t}MIN}{R_{g/t}MAX - R_{g/t}MIN} \right]^2 + \left[ \frac{GVV(X) - GVVMIN}{GVVMAX - GVVMIN} \right]^2 \quad (5.17)$$

The denominators of the above three terms are constants and represent the maximum variation of the  $TIO(X)$ ,  $R_{g/t}(X)$  and  $GVV(X)$  ratios, respectively, in the feasible design variable range. The numerators are the deviations of the objective functions from their ideal value. By applying weights  $W_1$ ,  $W_2$  and  $W_3$  to the three

terms in Eq. (5.17), the global criterion function can be rewritten as

$$F(X) = W_1 \left[ \frac{TIO(X) - TIOMIN}{TIOMAX - TIOMIN} \right]^2 + W_2 \left[ \frac{R_{g/t}(X) - R_{g/t}^{MIN}}{R_{g/t}^{MAX} - R_{g/t}^{MIN}} \right]^2 + W_3 \left[ \frac{GVV(X) - GVVMIN}{GVVMAX - GVVMIN} \right]^2 \quad (5.18)$$

#### 5.4.2 Solution Method

By selecting the three weighting factors as 0.15, 0.10 and 0.75 respectively, the three terms in the equation (5.18) were plotted against the gas pressure and are shown in Figs. 5.8 and 5.9 for natural gas and hydrogen. The global objective criterion is also shown in the figures. From these graphs, it can be seen that a gas pressure of about 430 bar for natural gas and 470 bar for hydrogen is recommended.

The global criterion function was also solved as a constrained non-linear optimization problem using interior penalty function method [50-52]. The pseudo-objective function  $\phi(X)$  can be defined as

$$\phi(X) = F(X) - r_p \sum_{j=1}^m \frac{1}{g_j(X)} \quad (5.19)$$

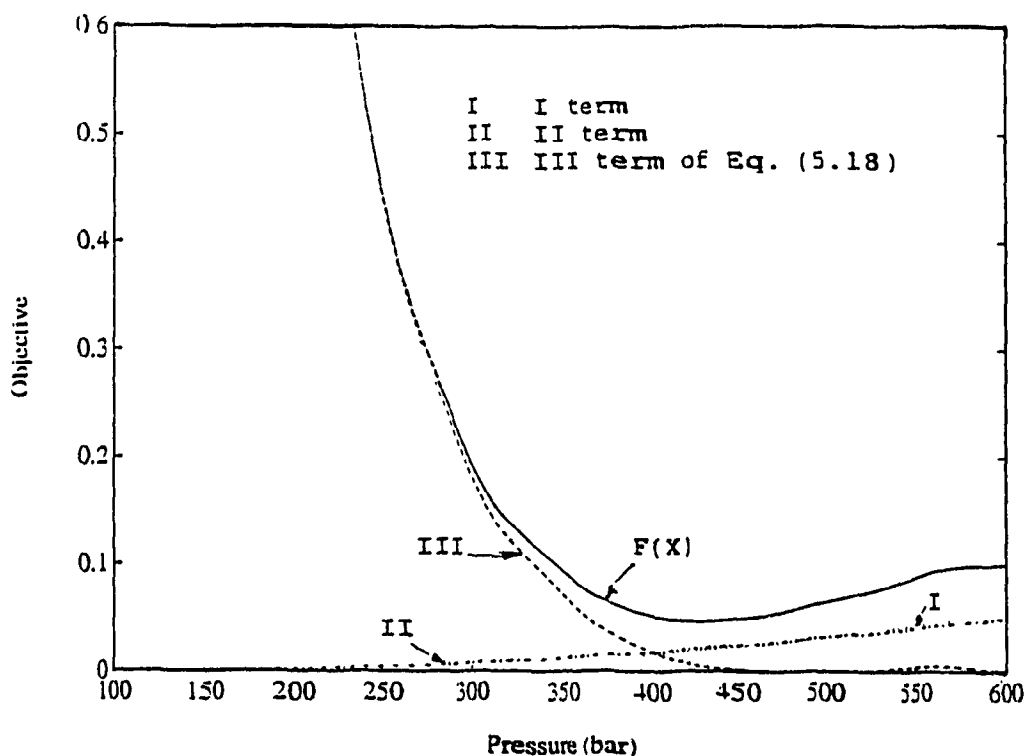


Fig. 5.8 Variation of Global Objective Criterion Vs Pressure for Natural Gas

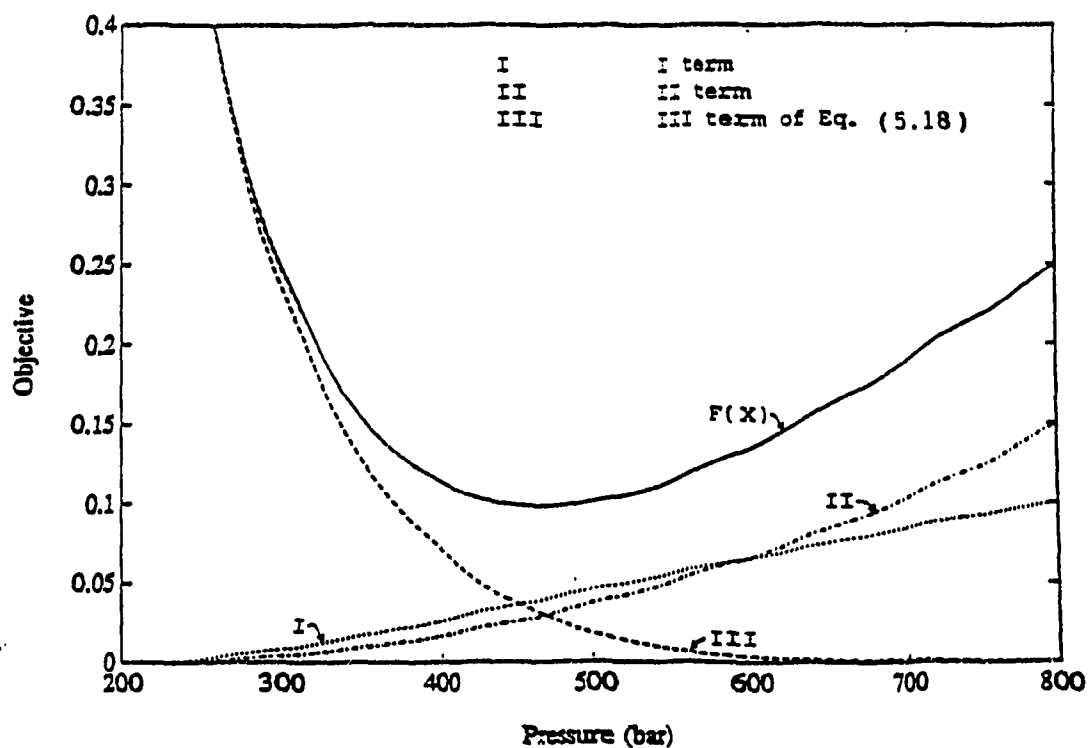


Fig. 5.9 Variation of Global Objective Criterion Vs Pressure for Hydrogen

where  $r_p$  is the penalty parameter whose value at the initial feasible starting point  $X_1$  was selected as

$$r_p = \frac{F(X_1)}{\left[ -\sum_{j=1}^m \frac{1}{g_j(X_1)} \right]} \quad (5.20)$$

and the subsequent values were decremented by multiplying with 0.1. Hooke and Jeeves method was used to find the minimum of the pseudo-objective function. Fig. 5.10 describes the flow chart of the optimization program used in this work. Fig. 5.11 shows the update of design variables in each iteration for hydrogen. It was found that the optimum design is:

For natural gas:

Pressure:	430 bar
Max. material stresses:	320 MPa
Sp. heat of material:	0.6 kJ/kg K

For hydrogen:

Pressure:	470 bar
Max. material stresses:	450 MPa
Sp. heat of material:	0.6 kJ/kg K

If the designer is not satisfied with the solution, he can change the weighting factors and repeat the process to get another optimum value better corresponding

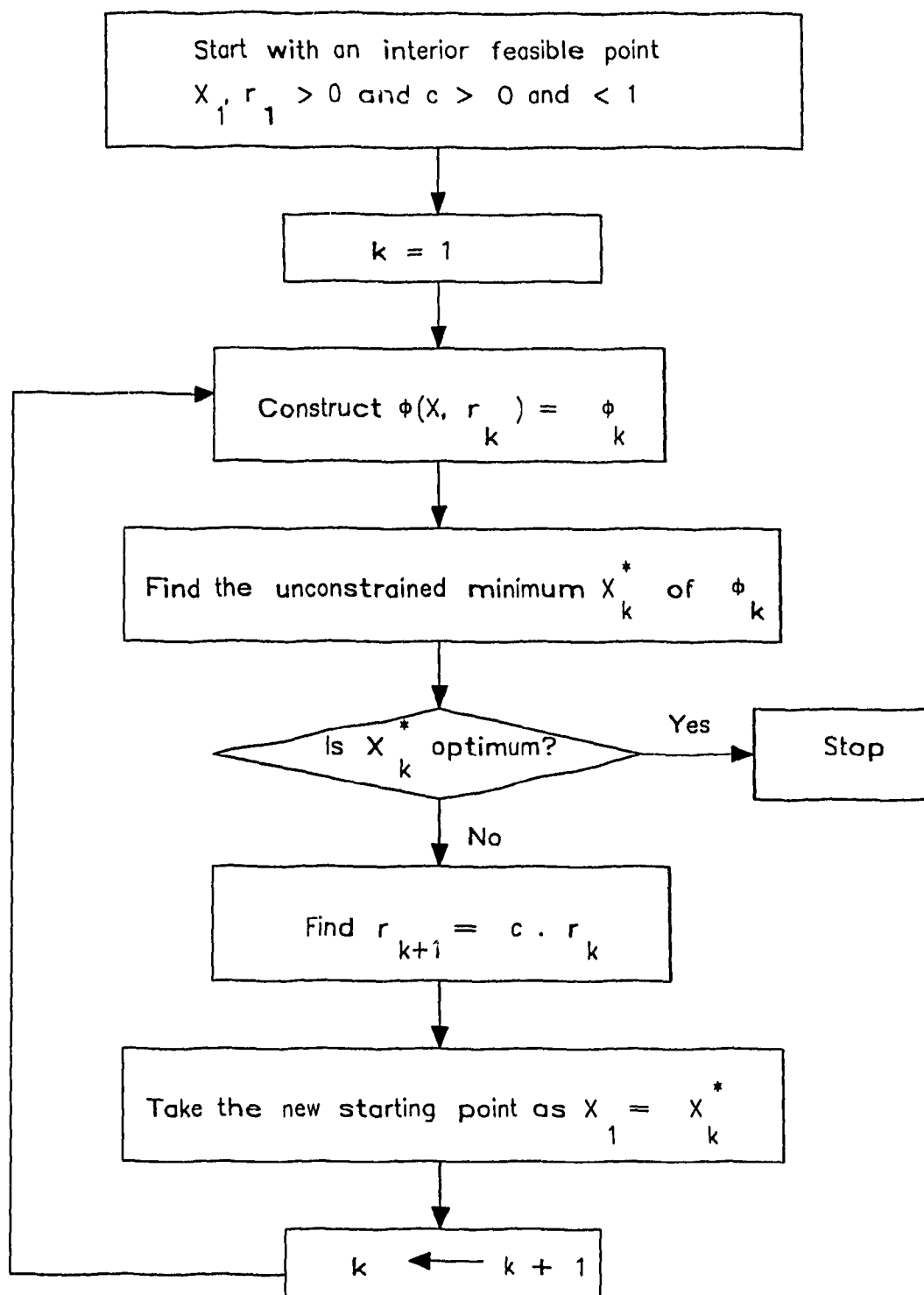


Fig. 5.10 Flow Chart of the Optimization Process

to his design approach. The internal diameter of the cylinder was earlier found to change the three objectives very little. Therefore the internal diameter of the cylinder was selected as 0.25 m for both the fuels. This is because of the fact that at larger diameters, the stresses will be higher and also these values closely match with the vessel diameter that are currently being used in gaseous fuelled vehicles.

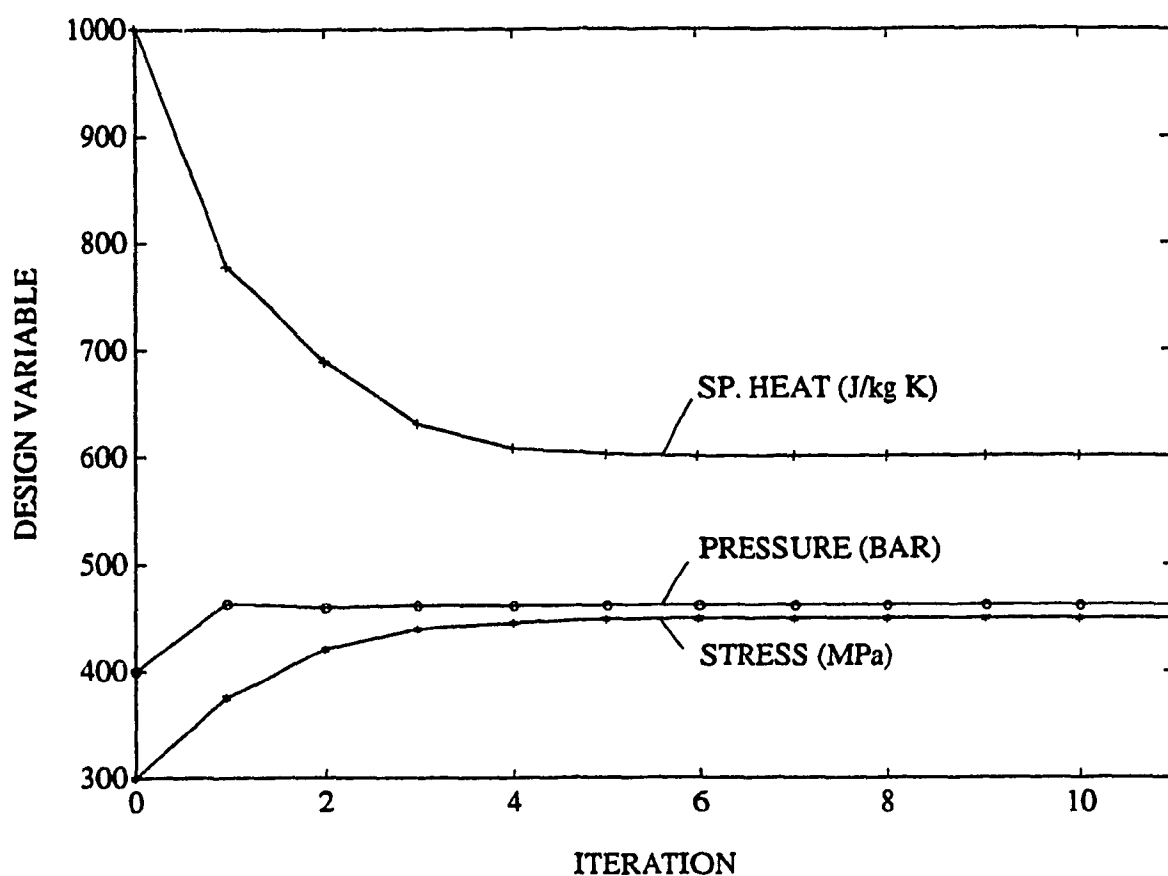


Fig. 5.11 Iteration History of Design Variables During Optimization for Hydrogen

## 5.5 Conclusions

The following conclusions could be drawn regarding the results of the vessel design optimization:

For natural gas and hydrogen, the optimum values for each of the three objectives are:

Initial Operational Temperature  $T_{io}$

	<u>Natural gas</u>	<u>Hydrogen</u>
Pressure, bar:	100	200
Max. material stresses, MPa:	320	450
Sp. heat of material, kJ/kg K:	0.6	0.6

Gas to Vessel Mass Ratio  $R_{g/t}$

	<u>Natural gas</u>	<u>Hydrogen</u>
Pressure, bar:	100	200
Max. material stresses, MPa:	320	450

Gas Mass to Tank Volume Ratio  $R_{m/v}$

	<u>Natural gas</u>	<u>Hydrogen</u>
Pressure, bar:	400	800
Max. material stresses, MPa:	320	450

As seen from the graphs, the vessel internal diameter was affecting these objectives to a small extent. It could therefore, have some impact if considered as

an objective.

Based on the results of this optimization, following would be the values of the proposed design parameters for the storage vessel.

	<u>Natural gas</u>	<u>Hydrogen</u>
Pressure, bar:	430	470
Max. material stresses, MPa:	320	450
Sp. heat of material, kJ/kg K:	0.6	0.6
Diameter of the tank, m:	0.25	0.25

Since the diameter is the same for both the fuels and maximum storage pressure is also approximately the same, the higher stresses for the hydrogen tank will make the tank lighter. But to have the same range for both the fuels, hydrogen storage tank volume should be increased, which means that a larger number of cylinders is required. This will make the total weight of hydrogen on-board storage system greater than that of the natural gas on-board storage system.

## **CHAPTER 6**

### **THERMOCONTROLLED TANK APPLICATIONS CONSIDERATION**

#### **6.1 Preliminaries**

After optimizing the thermocontrolled tank design for its diameter, specific heat and stress of the material and storage pressure [51,52], it has been considered for two types of vehicles, a bus and a car with two different operational patterns. The proposed location of the thermocontrolled tank and the gas supply system is discussed in this chapter for these two vehicles.

#### **6.2 Thermocontrolled Tank Considerations for a Bus**

The thermocontrolled tank is considered primarily for city buses, where there is a central refuelling station, which supplies fuel to a fleet of vehicles. In the morning, after fill-up, the buses wait until the required pressure of 100 bar for direct injection is attained and go into a prescheduled route. When they come back for the next fill-up, the residual fuel will be released into a collector cylinder and the filling process will be repeated.

It is proposed that the gas supply unit be located on the roof of the bus. This position for gas containers presents several advantages, such as protection against shock, space availability and accessibility. Furthermore this location conforms to

the regulation that, in case of leakage, the gas should escape without entering the bus interior. Both gaseous fuels: natural gas and hydrogen are lighter than air and, therefore, will escape upwards. In the presently made gas fuelled bus demonstration projects, such tank position is always proposed [53,54].

The size of the gas containers, as compared with the gasoline tank, is enormous, particularly for hydrogen gas. Therefore, compressed gas cylinders currently in service are as long as the bus itself. The vessels are placed longitudinally, side by side, creating a large battery of units connected with pipes and equipped with valves, pressure gauges and thermocouples. Fig. 6.1 shows the thermocontrolled gaseous fuel tank proposed for the bus adaptation. It is different from the conventional tank by the presence of an envelope made of metal sheet or composite cover, which allows the engine exhaust gases to flow over the cylinders to increase the heat transfer to the gas and to rise the gas temperature and pressure. This feature provides the tank with a thermal control which should be under microprocessor control.

The purpose of the thermocontrolled tank is to increase the energy content of the tank by filling it up with liquefied gas and allowing it to boil-off due to the heat transfer to the gas. Then, in the case of a bus, which will be operational a short time after fill-up, the gas extraction rate, depending on the gas consumption rate by the engine, could maintain the low gas temperature and would not allow the pressure in the tank to rise over the maximum design limit. Moreover, additional

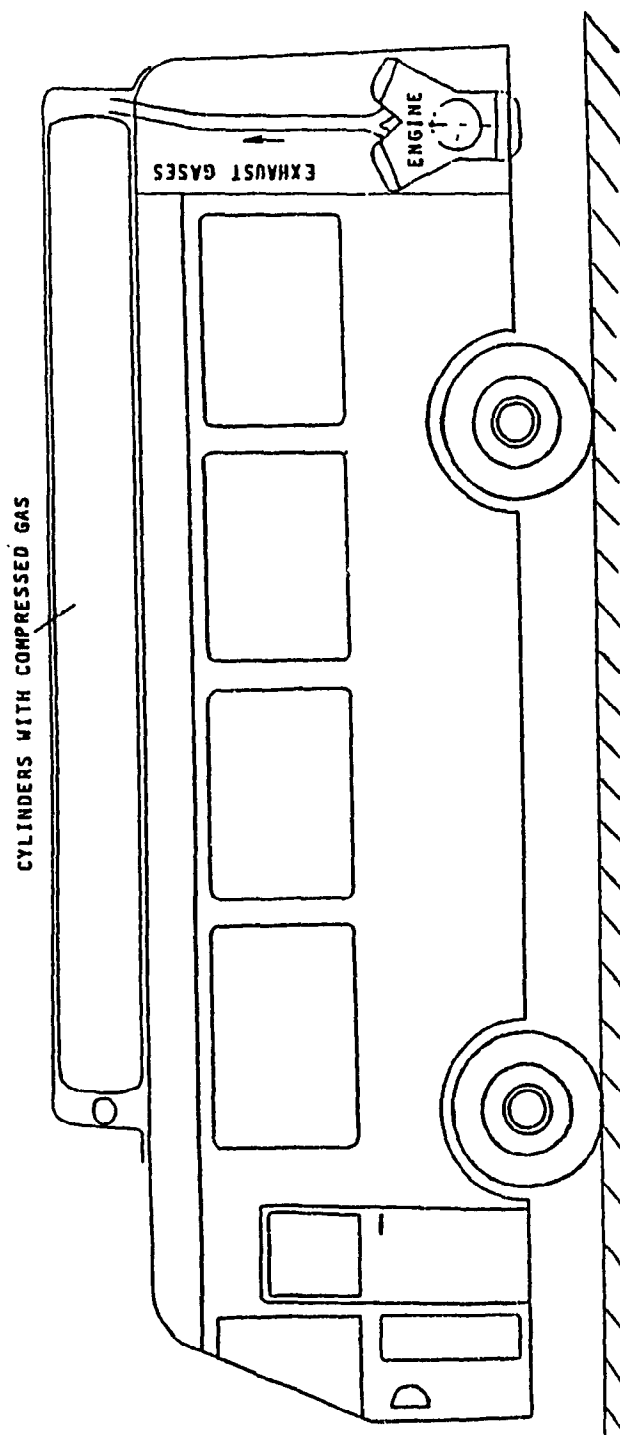


Fig. 6.1 Bus with a battery of thermocontrolled tanks installed on the roof

heat transfer might be required to increase the gas pressure when the mass of the gas in the tank will become lower, in order to help extract more gas before refuelling.

From the results of optimization in chapter 5, it was found that the storage pressure should be 430 bar for natural gas and 470 bar for hydrogen. When manufacturing a cylinder, it will be easier to specify the maximum pressure as a standard number, like 500 bar, rather than 430 bar or 470 bar. Hence the design maximum pressure will be referred to as 500 bar for both the fuels in the rest of the thesis. Increasing the pressure to 500 bar also reduces the residual fuel that is left unused in the tank at the end.

The bus considered for this study is a GM Coach equipped with a Detroit Diesel 6V-71 engine. It has a rated fuel consumption of 42 l/hr. of diesel oil, which translates to 1500 MJ/ hr. The bus roof area of 2.5 m x 6 m allows installation of 5 hydrogen bottles of 250 mm diameter and 3.7 m long, with a total volume of 0.9 cu.m. under 500 bar pressure containing hydrogen gas with a total energy of 6 600 MJ. In the case of natural gas, 4 bottles of 250 mm diameter and 4.7 m long with a total volume of 0.9 cu.m. can be installed containing a total energy of 17 000 MJ. Assuming that only 85% of the gas can be extracted under 100 bar pressure, the operational range of the bus on hydrogen can be predicted as 3.75 hr., and on natural gas as 9.5 hr. These data are preliminary and will be more accurately calculated based on the simulation of the bus operation.

The proposed gas storage and supply system is shown in Fig. 6.2. It consists of a cylinder containing the gaseous fuel which is fitted with a pressure transducer and a thermocouple, which deliver signals to the electronic microcontroller. A pressure regulator ensures that the gas leaving the tank and entering the gas conditioner is at 100 bar pressure. The tank envelope is designed so that the heat from the engine exhaust gases is transferred to the cylinders and to the gas inside the tank, to increase the gas pressure in the final phase of the gas release. Because the gas in the tank can come out at different temperatures, before entering the injectors, the gas flows first to the gas conditioner, where its temperature is maintained at about 350 K by heat transfer from the engine exhaust gases. A thermocouple and a pressure gauge monitor the temperature and the pressure in the gas conditioner. The two valves under electronic control: S1 and S2, divide the exhaust gas flow into three streams: to the tank envelope, to the gas conditioner and to ambient. The opening of these valves is under feedback control, based on the signals from the temperature and the pressure transducers in the gas conditioner in order to maintain the system operational. The exhaust gases produced by the engine have an entry temperature of 450 K, which is maintained by a thermostat operated valve S3.

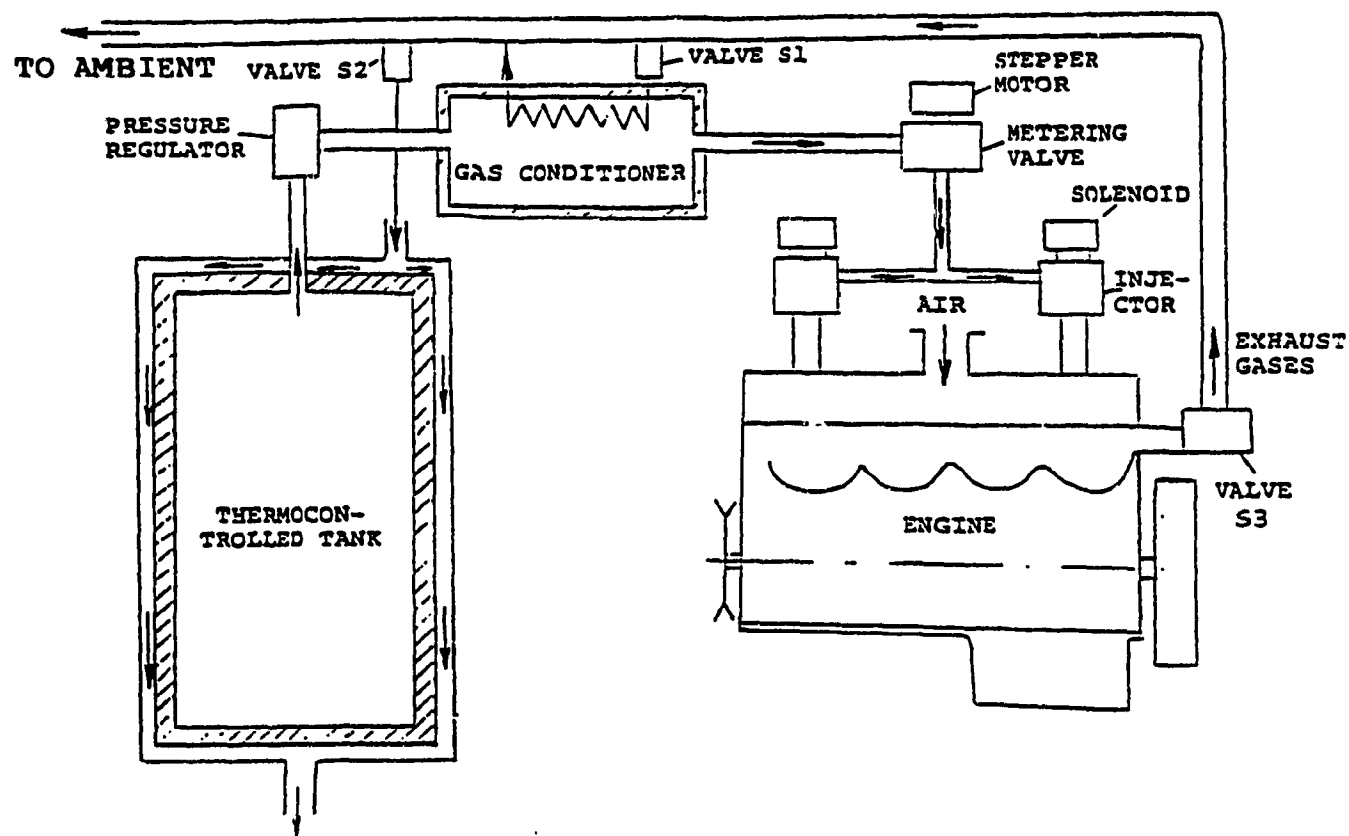


Fig. 6.2 Proposed gas storage and supply system for a bus

### 6.3 Thermocontrolled Tank Considerations for a Car

It is proposed that the gas supply unit be located in the trunk, in its front part, where it is well protected against damage in case of an accident. It is a typical place for compressed gas cylinders in the cars converted for natural gas or propane, with the cylinders installed perpendicular to the car axis.

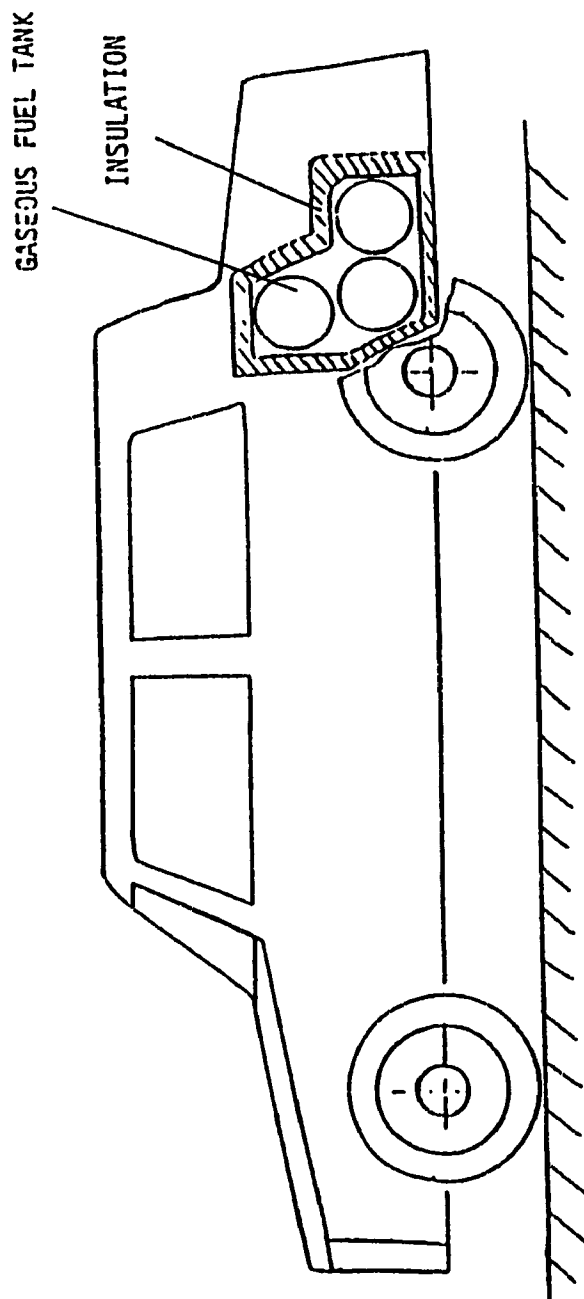


Fig. 6.3 Installation of thermocontrolled tanks in the trunk of a car

Fig. 6.3 shows the installation of gas cylinders in a car. The vessels may be insulated, using the foam glass closed cell insulation or a high performance closed cell insulation, similar to that used in cryogenic tanks. The exhaust gas preheating is through internal heat exchangers installed inside each cylinder. A system of electronically controlled valves, will provide the cylinders with the heat transfer to maintain the gas pressure required for direct gas injection into the cylinders of the engine.

The thermocontrolled tank for a car which would be operated intermittently requires insulation, which would prevent the gas pressure from exceeding the design maximum pressure limit. The vessel would also need gas heating, if the car has to run continuously for extended time periods or if the desired objective is to maximize the vehicle range.

The car considered is a mid size Peugeot 504 with a 2.2 l, 4 cylinder Indenor diesel engine, which has an average fuel consumption of 9 l/100 km of diesel fuel, which translates to 320 MJ/100 km. The trunk volume allows for installation of 3 hydrogen cylinders of 250 mm diameter and 1.1 m length with a total volume of 0.16 cu.m. under 500 bar pressure containing hydrogen gas with the total energy of 1 000 MJ. In the case of natural gas, 2 bottles of 250 mm diameter and 1.2 m length with a total volume of 0.12 cu.m. can be installed containing a total energy of 2 100 MJ. Assuming that only 85% of the gas could be used under 100 bar pressure, the operational range of the car run on hydrogen

can be predicted as 5 hr. and that on natural gas as 11 hr. These data are preliminary and will be more accurately calculated based on the computer simulation of the car operation in chapter 7.

The proposed gas storage and supply system is shown in Fig. 6.4. It differs from that of the bus, in that the exhaust gas heat exchanger would be installed inside the cylinders. Valve S2 which controls the exhaust gas flow to the cylinder, when opened allows the gas to flow to the internal heat exchanger. In this configuration, the exhaust gas entry temperature could reach temperatures as high as 500 K, if necessary.

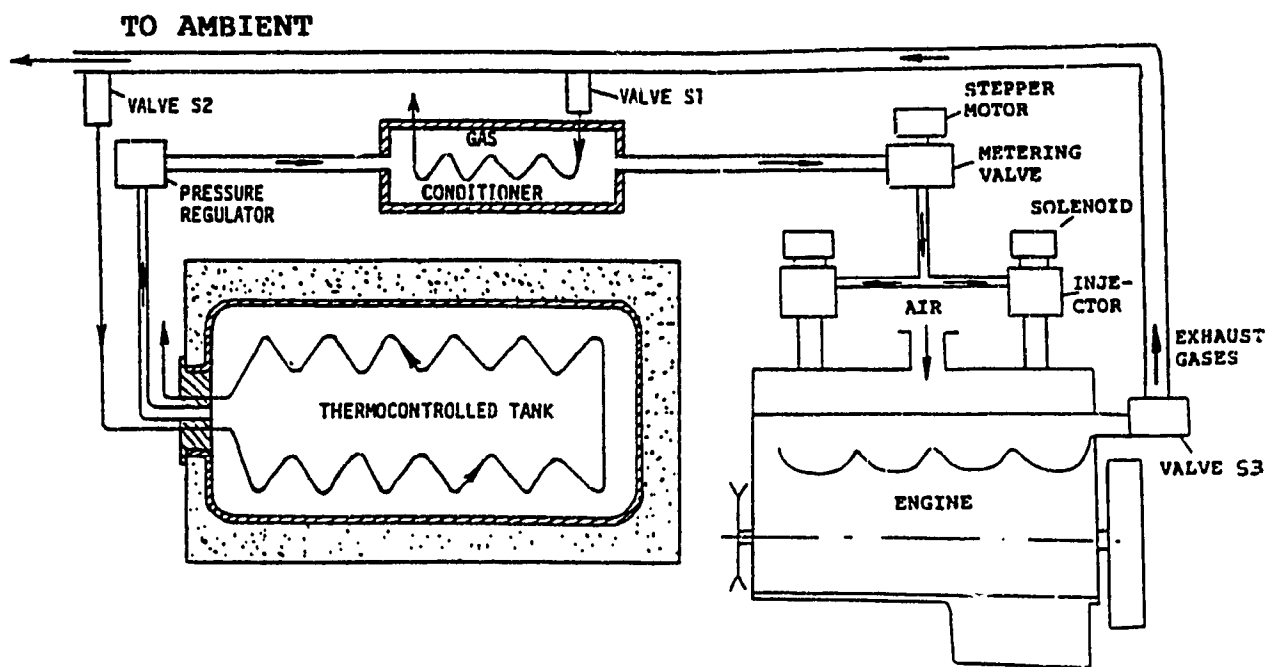


Fig. 6.4 Proposed gas storage and supply system for a car

#### **6.4 Practical Aspects of Thermocontrolled Tank Use**

At refuelling, the liquid fuel will be loaded first into the thermocontrolled tanks. Heat transfer from the tank walls to the cold fuel will then follow, causing evaporation of a portion of the liquid. This change in phase is anticipated as a factor providing the required temperature and pressure increase inside the tank. After the scheduled portion of the liquid fuel is introduced into the tank, some compressed gas could be added, if required to increase the gas pressure to over 100 bar (pressure required for direct injection of the fuel into the cylinder) so that the vehicle may be operated immediately.

When the vehicle comes for refuelling with the tank still filled with residual gas under pressure, that gas would be first released into a storage container at the refuelling station until the pressure in the tank drops allowing for subsequent charging with the liquid fuel.

During operation of the vehicle, the gas pressure would be maintained at a level higher than 100 bar by heating the gas in the tank by means of the engine exhaust gases. The heating process would be controlled using the microprocessor. The minimum value of 100 bar gas pressure inside the thermocontrolled tank is dictated by the requirement for direct injection of gaseous fuels into the cylinder of the internal combustion engine.

**CHAPTER 7**  
**SIMULATION OF GASEOUS FUEL PROPERTIES**  
**IN A THERMOCONTROLLED TANK DURING VEHICLE OPERATION**

**7.1 Preliminaries**

The mathematical model which was developed in Chapter 3 had been validated in Chapter 4. Also a thermocontrolled tank design had been optimized in Chapter 5 for use in vehicles. The objective of this chapter is to study the pressure and temperature variation of the gaseous fuels inside the optimized thermocontrolled tank during the vehicle operation using the validated mathematical model. This will enable us to know how many hours the vehicle can be operated after each fill-up.

**7.2 Mathematical Model for Thermocontrolled Tank Installed in a Vehicle**

During operation of the vehicle, energy will be transported out of the tank at a rate depending on the engine fuel consumption. Taking this energy into account, the energy balance on the gaseous fuel inside the tank yields:

$$m_g C_g \frac{dT_g}{dt} = \frac{T_h - T_g}{R_{hg}} + \frac{T_t - T_g}{R_{gt}} - \dot{m}_g C_g T_g \quad (7.1)$$

The mass of the gaseous fuel,  $m_g$  in the tank is a function of time, depending on the driver's operation pattern and on the fuel consumption,

$$m_g = m_{gi} - \int \dot{m}_g d\tau \quad (7.2)$$

The other equations for the energy balance on the exhaust gas, Eq. (3.3), heat exchanger pipe, Eq. (3.5) and the tank wall, Eq. (3.7) have been presented previously in Chapter 3 and remain the same.

### 7.3 Simulation of Gaseous Fuel Properties during Bus Operation

The objective of this simulation is to find out:

- 1) How much time is required after the filling up, to increase the gas pressure in the tank and to reach the required pressure for direct gas injection, i.e., the 100 bar pressure limit.
- 2) How long the vehicle could be parked safely after refuelling, without releasing any gas from the tank.
- 3) How long will the bus operate before the pressure falls down to the level below 100 bar without additional heating.
- 4) How long will the bus operate with additional gas heating, using engine

exhaust gases.

- 5) How much fuel would be left over in the tank before next refuelling.

The bus operation schedule, based on the data derived in Chapter 6, is shown in Fig. 7.1 for both, hydrogen and natural gas. As could be predicted, the time between refuelling for the bus is twice as many times for hydrogen than for natural gas. Still the operation on hydrogen is feasible, assuming that the bus will more frequently return to its initial point, where the central refuelling facility is available and that the bus operational schedule will be not much affected by the refuelling procedure.

When the tank of the bus is being filled-up with liquefied fuel, the heat from the tank walls immediately starts to vaporize part of the liquid. Therefore, the filling of the tank should be under high enough pressure from a pressurized cryogenic tank, with a vent in the tank open so that the pressure in the tank does not rise too high making the filling process difficult.

After the strictly determined portion of the liquefied gas has been delivered to the tank, the valves will be closed and the gas temperature and pressure will rise, due to the heat transfer, first from the cylinder walls and next through the walls from the ambient. When the bus is in operation, mass and energy is carried out of the cylinder by the gaseous fuel flow. The gas which remains in the tank undergoes an expansion process. The gas temperature and pressure in the tank are the result of two processes: the heat transfer to the tank, which increases the gas

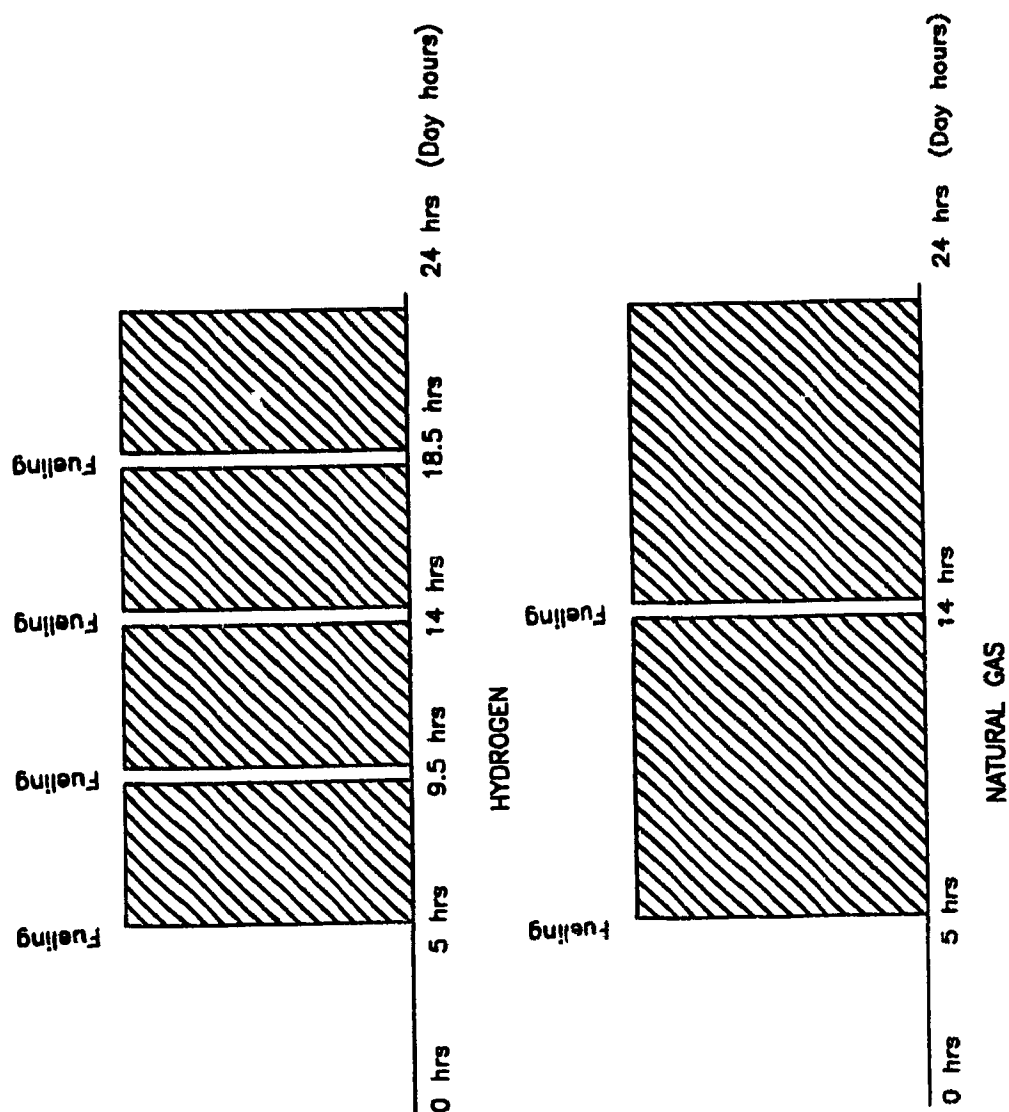


Fig. 7.1 Bus operational schedule for gaseous fuel use

temperature and the gas extraction, which lowers the gas temperature. The resulting temperature can be controlled by the exhaust gas circulation around the tank.

### 7.3.1 Simulation of Hydrogen Properties

Computer simulation of the bus operation has been carried out based on the following assumptions:

- 1) The bus tank content is 55 kg of hydrogen and the gas consumption is 12 kg/hr.
- 2) The bus is running continuously; bus stops to take passengers are not taken into consideration.
- 3) The hydrogen pressure should not exceed 500 bar and should not be lower than 100 bar during the bus operation.

Two cases have been simulated, namely: operation starts at 100 bar (case H1) and operation starts when pressure is 500 bar (case H2). The corresponding results are as follows:

**Case Bus H1, Fig. 7.2** Bus starts its operation just after the pressure in the tank reaches 100 bar; gas heating impact is shown to maintain the pressure required for direct injection and to use the fuel in the tank to the maximum possible extent.

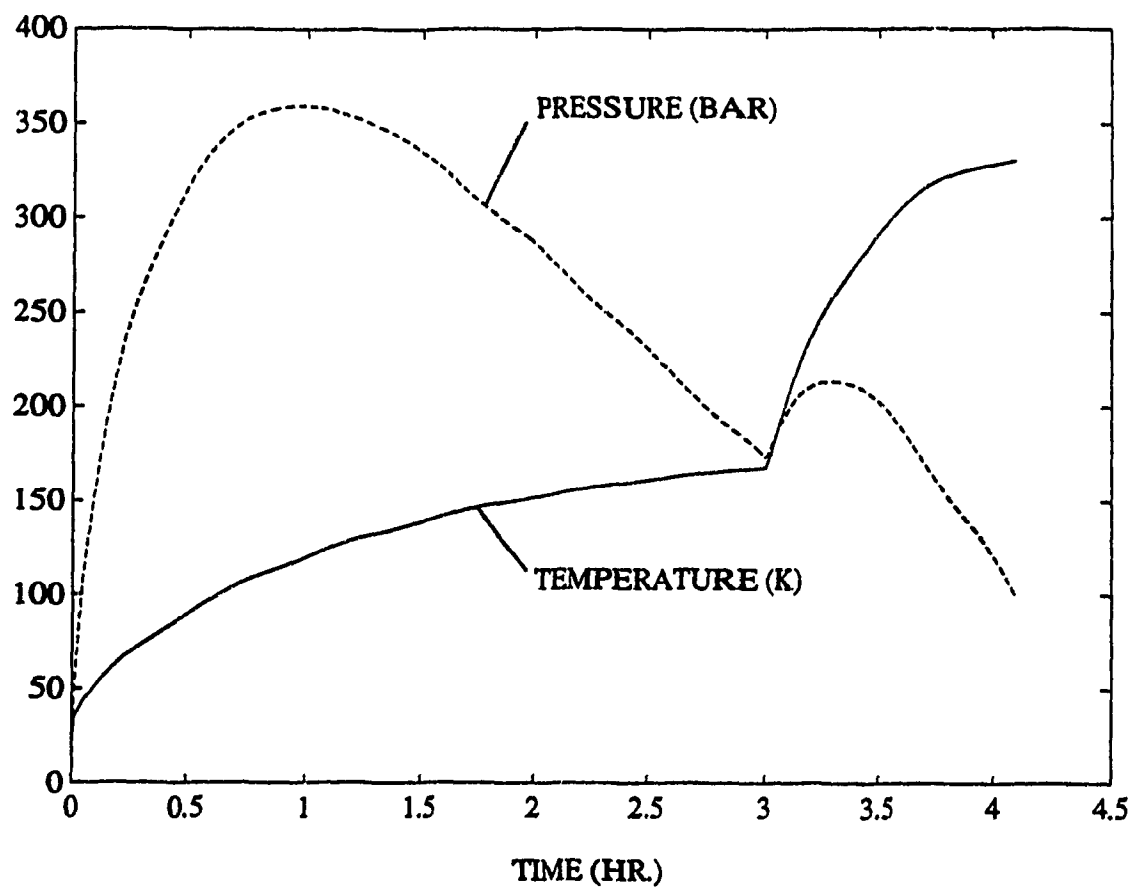
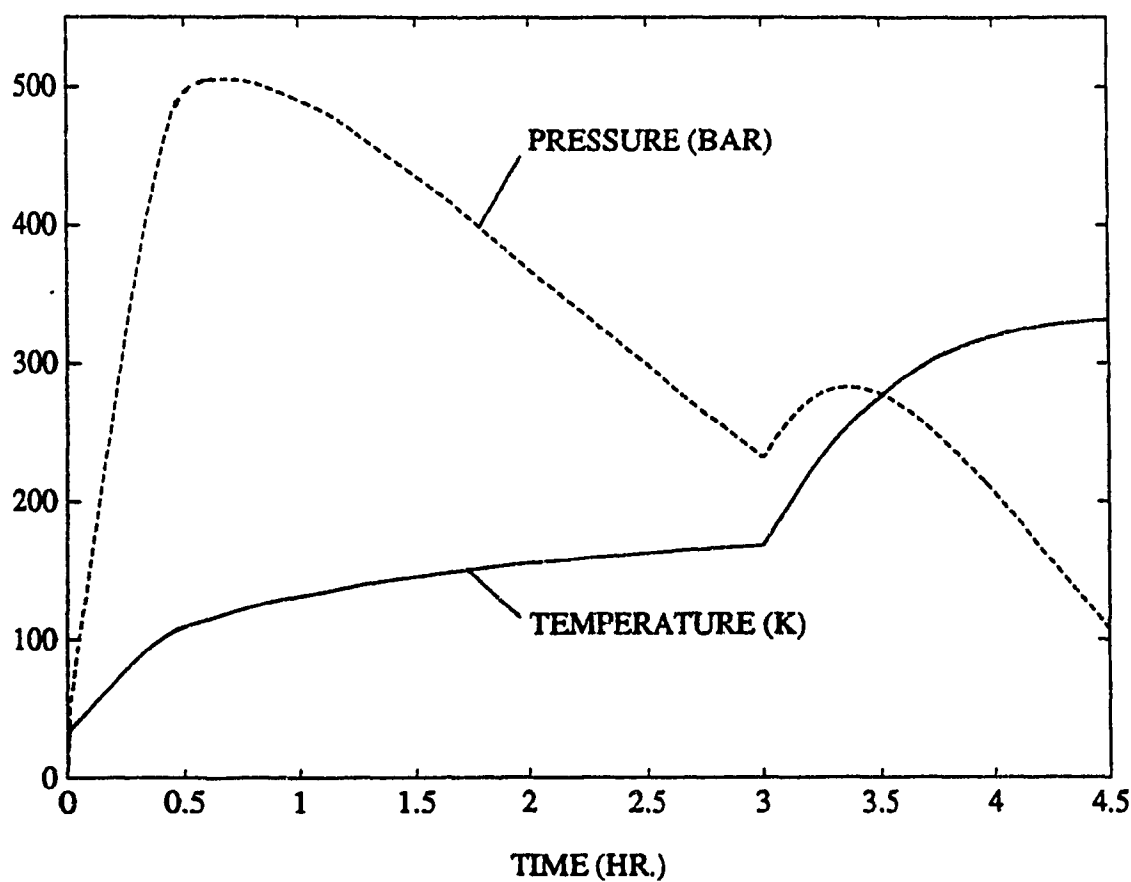


Fig. 7.2 Case Bus H1: Bus starts operation just after the pressure in the tank reaches 100 bar

**Case Bus H2, Fig. 7.3** Bus starts its operation just before the gas pressure reaches 500 bar; gas heating impact is also shown.



**Fig. 7.3** Case Bus H2: Bus starts operation just before the pressure in the tank reaches 500 bar

From the simulation results of the two cases, Fig. 7.2 and Fig. 7.3, it can be seen that the initial pressure of 100 bar required for direct injection can be achieved in less than 5 min. time after closing the valves of the tank. So the driver does not have to wait longer for the pressure to build up. On the other hand, the driver has a maximum time limit of about 0.5 hr to start the bus, in order not to release any gas from the tank. This time limit gives the driver some flexibility to start the vehicle. Also it was observed that heating the hydrogen gas using exhaust gases increases the operational time of the vehicle by upto 15%.

### **7.3.2 Simulation of Natural Gas Properties**

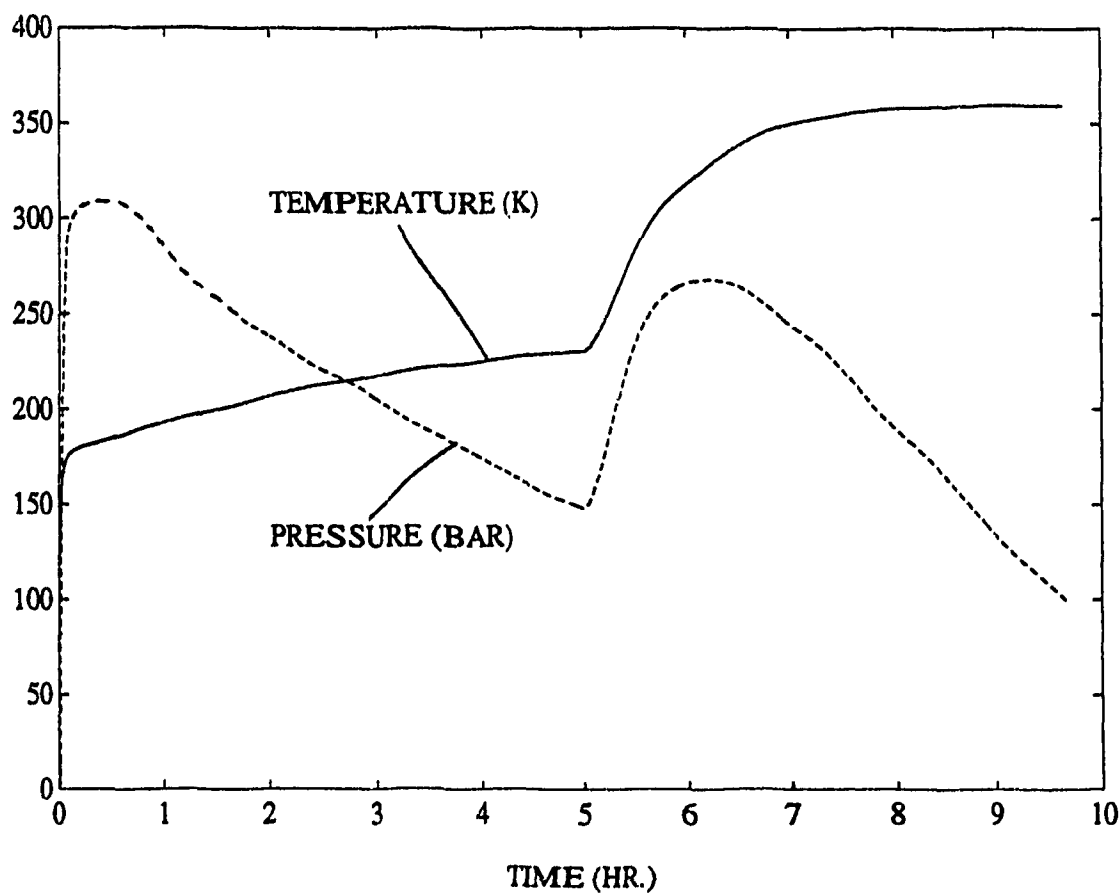
Computer simulation of the bus operation has been carried out based on the following assumptions:

- 1) The bus tank content is 340 kg of natural gas and consumption of the gas is 30 kg/hr.
- 2) The bus is running continuously; bus stops to take passengers are not taken into consideration.
- 3) The natural gas pressure should not exceed 500 bar and should not be lower than 100 bar during the bus operation.

Two cases have been simulated, namely: operation starts at 100 bar (case N1) and operation starts when pressure is 500 bar (case N2). The corresponding results are

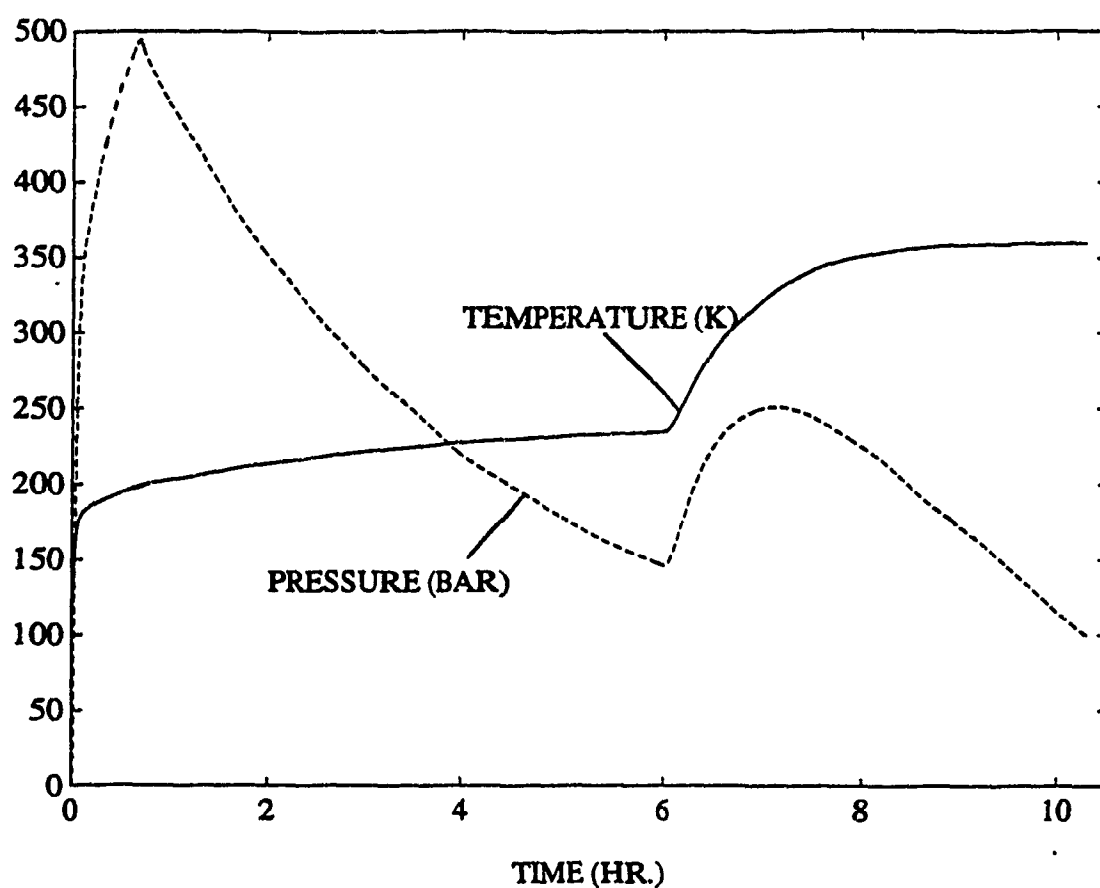
as follows:

**Case Bus N1, Fig. 7.4** The bus starts its operation just after the pressure in the tank reaches 100 bar; gas heating impact is shown to maintain the gas pressure required for direct injection and increase the utilization of the fuel content in the tank.



**Fig. 7.4** Case Bus N1: Bus starts operation just after the pressure in the tank reaches 100 bar

**Case Bus N2, Fig. 7.5**     Bus starts its operation just before the gas pressure reaches 500 bar; gas heating impact is also shown.



**Fig. 7.5**     Case Bus N2: Bus starts operation just before the pressure in the tank reaches 500 bar

From the Fig. 7.4 and Fig. 7.5, it can be seen that the raise in temperature is not large when compared with the rise in pressure at the beginning. This is because of the presence of a greater mass of liquefied natural gas in the tank as compared with hydrogen and, therefore, it takes more time and energy to evaporate and raise the temperature. When the vehicle is started after 100 bar pressure is reached (Fig. 7.4), the temperature and pressure of the gas inside the tank continue to raise for some time until all the stored energy from the vessel walls is transferred to the gas; then the pressure starts to drop. The rise in temperature is a result of two processes, which can be explained as follows: when the vehicle is in operation, mass and energy are carried out of the tank by the fuel flow. The gas that remains in the tank undergoes an extraction process. Also heat flows from the ambient through the tank wall to the gaseous fuel.

After 6 hrs. of continuous bus operation, the pressure falls to 100 bar level and at that time it is required to circulate the exhaust gases over the tank. It can be concluded that in this type of tank, heat addition from exhaust gases could be avoided if the tank wall design would provide the tank with higher heat transfer through the walls, so that the ambient gas temperature and a higher gas pressure could be reached at the end of the run.

#### **7.4 Simulation of Gaseous Fuel Properties during Car Operation**

The operation with the thermocontrolled tank, in case of a car which has to run and stop at different time intervals, requires an insulated tank, which would prevent the gas pressure to exceed the design maximum pressure limit. It would also need gas heating if the car has to run continuously. Simulation of the tank behaviour has been carried out to determine:

- 1) How much time is needed after the vehicle refuelling, to increase the gas pressure in the tank to 100 bar level.
- 2) How much time is available prior to the start of the car operation i.e., the gas extraction from the tank before it reaches the maximum design pressure.
- 3) How long will the car operate continuously with and without gas heating, before the tank pressure falls back to 100 bar.
- 4) How will the properties of the fuel inside the tank change on a week-schedule of the car, assuming regular commuting and parking of the car. In this case, it is assumed that the owner drives the car in the morning to work, parks there for 8 hrs. and drives back home.
- 5) How much gas would be left unused in the tank before the car needs to be refuelled.

The car operation schedule, based on the data derived in Chapter 6, is shown

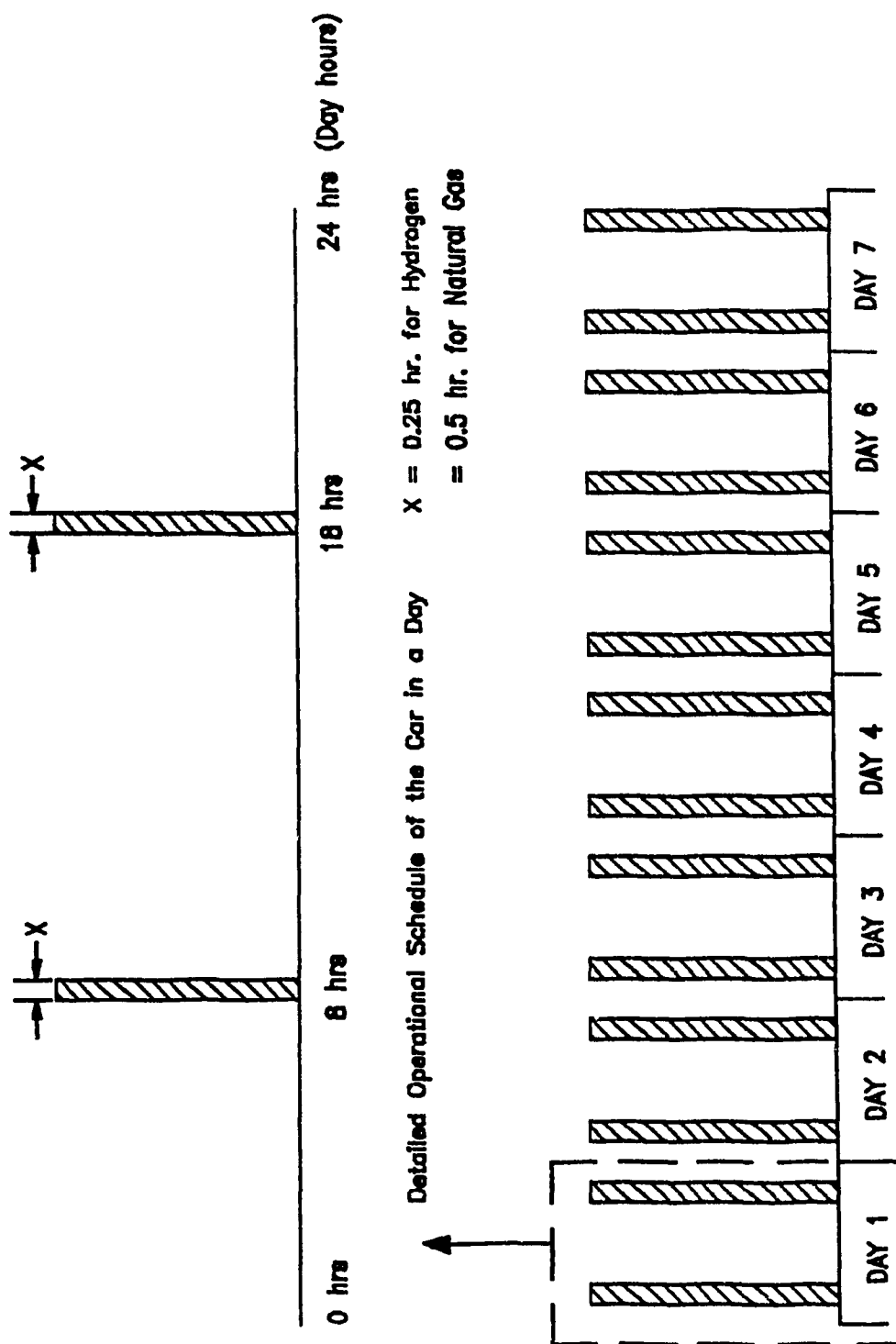


Fig. 7.6 Car operational schedule for natural gas and hydrogen

in Fig. 7.6, for both hydrogen and natural gas on a week schedule. Due to the tank insulation, the car could be parked for a longer time, particularly, after a part of the gas content has been consumed. This would require some attention from the car owner to confirm to the car refuelling pattern. Again, it can be expected that with natural gas the range of the car before refuelling can be several times longer than with hydrogen.

#### **7.4.1 Simulation of Hydrogen Properties**

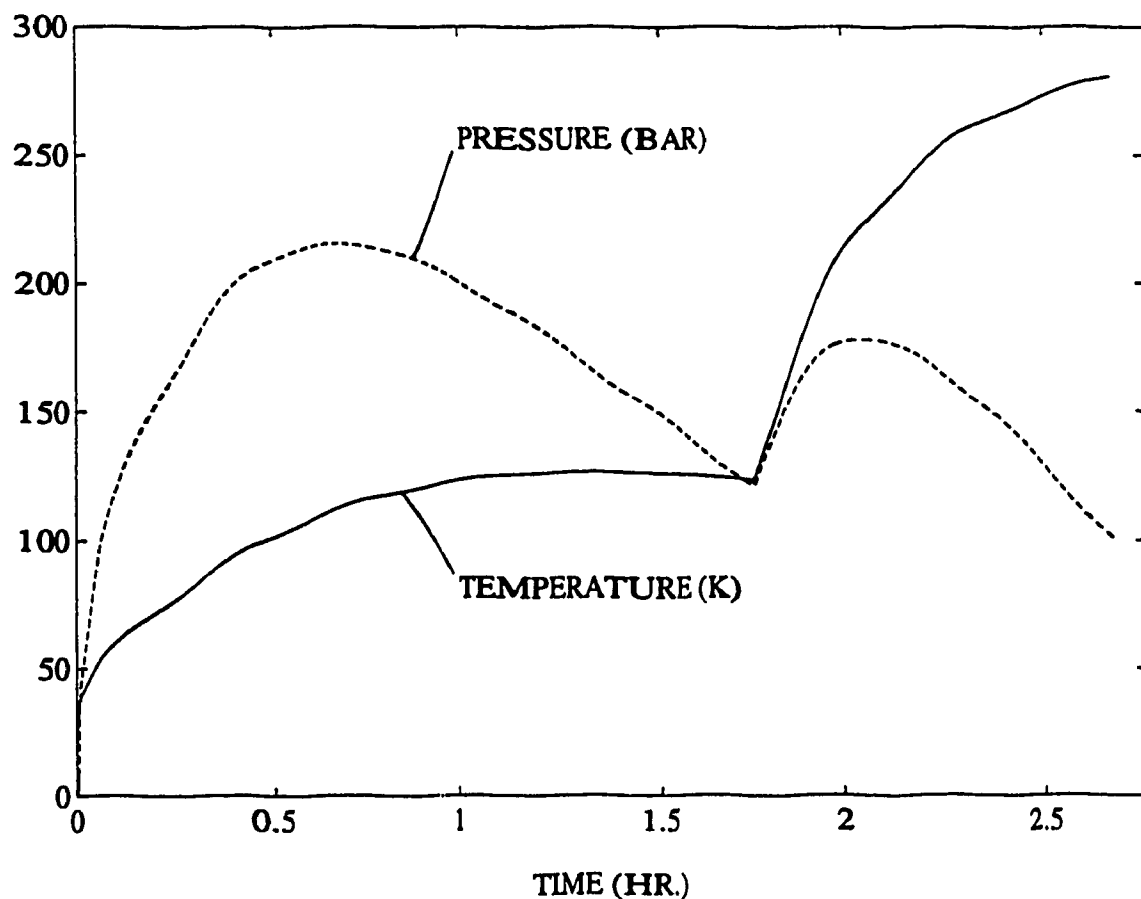
Computer simulation of car operation has been carried out based on the following assumptions:

- 1) The car tank content is 9 kg of hydrogen and the gas consumption is 2.2 kg/hr.
- 2) The car is running in two different modes: continuously or in a week commuting and parking schedule.
- 3) The hydrogen pressure should not exceed 500 bar and should not be lower than 100 bar during car operation.

Three cases have been simulated, namely: operation starts at 100 bar and runs continuously (case H1), the tank is charged with 25% more gas, assuming that it will start operation immediately after refuelling (case H2) and operation starts at the beginning of the week-schedule with a short commuting trip (case H3). The

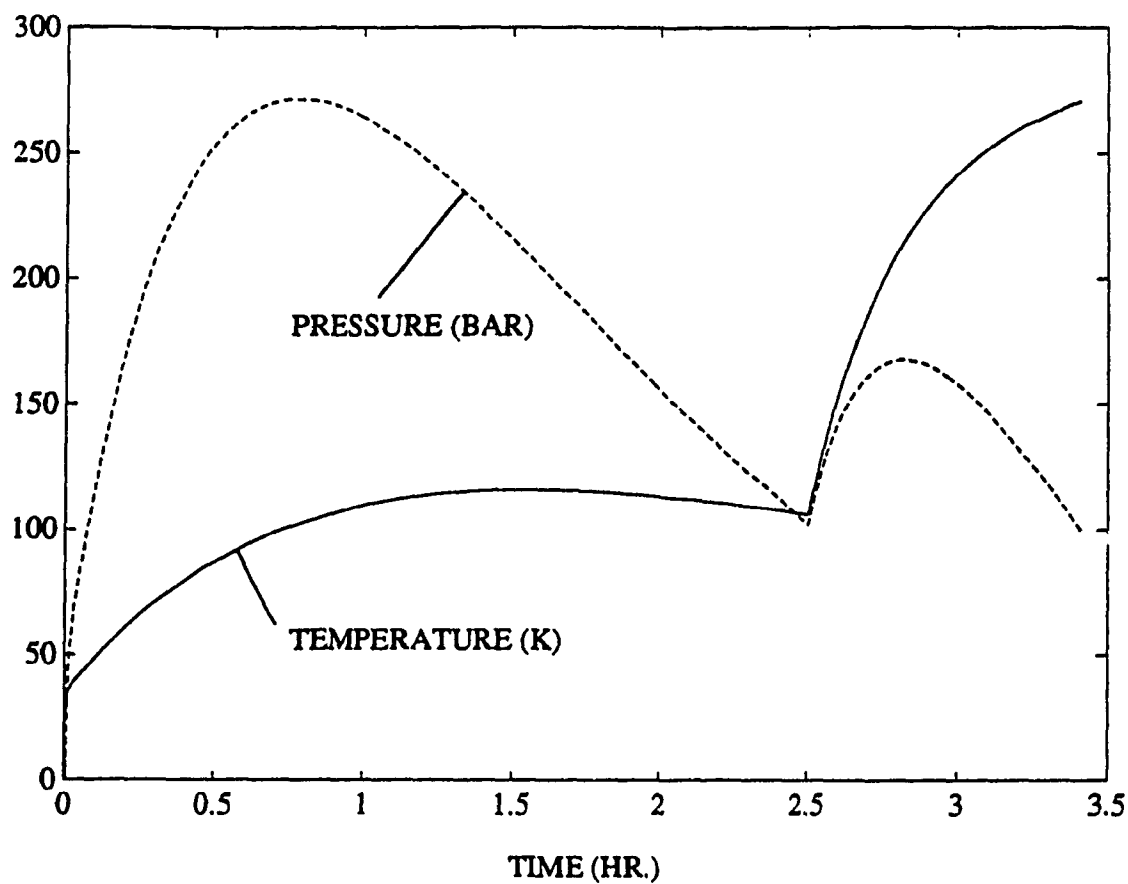
corresponding results are as follows:

**Case Car H1, Fig. 7.7** Car starts its operation just after the pressure in the tank reaches 100 bar. It runs continuously, until the pressure drops to 100 bar; gas heating impact is shown to maintain the pressure required for direct injection before the end of operation.



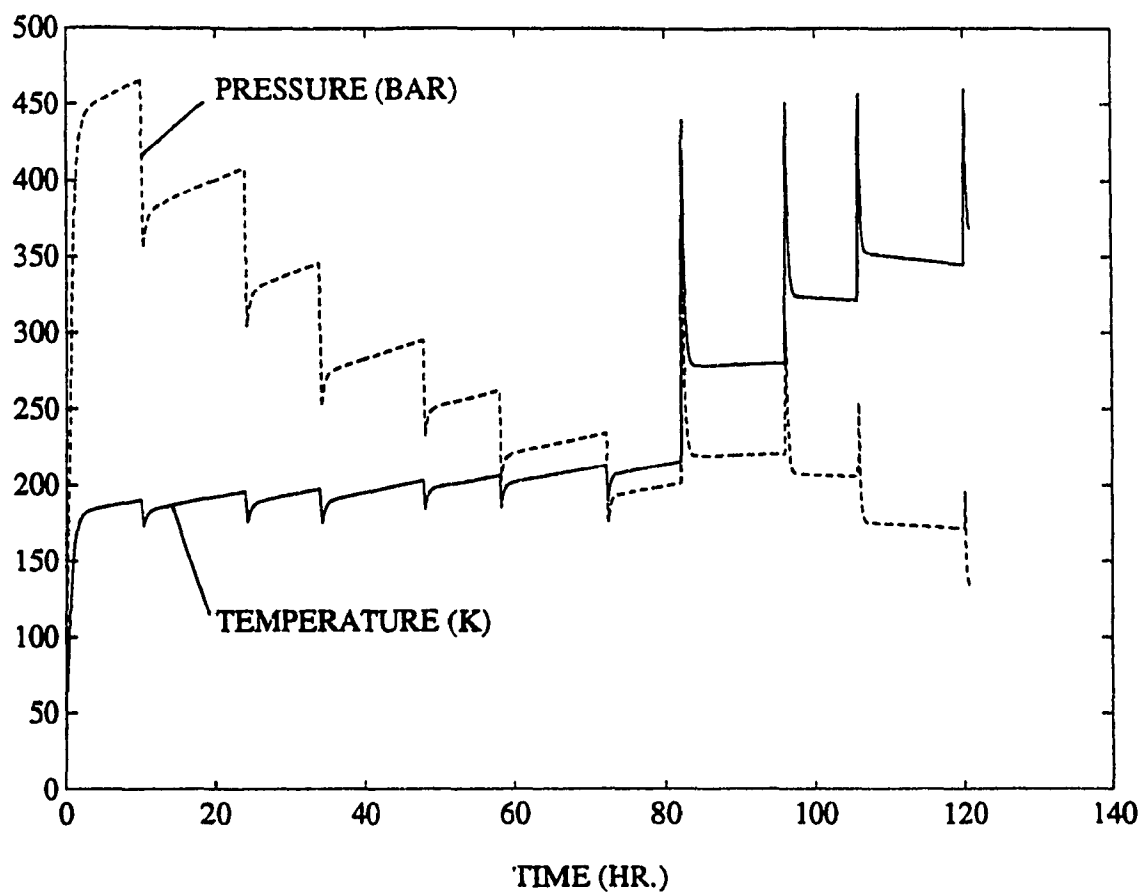
**Fig. 7.7** Case Car H1: Car starts operation just after the pressure in the tank reaches 100 bar; it runs continuously until the pressure drops to 100 bar

**Case Car H2, Fig. 7.8** The tank of the car is charged with 25% more gas, taking into account the fact that it will start its operation immediately after refuelling so that the pressure in the tank does not rise too high.



**Fig. 7.8** Case Car H2: The tank of the car is charged with 25% more gas, assuming that it will start operation immediately after refuelling

**Case Car H3, Fig.7.9** Car starts its operation at the beginning of the Week-schedule with a short commuting trip; the gas heating impact is also shown.



**Fig. 7.9** Case Car H3: Car starts its operation at the beginning of the week-schedule with a short commuting trip

When the car is refuelled with hydrogen, the initial pressure of 100 bar required for direct injection can be obtained in less than 5 min. time. In the continuous mode when the vehicle is running (Fig. 7.7), after 1.5 hrs. of operation, the exhaust gas circulation through the heat exchanger should be started to keep the pressure above 100 bar. Also if the driver wants to go on a longer trip, the same tank could be filled with 25% more gas. This was shown in Fig. 7.8. In this case, the maximum pressure reached is more than in case 1 (Fig. 7.7), but well under the operating maximum pressure of 500 bar.

In a weekly commuting and parking schedule, just after the refuelling, the car will be driven for 15 min. to work. Initially the pressure and temperature drop cannot be seen because of the gas expansion being dominated by the temperature rise resulting from the heat transfer directly from vessel walls. A drop in hydrogen pressure is observed, accompanied by a smaller temperature drop when driving back from work for 15 min. However, the drops in temperature during the run are compensated by the heat transfer through the tank insulation during the parking time, so that the temperature remains almost constant. At the end of the fourth day, heat is added from the exhaust gases to increase the gas temperature in the tank to increase the gas pressure. Finally, during the sixth day, the pressure level drops below 100 bar, when refuelling is required.

The following observations can be made from this simulation: first, when hydrogen is drawn from a well insulated tank, not only the pressure but also the

temperature falls, according to the equations of state. Then, even if the temperature increases, due to some heat transfer through the insulation, it cannot reach the ambient temperature without additional tank preheating by the exhaust gases. Second, in the insulated tank, not only the gas, but also the tank walls must be heated to maintain the gas pressure. This indicates that the heat transfer mechanism from the exhaust gas to the tank, i.e., the size and effectiveness of the heat exchanger, are critical to this concept. It is also observed that at the end of each run with heat transfer from exhaust gases, the hydrogen temperature falls down for a while before stabilizing at a new level. This is due to the fact that the heat received from the heat exchanger is absorbed by the tank walls.

#### **7.4.2 Simulation of Natural Gas Properties**

Computer simulation of car operation on natural gas has been carried out based on the following assumptions:

- 1) The car tank content is 42 kg of natural gas and the gas consumption is 4 kg/hr.
- 2) The car is running in two different modes: continuously or in a weekly commuting and parking schedule.
- 3) The natural gas pressure should not exceed 500 bar and should not be lower than 100 bar during the car operation.

Two cases have been simulated, namely: operation starts at 100 bar and runs continuously (case N1) and operation starts at the beginning of the week-schedule with a short commuting trip (case N2). The corresponding results are as follows:

**Case Car N1, Fig. 7.10** Car starts its operation just after the pressure in the tank reaches 100 bar. It runs continuously until the pressure drops to 100 bar; gas heating impact is shown to maintain the pressure required for direct injection before the end of operation.

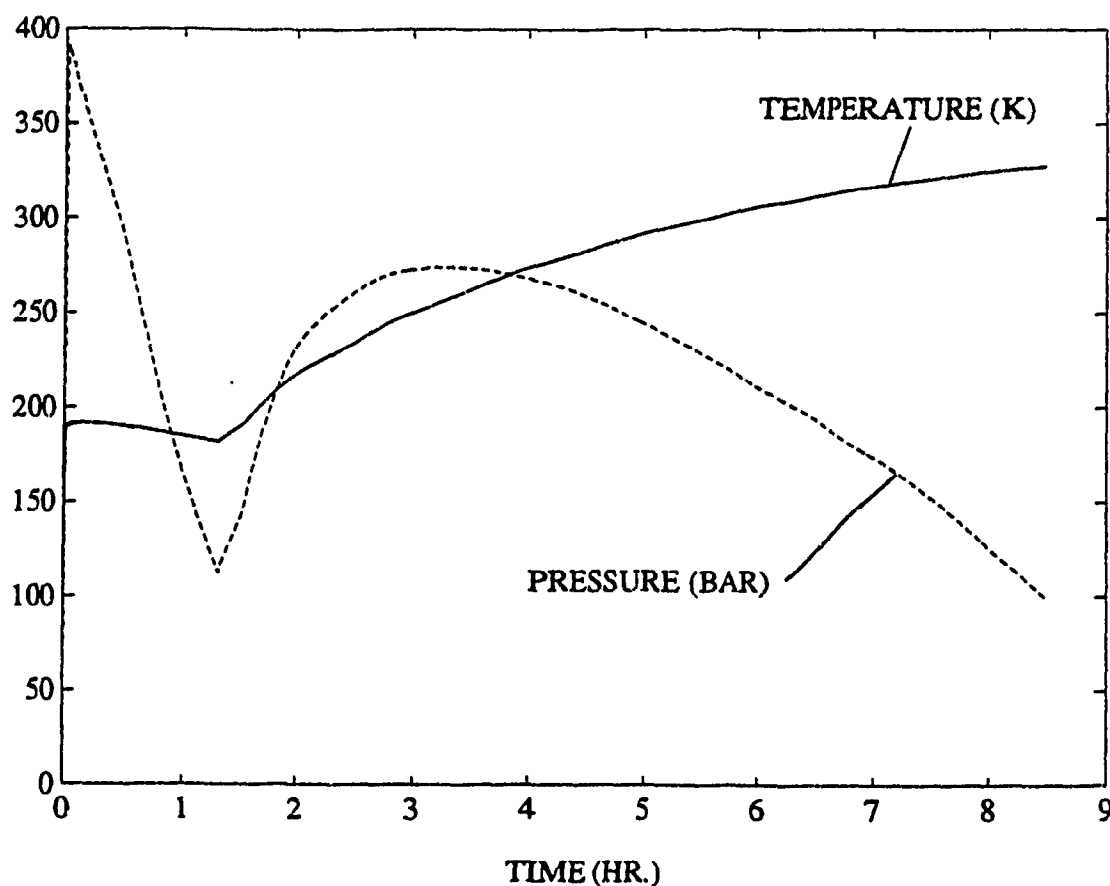
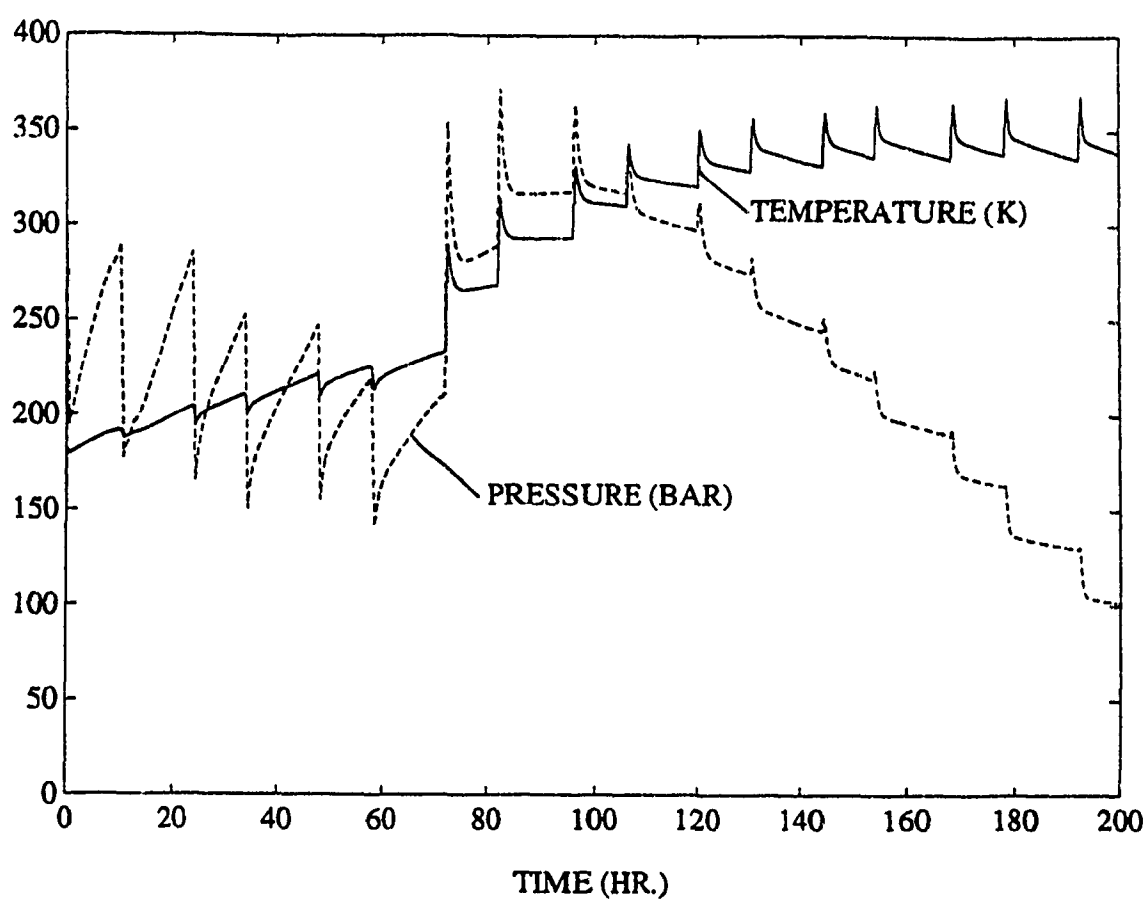


Fig. 7.10 Case Car N1: Car starts operation just after the pressure in the tank reaches 100 bar; it runs continuously until the pressure drops to 100 bar

**Case Car N2, Fig. 7.11** Car starts its operation at the beginning of the week schedule, with a short commuting trip. The gas heating impact is also shown.



**Fig. 7.11** Case Car N2: Car starts its operation at the beginning of the week-schedule with frequent commuting trips

Since the gas mass to vessel weight ratio of natural gas is higher than that of hydrogen (0.4 vs 0.05), the amount of liquefied natural gas that can be filled into the tank will be more compared with hydrogen. Because of the larger mass of liquefied gas present in the tank, the initial temperature rise will be slower and will result in a high pressure build-up at a relatively low temperature. The initial temperature rise is the result of the energy transfer between the liquefied gas and the tank walls which are at the room temperature. Once the energy stored in the vessel walls is transferred to the natural gas, the heat transfer has to start from the ambient air. Since the tank in a car is well insulated, the heat transfer rate from the ambient air to the gas is very low. Also the vehicle is in operation at that time (Fig. 7.10) and the resulting temperature drop inside the tank, due to the expansion process, limits the temperature rise resulting from the heat transfer from ambient. Hence, a longer heating period is required in this case to prevent the pressure drop below 100 bar level and to make the concept feasible.

In a weekly commuting and stopping schedule (Fig. 7.11), the car will be driven in the morning for 30 min. to work. It will be parked for 8 hrs and driven back home in the evening. The small pressure and temperature drops during each run are compensated by the heat transfer through the tank insulation during the long parking time. The operational time of the car with additional heat transfer from exhaust gases is smaller, as compared with the case 1, but, is still much higher, as compared with the corresponding case of hydrogen car (Fig. 7.9).

## 7.5 Conclusions

The following general observations could be made regarding the results of computer simulation of different thermocontrolled tank applications:

It is clearly seen, that the operation on hydrogen is much handicapped by the low density of the gas, as compared with natural gas; however, for both applications: the bus and the car, it might be still feasible if a limited, strictly determined operational schedule could be imposed. This is particularly possible for a bus, which can have an exact timing and usually operates from the same place, where the central refuelling facility could be located.

Operation on natural gas seems not to be a problem, providing that the gas storage and supply system would be reliable and affordable. It was also observed that the pressure inside the natural gas tank drops very fast, which requires an early start for the heating of the stored fuel using exhaust gases. Also, the temperature drop resulting from the gas extraction is smaller than for hydrogen, mainly due to the larger mass of gas in the tank, as compared with the extraction rate.

In a car, the tank has to be insulated to allow for some longer waiting periods without allowing the gas to reach excessive pressure. Then, of course, higher heating rate is required to maintain the gas pressure and to extract more gas from the tank. So, a trade-off between heating and insulation could be made, heating being a more controllable factor. In the case of a car, which could be

parked for a long time after refuelling, there is a need for much better insulation, which, with the existing cryogenic technology, does not create a major problem; however, it might be expensive. Hence, for the best tank performance, a strict car operation schedule is important.

## **CHAPTER 8**

### **OPTIMIZATION OF ON-BOARD GAS STORAGE SYSTEMS**

#### **8.1 Preliminaries**

In this chapter, the on-board storage system for natural gas and hydrogen fuels has been optimized for use in a car and a bus. The basic vessel design, which was optimized in Chapter 5 has been used here. Also, the mathematical model which was developed for simulation in Chapter 7, has been used in this optimization.

#### **8.2 Design Objectives and Variables**

The following objectives have been identified as the important parameters which govern the performance of the gaseous fuel storage system.

##### **1. Initial Waiting Time**

The *initial waiting time* is the time elapsed between closing the tank valves after refuelling and the time to get the required pressure for direct injection, i.e., 100 bar pressure limit. The initial waiting time should be as short as possible in order to start the vehicle immediately after refuelling.

##### **2. Parking Time**

*Parking time* is the time during which a vehicle can be parked safely after

refuelling, without releasing the gas from the tank. This time should be maximum to allow the driver to park the vehicle, if needed, a short time after refuelling.

### 3. Range

This objective is to maximize the operational range of the vehicle at given storage conditions. It means that with the full fuel charge, the vehicle should be able to run longer, after the tank is filled up and closed.

### 4. Safe Pressure Ratio

The *safe pressure ratio* is defined as

$$\frac{\text{Max. gas pressure in the tank at any time during the vehicle operation}}{\text{Design maximum pressure}} \quad (8.1)$$

This ratio should always be low enough, to avoid any possible chances of gas release and wastage. If the vehicle is not running or during the traffic jams, the gas pressure should not exceed the design maximum pressure leading to the release and the loss of the gas through a safety valve.

The various design variables considered as factors affecting the optimal performance, are as follows:

#### 1. Mass of the Fuel

This is the amount of fuel present in the tank after refuelling and before starting the vehicle. The amount of fuel dictates the size of the tank, and hence the total weight of the vehicle which, in turn affects the fuel consumption of the vehicle.

## **2. Fuel Consumption**

*Fuel consumption* is the fuel consumed by the engine propelling the vehicle per unit time. It changes with several factors like the weight of the vehicle, speed, etc. In gas fuelled vehicles with thermocontrolled tanks, the fuel consumption is an important factor; if the fuel is not utilized in time, the pressure inside the tank may exceed the designed maximum value and the gas can be lost.

## **3. Heat Addition**

*Heat addition* is the amount of heat added to the gaseous fuel in the tank from the engine exhaust gases. When heat is added to the fuel in the tank, the pressure and temperature of the gaseous fuel will increase, allowing more gas to be extracted and the vehicle to run longer. The amount of heat added to the gaseous fuel from the engine exhaust gases can be controlled by the mass flow rate of exhaust gases using valves as indicated in Chapter 6.

## **4. Inside Volume of the Tank**

This represents the total inside volume of the storage tank. The total inside volume of the tank can be altered by changing the number of vessels or the length of the vessel unit.

## **5. Insulation Resistance**

*Insulation resistance* acts as a barrier towards the transfer of heat from the ambient to the gaseous fuel inside the thermocontrolled tank. This can be altered by either changing the thickness of insulation or by changing the thermal conductivity of the

insulating material. In vehicles where the space is not a constraint, such as buses, a thick layer of a low cost insulating material can be used. In passenger cars, where the trunk volume is limited, a thin layer of low thermal conductivity materials should be used, which might cost more.

### **8.3 Optimization of the Storage System for a Car**

#### **8.3.1 Design Parameter Sensitivity Study**

The effect of the design variables on particular objectives was studied by varying one of the variables and keeping the other variables fixed at their nominal values. Each time this variable was changed, the mathematical model was used to evaluate the objective function.

##### **8.3.1.1 Initial Waiting Time**

Fig. 8.1 and Fig. 8.2 present the results of initial waiting time for hydrogen and natural gas respectively. It can be seen from these figures that by increasing the amount of liquefied fuel charged into the vessel, the initial waiting time is decreased. Also the reduction of the total inside volume of the tank will have similar effect on the initial waiting time. This is because of the fact that when the volume of the tank is decreased, the gas present in the tank becomes more

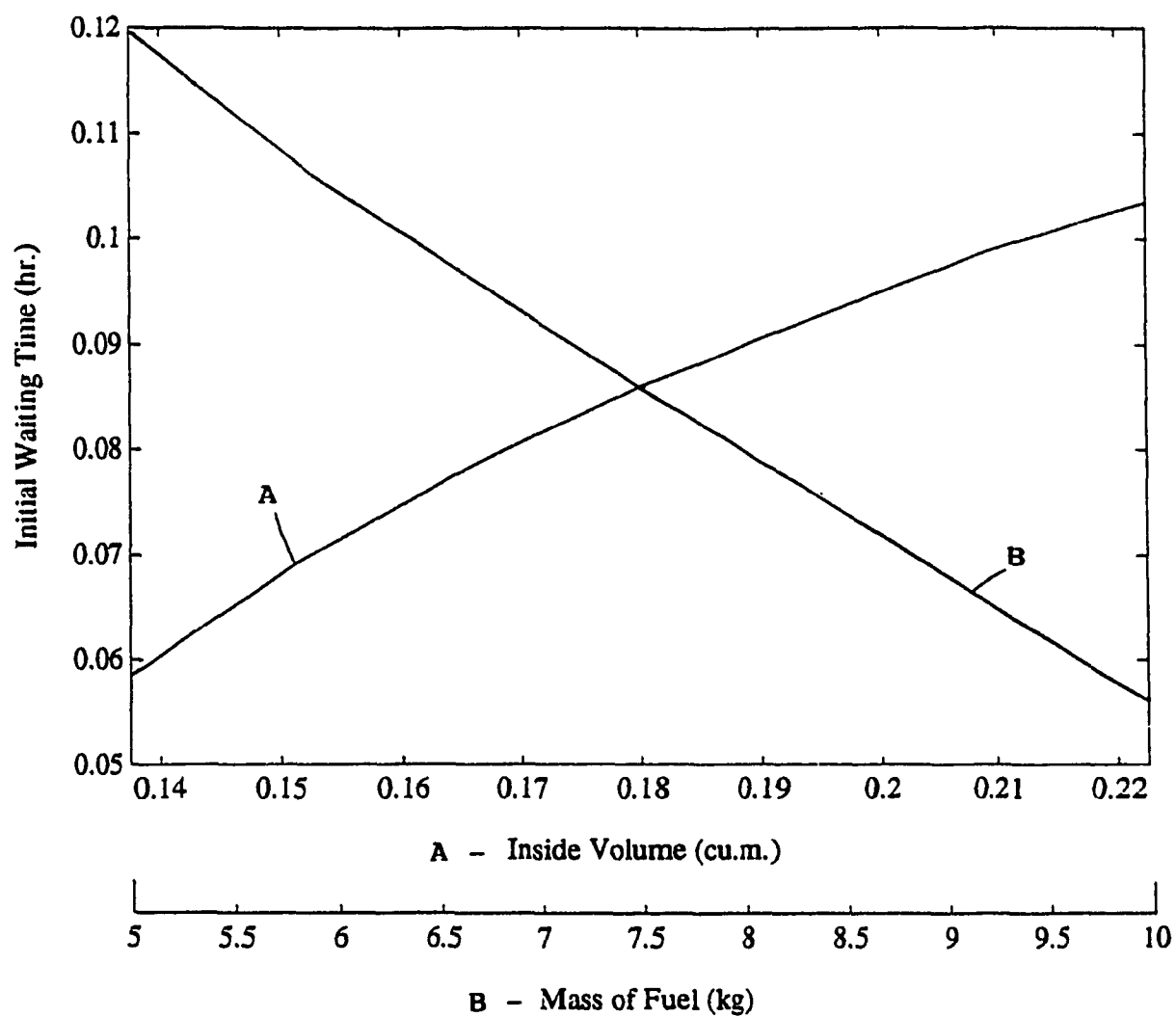


Fig. 8.1 Variation of initial waiting time with the change in variables for hydrogen car

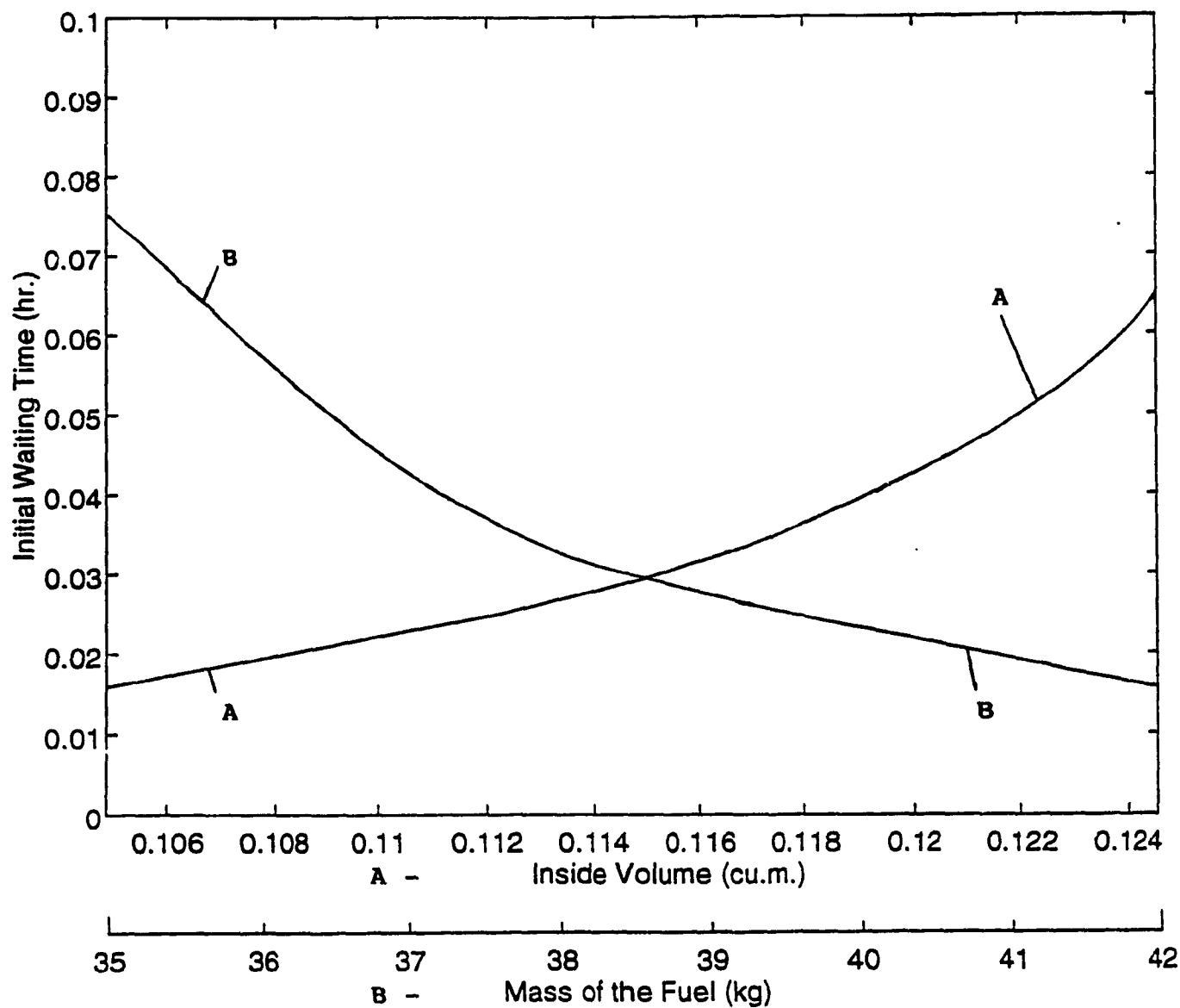


Fig. 8.2 Variation of initial waiting time with the design variables for natural gas car

compressed and then it takes less time to reach the 100 bar pressure level.

#### **8.3.1.2 Parking Time**

The simulation results of parking time for the hydrogen and the natural gas car are respectively presented in Fig. 8.3 and Fig. 8.4. The difference between these two sets of graphs (Fig. 8.1, 8.2 and 8.3, 8.4) is that the parking time can be well controlled by the insulation resistance, while the insulation resistance does not have much impact on the initial waiting time. This is because of the fact that the initial temperature rise and the resulting pressure increase are due to the heat transfer to the liquefied fuel from the walls of the vessel. Also, increasing the initial specific volume, either by increasing the total inside volume of the vessel or by decreasing the amount of fuel inside the vessel, increases the parking time of the car.

#### **8.3.1.3 Safe Pressure Ratio**

The impact of the design variables on the safe pressure ratio is shown in Fig. 8.5 and Fig. 8.6 for hydrogen and natural gas respectively. It can be seen that increasing the specific volume of the gas keeps the safe pressure ratio lower. Also, when the fuel is extracted at a higher rate or when the insulation resistance is

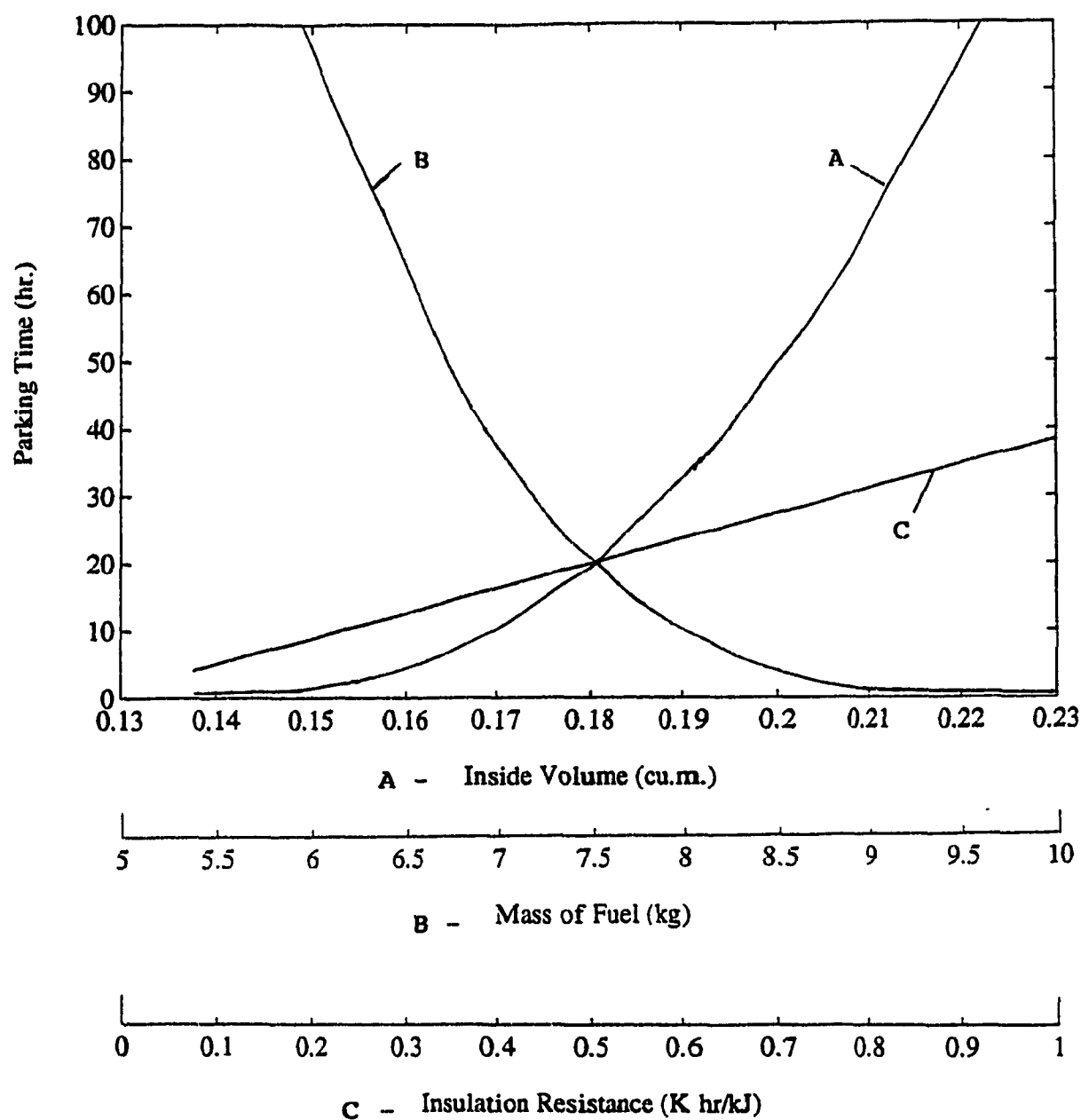


Fig. 8.3 Variation of parking time with the design variables for hydrogen car

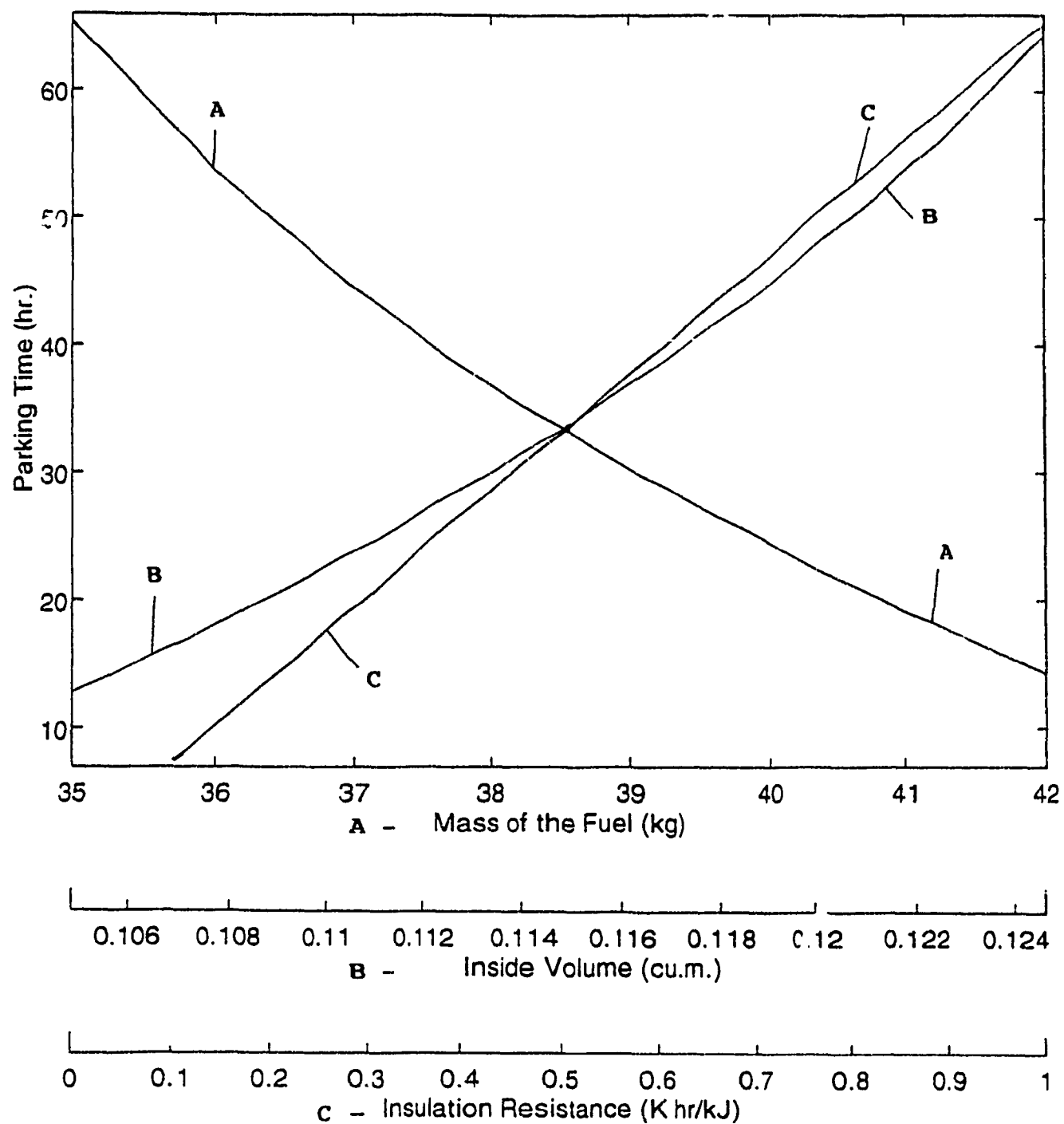


Fig. 8.4 Variation of parking time with the design variables for natural gas car

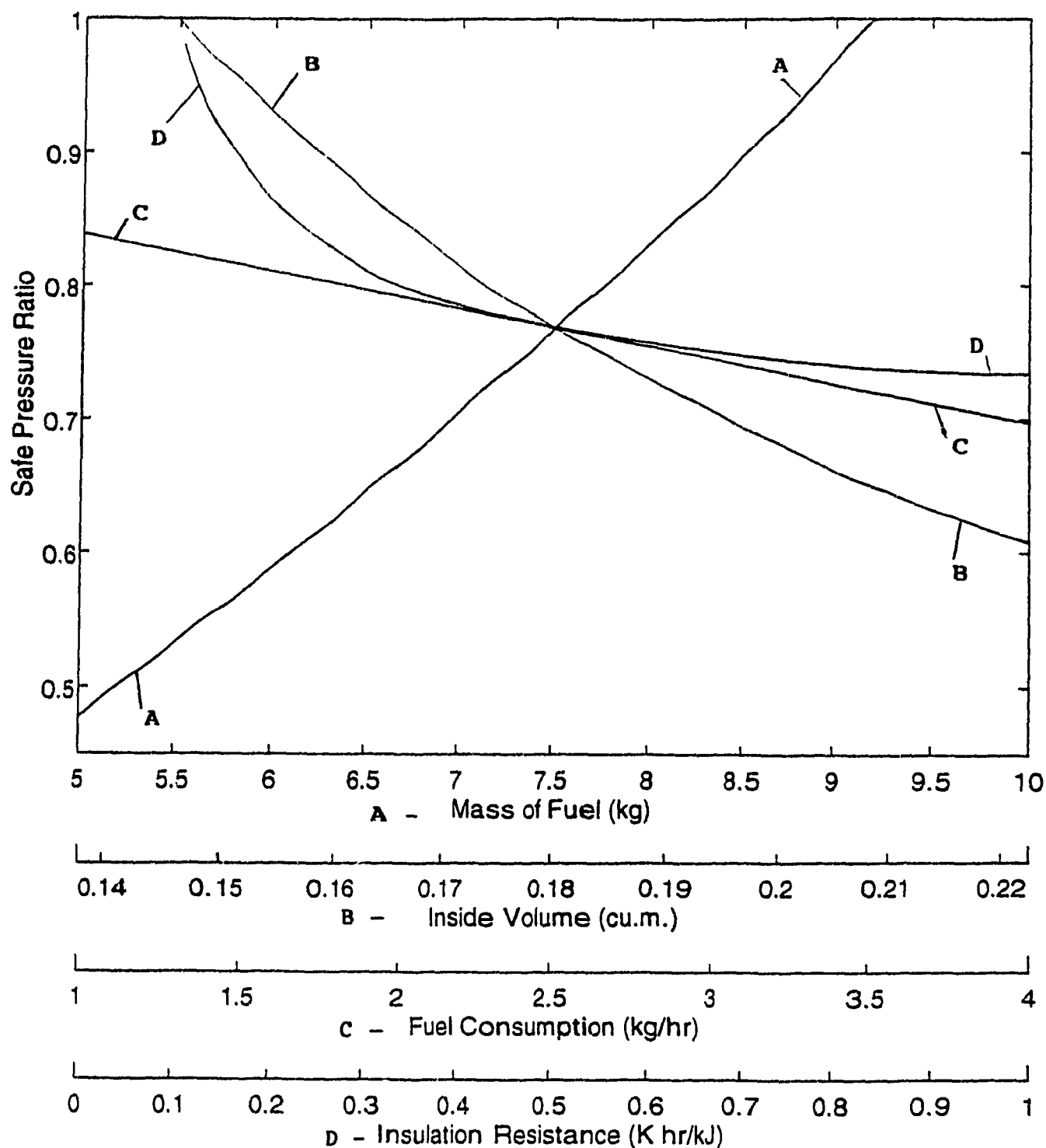


Fig. 8.5 Sensitivity of safe pressure ratio with design variables for hydrogen car

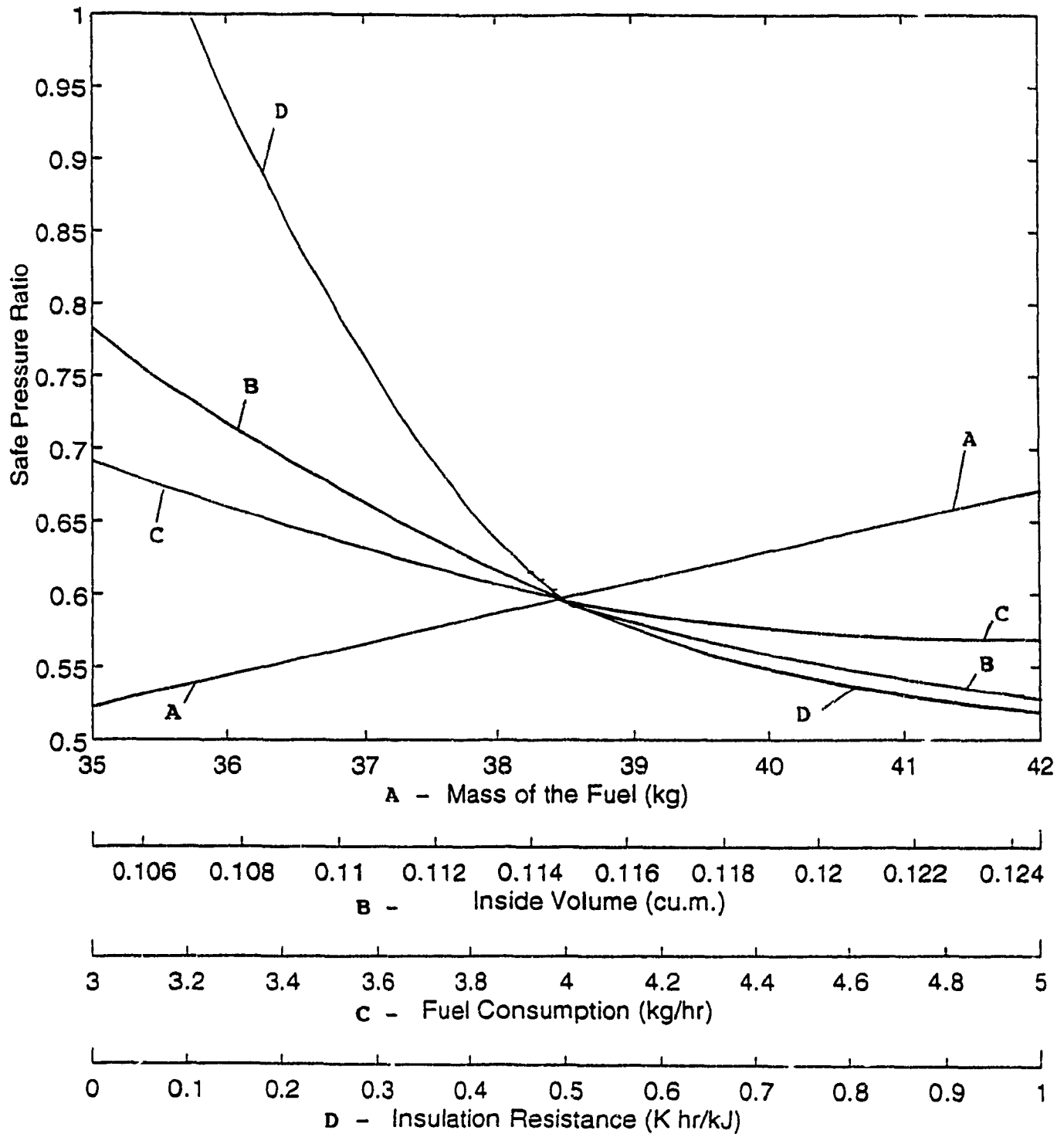


Fig. 8.6 Variation of safe pressure ratio with the design variables for natural gas car

increased, the safe pressure ratio will be lower. By comparing Fig. 8.5 and Fig. 8.6, it can be seen that the insulation resistance has a greater impact on the safe pressure ratio in natural gas tank when compared with the hydrogen tank. This is because the percentage filling (volume utilized/volume available \*100) of the tank with the liquefied natural gas is higher (70-85%) as compared with liquefied hydrogen (50-80%). This results in a higher pressure build-up in case of natural gas car when the vehicle is parked. By using a better insulating material, this rate of pressure rise could be reduced.

#### **8.3.1.4 Range**

For the vehicle range calculation, it was assumed that the car would be travelling at an average speed of 50 kmph. The simulation results of the range for hydrogen and natural gas cars are shown in Fig. 8.7 and Fig. 8.8. It was observed that, when all the other variables are kept constant at their nominal values, the heat addition will increase the range to a particular maximum value.

#### **8.3.2 Formulation of the Problem**

From the simulation results, four different expressions were established for the four objectives by linear multivariate regression analysis. Then, from the

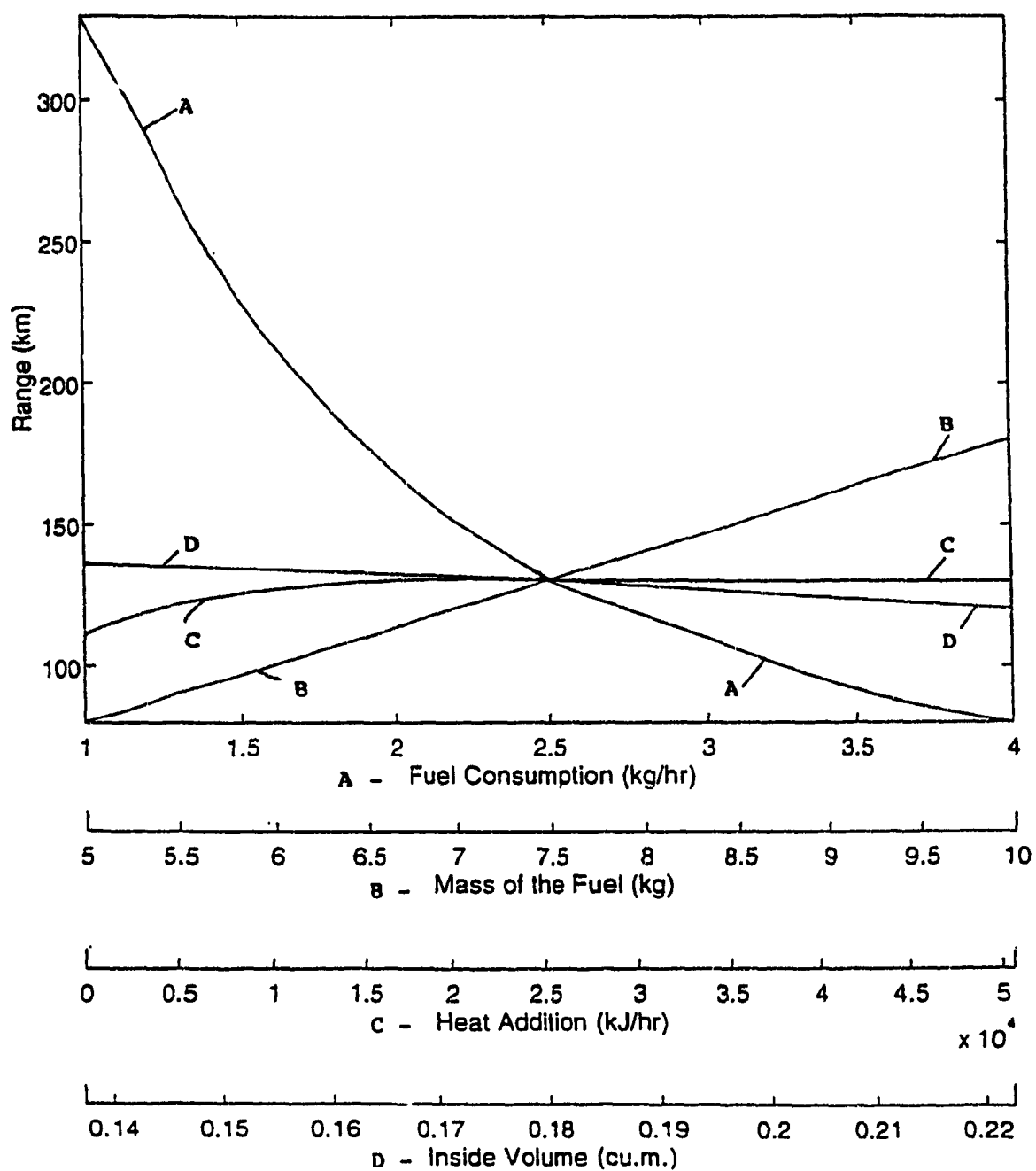


Fig. 8.7 Sensitivity of the range with design variables for hydrogen car

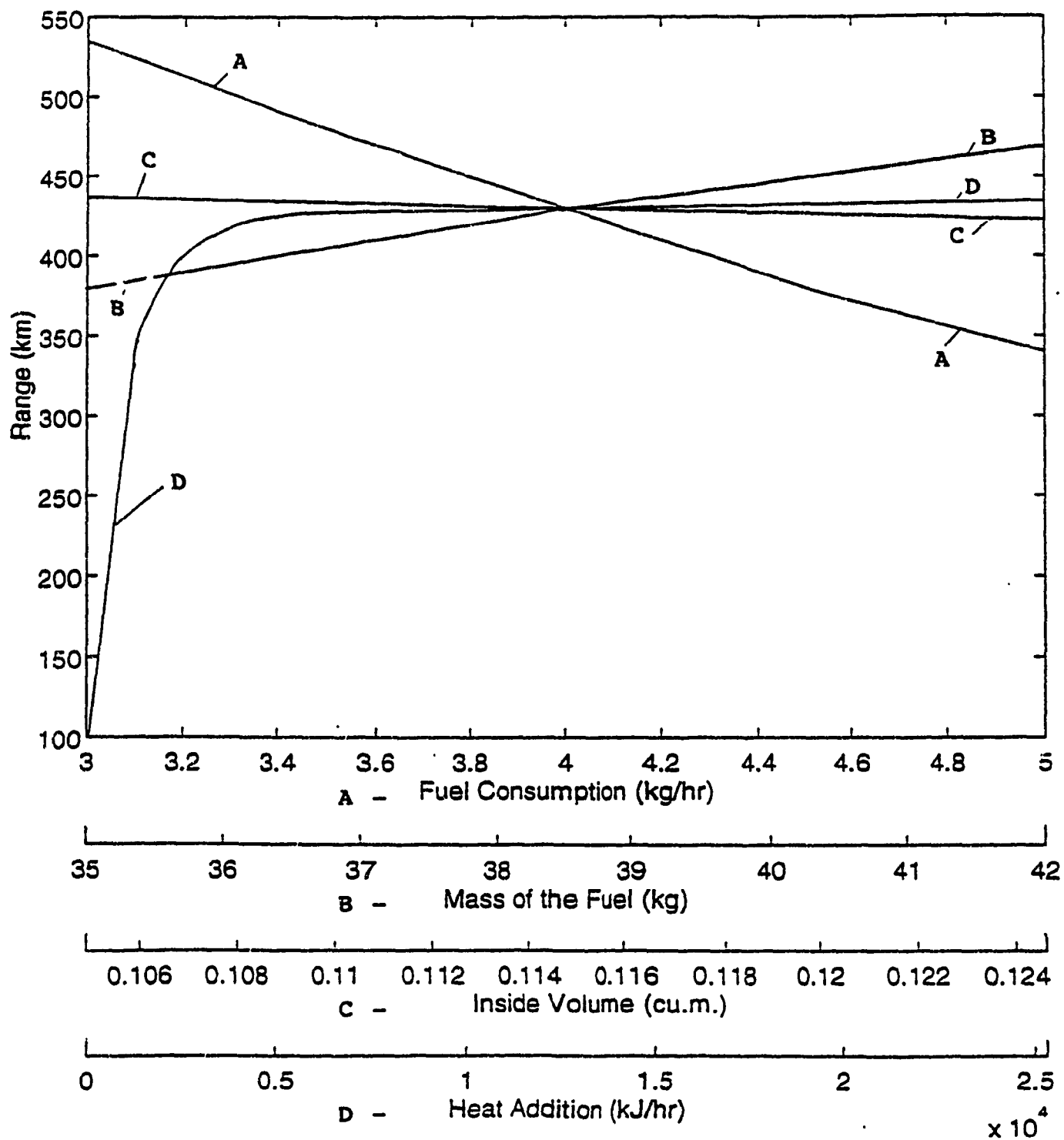


Fig. 8.8 Variation of the range for natural gas car with the design variables

monotonicity analysis, it was concluded that the insulation resistance should be made higher to keep the safe pressure ratio lower. Hence this variable was eliminated from the search for optimum design values and the maximum value from the feasible region was assigned to it. Now the multi-objective constrained non-linear optimization problem has been formulated as:

$$\text{Minimize } Z(X) = [\text{IWT}(X), -\text{PT}(X), \text{SPR}(X), -\text{RAN}(X)] \quad (8.2)$$

subject to the following side constraints:

$$m_{gl}^l \leq m_{gl} \leq m_{gl}^u \quad (8.3)$$

$$\dot{m}_g^l \leq \dot{m}_g \leq \dot{m}_g^u \quad (8.4)$$

$$V_t^l \leq V_t \leq V_t^u \quad (8.5)$$

$$q_{ex}^l \leq q_{ex} \leq q_{ex}^u \quad (8.6)$$

In this optimization, it is required to simultaneously minimize the initial waiting time,  $\text{IWT}(X)$  and the safe pressure ratio and maximize the parking time and the range. Hence a negative sign has been assigned for the parking time,  $\text{PT}(X)$  and range,  $\text{RAN}(X)$  in the Eq. (8.2).

### 8.3.3 Solution Method

The weights have been selected as 0.1, 0.4, 0.4 and 0.1 for the objectives initial waiting time, parking time, safe pressure ratio and range, respectively. The optimization problem has been solved using interior penalty function method. The following are the results of optimization:

For hydrogen:

Mass of the fuel (kg)	8.75
Total inside volume (cu.m.)	0.22
Fuel extraction rate (kg/hr)	1.0
Heat addition from engine exhaust gases (kJ/hr)	30464
Insulation resistance (K hr/kJ)	1.0

For natural gas:

Mass of the fuel (kg)	37.52
Total inside volume (cu.m.)	0.11
Fuel extraction rate (kg/hr)	3.0
Heat addition from engine exhaust gases (kJ/hr)	18340
Insulation resistance (K hr/kJ)	1.0

Fig. 8.9 and Fig. 8.10 show the convergence of design variables during the optimization process for hydrogen and natural gas. The variables shown in these graphs are normalized by dividing each of the variables by its optimum value.

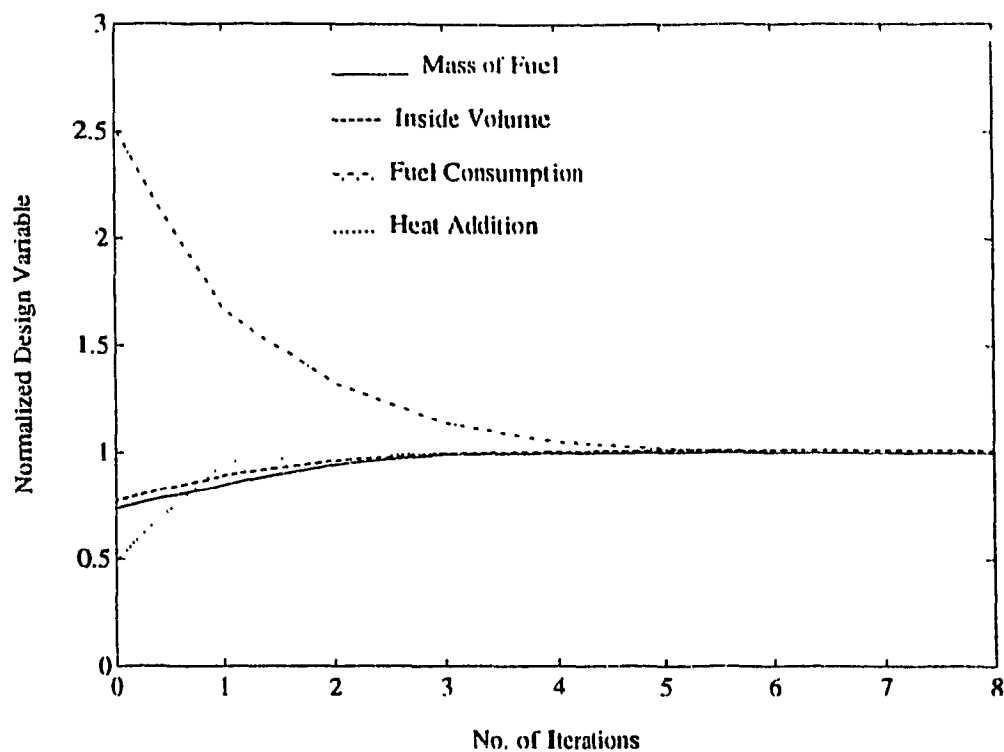


Fig. 8.9 Progress of optimization for hydrogen car

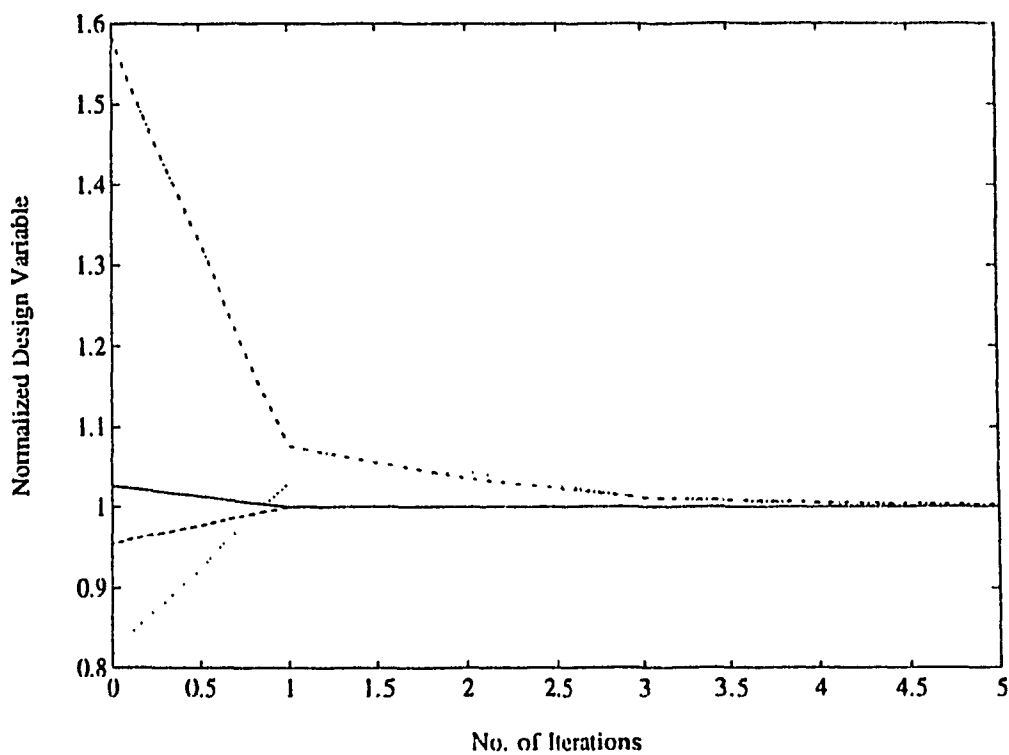


Fig. 8.10 Progress of optimization for natural gas car

## **8.4 Optimization of the Storage System for a Bus**

### **8.4.1 Design Parameter Sensitivity Study**

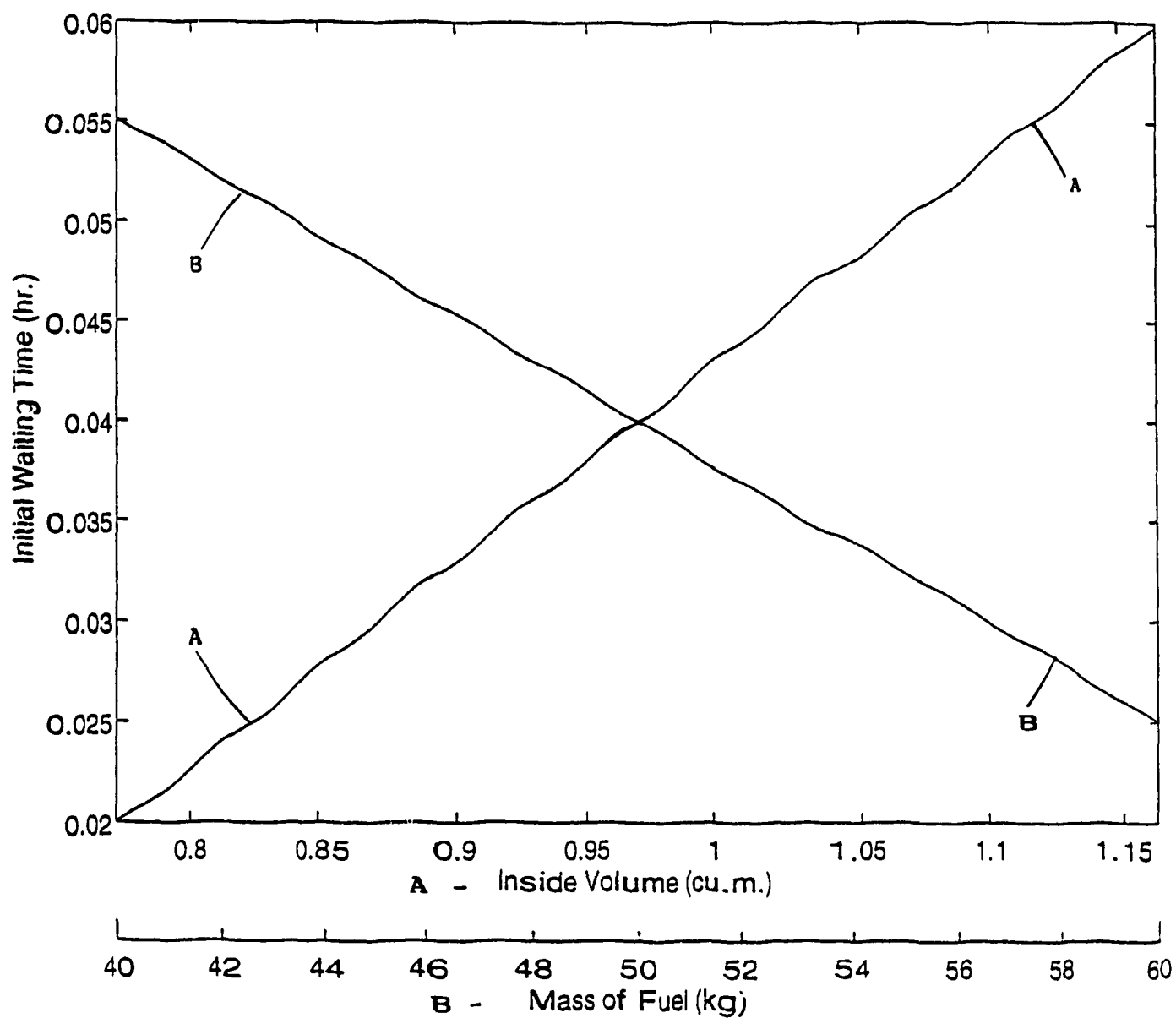
Prior to optimization of the model a detailed parametric study was carried out to obtain an indepth understanding of the system behaviour. Influence of system parameters on important design objectives are examined in this section.

#### **8.4.1.1 Initial Waiting Time**

Fig. 8.11 and Fig. 8.12 present the results of initial waiting time for hydrogen and natural gas buses respectively. It can be seen from these figures that decreasing the initial specific volume of the gas, either by increasing the amount of gas filled into the tank or by decreasing the internal volume of the container, decreases the initial waiting time.

#### **8.4.1.2 Parking Time**

The simulation results of parking time of the hydrogen bus and the natural gas bus are shown in Fig. 8.13 and 8.14. By comparing the Fig. 8.3 with Fig. 8.13 and Fig. 8.4 with Fig. 8.14, we can see that the parking time for a car is much longer than that of a bus. This is because the tank in a bus is not insulated, while the tank in a car is insulated.



**Fig. 8.11** Variation of initial waiting time with the change in variables for hydrogen bus

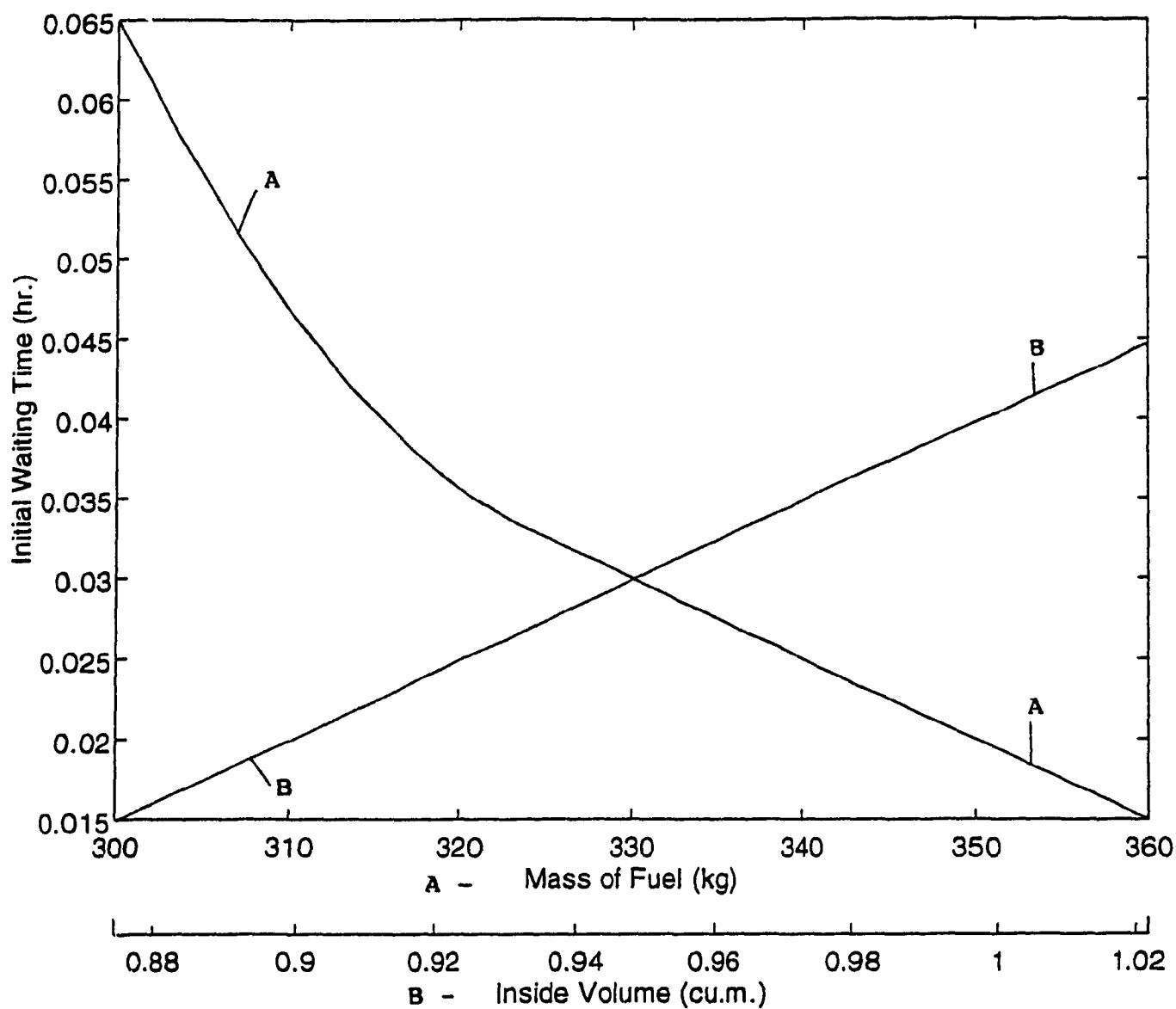


Fig. 8.12 Variation of initial waiting time with the change in variables for natural gas bus

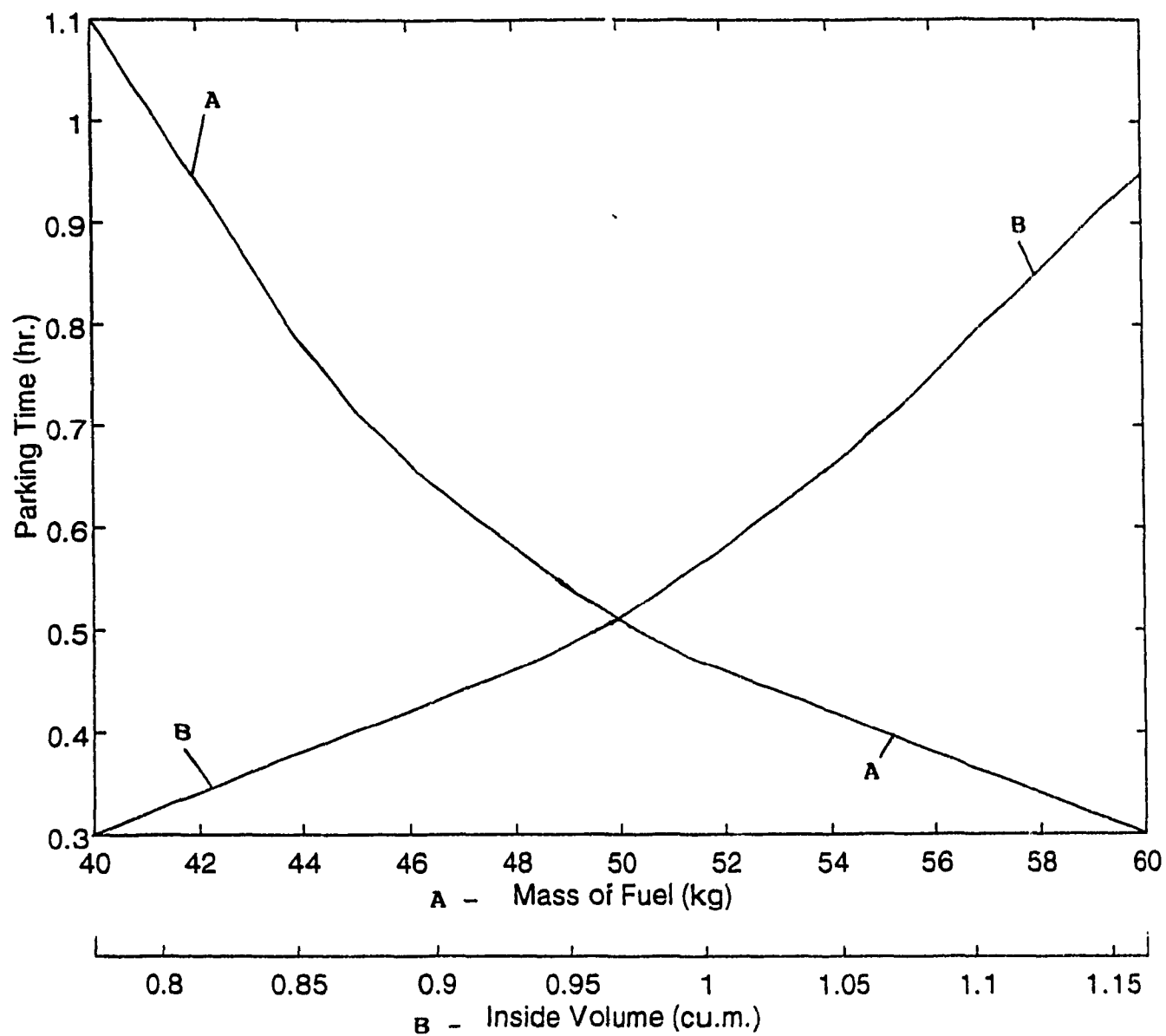


Fig. 8.13 Variation of parking time of hydrogen bus with the change in variables

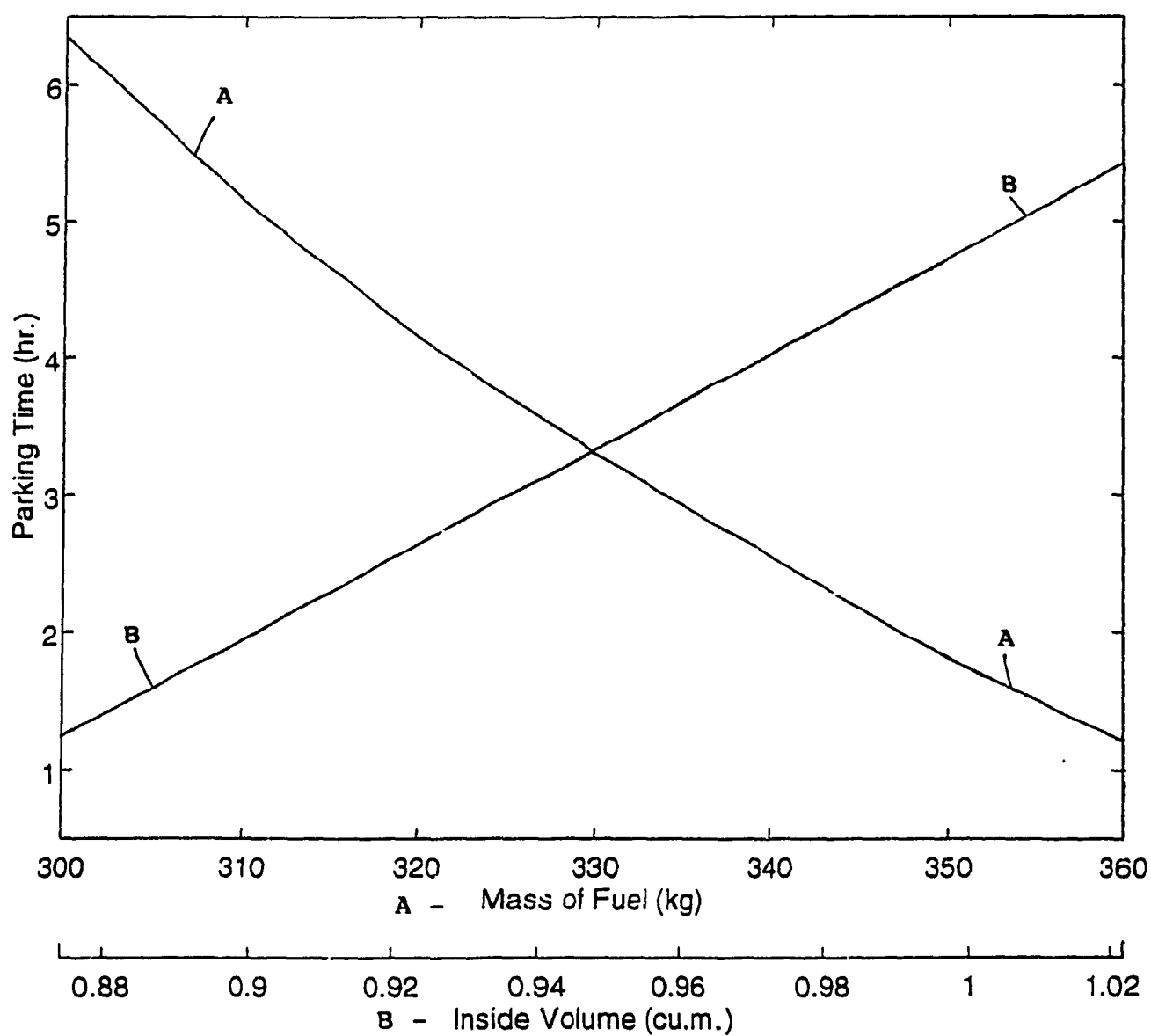


Fig 8.14 Variation of parking time of natural gas bus with the change in variables

### 8.4.1.3 Safe Pressure Ratio

The safe pressure ratio is shown in Fig. 8.15 and Fig. 8.16 for hydrogen and natural gas respectively. It decreases with the increase in the initial specific volume of the fuel in the tank and also decreases with the increase in the fuel extraction rate. By comparing the Fig. 8.6 with Fig. 8.16, we can conclude that the safe pressure ratio is low in the case of a bus when compared with a car. This is because of the following reason: the bus was assumed to start its operation immediately after reaching the 100 bar pressure and to run continuously until the pressure in the tank drops below 100 bar. The car was assumed to be running in a weekly schedule, where it drives the owner to work in the morning and brings him back home in the evening. Because of the longer parking time, the pressure buildup will be higher in the tank installed in a car. Hence, insulation is a key factor for the car in this type of operation schedule.

### 8.4.1.4 Range

The variations of the driving range for the hydrogen and natural gas buses are shown in Fig. 8.17 and Fig. 8.18 respectively, with the change in different variables.

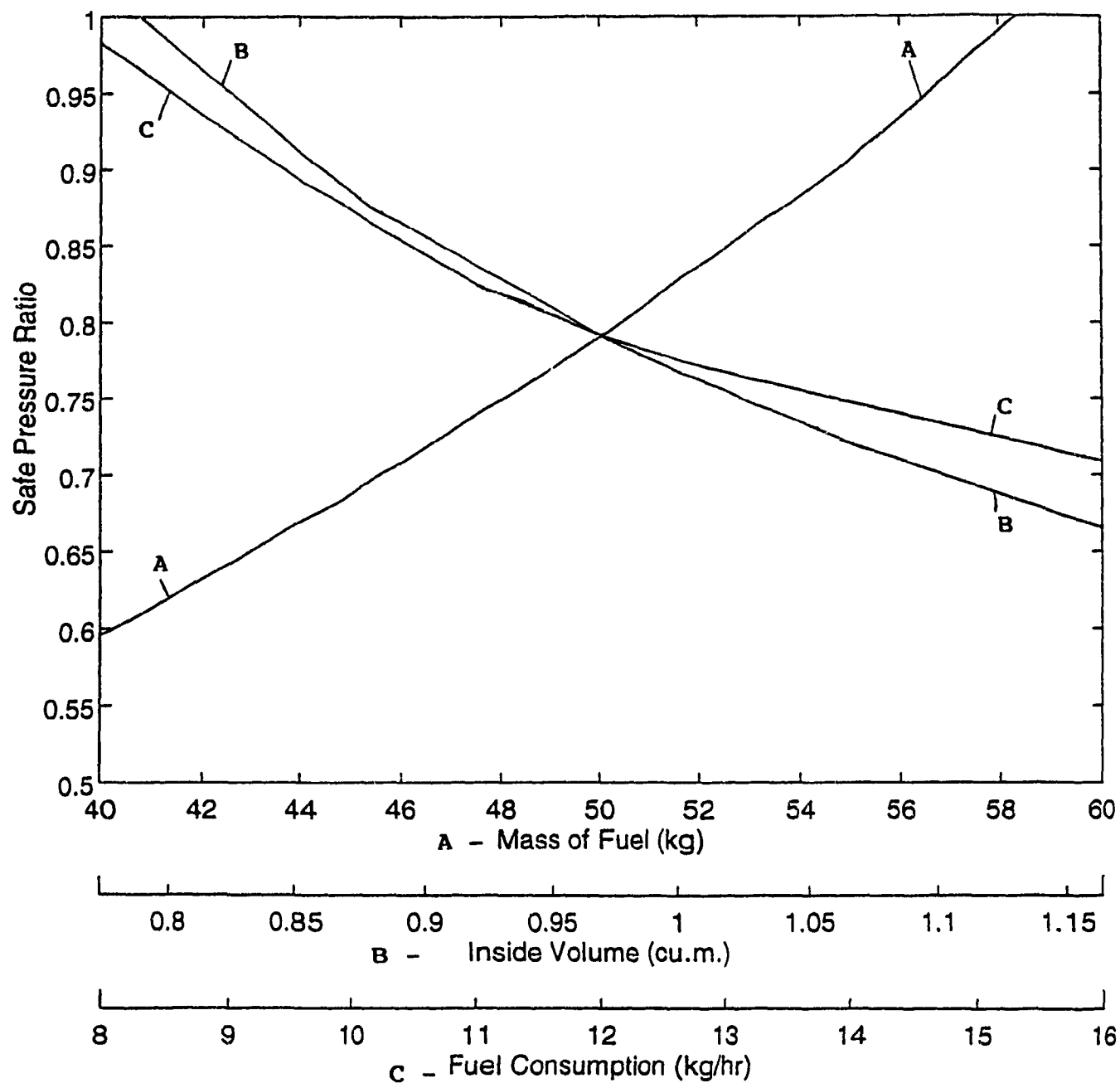


Fig. 8.15 Sensitivity of safe pressure ratio to design variables for hydrogen bus

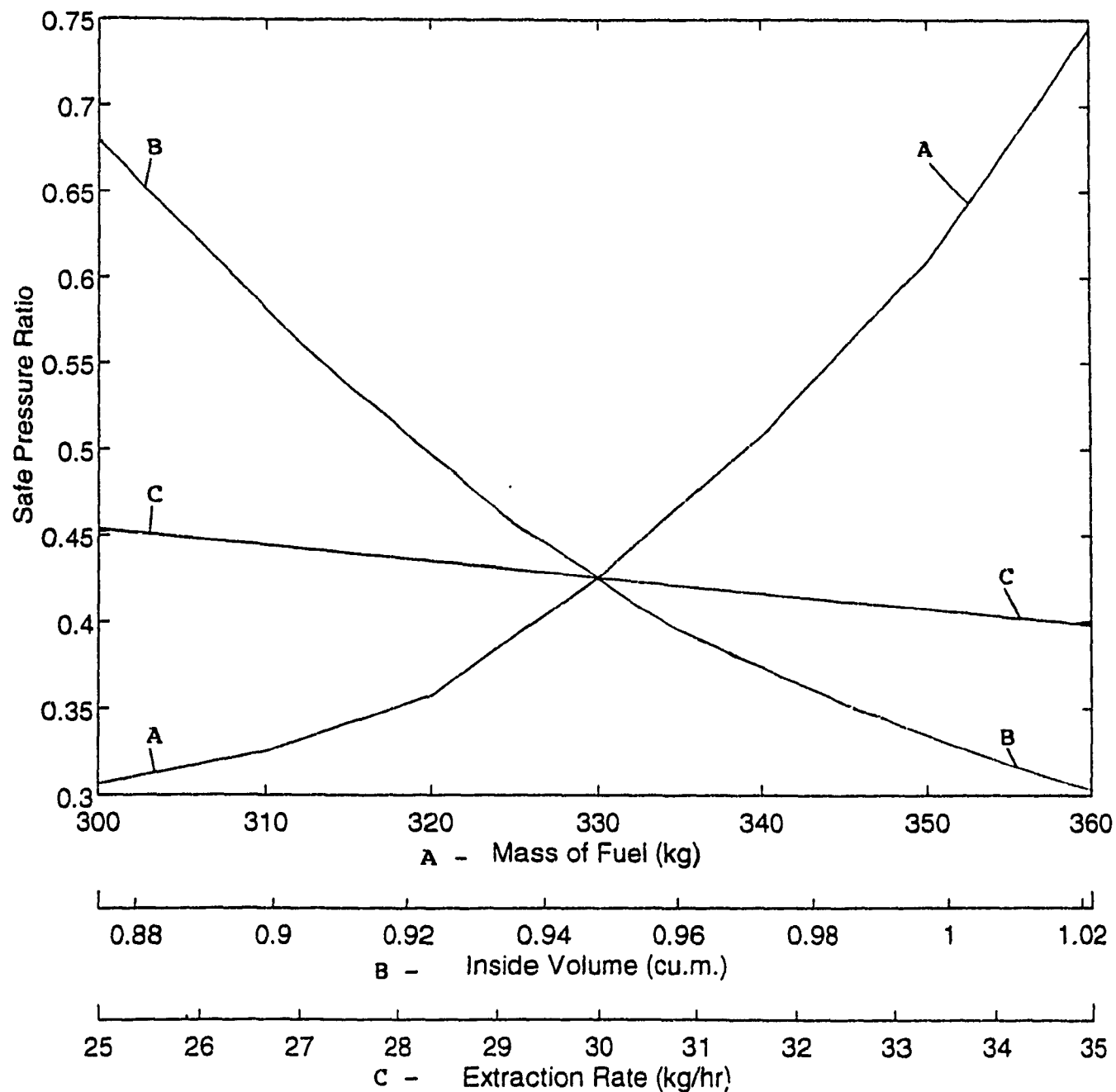


Fig. 8.16 Sensitivity of safe pressure ratio to design variables for natural gas bus

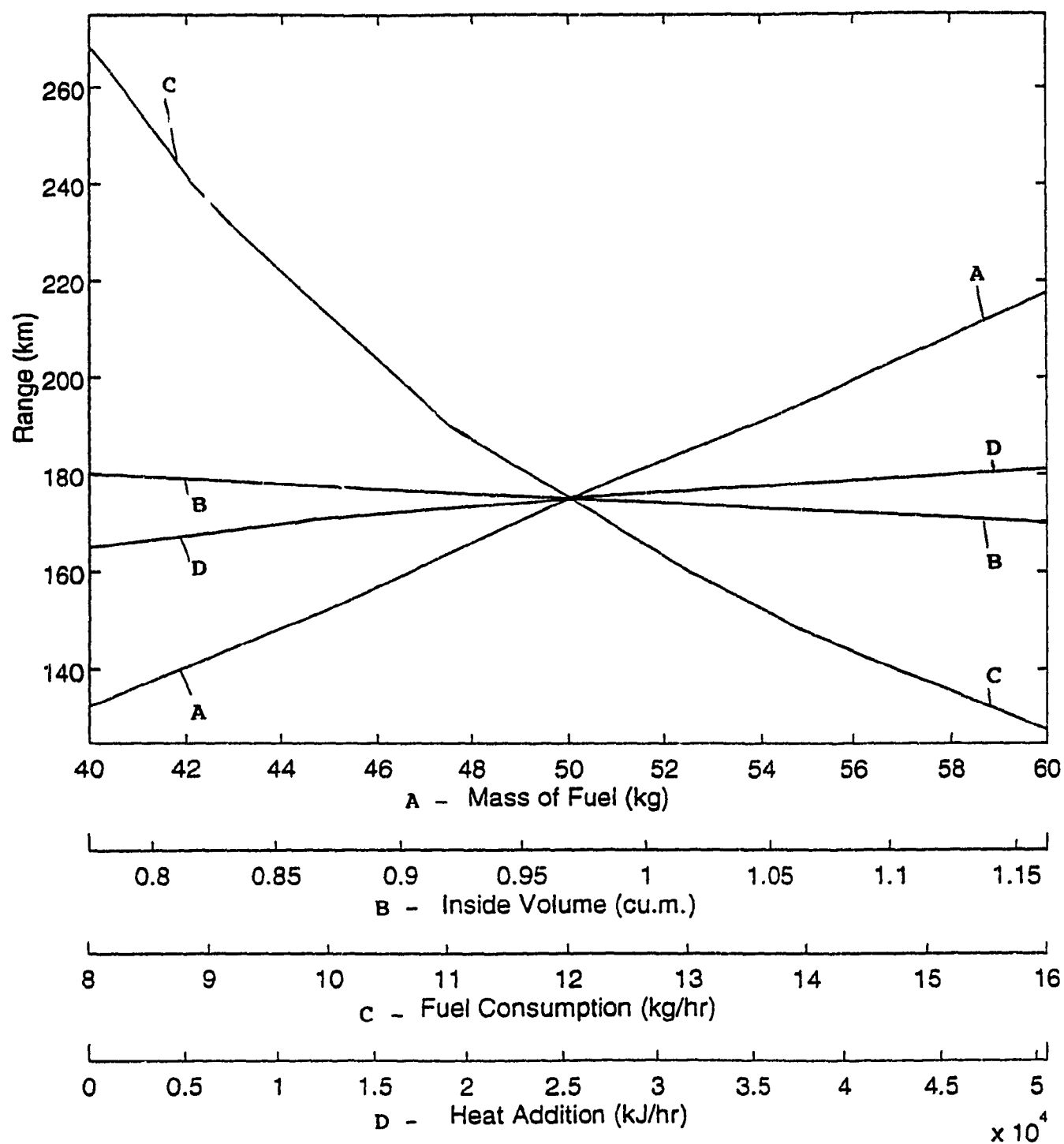


Fig. 8.17 Variation of range with the change in design variables for hydrogen bus

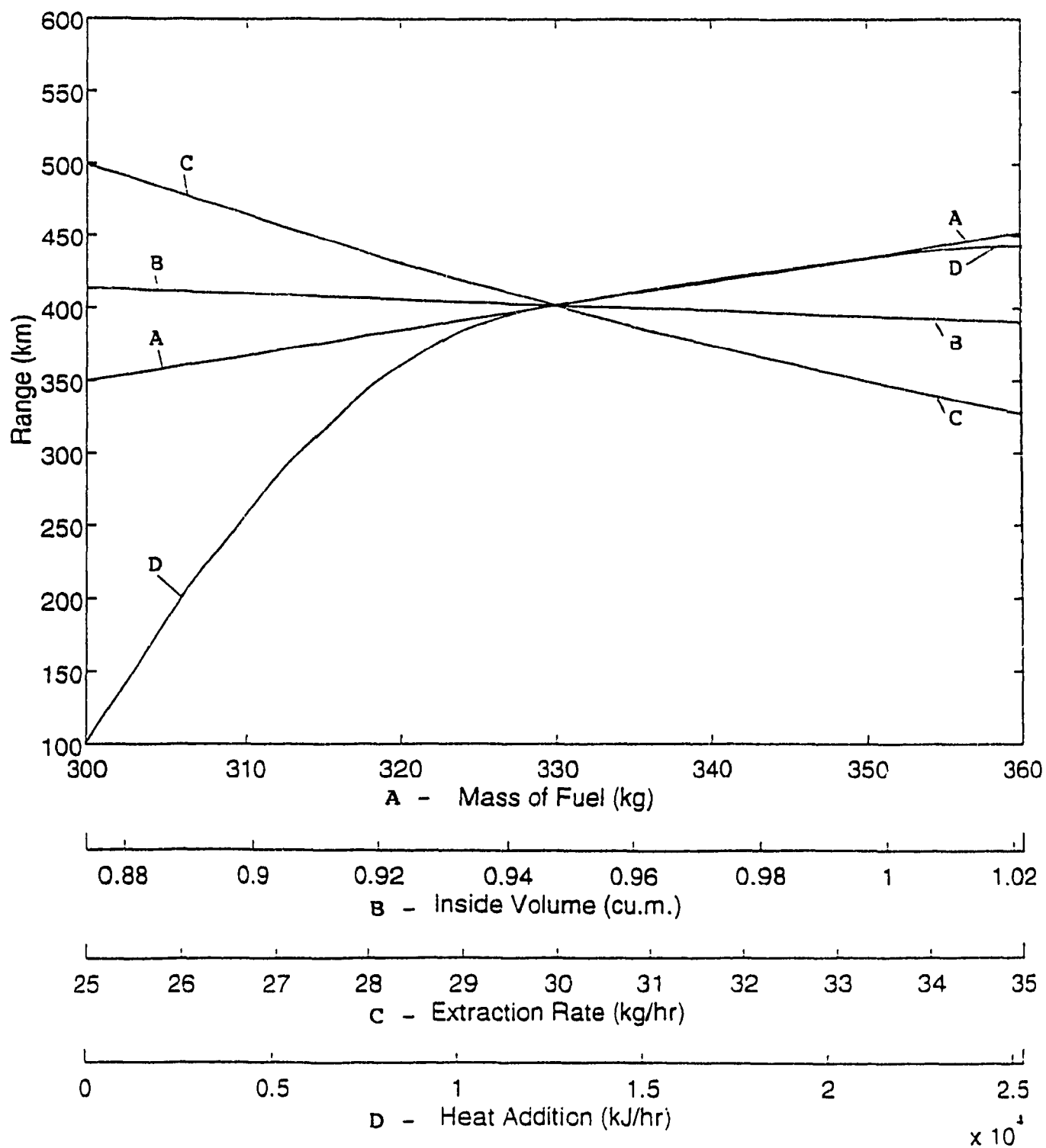


Fig. 8.18 Variation of range with the change in design variables for natural gas bus

### 8.4.2 Solution Method

The weights have been selected as 0.3, 0.1, 0.4 and 0.2 for the objectives; initial waiting time, parking time, safe pressure ratio and range, respectively. The storage and supply system parameters were optimized in the same way as it was done for a car and the results are shown below:

For hydrogen:

Mass of the fuel (kg)	56.8
Total inside volume (cu.m.)	1.1567
Fuel extraction rate (kg/hr)	12.4
Heat addition from engine exhaust gases (kJ/hr)	41160

For natural gas:

Mass of the fuel (kg)	348.9
Total inside volume (cu.m.)	1.02
Fuel extraction rate (kg/hr)	34.95
Heat addition from engine exhaust gases (kJ/hr)	25269

The progress of optimization is shown in Fig. 8.19 and Fig. 8.20 for hydrogen bus and natural gas bus. The design variables have been normalized by dividing by the optimum value and shown in the graphs.

The following conclusions can be drawn from the results of optimization:

1. In order to have a comparable range for hydrogen vehicle with that of

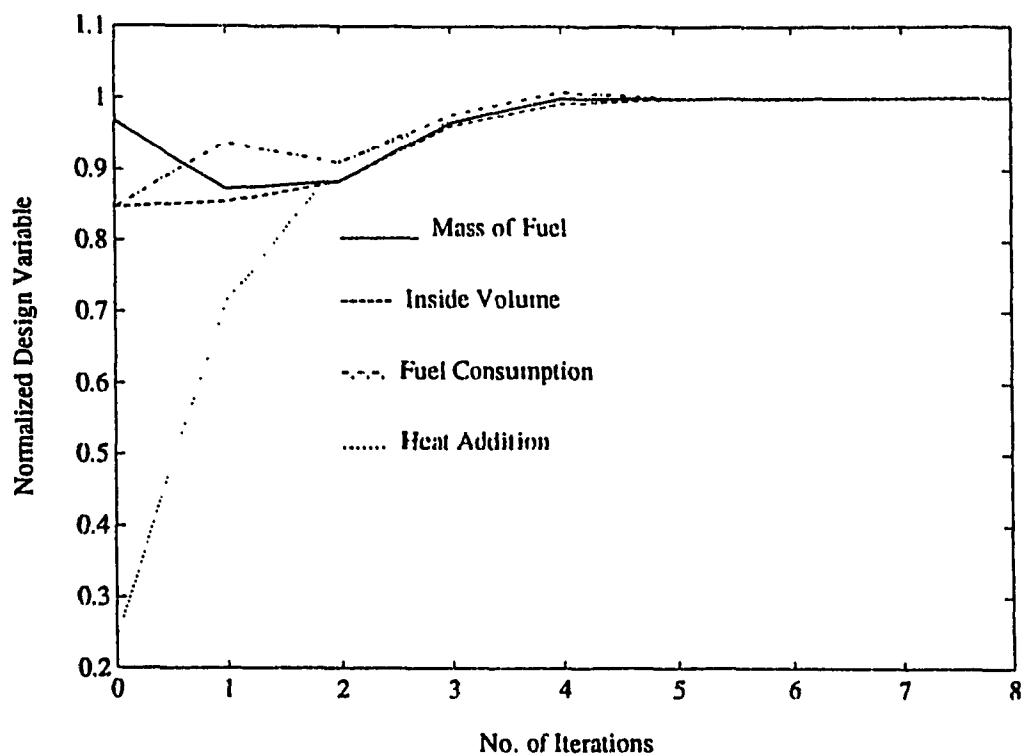


Fig. 8.19 Convergence of design variables during optimization for hydrogen bus

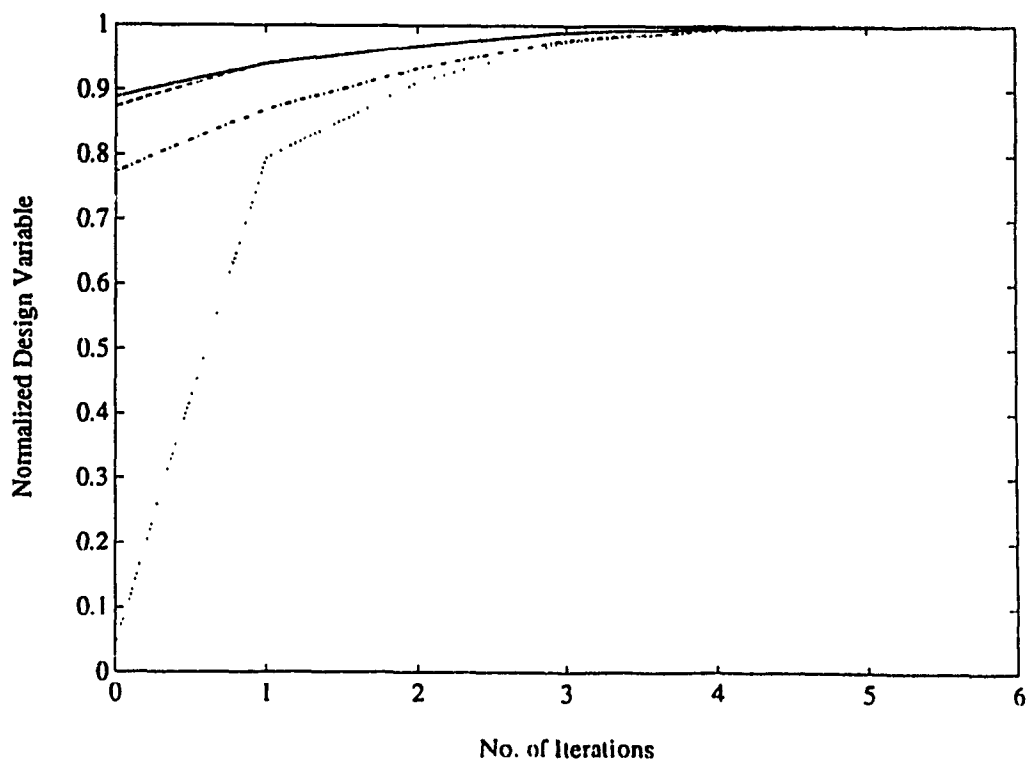


Fig. 8.20 Convergence of design variables during optimization for natural gas bus

natural gas vehicle, the volume of the tank should be very much increased.

2. Insulation is a key factor for the car to allow for longer parking time and to avoid gas release through safety valve.
3. If the vehicle is required to start immediately after refuelling, in which case reduction of the initial waiting time will have a priority, the weighting factors could be altered and new optimum operating conditions would be achieved.

## CHAPTER 9

### NATURAL GAS-HYDROGEN MIXTURES FOR VEHICLES

#### 9.1 Preliminaries

Adding some quantities of hydrogen to natural gas creates *Hythane*, a vehicle fuel which could bring significant reductions in pollutants along with other benefits [4]. Compared to gasoline, natural gas burns slower and is harder to ignite. The addition of about 5% hydrogen by energy content to the typical natural gas results in combustion rates equivalent to that of gasoline. On a volume basis, the mixture is a composition of 15% hydrogen and 85% natural gas. Burning pure hydrogen results in virtually no CO, hydrocarbons, sulphur compounds or particulate emissions. Even  $\text{NO}_x$  can be minimized with the correct combustion. Just adding 5% hydrogen could reduce emissions by 5% because of simple displacement of natural gas with zero-emission hydrogen. Further reduction can result because of improvements in combustion efficiency, particularly with very lean mixtures.

In this chapter, the on-board storage of natural gas/hydrogen mixture for vehicular applications is discussed. Fig. 9.1 shows the specific volume details of 100% natural gas, 100% hydrogen and 85% natural gas + 15% hydrogen mixture at 200 K temperature and at 100 bar, 300 bar, 500 bar and 800 bar pressure. As can be seen from the figure, the addition of 15% hydrogen increases the specific

volume of natural gas by four times. On the other hand, the lower heating value of the mixture will be only 21% higher than that of natural gas. Because of this the amount of energy that can be stored in a given volume will be smaller, which eventually reduces the range of the vehicle. Fig. 9.2 describes the vehicle range provided by different sizes of the tank for the mixture and for pure natural gas. The calculations are based on the bus, which was described in Chapter 6. A bus which has a tank volume of 1.0 cu.m. will have a range of approximately 500 km with 100% natural gas and 250 km with the mixture.

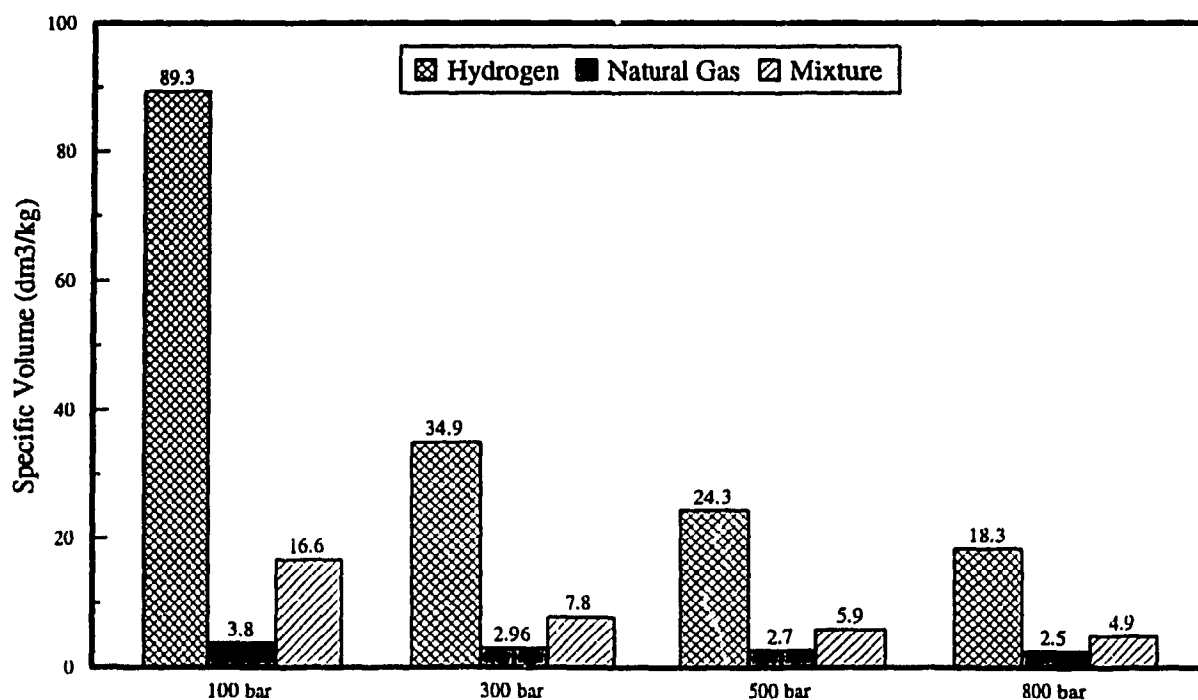


Fig.9.1 Specific Volume of Natural Gas, Hydrogen and the Mixture at 200 K

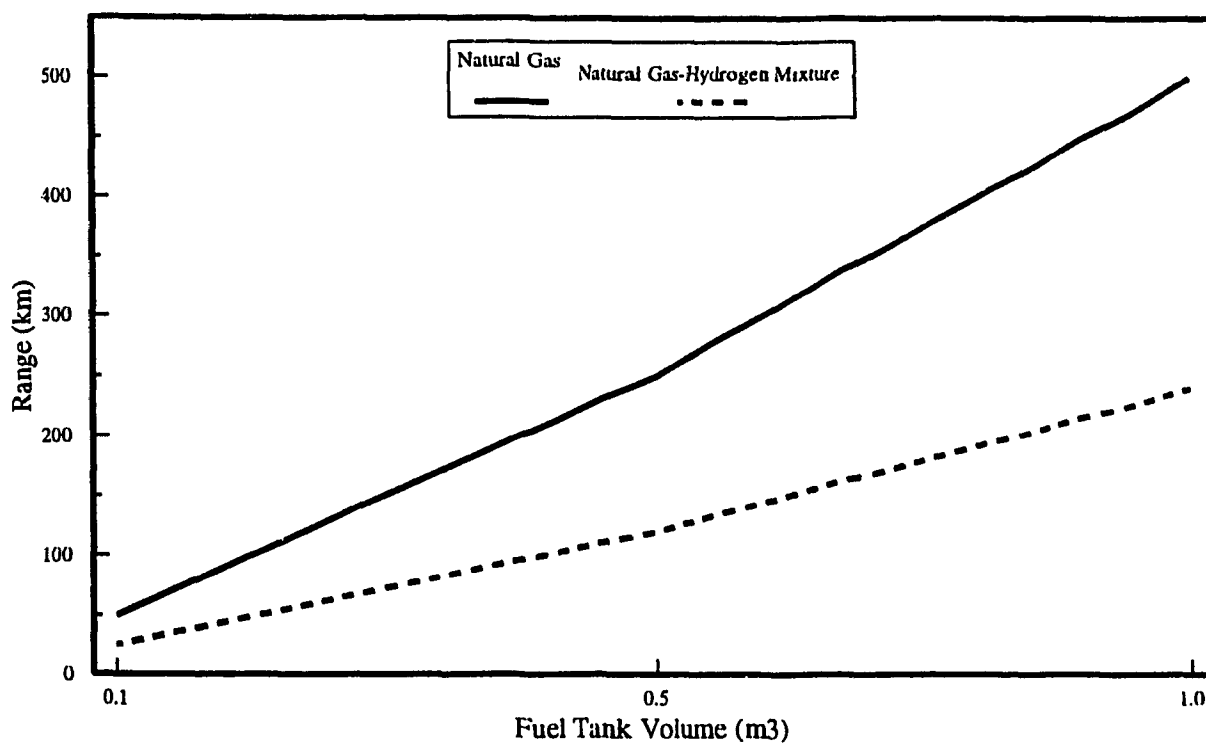


Fig. 9.2 Range Covered by Natural Gas and Natural Gas-Hydrogen Mixture Vehicles

When the vehicle comes for refuelling, liquid natural gas (LNG) will be inserted first into the thermocontrolled tank and gaseous hydrogen ( $\text{GH}_2$ ) can be added to it, as required to obtain the natural gas-hydrogen mixture. Since the gaseous hydrogen is available at ambient temperature and high pressure, it could be inserted into the container which is first filled-up with liquid natural gas. The  $\text{GH}_2$  will help in faster boil-off of LNG and will create the high pressure required for direct injection. Once the necessary pressure is attained, the vehicle can be started.

## **9.2 Simulation of the Mixture Properties in Thermocontrolled Tank during Vehicle Operation**

### **9.2.1 Natural Gas-Hydrogen Mixture for Bus Operation**

The thermocontrolled tank is well suited to city bus operation, where a centrally located refuelling station is being used and the vehicles run in a pre-scheduled fashion. The refuelling station can be designed to provide the vehicle with both liquefied natural gas and gaseous hydrogen.

Computer simulation of the bus operation on natural gas-hydrogen blend has been carried out based on the following assumptions:

- 1) The bus tank content is 25.5 kg of hydrogen and 144.5 kg of natural gas, together 170 kg of the gaseous fuel mixture.
- 2) The bus fuel consumption is 27 kg/hr for the mixture.
- 3) The bus is fitted with a battery of thermocontrolled tanks, with a total inside volume of 0.9 cu.m.
- 4) The gas pressure in the tank should not be lower than 100 bar during the bus operation.

Fig. 9.3 shows the simulation results for a city bus operating continuously for about 5 hrs. It was assumed that at the time of starting the bus, the temperature inside the tank is 200 K. Without adding the heat from exhaust gases, it is possible to use only 20% of the tank content, because of the lower initial pressure in the

tank. The addition of heat helps in increasing the utilizable fuel in the tank by upto 75%. It can be concluded that in such a tank, the heat addition from exhaust gases can be avoided if the tank wall design would provide the tank with higher heat transfer rate through the walls so that the ambient gas temperature could be reached at the end of the run.

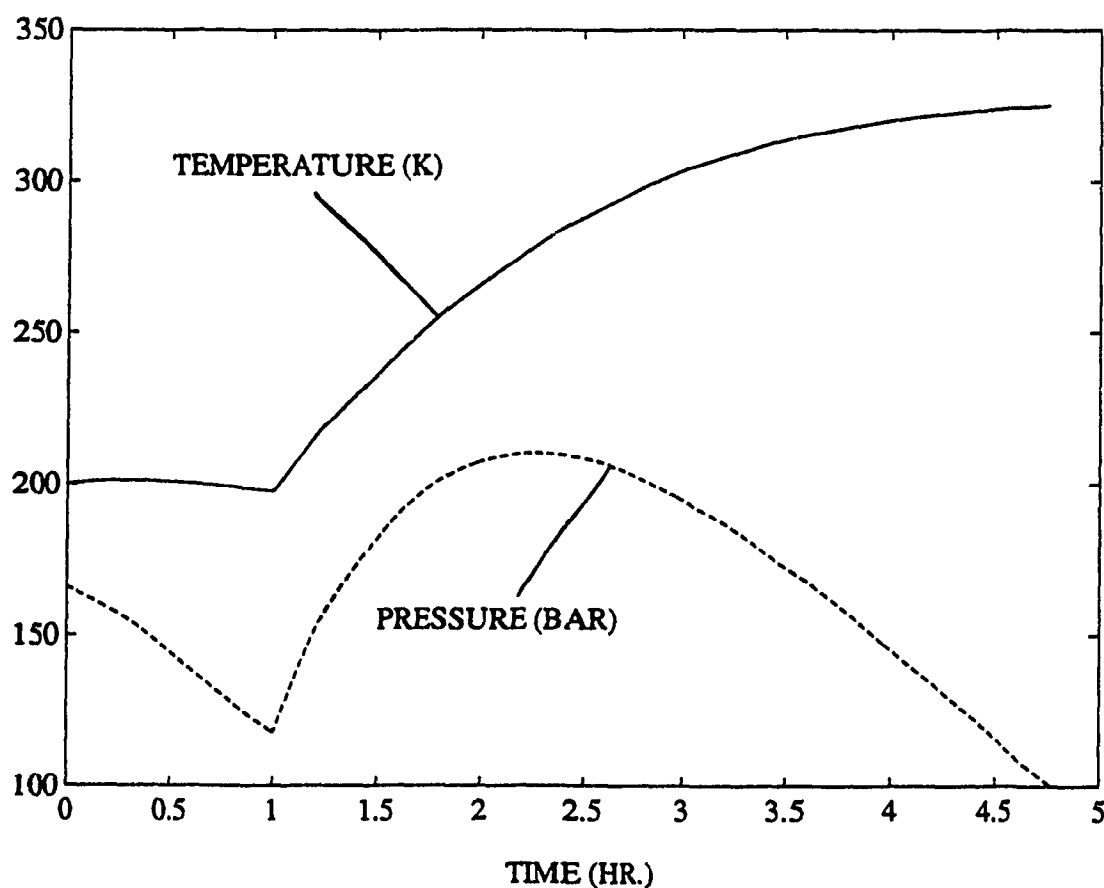


Fig. 9.3 Simulation of the mixture properties inside thermocontrolled tank during the bus operation

### **9.2.2 Natural Gas-Hydrogen Mixture for Car Operation**

The car is assumed to be refuelled once a week by filling-up the tank with 4 kg of hydrogen and 21 kg of natural gas, so that the total fuel in the tank would be 25 kg. The total inside volume of the tank is 0.12 cu.m. The car is used twice a day for 0.5 hr each time to drive from home to work and to come back. Due to the tank insulation, the car can be parked for a longer time, particularly, after part of the gas content has been consumed. This would require some attention from the car owner regarding the car refuelling pattern.

Fig. 9.4 shows the temperature and pressure changes in a well insulated tank during the car operation. When the car is being driven, a drop in the mixture pressure is observed accompanied by a smaller temperature drop. However, the drop in temperature during the run is compensated by the heat transfer through the tank insulation during the parking time so that the gas temperature returns each time to a similar level. After three days, heat is required to be added from the exhaust gases to increase the gas temperature in the tank to cause a rise in the gas pressure. Finally during the seventh day, the pressure level drops below 100 bar, and refuelling is required.

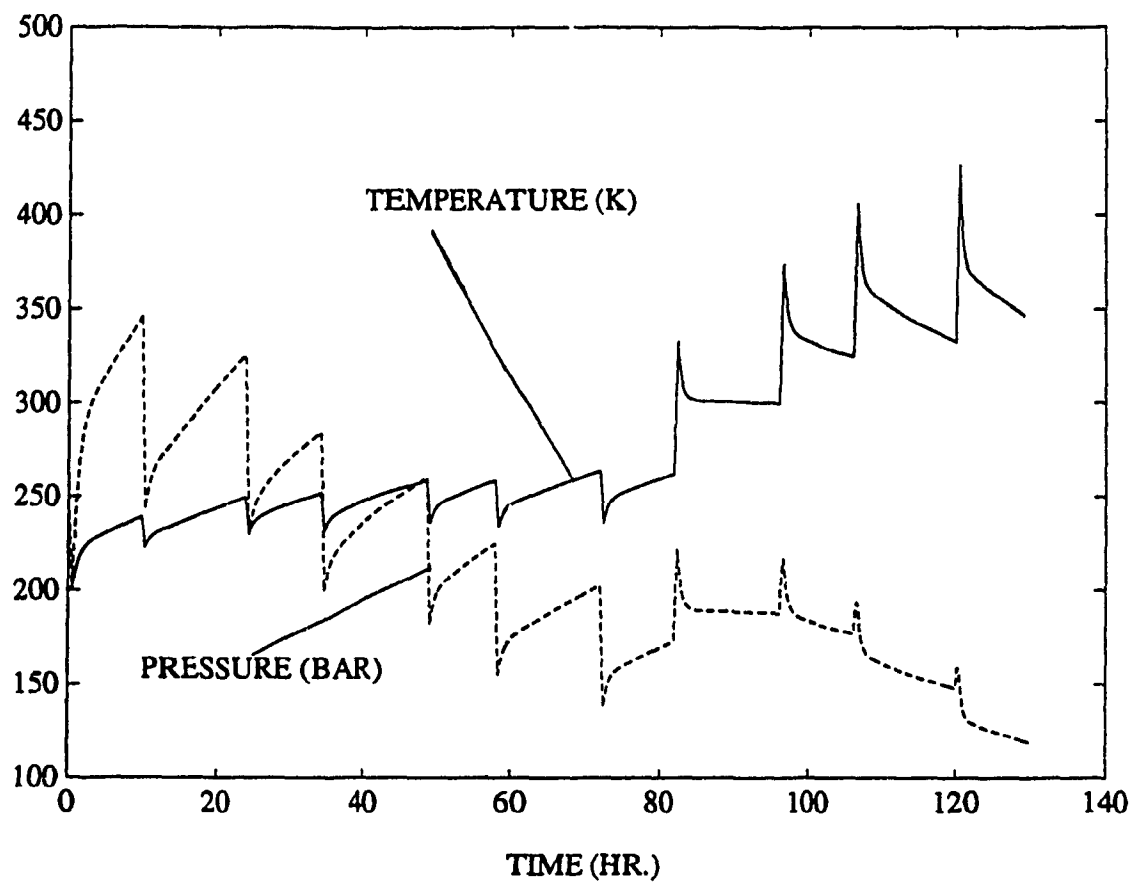


Fig. 9.4 Simulation of the mixture properties inside thermocontrolled tank during the car operation

## **CHAPTER 10**

### **SUMMARY, CONCLUSIONS AND RECOMMENDATIONS**

The present technology of supplying the vehicle with gaseous fuels is limited to the manifold injection. For direct injection of gaseous fuels into the combustion chamber of an engine, gas under high pressure is required. The requirement to provide the gaseous fuel under high pressure, reduces the range covered by a vehicle with direct gas injection. To increase the operational range of a vehicle equipped with a direct gas injection system and to eliminate the problems associated with the high pressure cryogenic pumps, a concept called thermocontrolled tank was investigated in this thesis. The amount of gas that could be stored in such a tank would be higher than in regular pressurized cylinders, but lower than in a typical cryogenic tank. Liquefied gaseous fuel would be introduced into an insulated vessel and the rise in gas temperature and pressure would be controlled by the heat transfer to the tank. To control the build-up of the gas pressure, both, insulation and preheating of gas, the latter utilizing the engine exhaust gases, could be used. Necessary gas pressure required would thus be maintained for the direct injection and to increase the utilizable portion of the tank content.

Based on this concept, two thermocontrolled tank prototypes have been manufactured and tested. The first vessel, called steel tank was designed for a maximum pressure of 250 bar. The second vessel, called composite high pressure

vessel, was designed for a maximum pressure of 1000 bar. The steel vessel was covered with insulation and was fitted with a heat exchanger inside. Both vessels have been tested with liquefied nitrogen to observe the temperature and pressure increase inside the tank. A mathematical model for the heat transfer process in the tank has been developed and the process simulated.

To find the optimum design of a composite vessel that can be used as a thermocontrolled tank, different aspects of storage, such as the initial operational temperature, gas mass to vessel weight ratio and gas mass to vessel volume ratio have been investigated. The thermocontrolled tank design has been then optimized for both natural gas and hydrogen using the theory of non-linear multi-objective optimization.

The thermodynamic properties of natural gas and hydrogen inside the thermocontrolled tank installed on board a vehicle have been simulated to find out how long the vehicle can be run after each fill-up. A city bus in continuous running mode and a car in start-stop weekly schedule have been investigated.

The optimum performance requirements of a thermocontrolled tank installed in a vehicle have been quantified for two different vehicles, with two different operational schedules. The initial waiting time, parking time, safe pressure ratio and range of the vehicles have been investigated and then optimized, to define the performance requirements.

Finally, the storage of *Hythane*, a mixture of natural gas and hydrogen, has

been also investigated on-board a vehicle. This concept could bring significant reductions in engine emitted pollutants, as compared with only natural gas and an increase in the vehicle range, as compared with only hydrogen.

Based on the investigations on thermocontrolled tank concept, the following conclusions were drawn:

1. The test results showed that the liquefied fuel can be brought from atmospheric pressure to the high pressure required for direct injection (100 bar) in reasonable time and that the pressure increase can be limited by tank insulation.
2. The tank filling time was found to be an important parameter, since by reducing this time, gaseous fuel wastage can be avoided. The shorter filling time could be achieved by specially designed automatic filling stations.
3. From the simulation results, it was observed that, even if the vessel would be completely isolated from the atmosphere, the internal energy stored in the walls of the tank would bring the liquefied gaseous fuel to a certain temperature and pressure, called initial operational temperature and pressure. The heavier the tank, as compared with the mass of inserted gas, the higher would be the initial operational temperature. For the best performance of this thermocontrolled tank concept, the initial operational temperature of the gas should be as low as possible, to increase the mass of the stored gas.
4. It was learned from the optimization results that the gas should be stored

under approximately 500 bar pressure for both the fuels. This high pressure enables one to store more fuel and provides for maximum utilization of the fuel from the tank.

5. In a city bus, the tank may not be insulated to allow for more heat transfer through the tank walls, which will increase the pressure and temperature of gas inside the tank. In a car or a truck, the tank has to be insulated to allow for longer parking periods, without bringing the gas to an excessive pressure. Also, for a hydrogen vehicle, the number of refuellings will be 3 times higher than that for a similar natural gas vehicle.
6. For the best utilization of the thermocontrolled tank, the vehicle running and refuelling schedule is important; the thermocontrolled tank concept works best with fleet vehicles, where there is a centrally located refuelling station and the operation schedule of the vehicles can be predicted.
7. It was observed from the optimization of on-board storage system results that, to have a comparable range for hydrogen vehicle with that of natural gas vehicle, the volume of the tank must be increased substantially.

Based on the thorough investigation presented in the thesis, it appears that the thermocontrolled tank is better suited for vehicles such as city buses which follow a regular schedule. Some of the topics that are recommended for further work are as follows:

1. First a tank should be built and tested in the laboratory to find out what the

life expectancy would be when the predicted duty cycle is imposed. A demonstration project should then be carried out to test the thermocontrolled tank fuel storage system for a bus.

2. A model should be developed for simulation of the refuelling process in a thermocontrolled tank. The feasibility of refuelling without emptying the residual fuel in the tank should be explored.
3. An optimization procedure should be developed to find the best proportion of hydrogen and natural gas for the use of hythane fuel.

## REFERENCES

1. Dahlberg, R., *Replacement of Fossil Fuels by Hydrogen*, Int. J. Hydrogen Energy, Vol. 7, No. 2, pp. 121-142, 1982.
2. Fisher, A., *Global Warming: Part Two, Inside the Greenhouse*, Popular Science, Sept. 1989.
3. Valenti, M., *Alternative Fuels: Paving the Way to Energy Independence*, ASME Mechanical Engineering, pp. 41-46, Dec. 1992.
4. Lynch, F.E. and Egan, G.J., *Near Term Introduction of Clean Hydrogen Vehicles via H<sub>2</sub>-CNG Blends*, Presented at the Fourth Canadian Hydrogen Workshop, Toronto, Nov. 1-2, 1989.
5. *Nonpetroleum Vehicular Fuels*, Symposium Papers Sponsored by Institute of Gas Technology and Presented at Arlington, Virginia, Feb. 11-13, 1980.
6. Shiells, W., Garcia, P., Chanchaona, S., McFeaters, J.S. and Raine, R.R., *Performance and Cyclic Variability of Natural Gas Fuelled Heavy Duty Engines*, SAE Paper No. 892137, 1989.
7. Watson, H.C. and Milkins, E.E., *Comparison and Optimization of Emission Efficiency and Power of Five Automotive Fuels in One Engine*, Int. J. of Vehicle Design, Vol. 3, No. 4, pp. 463-476, 1982.
8. Furuhamma, S. and Fukuma, T., *High Output Power Hydrogen Engine with High Pressure Fuel Injection, Hot Surface Ignition and Turbocharging*, Int. J. of Hydrogen Energy, Vol. 11, No. 6, pp. 399-407, 1986.

9. Peschka, W., *Hydrogen Combustion in Tomorrow's Energy Technology*, Int. J. of Hydrogen Energy, Vol. 12, No. 7, pp. 481-499, 1987.
10. Lapedes, D.N., *Encyclopedia of Energy*, McGraw-Hill Book Company, New York, pp. 373-377, 1981.
11. Song, Y.K., Acker, G.H., Schaetzle, W.J. and Brett, C.E., *Knock Limitations of Methane-Air Mixtures in a Turbocharged Dual-Fuel Engine*, SAE Paper No. 870794, 1987.
12. Golovoy, A. and Braslaw, J., *On-board Storage and Home Refuelling Options for Natural Gas Vehicles*, SAE Paper No. 830382, 1983.
13. Weaver, C.S., *Natural Gas Vehicles-A Review of the State of the Art*, SAE Paper No. 892133, 1989.
14. Colavincenzo, O., *Trip Report to Beech Aircraft to Review Liquid Natural Gas Powered Automobile*, Automotive Energy Research and Development Branch, Ontario Ministry of Transportation and Communications, Ontario, Canada, Nov., 1980.
15. Fisher, F.L., *Introduction of a Commercial System for Liquid Methane Vehicles*, Nonpetroleum Vehicular Fuels III, Symposium Papers, Institute of Gas Technology, Chicago, pp. 125-142, 1983.
16. The Aerospace Corporation, Energy Conservation Directorate, *Assessment of Methane-Related Fuels for Automotive Fleet Vehicles*, Volumes II and III, DOE/CE/50179-1, Office of Vehicle and Engine R&D, U.S. Department of

- Energy, Washington, D.C., Feb., 1982.
17. Nichols, R.J., *Ford's CNG Vehicle Research*, Presented at the 10th Energy Technology Conference, Washington, D.C., March, 1983.
  18. Duncan, R.W., Jenkins, W.D. and Webb, R.F., *Demonstration of Propane and Natural Gas as Fuels for City Buses*, Proc. of the Conf.: Gaseous Fuels for Transportation, Vancouver, Aug. 7-10, 1986.
  19. Noon, A., *A Bus Operator's Experience in the Conversion of Horizontal Diesel Engines to Operate on Both CNG and Propane*, Proc. of the Conf.: Gaseous Fuels for Transportation, Vancouver, Aug. 7-10, 1986.
  20. Krepec, T., Miele, D. and Sudano, A. *Preliminary Concept of Semicryogenic Tank for Storage and Direct Injection of Natural Gas in Internal combustion Engines*, SAE Paper No.880148, 1988.
  21. Bowles, J., *New Orion CNG Bus*, Review Newsletter, Center for Alternative Transportation Fuels, Issue No. 10, July 1989.
  22. Adams, J., *Natural Gas/Diesel Tractor Takes on Regular Highway Haul*, Review Newsletter, Center for Alternative Transportation Fuels, Issue No. 10, July 1989.
  23. Akhtar, A., *Cylinder Research at Powertech*, Review Newsletter, Center for Alternative Transportation Fuels, Issue No. 10, July 1989.
  24. Davies, J.G. and Sulatisky, M.T., *Natural-Gas-Fired Agricultural Tractors*, Automotive Engineering, Vol. 97, No. 9, 1989.

25. Fawley, N.C., *Report of Severe Abuse Tests Conducted on Composite Reinforced Aluminium CNG (Compressed Natural Gas) Cylinders*, SAE Paper No. 831068, 1983.
26. Tison, R., Sprafka, R.J., Bechtold R.L. and Timbario, T.J., *Safety Issues Surrounding the Use and Operation of Compressed Natural Gas Vehicles*, SAE Paper No. 831078, 1983.
27. Strobl, W. and Peschka, W., *Liquid Hydrogen as a Fuel of the Future for Individual Transport*, BMW AG Press, 1986.
28. Furuhashi, S. and Kobayashi, Y., *A Liquid Hydrogen Car with a Two Stroke Direct Injection Engine and LH<sub>2</sub> Pump*, Int. J. of Hydrogen Energy, Vol. 7, No. 10, pp. 809-820, 1982.
29. Buchner, H. and Povel, R., *The Daimler-Benz Hydride Vehicle Project*, Int. J. of Hydrogen Energy, Vol. 7, No. 3, pp.259-266, 1982.
30. Krepec, T., Miele, D. and Lisio, C., *New Concept of Hydrogen-Fuel Storage and Supply for Automotive Applications*, Proc. of the 7th World Hydrogen Energy Conference, Moscow, 25-29 Sept., 1988.
31. Feucht, K., Holzel, G. and Hurich, W., *Perspectives of Mobile Hydrogen Application*, Proc. 7th World Hydrogen Energy Conference, Moscow, U.S.S.R., Vol. 3, pp. 1963-1969, 1988.
32. Deluchi, M.A., *Hydrogen Vehicles: An Evaluation of Fuel Storage, Performance, Safety, Environmental Impacts and Cost*, Int. J. Hydrogen

Energy, Vol. 14, pp. 81-130, 1989.

33. Hynek, S., Bentley, J., Barnett, B., Shanley, E. and Melhem, G., *Hydrogen Storage Technologies: Present and Future*, Presented at Technical Seminar on Storage Technologies, Hydrogen Industry Council, Montreal, 9 Dec. 1992.
34. Krepec, T., Giannacopoulos, T. and Miele, D., *New Electronically Controlled Hydrogen Gas Injector - Development and Testing*, Int. J. Hydrogen Energy, Vol. 12, pp. 855-861, 1987.
35. Binder, K. and Withalm, G., *Mixture Formation and Combustion in a Hydrogen Engine Using Hydrogen Storage Technology*, Int. J. Hydrogen Energy, Vol. 7, pp. 651-659, 1982.
36. Holman, J.P., *Heat Transfer*, Fifth Edition, McGraw-Hill Book Company, 1981.
37. Wark, Jr., K., *Thermodynamics*, Fifth Edition, McGraw-Hill Book Company, 1988.
38. Machado, J.R.S. and Streett, W.B., *PVT Measurements of Hydrogen/Methane Mixtures at High Pressures*, J. of Chem. Eng. Data, Vol. 33, No. 2, 1988.
39. Goodwin, R.D. and Prydz, R., *Densities of Compressed Liquid Methane and the Equation of State*, J. of Research of the National Bureau of Standards - A. Physics and Chemistry, Vol. 76A, No. 2, 1972.

40. Kosov, N.D. and Brovanov, I.S., *Compressibility of a Binary Mixture of Argon and Nitrogen at Different Concentrations in the 59-590 bar Pressure Range*, J. of Engineering Physics, Vol. 36, No. 4, 1979.
41. Wilsak, R.A. and Thodos, G., *An Equation of State: Its Development from Argon Data and its Application to other Substances*, AIChE Journal, Vol. 31, No. 5, 1985.
42. Georgantas, A.I., Hong, H., Krepec, T., Lisio, C., Miele, D. and Wojciechowski, J., *Research and Development of New Concept for On-Board Storage, Direct Injection and Ignition of Gaseous Fuels in Automotive Internal Combustion Engines*, Progress Report No. 3, PROTOTYPES MANUFACTURING, CIC-0034, Concordia University, Montreal, Canada, October 1990.
43. Vargalftik, N. B., *Tables on the Thermophysical Properties of Liquids and Gases - In Normal and Dissociated States*, Second Edition, John Wiley & Sons, 1976.
44. Lubin, G., *Handbook of Composites*, Van Nostrand Reinhold Company, New York.
45. Hong, H., Krepec, T. and Tummala, M., *Research and Development of New Concept for On-Board Storage, Direct Injection and Ignition of Gaseous Fuels in Automotive Internal Combustion Engines*, Progress Report No. 5, DESIGN OPTIMIZATION, CIC-0047, Concordia University, Montreal,

Canada, December, 1991.

46. Baumeister, T., Avallone, E. A. and Baumeister III, T., *Mark's Standard Handbook for Mechanical Engineers*, McGraw-Hill Book Company, New York, 1978.
47. Rao, S.S., *Design of Vibration Isolation Systems Using Multiobjective Optimization Techniques*, ASME Paper No. 84-DET-60, 1984.
48. Papalambros, P.Y. and Wilde, D.J., *Principles of Optimal Design*, John Wiley & Sons, 1988.
49. Carrese, G. and Krepec, T., *Simulation, Testing and Optimization of a New Low Cost Electronic Fuel Control Unit for Small Gas Turbine Engines*, SAE Paper No. 901027, 1990.
50. Rao, S.S., *Optimization - Theory and Practice*, John Wiley & Sons, 1984.
51. Tummala, M., Krepec, T. and Ahmed, A.K.W., *Simulation, Testing and Optimization of Natural Gas On-Board Storage System for Automotive Applications*, SAE Paper No. 931820.
52. Tummala, M., Krepec, T. and Ahmed, A.K.W., *Optimization of Thermocontrolled Tank for Hydrogen Storage in Vehicles*, Proceedings of the 10th World Hydrogen Energy Conference, pp. 975-984, Volume 2, Cocoa Beach, Florida, U.S.A., 20-24 June 1994.
53. Krepec, T., *Dual-Fuel Urban Bus Transport System*, Report Prepared for Hydrogen Industry Council, Montreal, Aug. 1989.

54. Hong, H., Krepec, T. and Tummala, M., *Research and Development of New Concept for On-Board Storage, Direct Injection and Ignition of Gaseous Fuels in Automotive Internal Combustion Engines*, Progress Report No. 6, ADAPTATION AND APPLICATION, CIC-0048, Concordia University, Montreal, Canada, February, 1992.
55. Kroeger, C.A., *A Neat Methanol Direct Injection Combustion System for Heavy-Duty Applications*, SAE Paper No. 861169, 1986.
56. Watson, H.C. and Milkins, E.E., *Hydrogen and Methane - Automotive Fuels of the Future*, J.S.A.E. (Australia), Vol.35, No.2, 1975.
57. Gopal, G., Rao, S. P., Gopala Krishnan, K.V. and Murthy, B.S., *Use of Hydrogen in Dual-Fuel Engines*, Int. J. of Hyd. Energy, Vol. 7, No. 3, 1982.
58. Peschka, W., *Liquid Hydrogen - Fuel of the Future*, Springer-Verlag Wien New York, 1992.
59. Krepec, T., Miele, D. and Lisio, C., *Improved Concept of Hydrogen On-board Storage and Supply for Automotive Applications*, J. Hydrogen Energy, Vol. 15, No. 1, pp. 27-32, 1990.

## **APPENDICES**

## APPENDIX A

### PROPERTIES OF DIFFERENT FUELS USED IN VEHICLES

	Gasoline	Methane	Hydrogen	Nitrogen
Flammability limits (Vol %)	1-7.6	5.3-15	4.0-75	-
Stoichiometric air/fuel ratio	14.9:1	17.2:1	34.7:1	-
Laminar flame speed (m/sec)	0.33-0.47	0.39	2.78	-
Research Octane number	92-98	130	106	-
Ignition temperature (K)	663	905	845	-
Minimum ignition energy (MJ)	0.24	0.29	0.02	-
Specific gravity of liquid	0.75	0.42	0.07	0.81
Molecular weight	107	16.043	2.016	28.016

Specific heat, $c_p$ (kJ/kg-K)	1.62	2.25	14.31	1.04
Specific heat, $c_v$ (kJ/kg-K)	1.54	1.74	10.2	0.74
Critical pressure (bar)	24.5-27	45.8	12.8	33.5
Critical density (kg/m <sup>3</sup> )	230	162	31.4	304
Critical temperature (K)	540-569	190.7	33.2	126.1
Boiling point (K)	311-478	111	20	77
Lower heating value (MJ/kg)	43.7	50	120	-
Upper heating value (MJ/kg)	47	55.2	141.86	-
Heat of evaporation (kJ/kg)	330	510	446	197
Flame temperature in air (K)	2470	2148	2318	-

Note: Nitrogen is not a fuel for vehicles. Its properties were given only for comparison purpose, since liquid nitrogen was used in all the tests as a replacement for LNG and LH<sub>2</sub>.

Source: Ref. 55-58

**APPENDIX B**

**TECHNICAL DETAILS AND CALIBRATION CURVES**

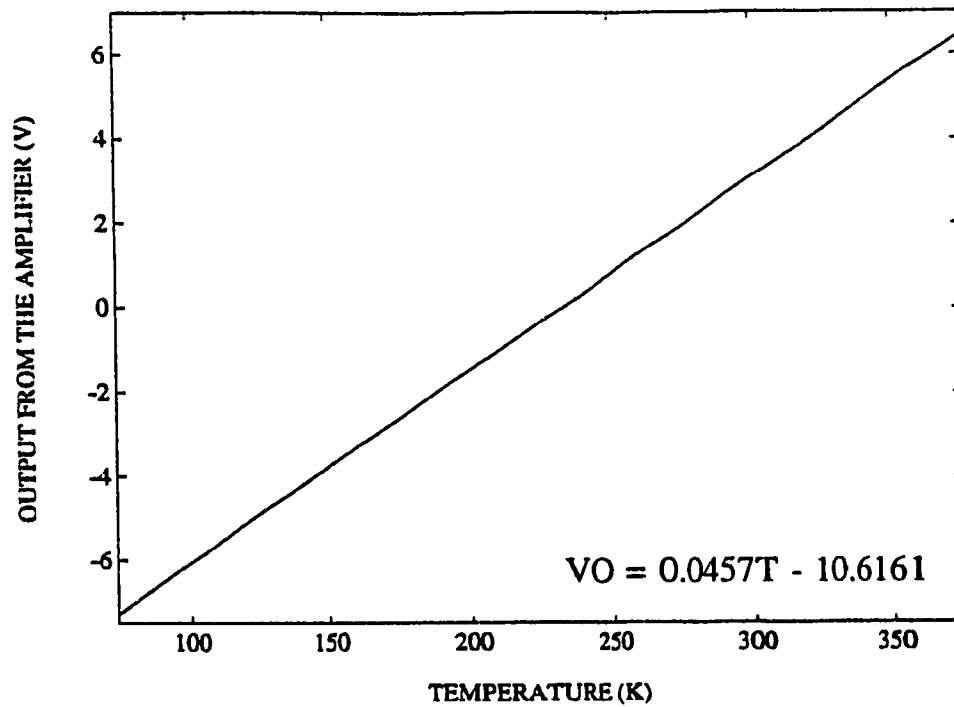


Fig. B.1 Calibration curve for OMEGA thermocouple

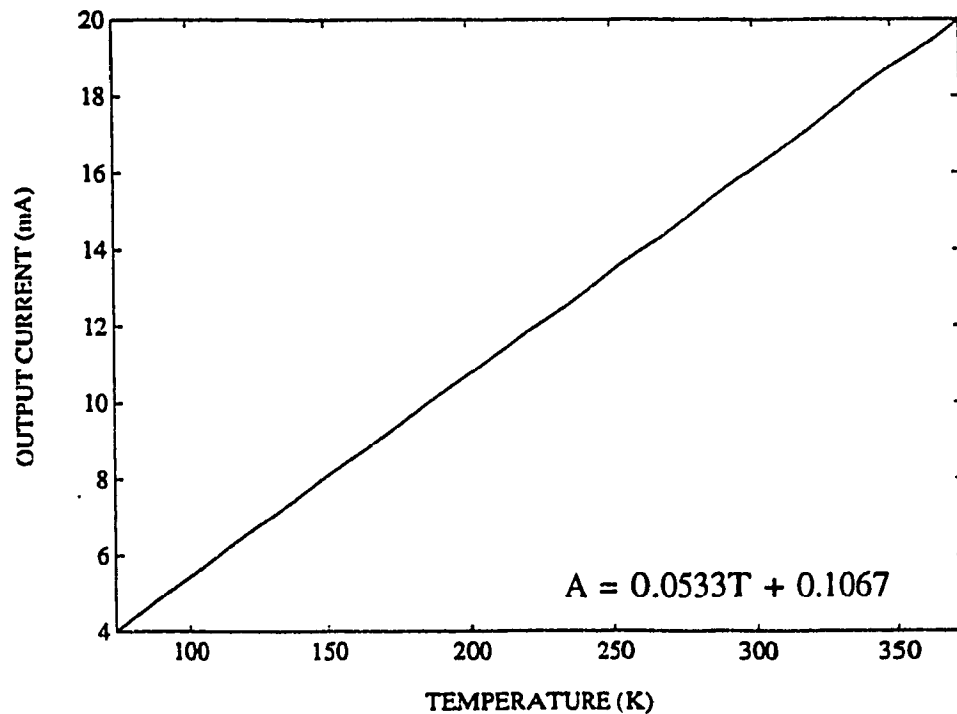


Fig. B.2 Calibration curve for RTD thermocouple

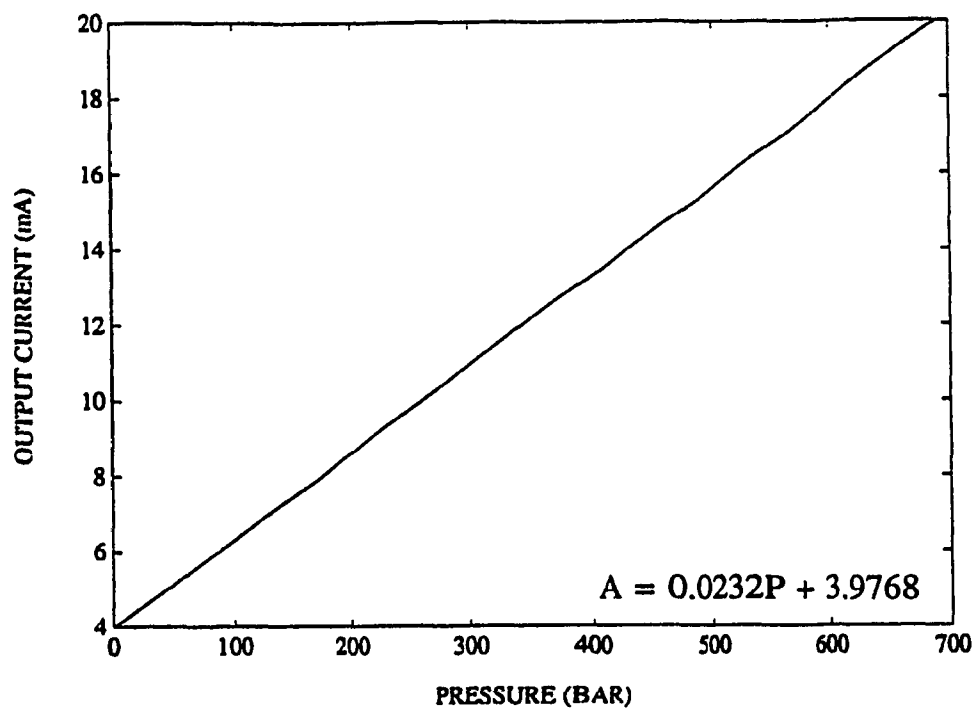


Fig. B.3 Calibration curve for OMEGA pressure transducer

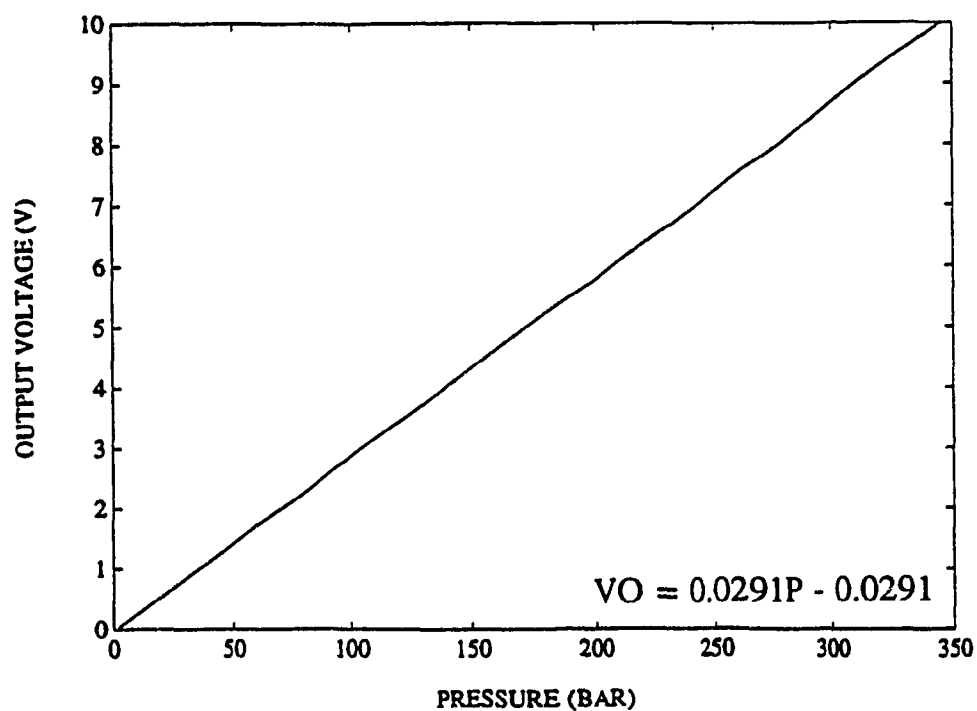


Fig. B.4 Calibration curve for VALIDYNE pressure transducer

FEATURE SELECTION IN THE CLASSIFICATION  
OF TIME-VARIANT PATTERNS

Khalid J. Siddiqui

A Thesis  
in  
The Department  
of  
Computer Science

Presented in Partial Fulfillment of the Requirements  
for the Degree of Doctor of Philosophy at  
Concordia University  
Montreal, Quebec, Canada

May 1994

© Khalid J. Siddiqui, 1994

## SCHOOL OF GRADUATE STUDIES

**This is to certify that the thesis prepared**

**By: Khalid J. Siddiqui**

**Entitled: Feature Selection in the Classification of Time-Variant Patterns**

and submitted in partial fulfillment of the requirements for the degree of

**DOCTOR OF PHILOSOPHY (Computer Science)**

**complies with the regulations of the University and meets the accepted standards with respect to originality and quality.**

**Signed by the final examining committee:**


K. Thulasiraman Chair

  
\_\_\_\_\_  
Dr. G. Stamon External Examiner

K. S. Ramamurthy External-to-Program  
Dr. A.S. Ramamurthy


Dr. T. Kasvand Examiner

Dr. I. Kasvand



\_\_\_\_\_ Examiner

Dr. H.F. Li

 Co-Thesis Supervisor  
Dr. C.Y. Suen

\_\_\_\_\_  
Dr. R. Hay Co-Thesis Supervisor

Approved by X211  
Chair of Department or Graduate Programme Director

August 23 19Am

Dean F. Kees  
Dean of Faculty

## ABSTRACT

### Feature Selection in the Classification of Time-Variant Patterns

Khalid J. Siddiqui, Ph.D.  
Concordia University, 1994

A bottleneck in building and using the knowledge base in an intelligent system is combining the appropriate problem solving knowledge with physical observations. Another problem is to derive pertinent information that is subtly available in physical observations. These problems are resolved by using the information and knowledge processing techniques available in the fields of signal processing, pattern recognition and knowledge engineering. Methods are developed to automatically measure, recognize and interpret the parameters (features) from the physical observations. A Successive Feature Elimination Scheme involving multiple steps is developed to eliminate poorly performing features. Pseudo-Similarity method which uses inter-class dissimilarity is introduced for feature ranking. To minimize the problems of information explosion and redundancy the concept of Pattern Association Hierarchy (PAH) is introduced to structure and organize the features and pattern classes in the form of a knowledge tree. Several classifiers including the two new algorithms PAH classifier and entropy based decision tree classifier are also developed. Based on the nature of the training data a number of meta rules are developed to select the best knowledge organization and classification algorithms. All these components and concepts are used as a basis to propose a structure of an intelligent waveform recognition system. This unified approach will not only automate and accelerate the knowledge acquisition and organization process, but will also formalize and structure the decision-making process, and thus reduce the reliance on a human expert.

The performance of these components is successfully demonstrated on several time-variant signals from non-destructive testing (NDT), and non-invasive testing (NIT) generated from materials (NDT signals), chemical mixtures (PNA spectra), human brain (EEG signals), and genetic cells (CEL signals). On the testing set from NDT data with 10 classes an overall performance reaching 84% was achieved and up to 95% when it is treated as a four class problem. Up to 95.67% of the EEG signals with 3 classes were correctly recognized whereas a perfect score of 100% was obtained on PNA data with 20 classes. On the CEL data with 19 classes the recognition performance reached 88.34%.

### Acknowledgements

I am grateful to the almighty Allah for granting me the wisdom curiosity, dedication, and endurance in pursuit of the goals I set.

I am sincerely thankful to my advisors Drs. D. Robert Hay and Ching Y. Suen for their continuous support, encouragement and guidance throughout the span of this research. Their patience and understanding, both work-related and personal have been most valuable for the completion of this endeavor.

I would also like to thank Dr. D. Eastwood of Lockheed Engineering and Sciences Company, Las Vegas, for providing knowledge and sharing thoughts pertaining to Chemistry and reading the sections which are carrying the information about the PNA problem. Thanks are also due to Dr. D.J. MacCrimmon, McMaster University, Hamilton, Canada for providing data on the EEG problem. The help that Dr. Y.-H. Liu, University of Nebraska, Omaha has provided in formulating the feature optimization problem is unforgettable. Some typesetting help received from Iftikhar is gratefully acknowledged. Akhtar's help in making few diagrams is appreciated as well. The software development, mainly, was done using Borland's Turbo Pascal and C in DOS and UNIX environments, the wordprocessing was done using Wordperfect, and the diagrams were drawn using Harvard Graphics. These vendors are sincerely acknowledged. The computing facilities at Concordia, Creighton, and at the University of Nebraska are appreciated very much. The office space and supporting facilities provided by Drs. M. Sketch, and S. Mohiuddin of The Cardiac Center, Creighton University, are acknowledged as well.

The comments, suggestions and the supply of NDT related literature by Dr. J.R. Matthews, Defence Research Establishment

Atlantic, Dartmouth, Canada, and Dr. A. Fahr, National Research Council, Ottawa, Canada are appreciated very much.

During my long period of studies at Concordia, I received much help from Stephanie, Halina, Angie, and Irene, the secretaries of the Computer Science department. Helene was very helpful in looking after the administrative matters at the Dean's office. I wish to thank them very sincerely. Mrs. C. Hay, Maureen, and other staff at Tektrend are also acknowledged for their share of support and well wishes.

I wish to express my gratitude to my peers, colleagues and dear friends in Montreal and Omaha, in particular, Drs. T. Fancott, R. Shinghal, S. Mohiuddin, D. Malik, and Mr. B. Qureshi for their encouragement, moral support in times of acute uncertainties and setbacks. My life-long friends, Alam in Chicago, Anzar and Ijaz in Montreal, and, Ismail, and Tahsin in Toronto provided transitory stay several times during these years of travelling; their hospitality and kindness is unforgettable.

Last, but not least I wish to thank my parents, siblings, and family for giving me support and kept praying for my welfare. I am particularly thankful to my wife and children for bearing with me during all these years of pain and miseries. Their understanding during eight years of shuttling between Omaha and Montreal is appreciated very much. The amount of time and money spent on this entire exercise is phenomenal. None other than my family deserves the acknowledgement, as often they sacrificed the acute necessities for making time and funds available.

Alas! the remaining errors, omissions, ambiguities, and misleading comments, if any, are the sole responsibility of the author.

Dedicated to my  
Homeland and my  
Family

## Table of Contents

Abstract	iii
Acknowledgement	v
Dedications	vii
Table of Contents	viii
Lists of Figures	xiv
List of Tables	xvi
List of Notations and Symbols	xxi
Glossary of Terms	xxiv

### Chapter One

#### Introduction

1.1 Intelligent Waveform Sensing .....	1
1.2 Signal and a Signal Processing System .....	5
1.3 Knowledge Based Systems .....	10
1.4 NDT Waveform Processing Systems .....	13
1.5 Medical Diagnostic Systems (MDS) .....	14
1.6 The Need for a Stand-alone System .....	18
1.7 Integration of Information Processing Technologies .....	20
1.8 A General Intelligent Recognition System (IRS)....	22
1.9 The Research Contributions .....	27
1.10 Thesis Organization .....	30

### Chapter Two

#### Common Elements of an Intelligent Recognition System

2.1 Introduction .....	32
2.2 Signal Interpretation - Current Practices .....	32

2.3	Modeling the Waveform Indications .....	34
2.3.1	NDT Indications Model .....	35
2.3.2	EEG Indications Model .....	38
2.3.3	PNA Indications Model .....	40
2.4	Ideal Knowledge Requirements .....	41
2.5	The Knowledge - Our Perspective .....	48
2.6	The Design of IRS System .....	51
2.6.1	The Knowledge Acquisition, Representation and Organization (KARO) Subsystem .....	52
2.6.2	Inference Engine .....	54
2.7	Signal Conditioning and Treatment .....	54
2.8	Mapping and Parameterization of Waveforms .....	56
2.8.1	Mapping Space .....	56
2.8.2	Parameter Extraction .....	60

### Chapter Three

#### Analytical Features and Pattern Association Hierarchy

3.1	Introduction .....	62
3.2	Fact Gathering Phase .....	62
3.2.1	The Pattern Data .....	63
3.2.2	Pattern Measurement Problems .....	63
3.2.2.1	Analytical Feature Extraction ....	66
3.2.2.2	Homogenizing the Analytical Features .....	67
3.3	Pattern Association Hierarchy .....	72
3.4	Clustering Procedures .....	77
3.4.1	The Bottom-up Organization .....	78
3.4.2	Generalized Variations Clustering Procedure	84
3.4.3	The Top-down (Divisive) Organization .....	87
3.4.4	Clustering Algorithm Selection Criterion - Meta Knowledge .....	89
3.5	Knowledge Organization Strategy .....	91

## **Chapter Four**

### **Feature Selection, Empirical Knowledge, and Organization of Knowledge Base**

4.1	Introduction .....	95
4.2	Selection of Optimal Features (Analytical) .....	95
4.2.1	The Size Selection .....	96
4.2.2	Feature (Label) Selection .....	97
4.2.2.1	Successive Elimination Process ...	98
4.2.2.2	Back-end Feature Dimensionality Reduction .....	103
4.3	Optimal Feature Selection - One by One Criterion..	103
4.4	Optimal Feature Selection - Simultaneous Selection Criterion .....	105
4.4.1	Pseudo-Similarity Algorithm .....	106
4.5	Weight Allocation to Features .....	111
4.6	Empirical Knowledge .....	113
4.7	Knowledge Formalization, Representation and Organization .....	116
4.7.1	Knowledge Formalization and Representation.	116
4.7.2	Hierarchical Knowledge Organization .....	117

## **Chapter Five**

### **Inference Engine and Machine Learning**

5.1	Introduction .....	120
5.2	Components of the Inference Engine .....	121
5.3	Inference Mechanism .....	123
5.4	Machine Learning .....	126
5.4.1	Learning by the Discrimination System .....	127
5.4.2	Learning by the Cognition System .....	131
5.5	Discrimination System - The Process .....	133
5.6	Cognition System - The Process .....	134
5.7	Entropy-based Decision Tree (EDT) Algorithm .....	135

5.7.1	Design of the EDT Algorithm .....	137
5.7.2	Computational Complexity and Problems .....	142
5.7.3	Merits of the EDT - Classifier .....	143
5.8	Failure Control .....	144

## Chapter Six

### Discrimination Subsystem

6.1	Introduction .....	146
6.2	Discrimination Subsystem .....	146
6.3	Classification Methodologies .....	147
6.3.1	Decision Theoretic Approaches .....	148
6.3.1.1	Parametric Approaches .....	148
6.3.1.2	Non-Parametric Approaches .....	150
6.3.1.2.1	Direct Decision Functions .....	150
6.3.1.2.2	Adaptive Decision Functions .....	151
6.3.2	Information - Theoretic Methods .....	154
6.3.3	Syntactic Approaches .....	154
6.3.4	Other Decision Making Strategies .....	155
6.3.4.1	Graph Theoretic Approaches .....	155
6.3.4.2	Heuristic Approaches .....	157
6.4	Trends in Decision Making Process .....	157
6.5	Classification (Search) Strategies .....	158
6.6	Hierarchical Decision Approaches .....	160
6.6.1	The PAH - Classifier .....	161
6.6.2	Design of the PAH - Classifier .....	162
6.6.3	Computational Complexity .....	164
6.6.4	Merits of the PAH - Classifier .....	168
6.7	Nodal Classifiers .....	169
6.7.1	Empirical Bayesian Classifier .....	169
6.7.2	K-Nearest Neighbor Classifier .....	172
6.7.3	Minimum Distance Classifier .....	173
6.7.4	Linear Discriminant Classifier .....	175
6.7.5	Quadratic Discriminant Classifier .....	176
6.8	Classification Process .....	178
6.9	Parametric Selection of a Classifier .....	179

## Chapter Seven

### Classification Experiments and Results

7.1	Introduction .....	188
7.2	The Functional View of Recognition Components ....	189
7.2.1	The Function of The Discrimination Sub-system .....	190
7.2.2	The Function of The Cognition Subsystem ...	192
7.2.3	The Function of The Failure Control Sub-system .....	193
7.3	System's Training .....	193
7.4	Performance of the Recognition Components .....	194
7.4.1	Implementation of MDC .....	194
7.4.2	Implementation of KNN .....	195
7.4.3	Implementation of LDC .....	195
7.4.4	Implementation of QDC .....	196
7.4.5	Implementation of BYC .....	196
7.4.6	Implementation of PAH .....	197
7.4.7	Implementation of EDT .....	198
7.5	Performance on NDT Data .....	198
7.5.1	Experiment A - MDC .....	200
7.5.2	Experiment B - KNN .....	204
7.5.3	Experiment C - LDC .....	206
7.5.4	Experiment D - QDC .....	206
7.5.5	Experiment E - BYC .....	209
7.5.6	Experiment F - PAH .....	210
7.5.7	Experiment G - EDT .....	212
7.5.8	Comments: Performance on NDT Data.....	214
7.6	Performance on EEG Data .....	218
7.6.1	Experiment A - MDC .....	222
7.6.2	Experiment B - KNN .....	229
7.6.3	Experiment C - LDC .....	232
7.6.4	Experiment D - QDC .....	233
7.6.5	Experiment E - BYC .....	236
7.6.6	Experiment F - PAH .....	237
7.6.7	Comments: Performance on EEG Data.....	239
7.7	Performance on PNA Data .....	242
7.8	Performance on CEL Data .....	248
7.8.1	Experiment A - MDC .....	253

7.8.2	Experiment B - QDC .....	258
7.8.3	Comments: Performance on CEL Data.....	262
7.9	Discussion: Overall Recognition Performance .....	263

## Chapter Eight

### Performance Review, Directions for Further Research, and Conclusions

8.1	Introduction .....	268
8.2	Performance Review .....	268
8.2.1	System Concept Level .....	269
8.2.2	Feature Extraction and Selection Level .....	269
8.2.3	Knowledge and Knowledge Representation .....	270
8.2.4	Knowledge Organization Level .....	270
8.2.5	Classification Level .....	271
8.2.6	Integration and Automation Level .....	272
8.2.7	Application Level .....	273
8.2.8	Overall Efficiency and Effectiveness .....	273
8.2.9	Expansion and Growth .....	274
8.3	Directions for Further Research .....	274
8.3.1	Future: Knowledge Acquisition .....	275
8.3.2	Future: Knowledge Formalization and Organization .....	275
8.3.3	Future: Modeling the Pattern Classes .....	276
8.3.4	Future: Inference Engine .....	277
8.3.5	Future: Expert/User Interface .....	277
8.4	The Research Contributions .....	278
8.5	Conclusions .....	280
8.5.1	NDT Problem .....	281
8.5.2	Medical Diagnosis Problem .....	282
8.5.3	Exploration/Classification of Oil and Minerals .....	284
8.5.4	General Remarks .....	284
	References .....	287
	Appendix - A Feature Extraction Details .....	311
	Appendix - B Acquisition and Characteristics of Data Sets .....	324

## List of Figures

1.1	A General Signal Acquisition and Processing System ..	6
1.2	A Typical ECG Waveform and its Information Contents .	8
1.3	A General Signal Classification/Diagnosis System ....	9
1.4	Components of an Expert System .....	11
1.5	The Proposed design of an Intelligent Recognition System .....	23
1.6	Skeletal View of components and techniques used in Intelligent Recognition System .....	28
2.1	NDT Indications .....	37
2.2	EEG Indications .....	39
2.3	PNA Indications .....	42
2.4	The Knowledge Acquisition, Representation, and Orga- nization (KARO) Subsystem .....	53
2.5	Pattern Measurement System [SIDD-90a] .....	57
2.6	Geometrical Interpretation of Envelope and Features Derived Therefrom .....	61
3.1	A few typical samples from NDT signals .....	65
3.2	Hierarchical Clustering Procedure .....	81
3.3	Block Diagram of Tree Organization .....	82
3.4	Bottom-up Algorithm for organizing the analytic feat- ures and corresponding classes in a tree structure .	83
3.5	Lower triangle .....	84
3.6	Top-down Algorithm for organizing the analytic feat- ures and corresponding classes in a tree structure .	90
3.7	Decision Tree for the Selection of a Clustering Procedure .....	94
4.1	A typical organization of knowledge frame .....	119
5.1	Schematic Design of the Inference Engine .....	122

### **List of Figures (Contd.)**

5.2	Inference Mechanism and Control Strategy .....	124
5.3	Supervised Learning and procedure for the Inference Tree .....	129
5.4	Nodal Training Scheme - Discrimination System .....	132
5.5	Tree Classification Mechanism of the Discrimination System .....	135
5.6	Information-theoretic organization of knowledge and pattern classes .....	136
5.7	Procedural steps of EDT Algorithm .....	138
6.1	PAH Classifier Design .....	161
7.1	Variations between different NDT Pattern Classes ..	199
7.2	A few samples from EEG Signals .....	219
7.3	Recognition Performance vs Number of Features .....	226
7.4	A few sample spectra of Petroleum Oils (PNA's) ....	243
7.5	Schematic structure of a nerve cell .....	250
7.6	The time course of action potentials .....	250

## List of Tables

2.1	Popular NDT Methods, their Application and useful Method Dependent Parameters .....	45
2.2	Theme Rules Describing Problem Domain Information ...	46
2.3	A priori knowledge - Test Specimen .....	47
2.4	Shape Factors of Some Common Defects .....	47
2.5	Test Apparatus & Test Conditions .....	48
2.6	Analytical knowledge features used .....	61
3.1	Sizes of Defect Areas and Their Identification .....	64
3.2	Analytical Features extracted for NDT Signal data [HAYD-88] .....	68
3.3	Parametric values for different clustering algorithms	78
3.4	Pattern Association Hierarchy using Single Linkage Method.....	80
3.5	Pattern Association Hierarchy using Centroid Method .	80
3.6	Pattern Association Hierarchy using Group Average Method.....	81
3.7	Pattern Association Hierarchy using Generalized Variations Procedure .....	87
3.8	Rule Set for the Selection of Clustering Procedure and Similarity Index .....	92
4.1	Stationary Features (NDT-data) removed .....	99
4.2	Features (NDT-data) rejected by t-test .....	101
4.3	Features (NDT-data) deleted by Collinearity test ....	101
4.4	Features (NDT-data) merged by 2nd Collinearity test .	103
4.5	Features (NDT-data) ranked using Fisher Index .....	105
4.6	Features (NDT-data) ranked using Pseudo-Similarity Algorithm .....	111
4.7	Empirical and Statistical Decision Parameters .....	114

## List of Tables (Contd.)

6.1	Complexity of Unweighed Pattern Classifiers .....	167
6.2	Properties of Classification Algorithms .....	184
6.3	Set of Rules used for the selection of Classification Procedures and Feature Weighing Criterion .....	185
7.5.A1	Classification Results on NDT Data Using Linear Orga- nization of Pattern Classes (MDC-Euclidean, Feat-A)	202
7.5.A2	Classification Results on NDT Data Using Linear Organi- zation of Pattern Classes (MDC-Mahalanobis, Feat-A)	202
7.5.A3	Classification Results on NDT Data Using Linear Orga- nization of Pattern Classes (MDC-Euclidean, Feat-F)	203
7.5.A4	Classification Results on NDT Data Using Linear Orga- nization of Pattern Classes (MDC-Euclidean, Feat-S)	203
7.5.A5	Classification Results on NDT Data Using Linear Organi- zation of Pattern Classes (MDC-Mahalanobis, Feat-F)	204
7.5.B1	Classification Results on NDT Data Using Linear Orga- nization of Pattern Classes (3NN-Euclidean, Feat-A)	205
7.5.B2	Classification Results on NDT Data Using Linear Organi- zation of Pattern Classes (3NN-Mahalanobis, Feat-A)	205
7.5.D1	Classification Results on NDT Data Using Linear Orga- nization of Pattern Classes (QDC, Feat-A) .....	207
7.5.D2	Classification Results on NDT Data Using Linear Organi- zation of Pattern Classes (QDC, Feat-A, wt=1/sd) ..	208
7.5.D3	Classification Results on NDT Data Using Linear Orga- nization of Pattern Classes (QDC, Feat-F) .....	208
7.5.D4	Classification Results on NDT Data Using Linear Orga- nization of Pattern Classes (QDC, Feat-S) .....	209
7.5.E1	Classification Results on NDT Data Using Linear Orga- nization of Pattern Classes (BYC, Feat-A) .....	210
7.5.1	Hierarchical Organization of Pattern Classes .....	211
7.5.F1	Classification Results on NDT Data Using Hierarchical Organization of Pattern Classes (MDC-Mahalanobis) 10 Class Problem .....	212

## List of Tables (Contd.)

7.5.F2 Classification Results on NDT Data Using Hierarchical Organization of Pattern Classes (MDC-Mahalanobis) 4 Class Problem .....	212
7.5.G1 Classification Results on NDT Data Using EDT Algorithm (10 Class Problem) .....	213
7.5.G2 Classification Results on NDT Data Using EDT Algorithm (4 Class Problem) .....	214
7.6.1 Features used for EEG Problem .....	220
7.6.2 EEG Problem: Features Deleted .....	221
7.6.3 EEG Problem: Feat-F and Feat-S .....	222
7.6.A1 EEG Problem: Design Set, Classification Results (MDC-Euclidean, Feat-A) .....	224
7.6.A2 EEG Problem: Testing Set, Classification Results (MDC-Euclidean, Feat-A) .....	225
7.6.A3 EEG Problem: Design/Testing Set, Classification Results (MDC-M, Feat-A) .....	226
7.6.A4 EEG Problem: Testing Set, Classification Results (MDC-Euclidean, Feat-F) .....	227
7.6.A5 EEG Problem: Testing Set, Classification Results (MDC-Euclidean, Feat-S) .....	228
7.6.B1 Classification Results on EEG Data Using Linear Organization of Pattern Classes (3NN-Euclidean, Feat-F) DesignSet .....	230
7.6.B2 Classification Results on EEG Data Using Linear Organization of Pattern Classes (3NN-Euclidean, Feat-F) TestingSet .....	231
7.6.B3 Classification Results on EEG Data Using Linear Organization of Pattern Classes (3NN-Mahalanobis, Feat-A)	232
7.6.C1 EEG Problem: Classification Results -LDC (Feat-A)	233
7.6.D1 Classification Results on EEG Data Using Linear Organization of Pattern Classes (QDC, Feat-A) .....	235
7.6.D2 Classification Results on EEG Data Using Linear Organization of Pattern Classes (QDC, Feat-F) .....	235

## List of Tables (Contd.)

7.6.D3	Classification Results on EEG Data Using Linear Organization of Pattern Classes (QDC, Feat-S) .....	236
7.6.E1	Classification Results on EEG Data Using Linear Organization of Pattern Classes (BYC, Feat-S) .....	237
7.6.4	Hierarchical Organization of Pattern Classes .....	238
7.6.F1	Classification Results on NDT Data Using Hierarchical Organization of Pattern Classes (MDC-Mahalanobis) .	238
7.6.F2	Classification Results on NDT Data Using Hierarchical Organization of Pattern Classes (MDC-Euclidean) Feature Sets: Feat-F & Feat-S .....	239
7.7.1	PNA Pattern Classes, their Labels .....	245
7.7.2	PNA Problem - Features Extracted .....	246
7.7.3	Pattern Association Hierarchy using Centroid Method	246
7.7.4	Classification Results .....	247
7.8.1	CEL Data Pattern Classes .....	251
7.8.2	CEL Problem - Features Deleted .....	252
7.8.3	EEG Problem: Feat-F and Feat-S .....	253
7.8.A1	CEL Problem: Design Set, Classification Results (MDC-Euclidean, Feat-A) .....	254
7.8.A2	CEL Problem: Design Set, Classification Results (MDC-Euclidean, Feat-A, wt = 1/sd) .....	255
7.8.A3	CEL Problem: Testing Set, Classification Results (MDC-E, Feat-A, wt = 1/sd) .....	256
7.8.A4	CEL Problem: Testing Set, Classification Results (MDC-M, Feat-A) .....	257
7.8.B1	CEL Problem: Testing Set, Classification Results (QDC, Feat-A) .....	259
7.8.B2	CEL Problem: Testing Set, Classification Results (QDC, Feat-F) .....	260

**List of Tables (Contd.)**

7.8.B3 CEL Problem: Testing Set, Classification Results (QDC, Feat-S) .....	261
7.9.1 Sensitivity of Classifiers on Different Data Sets .	267

## List of Notations and Symbols

$\{\}$	: Set symbol
$[\ ]$	: Vector symbol
$  \  $	: Determinant
$\neg$	: Logical negation
$\in$	: Inclusion of an element
$\alpha$	: Level of significance for t-test
$\varsigma$	: Correction factor to adjust the feature's weight
$\sigma_{ij}$	: Covariance of features $i$ and $j$
$\mathcal{S}$	: Feature Subset
$\psi$	: Ratio of pattern space to no. of features
$\Phi_j(X)$	: Characteristic function on a vector $X$
$U_x$	: Graph of pattern $X$
$a, b, c$	: Parameters of recursive distance function
$\text{cor}$	: Correlation threshold
$C$	: Label of a Pattern Class
$d(q, r)$	: Distance between classes (or groups) $q$ and $r$
$\bar{D}$	: Mean difference
$D_{ij}$	: Difference between feature
$D_j(X)$	: Discriminant function
$\delta$	: Expected value of feature difference
$G$	: Total number of cluster groups
$G_o, G_q, G_r$	: Group of Pattern Classes
$h, g, \text{ and } f$	: Three functions defining clustering environment: $h$ : maps input as vector $g$ : symbolic label of a class $f$ : clustering procedure
$H$	: Entropy function
$i, j, k$	: Indices for a feature, a sample, or a classes
$I_n$	: Entropy of input group
$I_o$	: Entropy of output group
$J$	: Optimization Criterion
$L$	: Level of the tree
$\ln$	: Natural logarithm
$M_i$	: Mean vector of class $i$
$M_o, M$	: Mean over $N$ classes
$m_i$	: Mean of feature $i$
$m_i$	: Mean of feature $i$ in reduced feature set
$\text{MAT}(ijr)$	: An element of the training matrix representing the conditional probabilities

Max	: A function to find maximum
Min	: A function to find minimum
$n'', n', n$	: Number of features at various stages of analysis
N	: Number of pattern classes
$p_i$	: Number of samples in class i
$p_o$	: Total number of samples in a problem space
$\rho_{ij}$	: Cell ij of the similarity matrix R
p	: Number of samples (equal) in each class
$P(i)$	: Probability of occurrence of class i
$P(\omega_j)$	: A priori probability of occurrence of class $\omega_j$
$P(X \omega_j)$	: Conditional probability of occurrence of X given that $\omega_j$ has occurred
r	: evaluated decision plane (function value) of a classification method
R	: Similarity matrix
$s^2$	: Pooled variance
$s_j$	: Standard deviation of feature j
S	: Variance-Covariance Matrix or pooled matrix
$S_w, S_b, S_t$	: Scatter matrices - within, between, and total
$S(q)$	: Number of comparison for a successful search in a binary tree
$U(q)$	: Number of comparison for an unsuccessful search in a binary tree
$\tau$	: Classification method dependent decision plane (threshold)
t	: Variable that holds the Student's t Distribution
$\tau'$	: range of feature values
$T^2$	: Distance (Hotelling's $T^2$ )
$t^2$	: Squared distance from the mean vector
$t'_\alpha$	: Tabulated value of t at significance level $\alpha$
$\theta_o, \theta_1, \theta_2, \theta_3$	: Threshold used successively to eliminate the features
$\theta_m$	: Majority vote threshold
$\theta_c, \theta_{min-c}$	: Threshold used for correlation
U	: Universe of a problem space
$v_i$	: Variance of feature i
$v'$	: Value of a feature
$\omega$	: A general pattern class
$w_i$	: Weight allocation to feature i
W, W'	: Weight vectors

$x_{ij}$	: Feature j of class i (transformed)
$x_{ij}'$	: Original value of feature j of class i
$x_j^o$	: j-th region of feature $x_j$
$x_{min}$	: Minimum value of $x_{ij}'$
$x_{max}$	: Maximum value of $x_{ij}'$
$\bar{x}$	: Maximum likelihood estimate for mean of a feature
$X$	: An arbitrary feature vector
$y_i$	: Measurement (feature) on a pattern
$Z$	: Design set

## Glossary of Terms

Analytical Knowledge	A set a parameters analytically derived from physical observations.
BYC	The Bayesian Probabilistic Discriminant Function/ Classifier
Class	One of many groups or divisions of a problem space
Classify	Arrange or sort in classes (during design phase), or assign to a class (during classification)
Classification	A procedure of deciding if a given input pattern belongs to a given class of patterns
Cluster	A group of patterns or feature vectors closely associated based on a given criterion
CEL	Cell Data
Clustering	The process of grouping data
Complex Heuristics	A composite of data, information, knowledge, and meta knowledge allowing or assisting to discover
Decision	A conclusion reached as to some procedural action to be taken in a pattern analysis system
Decision function	A scalar single-valued function that defines the statistical decision boundary
Decision boundary (surface)	An artificially created border between two or more classes or clusters
Deduction	A term used in the sense of classification
Decision theoretic	Mathematical theory of making optimal decision
Discrimination	The ability to distinguish between two or classes (or clusters) of patterns
Distribution	The arrangement of data in a feature set, both within class and between class

ECG	Electrocardiogram
EDT	Entropy based Decision Tree algorithm
EEG	Electroencephalogram
Empirical Knowledge	A set a parameters derived from analytical knowledge
Fact	Established knowledge about a problem domain
Feature	A distinctive characteristic measurement, or a structural component made on a pattern
Feature Extraction	The determination of a feature or feature vector from a pattern
Feature Selection	The selection of a smaller feature set to be used for classification, may also involve mapping the original pattern to a lower dimensional pattern
Feature space	For n features, the n-dimensional space
Heuristics	Problem solving knowledge explicitly derived from expert(s)
Homostat	A homogeneous pattern class or a cluster
Hybrid Machine	An embedded system that combines physical observations, rules of thumb, and heuristics
Indication	A signal pattern representing certain class
Induction	Inference of a general law from particular instances
Inference	The act of decision making - to deduce or conclude from facts
Information	The possible features a pattern may have
Interpret	Bring out the meaning of; explain or understand
KNN	K-nearest neighbor classifier

Knowledge Based Pattern Discrimination	A new problem solving approach that combines physical observations and heuristics to distinguish between patterns of different classes
Hierarchical Clustering	Process of hierarchically grouping patterns/classes
Learning/Training	Knowledge acquired by study; to gain knowledge by experience
LDC	Linear Discriminant Classifier
Likelihood estimates	Empirical probabilities of the parameters
Matching	To test the similarity of two or more entities in some essential respect
MDC-E	Minimum Distance Classifier - Euclidean
MDC-M	Minimum Distance Classifier - Mahalanobis
Meta Knowledge	A set of Rules derived from established theory of Statistics, Clustering methods and data characteristics
NDT	Non Destructive Testing
PAH	Pattern Association Hierarchy: A new concept proposed in [SIDD-93a] that organizes the knowledge components based on their proximity
PNA	Polynuclear Aromatic Hydrocarbons (Petroleum Oils)
Pattern	A numerical vector of parameters describing an event
Pattern Recognition	A process leading to, 1) classification, 2) detection, or 3) parameter estimation, of an input pattern
Piecewise linear boundary	Boundary constructed to approximate non-linear decision boundary
PR	Pattern Recognition
Proximity	A numerical measure of establishing association between two pattern vectors
QDC	Quadratic Discriminant Classifier

Sample	A single measurement of a pattern or signal
Segregates	Pattern class or cluster with significant intra-class/cluster variations
Signal	A function of one or more independent variables
Supervised	To oversee the execution of a machine pattern recognition task by providing labeled reference pattern vectors to train the system
Trainable Machine	An intelligent machine that is capable of learning as more knowledge becomes available
Unsupervised	Not supervised, or learning as more knowledge is gained

## Chapter 1

### INTRODUCTION

#### 1.1 Intelligent Waveform Sensing

A waveform which may be time-variant or time invariant, is an electronic signal and it is used to convey information in a wide range of sensing and recognition applications. In these applications a signal is generated by a physical, chemical, or a biological phenomenon and its form is governed by inherent characteristics of some phenomenon such as electrical activity of brain cells represented as EEG's. The waveform therefore carries information about the structure or the functioning of the source and/or about the path from the source to the receiver. In time-variant signals the waveform may change its structure over time whereas the time has no bearing in time-invariant waveforms. The information carried by the waveforms may be extracted directly, by known observations of the waveforms as usually done in manual inspection techniques; or indirectly, by applying appropriate synthesizing and analyzing tools to either the waveforms or the measurements derived from them as usually done in automatic signal processing systems.

A number of applications, particularly for time-variant signals from both physical and biological systems can be cited in this regard [CHEN-82, COHE-86a,b, NAGA-91]. Notable examples from the physical systems are non-destructive testing (NDT) or evaluation (NDE), and spectral analysis of polynuclear aromatic (PNA) compounds (petroleum oils). The applications from the biological systems are too many to enumerate. However, some of the examples of such systems include electrographs (EG's), such as Electrocardiographs (ECGs), Electroencephalographs (EEG's), and cell and tissue categorization.

It is obvious that the information carried by the signals is phenomenal and an ideal system for processing and interpretation of signals would include a comprehensive cause and effect analysis of all attributes of the signals. Different approaches and issues involved in building such systems are discussed in subsequent sections. A formal approach would be to model the signals using all measurable attributes comprising the source and phenomenon generating the signals, their structure, and variations between signals.

Although numerous attempts were made to exhaustively synthesize the structure of the signals using analytical and mathematical tools [KRAU-69, NJP-93, STAL-82, VARY-79], such a comprehensive model cannot be represented using a mathematical expression alone. Instead we need methods to determine and evaluate the information signals carry, and to process large volumes of information we need automated knowledge based tools. Emphasizing such need we propose, in this thesis, a system approach to solve the problems of this magnitude and developed several essential tools for information analysis and summarization, and organization and categorization to achieve the objectives. Modeling the information contents carried by the signals and utilizing methods and concepts from pattern recognition, statistical decision theory and knowledge engineering, we developed algorithms to, 1) eliminate redundant information, 2) rank and weigh the parameters based on their discrimination power and information contents, 3) structure and organize the knowledge, based on natural association among pattern classes, and 4) categorize and interpret the signal patterns using a suitable classification algorithm. In addition, we developed rules to select different algorithms and made efforts to minimize the subjective biases of an expert/user at each phase of processing. A number of existing tools and techniques, such as clustering algorithms, Fisher's feature ranking method, and several traditional classification

algorithms, wherever they found feasible, are used. However, appropriate adjustments, as found necessary, have been made in these tools and techniques to conform with the objectives. Wherever it become necessary, new methods and techniques are developed (see Section 1.9). These methods mainly include, feature elimination and ranking methods, a pattern organization scheme, and several classification methods. All these methods are essentially the contributions of this research.

The performance of all these tools and techniques are evaluated in two domains of applications, i.e., physical systems and biological systems. Two examples from the physical systems considered are non-destructive testing (NDT), and chemometric analysis and interpretation of oil spectra. One of the examples from the biological systems is non-invasive medical testing (NIT) as applied to the interpretation of electroencephalographs (EEG's). The other example is living-body tissue and cells classification. These applications are briefly introduced in the following paragraphs.

Obviously, any test which is "destructive" will prevent the tested object from functioning usefully after the test. A case in point questions whether a machine which is working well will continue to do so, or have defects, e.g., hidden cracks, corrosion, wear and tear, etc., which will likely lead to an early breakdown. Of course such defects cannot be determined by running a test under service conditions. Thus a "Non-Destructive Testing (NDT)" method is introduced to test the intended or actual performance of a component or a structure without impairing the usefulness of the structure or the component. Generally, any test method in which the test signal has no significantly measurable effect on the properties of a material can be considered as non-destructive. The aim of NDT is to obtain information on the performance of material component or structure. Generally, only some inter-

mediate effects can be measured, which in turn must be related to performance. For example, radiographic methods determine changes in density. These density changes are then interpreted or characterized in terms of defects, which in turn are attributed to actual performance criteria.

Analogous to NDT methods, medical diagnostic testing by non-invasive techniques (NIT) can be defined as any test method by which the performance of living organisms, generally human beings, can be determined without in any way harming the living substance or even causing pain.

The kind of problem we are dealing with in this study is that of classification and assumes an appropriate name according to the nomenclature of the problem area. If the signal source is an NDT application then the classification problem will be referred to as a recognition problem and if it is a biomedical application then, synonymously, the classification will be called a diagnostic problem. The analysis of spectra in chemistry can be referred to as a chemometric interpretation problem. The identification of genetic cells is a biological grouping problem. Thus NDT, NIT, chemometric interpretation, and cell identification methods pose a similar problem: classification or interpretation of signals, based on their structural characteristics. However, each application would require its own set of parametric measurements. The majority of currently available techniques for these typical problems are primarily based on visual inspection and thus are human operator-dependent. The transfer of such human knowledge into the computer provides a basis for use of an automatic knowledge-based system for the interpretation of waveforms.

Although knowledge-based systems have evolved over a period of two decades, their use in the classification of waveform signals is still scarce. First, in Section 1.2, a conventional

signal processing system is outlined and different tools constituting such a system are described. Later the field of knowledge-based systems is reviewed, in general, in Section 1.3. Those systems specially designed for NDT waveform processing are separately discussed in Section 1.4. Section 1.5 reviews the medical diagnostic systems. Section 1.6 establishes the need for an intelligent signal processing system whereas Section 1.7 presents a unifying scheme to build a multi-disciplinary integrated smart system. Section 1.8 outlines the details of each component of a generalized intelligent recognition system proposed in this thesis. The contributions this research offers are summarized in Section 1.9. Lastly, Section 1.10 presents the organization of this thesis.

## **1.2 Signal and a Signal Processing System**

A general signal measurement, classification, interpretation and diagnostic system is schematically shown in Fig. 1.1. Usually such a system consists of a transducer coupled with the information source and extracts the required information. The transducer, in fact, converts the information into an electrical signal (analog) which is conditioned and transmitted, digitized, and submitted to digital conditioning (salt and pepper noise removal), processing (transformation and manipulation) and/or classification (see Fig. 1.1). The transmitted signal may be corrupted with additive and multiplicative noise, and the information required may constitute only a part of the signal such that irrelevant portions are considered noise. In such situations signal conditioning techniques such as noise attenuation and cancellation techniques, or signal enhancement methods, can be applied in order to increase the signal-to-noise ratio and/or information contents. A variety of methods are available for the enhancement of the relevant information in a signal [COHE-86b, STEA-88].

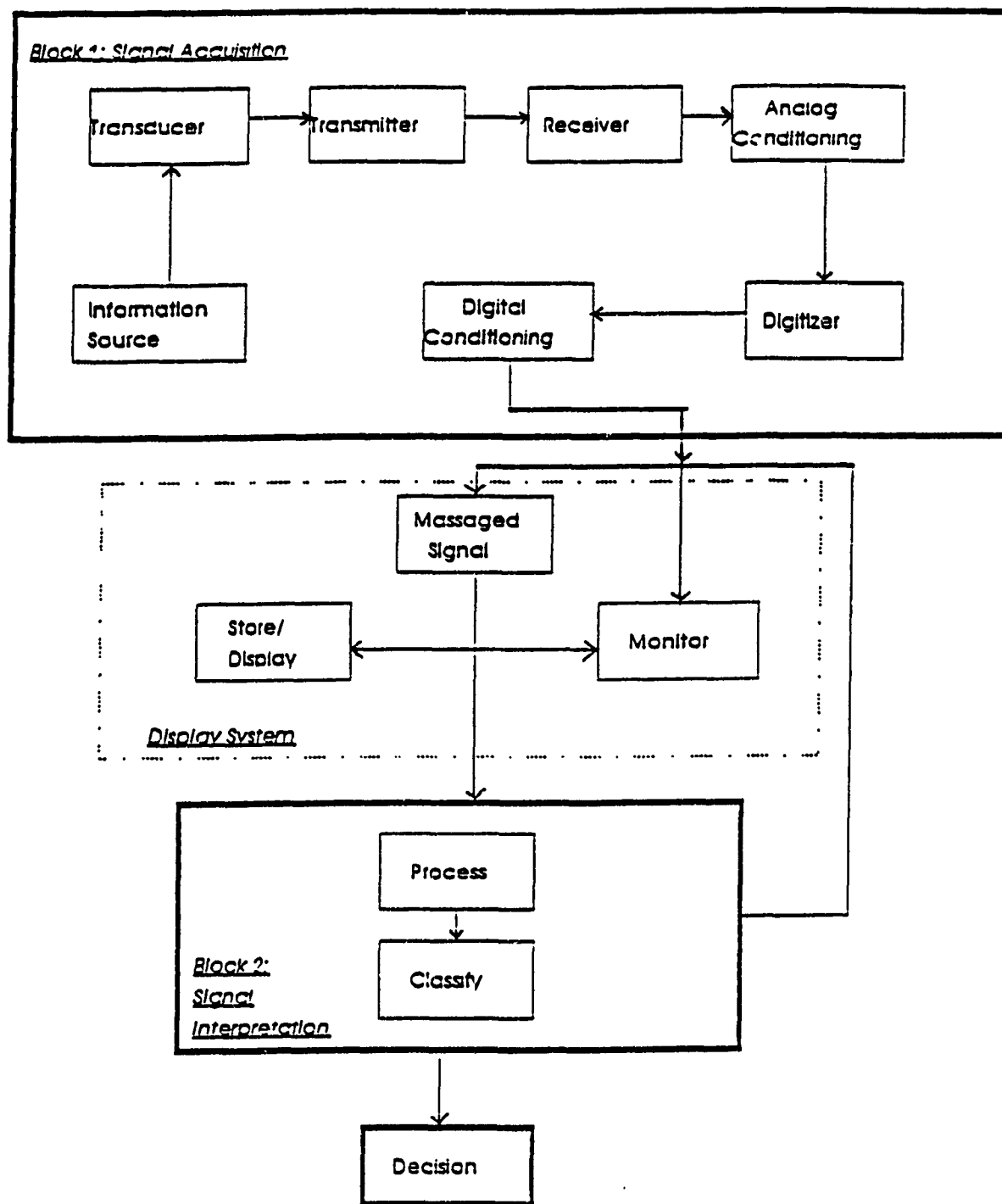


Fig. 1.1: A General Signal Acquisition and Processing System.

Sometimes the signals available may not yield the required information directly or the information conveyed by even a clean and massaged signal is not sufficient for high precision decision-making. In such cases the transformation of signal has been suggested in the literature [BRAC-86]. The most common transform applied in the majority of engineering applications is the Discrete Fourier Transform (DFT). The DFT is used to transform the signal, usually from the time domain into frequency domain, so that spectral information about the signal can be revealed explicitly. In addition to the frequency domain other properties of the transforms can also be used. In some other situations the signal may drastically change its properties with time, i.e., signal is time-variant. In such cases the observations and processes on the signal are performed only in a finite time window. The length and type of the window depends on the signal source and the processing objectives.

Very often only the general wave shape is known. A good example is the electrocardiographic signal, shown in Fig. 1.2, where the general shape of the wavelet, also called as PQRS complex in medical terminology, is known. In order to determine the patient's condition, the extraction of this wavelet present in the signal and its frequency of occurrence (defined in terms of number of cardiac cycles) is required [DICA-93, SIDD-93a,b, TRAH-89]. The wavelet can be extracted using segmentation or similar techniques. Other parameters of interest for this problem are identified in Fig. 1.2 [TRAH-89].

Once conditioning and/or preprocessing is done, the signal or the extracted wavelet is ready for processing (manipulation). Again not all the information conveyed by the signal is necessarily of interest. The signal itself may contain redundant information. When effective storing and transmission are required, or when the signal needs to be automatically classi-

fied, these redundancies have to be eliminated. The signal can be represented by a set of features that contain the required information. These features are subsequently used for storage, transmission and classification. Furthermore, such features are also needed for enhancement and reconstruction of the signal. The number and types of features used dictate, on one hand, the data reduction rate for efficient storage and transmission and, on the other hand, the error of reconstruction. For tasks such as classification and diagnosis, pattern recognition (PR) techniques are usually used. The processes shown in the heavy dotted block of Fig. 1.3 are some of the typical steps involved in PR systems.

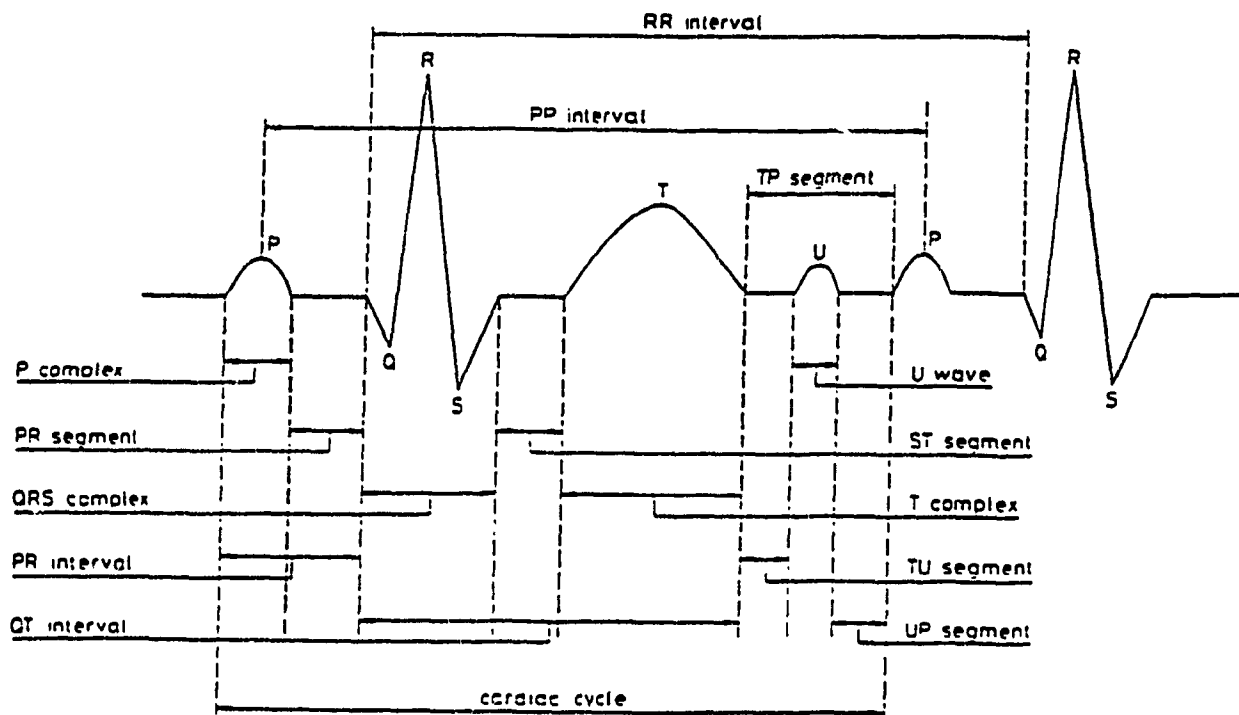


Fig. 1.2: A Typical ECG Waveform and its Information Contents.

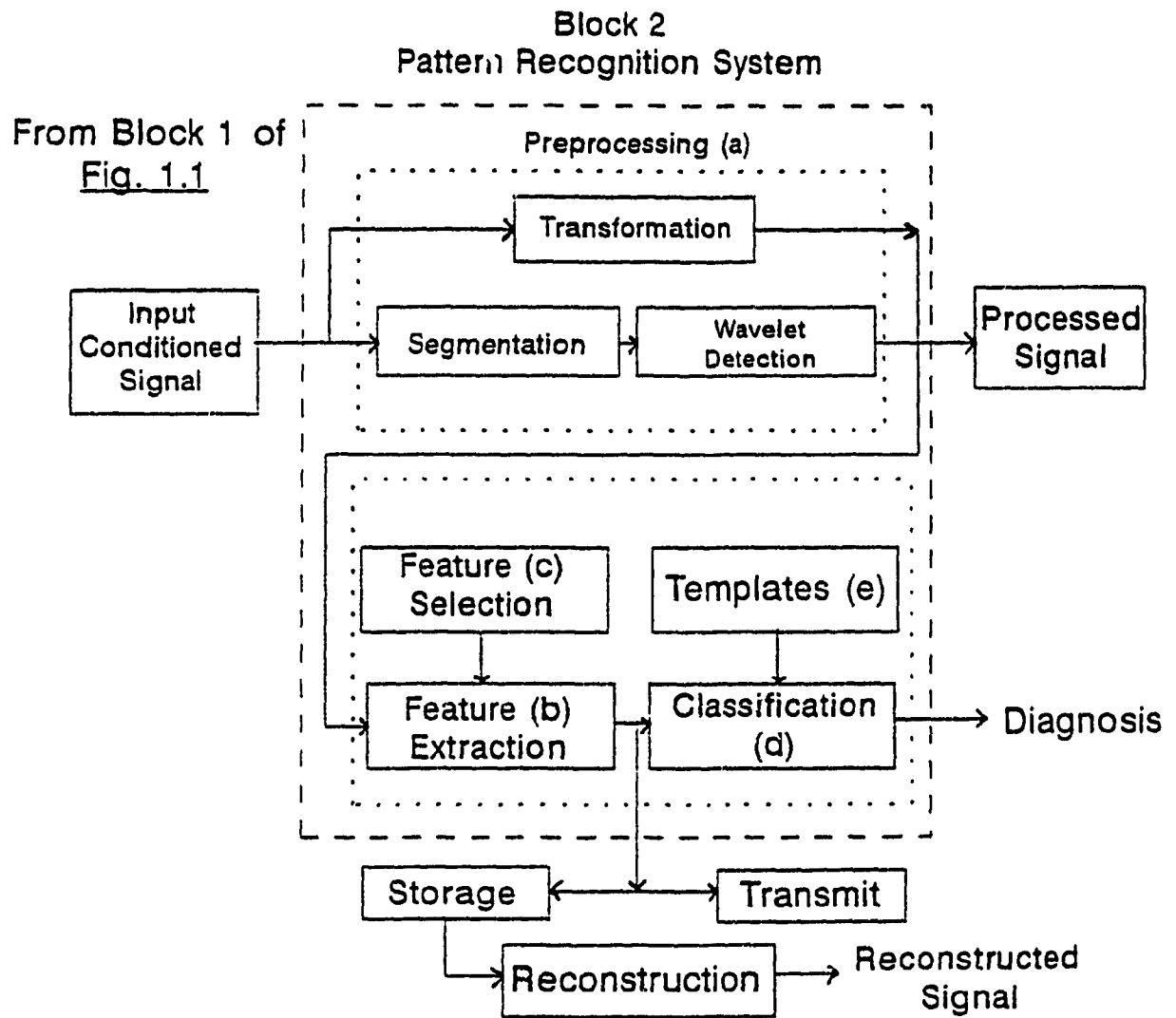


Fig. 1.3: A General Signal Classification/Diagnosis System.

The various functions thus needed in a signal processing and classification or interpretation/diagnosis system are depicted in the blocks of Fig. 1.3. The system shown in Fig. 1.3 is a general system. For specific applications, however, one may delete some of the components or add some other.

### **1.3 Knowledge Based Systems**

Scientists and engineers from every discipline are increasingly interested in including 'knowledge' among the materials from which they construct their artifacts. Knowledge based systems is a generic term and is used to characterize a general class of computer systems which incorporate knowledge as an integral component for decision making. When this knowledge is explicitly acquired from human expert(s), these systems are called expert systems.

Most knowledge-based systems that have been designed to date have been cited as expert systems. An expert system is a knowledge-intensive computer program that solves problems requiring human expertise so as to enable the computing system to perform convincingly as an advisory consultant or a decision maker. In some cases such human expertise is very expensive, rare, and occasionally, not replaceable. The scarcity of the experts and the need for an autonomous system has led the industry and the researchers to store the domain-dependent expertise into a data base and to computerize its subsequent utilization. Perhaps for this reason expert systems and knowledge based systems are growing in many areas, particularly in business applications. Industrial, medical (both clinical and electromagnetic diagnosis), and other scientific fields are beginning to find applications as well.

A typical knowledge based system is shown in Fig. 1.4. Such systems are usually composed of three principal components, a

knowledge base, an inference engine, and a user-interface. The knowledge base mostly contains declarative knowledge that is usually represented in the form of IF <premise> THEN <conclusion>, expressing a problem solving strategy that may be followed by an expert for the domain at hand. The inference engine is made up of decision rules that are used to control how the knowledge stored in the knowledge base is used or processed. The user-interface allows communication or interaction between the system and an end-user. A few examples will follow to illustrate the kinds of consultant services and

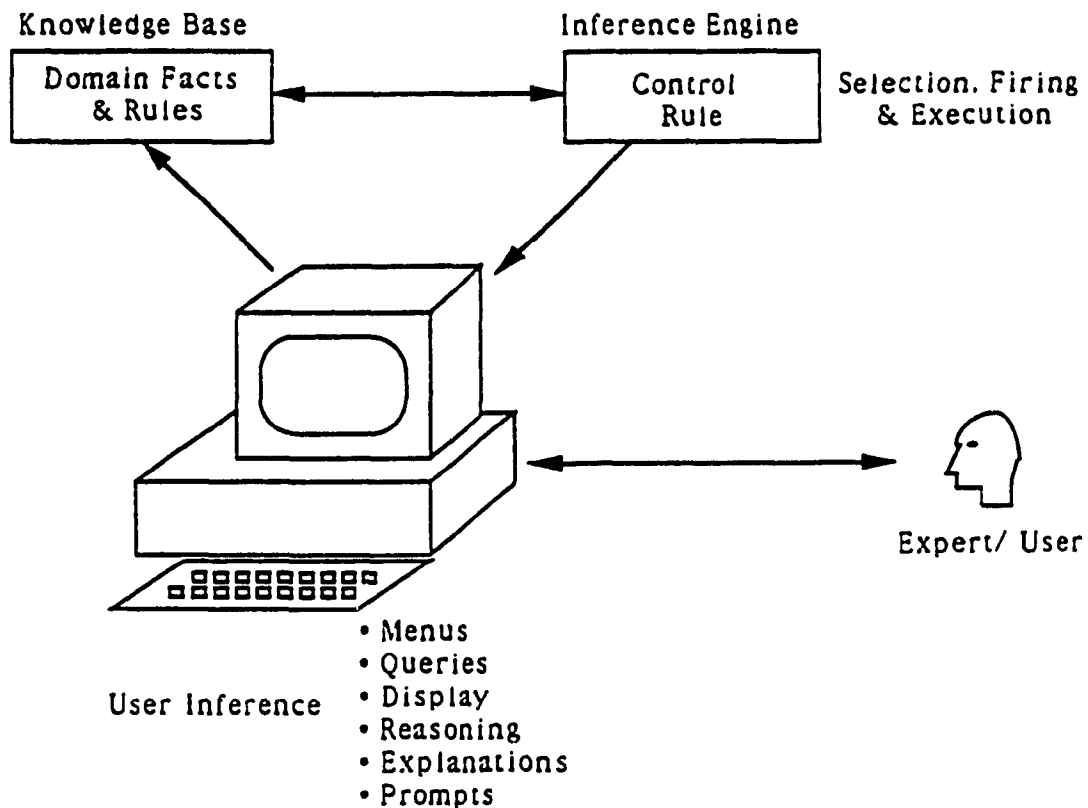


Fig. 1.4: Components of an Expert System.

skills which have been provided by such systems. MOLGEN [MARN-77, STEF-81] interactively aids molecular geneticists in the planning of DNA-manipulation experiments. SACON [BENN-78] guides engineers in the use of a large program which integrates structural analysis procedures. ITES [NAGA-91] deals with human images of feelings and translates them into ergonomic knowledge.

Well known examples of expert systems developed for industrial applications include PROSPECTOR [DUDA-78a,b] which has been successfully used to locate mineral deposits, Dipmeter Advisor, which is used for oil exploration [DAVI-81] and R1, which is used to configure computers [MCDE-82]. DENDRAL [BUCH-78, LIND-80] takes the pattern generated by subjecting an unknown organic chemical to a mass spectrometer and infers its molecular structure. SECS [WIPK-74] uses a 'knowledge base' of chemical transformations to propose schemes for synthesizing stated compounds. SES (Spectral Expert System) uses spectral information to characterize polynuclear aromatic compounds [SIDD-91a]. GUIDON is a knowledge-based tutoring system [CLAN-87]. End-game expert system deploys and discusses chessmaster knowledge and generates improved teaching texts [BRAT-78, BRAT-80]. Examples of other tutoring systems are [BRWN-74, BRWN-75, BURT-82, CARB-70].

A number of knowledge-based systems have also been developed for medical applications [ANBA-87, BETA-91, NAUD-83]. They will be reviewed separately in Section 1.5. The systems developed for applications in chemistry are reviewed by the author and others in [BROW-88, PAVE-86, SETT-87, SIDD-89a, SIDD-91a]. Further information on many of these systems and other applications is available in [BUCH-79, IRGO-90, LIEB-86, MOLD-87, NAUD-83, SIDD-88, SIDD-89a,b,c,d, SIDD-90c, SIDD-93a, SIDD-94a,b].

#### 1.4 NDT Waveform processing systems

Until the beginning of the 70's, non-destructive techniques (NDT) grew primarily as an experience-based technology. The field depended on skilled, experienced inspectors who progressed through certification programs based on knowledge of fundamentals and accumulated experience (expert knowledge) [MCGO-61]. While an underlying science base was developed through the 1960's and 70's, the qualified inspector remains the corner stone of the technology. Technological developments tended to be technique-based and explored new methods for interrogating materials. Since the 70's, there have been significant changes, there is not only a growing need for NDT technology, but there is also a broader perception and acceptance of its importance and applications.

A case in point concerns large engineering development projects, which characterize various new approaches to generate, transport, or use energy. These systems very often use materials close to their limits and the consequence of any failure can be catastrophic. The need for a timely and adequate inspection system is naturally obvious.

In recent years, because of the need for reliable and precise flaw classification techniques, the thrust of the research has been shifted from manual/analytical techniques to automatic multi-disciplinary techniques. Among the multi-disciplinary approaches, Shankar et al. [SHAN-78], Rose and Singh [ROSE-79a,b], Chan et al. [CHAN-85a,b], and Hay et al. [HAYD-84, HAYD-88] have demonstrated the feasibility of applying signal processing and pattern recognition techniques. Another approach combines signal processing and artificial intelligence [SING-83]. Other approaches combine two or more disciplines of image processing, holography, statistics, signal processing, artificial intelligence, and pattern recognition

[CHAN-80, CHAN-82, CHAN-85a,b, ELSL-83, HARR-80, HAYD-84, MAHL-85, ROSE-84, SIDD-86a, SIDD-88, SING-81].

As a result of these multi-disciplinary approaches, knowledge based systems and expert systems for NDT are beginning to emerge. For example, Mahalingam and Sharma [MAHL-85] reported a preliminary system called WELDEX for testing of welds and Siddiqui et al. [SIDD-87a] proposed the design of an expert system called KNOMES (Knowledge Monitoring Expert System). Primarily, the WELDEX system is derived from a medical system [GOME-81] and uses radiographic and other image processing techniques to diagnose the weld defects whereas the KNOMES system was based on signal processing and pattern recognition methods and was designed to classify NDT signals. None of these systems showed any experimental results. However, the work reported in this thesis uses the KNOMES' design approach [SIDD-87a] as the basis and provides experimental results on several application areas discussed above.

Another system of this type is ICEPAK (Intelligent Classifier Engineering Package). To the best of our knowledge this is one of the most effective and practically operating, and commercially available AI-based system which uses advanced signal processing and pattern recognition techniques for waveform characterization. This system has been successfully used on different kinds of waveforms from both material testing, and medical interpretation, to characterize flaw/defect and disease problems of 2 to 6 classes [CHAN-85a,b, HAYD-84, HAYD-88]. ICEPAK's design philosophy is partially used in the development of preprocessing and feature extraction modules.

### **1.5 Medical Diagnostic Systems (MDS)**

Physicians' diagnostic decisions are central to the treatment and care of patients. Often a physician's decision could mean

the difference between life and death. The question of how a physician should react to each new test result is persistent and pervasive. The information needed to answer a series of questions related to the outcome of such test results is based upon experience gained from training, and more immediately, information sources such as medical records, laboratory reports, textbooks, documented case histories, etc. In a majority of cases the answer requires simple list searches and comparisons, but the amount of information required to conduct the search, compare and remember is enormous. Human beings are not perfect. Given both the human limitations and extensive medical training of physicians, many medical errors may well be due to the limitations of endurance and instantaneous recall, rather than to remediable flaws in their funds of knowledge. There have been efforts made to reduce the chances of such errors [ANBA-87, BUCH-84, COOP-84, GOME-81, MILL-82, NATH-84, SHOR-76].

For example, WAMIS (German acronym for Vienna General Medical Information System) is an integrated knowledge-based medical system [ADLA-89] that combines medical information system with medical expert system CADIAG-2 [ADLA-86]. It links medical records, hospital testing facilities, pharmacy, patient's rooms, and outpatient clinics. By putting this information together, along with the factual and heuristic medical knowledge in its knowledge base, the knowledge system can interpret instrument readouts, suggest what the patient's illness might be, and advise on the proper drugs and treatment. Such consultant systems and several specialized disease-oriented systems have been in use since the middle 1970s. For example PUFF (PULmonary Function) system, developed at the Pacific Medical Center is a diagnostic system for pulmonary diseases [AIKI-83, KUNZ-78]. Ventilator Management (VM) [FAGA-78, FAGA-80] gives real-time advice on the management of intensive care patients' mechanical ventilation

at the same center. The Regenstrief Institute of Health Care (Indianapolis, Indiana) knowledge system called CARE, and the LDS Hospital (Salt Lake City, Utah) knowledge system named HELP, are both consultants that handle a more comprehensive range of physicians' chores [NATH-84, PRYO-83]. HELP has been shown to reduce healthcare costs. Some of the patients are treated even at remote locations. Barney Clark, the recipient of the first artificial heart was among such patients treated by HELP system. MYCIN [SHOR-74] and INTERNIST [POPL-77] have outperformed clinical consultants within the bounds of the systems' stored expertise. Foetus [BETA-91] is one of the most recent expert system developed for the assessment of fetus in a high-risk pregnancy. There are other computer programs such as, CADIAG-2 [ADLA-86], INTERNIST-1/CADUCEUS [MILL-84], ONCOCIN [BUCH-84], QUICK [FIRS-85], RECONSIDER [TUTT-83], that are practically operating in the hospital or physician's office. Some of these systems have already been tested with hundreds of clinical cases. Additional examples of medical diagnostic systems are cited in [ANBA-87, BENB-80, BUCH-84, COOP-84, FINK-89, GOME-81, HERN-89, LUGE-89, MILL-82, SIDD-93a, SHOR-74, SHOR-75]. Several medical tutoring systems are also reported in the literature [CLAN-81, HEID-88].

Most of the knowledge-based MDS systems are general care monitoring and analysis systems. The inference mechanism (problem-solving method) used in these systems is basically a variation of the hypothesize-and-test process. However, recently, a number of successful attempts of using elementary PR techniques and typical signal processing methods for simple classification and diagnostic problems in medicine have been reported [BENB-80, BUCH-84, LUGE-89, PAHL-87, SIDD-93b, SLAG-89].

Only a handful of the MDS systems mentioned above are capable of simultaneously analyzing, monitoring and diagnosing. Problems arise because of the complex nature of the input data and

number of parameters affecting it. Biomedical signals are usually extracted from living organisms. The living biological system is a very complex system governed by interactions of numerous biochemical, physical, and chemical subsystems not well understood as of yet [COHE-86a, PICT-88]. The complexity of the biological system introduces difficulties in measurement and processing procedures. In particular, many aspects of the complex hierarchical control of the brain and the nervous system, the genetic control, the neural information transfer and processing, and other systems are still under extensive investigation.

The large variations that exist in biomedical signals usually suggest the use of statistical methods. These variations exist in signals acquired from an individual and, of course, between populations. Consequently, the accuracies and confidence limits that come out of biomedical signal processing are usually not very high, at least in terms used in engineering disciplines. The measurement systems most often use Non-Invasive Techniques (NIT). This means that very often the requisite information cannot be acquired directly and one has to infer it from signals that are non-invasively available. Fetal heart monitoring is a good example. Rather than applying electrodes directly to the fetus' skin which is an invasive procedure, we non-invasively place the electrodes on the mother's abdomen. Unfortunately, the signals thus acquired are heavily contaminated with the mother's strong ECG and muscle activities (EMG).

Thus, one of the MDS problems is to extract pertinent pieces of information from highly contaminated signals and be able to analyze and diagnose (recognize) them using a machine. It appears that, as yet, no operative example of building such a stand-alone monitoring and diagnostic MDS system exists.

## 1.6 The need for a Stand-alone System

From the review of knowledge-based and signal processing systems presented in Sections 1.3 through 1.5, clearly two different problem-solving approaches have emerged, signal processing supplemented with pattern recognition methods and an expert-system approach.

Perhaps signal (waveform) sensing and processing systems which are primarily based on numeric processing are among the most powerful tools currently available for examining the internal structure of materials, chemical spectra and living biological substances. Using the waveforms, these systems have found wide application in industrial flaw detection, thickness gauging, spectroscopy to identify the components in chemical compounds, and very recently in medical diagnostic systems such as electrocardiography (ECG), electroencephalography (EEG), electro-neurography (ENG), electrooculography (EOG), etc. The other approach that heavily entails symbolic processing is that of expert systems which emulates human problem-solving in the form of hypothesize-and-test type symbolic processing.

While both of the above approaches have produced impressive performance at times, they currently face a number of limitations when applied to real-life problems [REGG-83, WEIS-84, SIDD-89d, SIDD-93a,b]. For example, problems where multiple pattern classes with complex representation are present simultaneously have proven very difficult to handle [POPL-77, SIDD-89d]. In addition, AI models of diagnostic reasoning are often criticized as being "ad hoc" because of the absence of a formal, domain-independent theoretical foundation [BENB-80]. Current systems are limited in size (of problem) and scope with limited learning capability and require extensive amount of expert/operator input. Rather, these systems provide enhanced displays and presentations to assist the human analyst in

his/her interpretations more likely with dated knowledge.

Ideally, for any computer software to be called an expert (intelligent) system, it should at least have the following characteristics:

- a mechanism to extract knowledge from raw observation and/ or from the expert, i.e., a mechanism that could combine numeric and symbolic processing.
- a mechanism to optimally associate observations to the pattern classes.
- a domain-specific knowledge base that may be updated as more knowledge becomes available.
- an optimal mechanism to represent and organize knowledge so that the problems such as information explosion and redundancy could be minimized.
- an inference mechanism that based on the knowledge available may choose an appropriate decision-making algorithm.
- an explanation/communication facility that may provide a logical explanation of the solution plan.

More recent efforts in AI research have stressed the use of large stores of domain-specific knowledge as a basis for high performance of expert systems. The knowledge base, which is the key component of this sort of program (e.g., Dendral [FEIG-71], MACSYMA [MART-71], Foetus [BETA-91]) is traditionally assembled manually. Such an assembly of a knowledge base is considered an ongoing task that typically involves numerous man-years of effort and continual interaction with expert(s). A key element in constructing a knowledge base is the transfer of expertise from human expert(s) to the computer program. The process of knowledge transfer is called knowledge engineering. Often, the domain expert is unfamiliar with the knowledge engineering process and usually unable to structure his strategic problem solving approach into a logical algo-

rithmic form. Also, it is virtually impossible for an expert to consistently extract the problem-solving information from physical observations. These factors make the acquisition of an expert's knowledge a very difficult task. Further, the manual acquisition of knowledge from a human expert is a very labor-intensive process. Therefore, we acknowledged a need to have automatic and formal aids for knowledge acquisition, formalization and its processing for the results, as part of the system.

### **1.7. Integration of Information Processing Technologies**

With the previous discussion it appeared to be essential that the methods available in a single field would not be able to provide us a complete set of tools to build the system we intended. A multi-disciplinary approach is essential. Now the question arises as to which disciplines to use and how to blend these disciplines to develop an integrated system to overcome some of the limitations discussed above. The approach we adopted is to borrow the concepts from a field only for those functions that the system can perform best. Thus considering the ideal characteristics, an intelligent system should have (see Section 1.6) the general objectives and scope of the problem we solved were established as below:

- Define a stand-alone signal classification and discrimination system that combines physical observations and expert knowledge.
- Minimize human biases in the selection of knowledge parameters, selection of knowledge processing techniques, and decision-making.
- Be able to solve a fairly large set of problems in a problem domain without degrading the performance.
- Be able to adapt itself to new problem domains by simply providing the system with a knowledge base in that problem domain.

- Be able to function both as an expert and as a consultant.

Two basic approaches of solving classification problems are discussed in previous sections, namely, pattern recognition (PR) and expert systems. Pattern recognition approaches primarily use numerical methods to automate the interpretation process by defining a set of characteristics for a pattern class. However, the PR techniques make no effort to identify the specific structure/property involved; they merely try to suggest structural elements (features) that the unknown may contain. In fact, this is the information that is used for the discrimination of a pattern class. A major advantage of these techniques is that they make no a priori assumption regarding the structural information used to discriminate a pattern class. As such, without imposing any solution, it is possible that useful new information may be uncovered. An expert system, on the other hand, uses the known interpretation logic of the human expert which is usually represented in symbolic form, and since it is stored in machine, the scope and effectiveness of decision-making is limited to the amount and depth of the knowledge stored.

The problem-solving approach adopted in this research uses a hybrid scheme that combines both of the above two approaches to build on their strengths rather than living within their limitations. The functional view of a unified system combining the set of approaches that have been shown diagrammatically in figures 1.1, 1.3 and 1.4 is presented in Fig. 1.5.

The techniques for signal registry and conditioning are borrowed, as is, from typical signal processing systems (Block 1 of Fig. 1.1) and used for information acquisition, conditioning and enhancement. The next set of techniques selected is PR techniques (Block 2 of Fig. 1.3). Pattern recognition

techniques are primarily evolved from the human process of vision, recognition and perception. Selection of good pattern recognition tools could reduce the burden on the human expert and save an unaccountable number of man-years which are otherwise required only to acquire the expert's knowledge. Moreover, since pattern recognition techniques use features which are easier to represent and easier to apply to decide the pattern identity, they will be very useful in formalizing and structuring the reasoning and explaining process for the actions of an inference engine. In addition to PR techniques, information transformation techniques such as Fourier or Hartley transform can be used to transform the signal to a more meaningful and explicit form.

The parameters extracted can be stored in a knowledge base and then usual expert systems' approach shown in Fig. 1.4, or knowledge-based pattern recognition methods can be used for classification. The inference engine, therefore, can be designed using both the declarative knowledge (from the expert) and the procedural knowledge. The procedural knowledge comprised of a set of pattern classification algorithms will use physical observations (pattern features) for decision making. To process the declarative and heuristic knowledge iterative dichotomization as suggested by Quinlan [QUIN-86], or any other algorithm with similar function can be used. Thus by combining these disciplines an intelligent waveform processing and recognition system, shown in Fig.1.5, is proposed. The details are presented in the following section.

### **1.8. A General Intelligent Recognition System (IRS)**

A general intelligent recognition system (IRS) is shown in Fig. 1.5. Before we describe the components of this system, several key terms and the context in which they are used will be defined.

# Knowledge Acquisition, Representation & Organization (KARO)

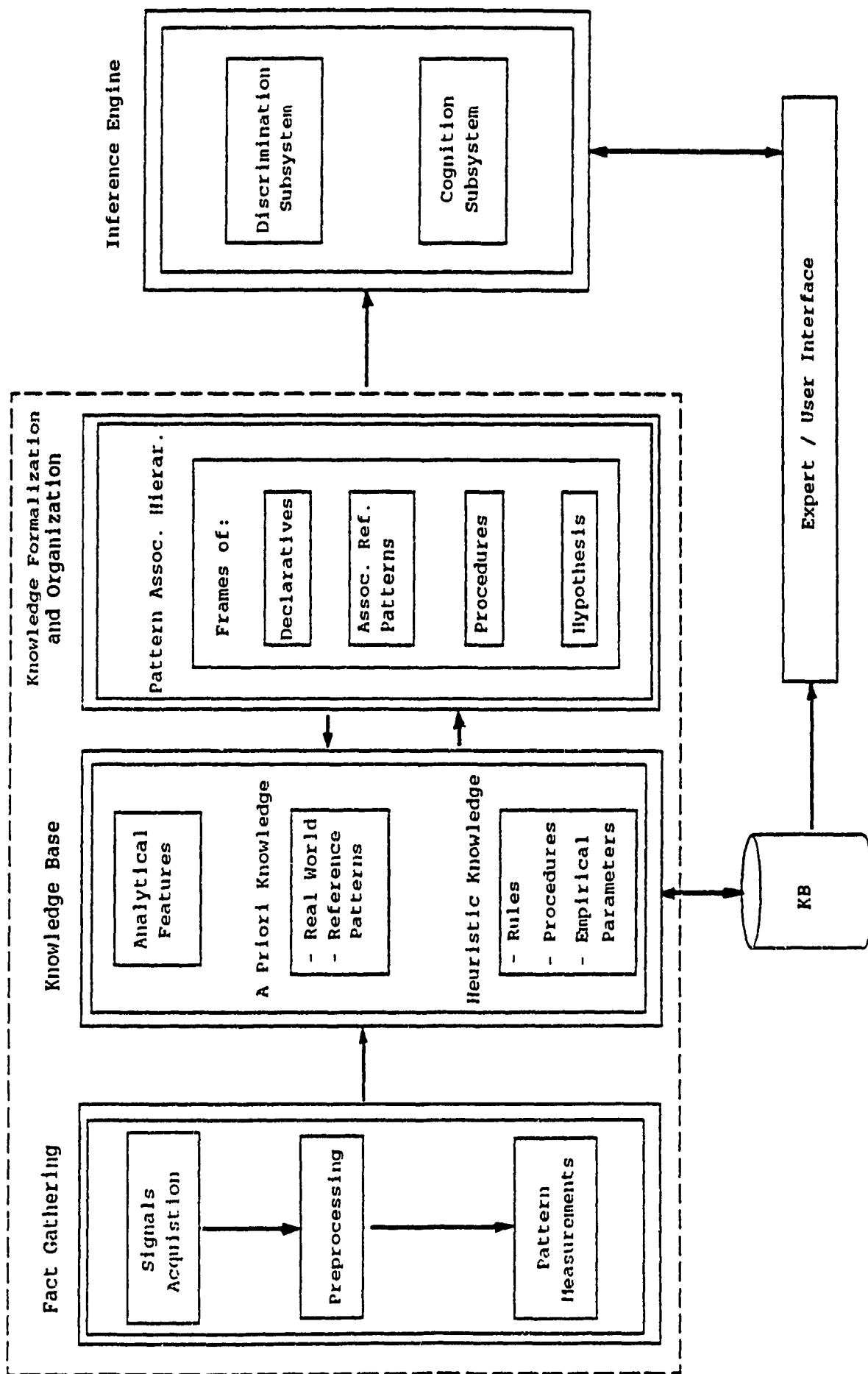


Fig. 1.5 A general design of an Intelligent Recognition System

The basic objects within the knowledge base are Facts and they refer to real-world knowledge about the problem domain which include the physical observation collected from the subject and any additional knowledge the signal may carry. These observations (signals) carry information about the source or the path which may be extracted in the form of pattern measurements (features). Based on their values, these features may indicate the pattern belongs to one particular class, i.e., indication.

The system shown in Fig. 1.5 is composed of three subsystems, 1) Knowledge Acquisition, Representation, and Organization (KARO) subsystem, 2) Inference Engine, and 3) the Expert/User Interface. The design philosophy and operational details of these components are presented in subsequent chapters, however, a functional overview of the system is presented in the following paragraphs.

The basic cycle of the KARO subsystem consists of three phases: namely, fact gathering, knowledge base, and knowledge formalization and organization. The fact gathering phase performs three main tasks, 1) acquisition of input data (waveform signals), 2) data preprocessing, and 3) pattern measurements. Each of these tasks further entails a series of operations. Since the pattern measurements are performed using analytical tools they will be called analytical features hereafter. Analytical features constitute a major portion of the knowledge base which is the next component of the KARO subsystem. A set of analytical features representing one physical observation constitutes a pattern vector. A set of pattern vectors representing the design set serves as a set of examples or reference patterns the system may be able to classify. Other components of the knowledge include a priori knowledge, and heuristic knowledge conforming the problem domain. A priori knowledge includes a number of parameters

pertaining to the physical and operating characteristics of the apparatus required for the recognition/interpretation experiment at hand. The analytical features are further used to derive empirical knowledge parameters some of which in turn are used to simulate human judgement and hence these parameters are considered as heuristic knowledge. Heuristic knowledge comprises of, 1) a set of rules representing expert's fixed (book) knowledge, 2) a set of procedures that an expert may apply on physical observations, and 3) a set of empirical knowledge parameters to formulate an expert's judgement and objectives. The function of a priori knowledge is to identify corrupted signals and based on stored knowledge, direct the preprocessing that the system should perform. The heuristic knowledge serves as meta knowledge and is used to select an appropriate algorithm at different stages of processing and controls its application on requisite data.

The next component of the KARO is knowledge formalization and organization wherein a series of operations are performed to sort, structure and organize the accumulated knowledge. Analytical knowledge takes advantage of the natural association that exists among patterns to build their pattern association hierarchy (PAH) which is a new concept introduced by the author in [SIDD-87a]. PAH supplemented with a priori and heuristic knowledge thus indicates the actions the system should initiate when some parameters reach certain thresholds. To use the knowledge base efficiently, the knowledge is formalized using a combination of knowledge structuring and rule building methods. The analytic features corresponding to an individual pattern are transformed into several sets of selected feature vectors. Empirical knowledge and heuristic knowledge pertaining to a set of associated patterns are stored as declaratives and procedures in structures called knowledge frames. A knowledge frame with appropriate node-dependent knowledge is placed at each intermediate node in the

PAH. Such organization of knowledge not only facilitates the storage and retrieval of pattern class-dependent information, but also increases the pattern recognition performance.

The same pattern association hierarchy is used by the inference engine to classify an unknown pattern. Using the known identity of the patterns, the inference mechanism of the engine is trained for an appropriate classifier at each node of the hierarchy. The classifier and the training information for each intermediate node is stored in the respective frames.

Once the knowledge is formalized and organized using the known identity of the signals, and the inference engine is trained on the problem at hand, the system can be used to characterize an unknown set of input signals.

Such a system could be designed to operate in two distinct modes, executive and consultant modes. In the executive mode, the system can operate autonomously by processing through the PAH and would not require any human input to solve a problem. To train the system for this mode of operations, supervised learning is required in which the system has the knowledge of the pattern classes it will be identifying. In the consultant mode, the system can be designed to function as a synthesizer that will allow the expert to monitor the pattern classification process by modifying a number of key decision parameters that we have identified for this purpose. To train the system for this mode of operation, unsupervised learning would be needed in which the expert has to provide initial input on identification of pattern classes.

If the dual mode of operation is implemented then the utilization of heuristic knowledge will depend on the operating modes of the system. If the system is in the executive mode, only the pre-stored fixed knowledge is utilized for the final

determination of pattern's identity. When the system is in the consultant mode, expert input is sought at each phase of the classification process. At present the system assumes the executive mode of operation only.

The last component of the system which is not implemented in this research, is the user/expert interface. The function of this component is to provide a communication and explanation facility for the actions which the system undertakes. A skeletal picture of the components and the techniques that are required for the development of the whole system are summarized in Fig. 1.6.

### **1.9 The Research Contributions**

The objectives discussed in Section 1.6 were established to define the context of the present work. To successfully achieve those objectives, a number of new algorithms and concepts which essentially constitute the contributions of this research were developed. Some of the notable contributions are listed below.

#### **1. System Concept Level**

Until the work reported in the thesis was carried out, the knowledge based approaches to system development were essentially isolated. That is, the systems were developed either using physical observations only or they were emulated using expert knowledge. This thesis proposes an integrated approach to a knowledge based pattern recognition system that combines both physical observations and empirical knowledge and develops several components (see below). Those components evaluated in this thesis demonstrate the general feasibility of the approach.

### **Knowledge Type**

A priori knowledge

- \* Facts about
  - problem domain
  - test equipment
  - test specimen characteristics
  - test conditions

Analytic knowledge (physical observations)

- \* Statistical features
- \* Waveform features

Heuristic knowledge (implicit/derived observations)

- \* From Expert
  - judgement & objectives;
  - specific methods/procedures including classification algorithms
- \* From System
  - empirical observation
  - meta knowledge

### **Knowledge Representation and Formalization**

Analytical feature vectors

Empirical knowledge and declarative rules

### **Knowledge Organization**

Declarative & Frames

Procedures

Pattern Association hierarchy

### **Inference Engine**

Machine Learning

- supervised/unsupervised

Inference Mechanism

- \* Discrimination strategy
  - parametric classification schemes
  - non-parametric classification schemes
- \* Cognitive strategy
  - information-theoretic decision tree

### **Operation (decision making environment)**

Executive (Tutorial)

Subordinate (Consulting)

### **Explanation/Reasoning Mechanism**

Forward/backward chaining through the hierarchy

Fig. 1.6: Skeletal View of the components and techniques used in the Intelligent Recognition System.

## 2. Feature Level

What features should be selected? Addressing this issue, we suggest to extract all useful features one can think of and then use 'Successive Feature Elimination Process' to weed out the poor performers and later use one of the two feature ranking and selection algorithms, i.e., Fisher discriminant index or Pseudo-Similarity method to select a smaller feature set. Successive Feature Elimination Process and Pseudo-Similarity method are the contributions introduced in this thesis.

## 3. Knowledge Organization Level

To minimize the problem of knowledge explosion and redundancy, a new concept called the pattern association hierarchy is introduced wherein several existing algorithms (a few were modified) and a new clustering algorithm called 'Generalized Variations' method are used to hierarchically organize the pattern classes and their associated knowledge. This arrangement thus always stores the knowledge pertaining to only two groups (or classes) at each non-terminal node of the PAH. Data-dependent 'Rules' are developed to select an appropriate clustering algorithm.

## 4. Classification Level

A number of observation-dependent parameters are designed to automatically determine the data statistics which in turn determine the pattern classification algorithm to be used. The new concept of pattern association hierarchy along with feature elimination and selection methods, data-dependent parameters, and, a number of parametric and non parametric classifiers at each node of the hierarchy gives birth to a flexible PAH-classifier. This method reduces the bias that

may be introduced by the human judgement while designing each of the above phases.

#### 5. Integration and Automation Level

Instead of human judgement, the system primarily relies on analytical tools to synthesize the available information. This synthesis evolves a set of new parameters (empirical knowledge) which are used to partially simulate human judgement. Using empirical knowledge a set of rules are designed to automatically select an appropriate algorithm among several available at different phases of processing. Thus a high level of automation and integration is achieved.

#### 6. Application Level

The project develops a generic signal classification scheme by successfully applying the system to three different application areas, namely, non-destructive testing, spectroscopy and medical diagnosis.

#### 7. Size of Problem, Performance, and Robustness

The algorithms we developed are not restrained by the size or the nature of the problem. We solved four problems with 3 to 20 pattern classes, up to 112 features and 2 to 200 samples in a pattern class with consistently high individual class performance of 60% to 100% mark for various problems.

#### 1.10 Thesis Organization

Altogether, the thesis comprises eight chapters. It begins with a chapter entitled, "INTRODUCTION" that describes waveform sensing and reviews some of the important systems developed for signal processing in first two sections. Review

on the knowledge based systems is included next. The systems developed for two of the application domains, i.e., the NDT signal processing and the medical diagnostic systems are briefly reviewed in the next two sections. After establishing the justifications for a knowledge based intelligent recognition system, the components of the proposed system are described together with a list of contributions this research makes.

Chapter two presents a general IRS system and describes its components. It further describes how the physical observation and other knowledge components pertaining to a problem domain are gathered, and analyzed. Several generic algorithms developed for knowledge organization and selection of optimal parameters for pattern discrimination are described in Chapter 3. Chapter 4 describes the components of the empirical and meta knowledge concentrating on techniques for knowledge abstraction and organization. A priori knowledge, physical observations, and empirical knowledge specifically for the NDT-domain are described in these chapters. The architecture of the inference engine is described in Chapter 5. The inference engine is a composite of two independent solution strategies, discrimination and cognition. The cognition algorithms used are also described in this chapter. The algorithms which formulate the discrimination strategy are presented in Chapter 6.

Chapter 7 presents the results of several experiments conducted on four data sets. These results are studied in detail and the observations made are discussed.

Finally, Chapter 8 concludes the research, reviews individually all the components of the system and summarizes the contributions of this research. It also presents the directions for future research in this area.

## Chapter 2

### Common Elements of an Intelligent Recognition System

#### 2.1. Introduction

We observed four levels of abstraction in knowledge hierarchy. They include primary concepts, physical observations, derived facts, and heuristics. Primary concepts refer to a priori knowledge pertaining to a problem domain. The information that the physical observations (raw signals) may carry is considered as facts. The derived facts and the knowledge derived from the primary concepts are referred to as the empirical knowledge. Using empirical knowledge and statistical decision theory a set of meta-rules were derived. Meta-rules are considered as heuristics and hence these two terms will be used interchangeably. Using this quadruple concept of knowledge abstraction the first subsystem, Knowledge Acquisition, Representation, and Organization (KARO) subsystem, of the intelligent recognition system is designed which forms the main subject of this chapter. The information a waveform carries is modeled and requisite knowledge pertaining to the NDT problem is structured. Some thoughts on how to incorporate instrumentation and operating conditions of apparatus are also presented in this chapter. The empirical and meta-knowledge concepts are the subjects of Chapters 3 and 4 respectively.

#### 2.2 Signal Interpretation - Current Practices

To conceptualize the knowledge requirements for individual problem-domains, it was essential to study how different types of problems included in the present study are being currently solved. After carefully reviewing the current state of the technology we noticed that the majority of such techniques are

based on visual inspection. In visual inspection techniques the discrimination is largely based on the indications of amplitude and arrival time (or intensity and wavelength), or in some cases using the signals in the transformed domains (see Sections 1.1 and 1.2, and Fig. 1.1 and Fig. 1.3) and the discrimination process simply decides on an accept/reject criterion. For large scale interpretation and data synthesis, however, analytical methods for evaluating the signal artifacts have been used [STAL-82].

In current methods for spectroscopy, since a majority of polynuclear aromatic compounds (PNA) have unique peaks at a given wavelength, frequency domain transforms are usually used whereas in electroencephalographs (EEG) analysis, time domain signals are considered important. In NDT-testing, however, the inspection records are usually obtained in three forms, A-scan, B-scan and C-scan. The A-scan is amplitude/time display for a specific point on the specimen and basically a time-domain signal as described above. B-scan is an amplitude curve along a scan line whereas the C-scan is a planar view (2 dimensional) image and is obtained through a series of scans covering the surface of the specimen.

Among the recent practices for NDT-testing the A-scan is further submitted to analysis using signal processing techniques. In most signal processing applications, an important waveform transformation called Fourier Transform is employed. This transform has been used to translate a time domain signal into what is known as power domain signal. A power domain signal can also be referred to as a frequency signal because it actually shows the power of the signal at each frequency. These domains have been used to improve classification considerably [HAYD-84, MATT-89]. A reference signal is often used to remove the local geometry and grain properties, in addition to transducer characteristics. Other techniques involve using

deconvolution for separating signals. The deconvolved signal can then be analyzed in two other domains in addition to the frequency domain. By taking the inverse transform of the deconvolved signal, a time domain signal is obtained. According to the theoretical model, this signal should be trapezoidal function whose dimensions are related to the defect dimensions. Taking the complex logarithm of the spectrum and then performing the inverse Fourier transform yields the cepstrum, where peak locations in quefrency are also indicative of crack dimensions.

The above discussion thus suggests that any automatic inspection system should select features based on physics and mechanics of the problem with respect to expected modification and changes in the signal amplitude versus time waveform or versus wavelength (frequency domain). Time and frequency are important domains for information synthesis since many phenomena occur only at a specific frequency or within a particular range of frequencies. To enhance the performance of the categorization process, however, these observations (features) must be supplemented with the additional knowledge that may either be obtained from a priori (real world) knowledge, or the expert knowledge of the operator.

### 2.3 Modeling the Waveform Indications

Reviewing the signal interpretation process presented in previous section, we modeled the information a waveform signal carries. EEG signals, PNA spectra, and NDT applications, or perhaps any application that can be represented by signals, all require electronic data acquisition, preprocessing and other conditioning according to the factors which contribute to the nature of the signal and their information contents. Since each problem domain involves different instrumentation and different test subjects (or specimens) having a different

set of inherent characteristics, the factors affecting the indications would vary from problem to problem. For example, the EEG signals are corrupted by noise and/or artifacts, introduced by the electrodes, eye blinks and other body movements, instrumentation fit-up and other elements in the measurement set up. Here, the application of more complex methods is needed for a proper evaluation of the differences in the received indications regarding disease (defect) signals and interfering signals.

In this section we will individually model the accumulated effect of surrounding factors on NDT, EEG and PNA signals. Several parameters are designed to accommodate these factors individually.

#### **2.3.1 NDT Indications Model**

The inspection and evaluation process poses a special challenge to NDT engineers due to a variety of reasons related to complex metallurgy, structural geometry, unpleasant or hostile radioactive environment, high temperature, noise from the equipment and environment, random variations in signals, varied properties of the test objects including their geometry and thickness, limited access to the component, NDT-method dependent parameters, and the presence of defects as well as distance and orientation of test equipment with respect to the test object and the testing conditions.

Modeling the indications requires that a candidate set of input parameters to the model be defined. This candidate set must be a summary description of the known and instrumental variables. In addition, the parameters input must be related to the physics of the underlying process or at least to an intuitive understanding of the process. Since human interpretation of NDT signals, or EEG/PNA signals for that matter,

is dependent solely on the observed characteristics of the signals, the input parameters should be attributable to mathematical characteristics of the signals.

To sort the indications a variety of contributors to NDT-indications mentioned above have to be considered. With the knowledge pertaining to the source of these factors their influences can be minimized considerably. Considering these factors a waveform can be defined as the sum of overlapping defect and geometrical or structural indications.

Based on simple accept/reject criterion the NDT-indications could be divided into defects, and non-defects. The contributors to the non-defect indications primarily include the parameters from test equipment, operating conditions and the material properties. Based on the dichotomy of indications (defects/non-defects) the parameters which contribute to NDT indications are hierarchically organized in Fig. 2.1.

Thus the basis for modeling these indications in a waveform (NDT) is a measurement model that relates the output indications of the system (test equipment),  $W(n,d)$ , to its various signal and noise components shown in Fig. 2.1. In designing the model we assumed that the effect of the components is independent of each other and used an additive measurement model as defined by:

$$W(n,d) = W(d) + W(E) + W(C) + W(P) \quad \dots 2.3.1$$

where

$W(d)$  : is the indication produced by the defect,  $d$ , in the absence of non-defect artifacts,

$W(E)$  : is the indication (artifact) produced by the equipment,  $E$ , and is the sum of artifacts from wave mode,  $W(mode)$  and electromechanical artifacts,  $W(a)$ , that is,

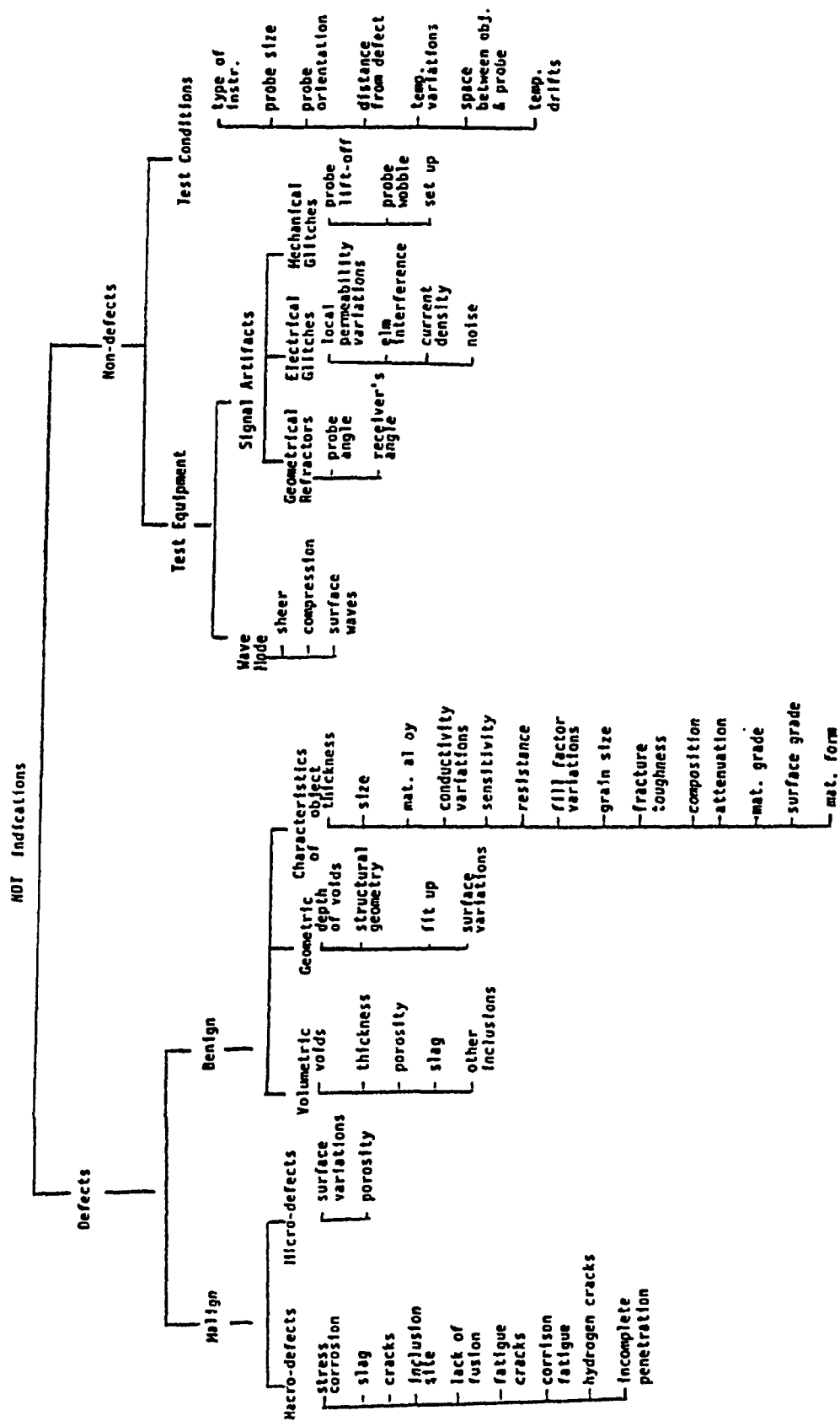


Fig. 2.1: NDT Indications

$$W(E) = W(mode) + W(a) \quad \dots 2.3.2$$

$W(C)$  : is the indication (artifact) produced by the operating conditions, C, of the equipment,

$W(P)$  : is the indication (artifact) produced by the material properties, P,

$W(n)$  : is the accumulated indication (total noise) produced by the non-defect parameters together, i.e.,

$$W(n) = W(E) + W(C) + W(P) \quad \dots 2.3.3$$

$W(n,d)$  : is the composite indication and consists of both signal and artifact indications.

By collecting the parameters shown in Fig. 2.1 the factors in equation 2.3.1 which contribute to corrupt the signals can be eliminated and the quality of the signal can be enhanced right at the source. The components pertaining to NDT-problem domain which would contribute to increased performance are described in the following sections.

### 2.3.2 EEG Indications Model

It has been long known that the brain generates waves called electroencephalographs (EEG) [GEVI-80]. An EEG is a slow (0.01-100 Hz) electromagnetic wave that pervades the brain tissue [PICT-88]. It can be recorded either with electrodes implanted in the brain or with an array of electrodes affixed to the scalp. Of special interest are experiments with evoked responses, for example, see Siddiqui et al. [SIDD-90c].

The evoked responses or event-related potentials (ERP) result from a stimulus applied to a person. The stimulus can be an electrical pulse, a drug, sound, a (soothing) touch, and so on. The result is a wave representing different aspects of the brain's response.

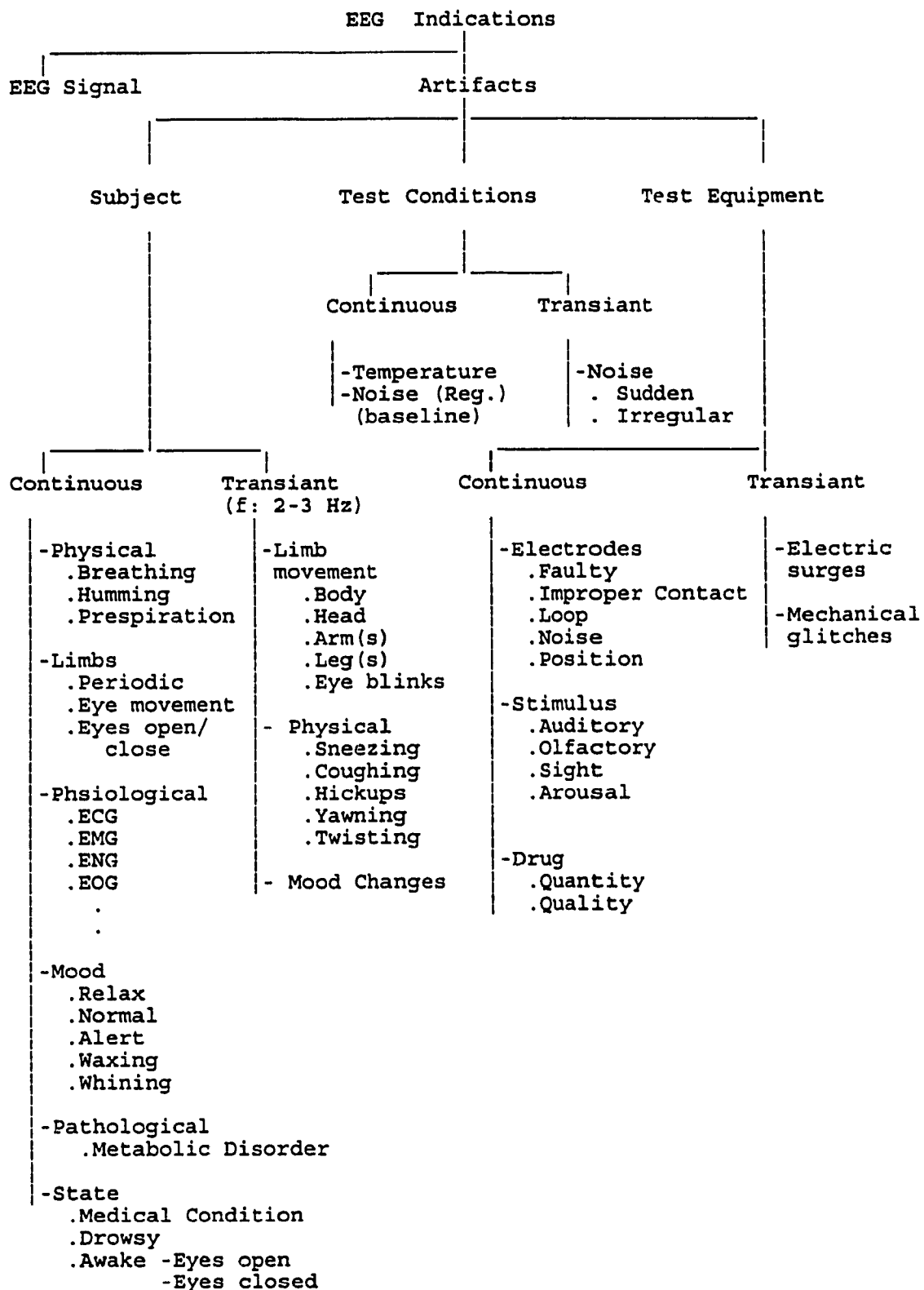


Fig. 2.2: EEG Indications

Following the model we developed in equation 2.3.1, the indications in the EEG type of problems were structured in Figure 2.2. However, the components would have the following interpretation:

W(d) : is the indication produced by the disease, d, in the absence of non-disease artifacts,

W(E) : is the indication (artifact) produced by the equipment, E, and is the sum of artifacts from wave mode, W(mode) and electromechanical artifacts, W(a), that is,

$$W(E) = W(\text{mode}) + W(a)$$

W(C) : is the indication (artifact) produced by the operating conditions, C, of the equipment,

W(P) : is the indication (artifact) produced by the limbs and other organs of the body, P,

W(n) : is the accumulated indication (total noise) produced by the non-disease parameters together,

W(n,d) : is the composite indication and consists of both brain signal and artifact indications.

W(mode) : is the indication of the subject in question under normal (healthy) conditions.

### 2.3.3 PNA Indications Model

A PNA-waveform is an ultra violet visual fluorescence (uv-vis fluorescence) composed of discrete spectrum produced by measuring intensity of emission versus wavelength scanned during a certain time which usually excites with steady state light at a fixed wavelength [EAST-83, SOGL-85]. These spectra, like NDT-signals and EEG waveforms are not noise free. In addition to the usual noise from the equipment and experimentation, peak-jitters, optical noise from the mixture and the solvent blank are some of the common factors which corrupt the quality of the spectra. Adopting the same model

of equation 2.3.1, we developed the model for PNA spectra. The PNA indications are structured in Figure 2.3. The components in equation 2.3.1, however, have the following interpretation:

W(d) : is the indication produced by the PNA-compound, d, in the absence of impurities,

W(E) : is the indication (artifact) produced by the equipment, E, and is the sum of artifacts from wave mode, W(mode) and electromechanical artifacts, W(a), that is,

$$W(E) = W(\text{mode}) + W(a)$$

W(C) : is the indication (artifact) produced by the operating conditions, C, of the equipment,

W(P) : is the indication (artifact) produced by the constituents of the compound, P,

W(n) : is the accumulated indication (total noise) produced by the impurities and other non-concerned constituents present in the compounds,

W(n,d) : is the composite indication and consists of both spectra and artifact indications.

W(mode) : is the indication when running a blank mixture under the same operating conditions.

#### 2.4 Ideal Knowledge Requirements

To evaluate the components of equation 2.3.1 and to acquire pertinent knowledge for signal processing and recognition, accumulated effect of all their constituent parameters has to be evaluated. To simplify the task we considered the major noise contributors which are usually known before the experiment - a priori knowledge. These contributors are described below.

A priori knowledge is considered to be problem-domain dependent generic knowledge that is independent of the presence of

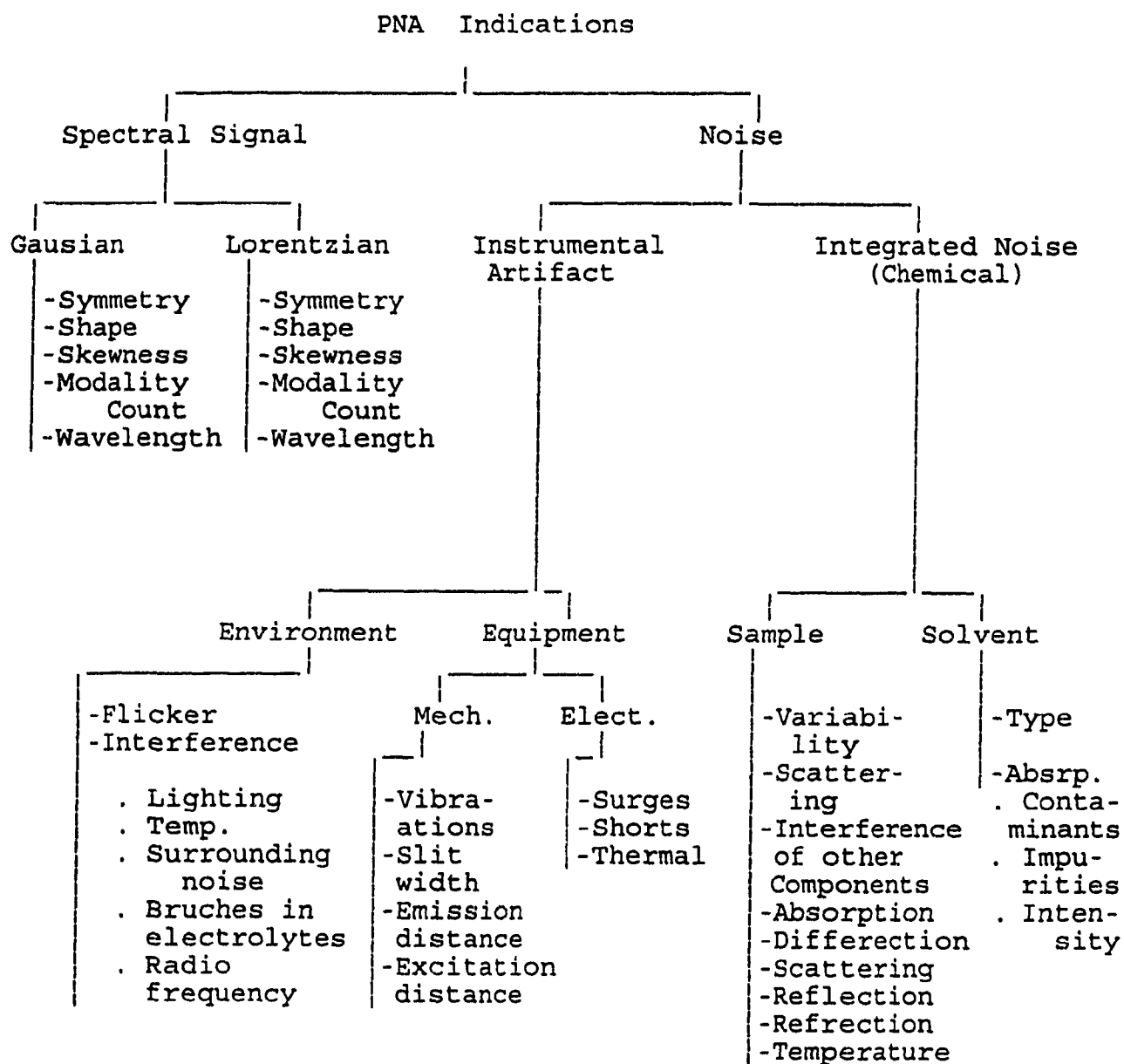


Fig. 2.3: PNA Indications

any pattern class. We defined it as the hard core real world knowledge which can be used for, a) identification of sources of noise and artifacts, b) reduction/elimination of noise contributors, c) preliminary interpretation of signals, d) preparatory arrangements for problem solution and establishment of the scope of the problem.

A defect is a material inhomogeneity which significantly affects the performance of material or component. Considering the factors shown in Fig. 2.1, in NDT-problems, a priori knowledge about the defects could be divided into six basic inputs: 1) domain-specific parameters, 2) method-specific parameters, 3) test specimen characteristics, 4) detailed defect (source) characteristics including location and orientation of defect(s), 5) test equipment characteristics, and, 6) the operating parameter ranges of the test.

The domain specific parameters include the general principles and guidelines that an expert may adopt for, a) describing the pattern classes and label assignment to pattern classes, b) selecting the physical (NDT) method and apparatus for signal acquisition, c) selecting the information physical observations may carry, d) selecting the methodology and algorithms in each phase of solving a problem, and, e) the methods to interpret the results and methods to associate pattern class to a physical phenomena.

To correlate defects with appropriate properties of signals and materials the NDT technology provides a large number of methods. Most commonly used methods are; eddy currents [AULD-83, MARZ-83], ultrasound [KRAU-69, VARY-79], acoustic emission [HAYD-84], and acousto-ultrasound [DESR-86, KAUT-86, VARY-82, VARY-87]. Each method encompasses its own set of principles and characteristics which should be considered when a method or application is selected. The selection of an NDT method is

highly dependent on a large number of factors such as components to be tested, the kind of defects to be identified, the kind of defects a method can determine, etc. These factors are summarized in Table 2.1. A set of theme enquiries designed to establish method versus defect relationship and to determine the kind of knowledge required in the NDT problem domain are shown in Table 2.2.

The NDT-signals also affected by inherent characteristics of the test object. These characteristics include material property data, shape and geometry of the object, and the knowledge pertaining to the defects the specimen may contain. For example, natural materials produce a more or less pronounced effect which usually weaken the propagation of sound. This results from attenuation, which is the sum of scattering, and absorption losses. The studies in material science suggest not measuring the individual effect of waves propagation based on grain [KRAU-69], and geometry or structure [MOYZ-82]. The point, however, to be made is that the inherent properties of the material should not be confused with artifacts or defects. Important characteristics to consider are listed in Table 2.3. An expert, perhaps reviews them in some logical fashion.

Defect characteristics are normally suspected with high certainty by experts or seasoned operators, if a material specimen is presented to them implying that they have sufficiently learned the properties of different defects and can recognize them by simply eye-balling a few samples. A number of physical characteristics of commonly found defects are shown in Table 2.4.

Test equipment characteristics pertaining to initial set-up and calibration of the testing equipment have immediate effect on the quality of signals. It is a well known fact that the pattern recognition techniques are sensitive to an input

signal which is dependent on the characteristics of the system. Proper selection of the test equipment is essential for an acceptable reliability of a system and this would basically improve signal-to-noise ratio by reducing the electrical artifacts, mechanical glitches and other electromechanical artifacts and hence would lead to a high resolution data requiring the least amount of preprocessing and other rectifying measures for improving the quality of data.

Table 2.1

Popular NDT Methods, their Applications and  
useful Method dependent Parameters

Method	Measures/Detects	Test Specimen/ Application	Method dependent Parameters
Acoustic Emission	Crack initiation & growth rate; internal cracking in welds during cooling, boiling or cavitation; friction or wear; plastic deforma- tion; phase transformations;	Pressure vessels; stressed struct- ures; turbine or gear boxes; fracture; mechanics; weldments;	Transducer must be placed on part's surface; highly ductile material yield low amplitude emissions; part must be stressed; operating test system noise needs filtered out;
Ultra- sonics	internal defects & variations; cracks; lack of fusion; porosity; inclusions; delaminations; lack of bond texturing; thickness;	Wrought metals; welds; brazed joints; adhesive bonded joints; non-metallics; in-service parts;	Couplant required; small, thin, complex parts may be diffi- cult to check; reference standards required; special probes;
Acousto Ultra- sonics	bonded joint defects & stren- gth variations; hidden impact damage; degradat- ion from cyclic fatigue; hydro- thermal; aging; overt flaws; de- lamination; erosion; corrosion;	Metals; compo- sites; structu- ral composites; ceramic mat- erials; porous metals; fiber glass composites;	broadband transducer; sending & receiving transducer on the same side of the specimen; couplant required; distance between transmitting & receiving transducer, location; amount of pressure applied;

Table 2.2

Theme Rules Describing Problem Domain Information

- 
1. Define the problem and determine the nature of defects (classes) to be identified and also determine the desired extent of the solution(s), that is, the knowledge pertaining to:
    - Number of pattern classes and their identity
    - Number of pattern samples in each class
    - Number of features and their identity that could best describe each class
  2. Observe the methods given in Table 2.1 and determine the method to solve the given problem?
  3. Using the above methodology search through Tables 2.1 through 2.5; identify the knowledge required to solve the problem and search the answers to the questions:
    - What are the known physical properties of the test object?
    - What is the geometry of the test specimen?
    - What potential defects are we looking for?
    - What is the test goal?
    - What test apparatus is available?
    - What are the Operating parameters of the apparatus?
    - What are the operating conditions?
  4. Set up the design data set.
  5. Expert Choices
    - Method to be used at each step of processing
    - Solution strategy
    - Decision parameters and their thresholds
- 

An NDT-test equipment is usually a transducer/pulsar system. As a general guideline a rather strict acceptance criterion is necessary for acquisition of the test equipment. In addition, a transducer acceptance check should be made before acquiring test data on a particular day which involved acquiring a maximized echo from the edge of the component, and then comparing it with the reference echo in time and frequency domains. Necessary factors for proper set-up and calibration of the test equipment are listed in Table 2.5.

Table 2.3

## A priori knowledge - Test Specimen

Material Properties	Specimen Geometry	Visually Confirmed Defects
Material alloy	Dimensions: height, width, length;	Type (Class or Candidate classes)
Material Grade	Shape	Dimensions (size)
Base Material	Surface conditions:	Shape
Weld,	degree of roughness;	Orientation
Material Form	inspection area:	Location
Surface conditions:	plane, cylindrical,	Causes of defect
roughness, porosity,	machine parts,	(Procedure for producing defects)
coatings	bar-type	Confidence levels of Observation
Thermomechanical history - grain structure & size		Method of actual crack size determination
Organic structure		
Anisotropy, Texture		
Density, Acoustic Impedance		

Table 2.4

## Shape Factors of Some Common Defects


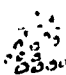


	Cracks	Porosity	Slag	Erosion
Shape				
Description	Vertical Planer Sharp edges	Spherical Volumetric smooth edges	Variable Shape Volumetric Sharp/smooth edges	Vertical Planer Concave/convex Sharp edges
size	singular	singular/ clusters	singular	singular

Table 2.5

## Test Apparatus &amp; Test Conditions

Transducer	Other Components	Operating Parameters
size	couplant: type, amount	skip distance;
Frequency	and distribution	motion control:
Material length	wedge angle	auto-indexing,
focal length, if	Reference Block	manual-indexing,
focused		digital-indexing;
Damping media		preparation of part
Frequency spectrum		Operating Temperature
Beam width (2 axes)		Scanning area, angle
Focal length/water		Location of Transducer
path		Incidence angle
Wavelength		Transient angle
emission rate		Sampling period
		Cleanliness
		Surface preparation

Proper selection of equipment goes in hand with its proper usage. As discussed above, proper calibration of the equipment for the type of the experiment at hand is essential for high quality of data. The operating parameters indicative of effects on signals are listed in Table 2.5.

Although it might be ideal to know all the parameters listed in Tables 2.1 through 2.5 encompassing the problem at hand, acquisition of knowledge pertaining to all six areas in addition to the structural properties of the signals would be a formidable task. Therefore, we decided to consider an overall effect of the material properties. Once assured of the proper quality, the signals based on their structure are carefully reviewed. The defects identified can be attributed to decisions later such as retirement of material for cause, remaining life analysis, life extension probability, etc.

## 2.5 The Knowledge - Our Perspective

Traditionally, a knowledge-based system is meant to mimic the decision making process of human experts in a specific problem

domain. It contains large amounts of subtle knowledge of expert(s) organized into a knowledge base yet separate from the decision making process.

In these systems, the knowledge pertaining to a given domain consists of descriptions, relationships, and procedures [JACK-90]. The descriptions which identify and differentiate objects and classes are sentences in some functional or object oriented language such as Lisp, Prolog [CLAR-82], OPS5 [BRWR-85, FORM-77], and KL-One [BRAH-85] whose elementary components consist of either logical constructs or primitive concepts. A description system generally includes rules or procedures for applying and interpreting descriptions in specific applications. A knowledge base also contains particular kinds of descriptions known as relationships. They express dependencies and associations between items in the knowledge base. Typically, such relationships describe taxonomic, definitional and empirical associations. Procedures specify operations to be performed when attempting to reason or solve a problem [HAYE-83].

This traditional concept of knowledge and its representation and organization tends to provide a rigid mechanism which can be constructed only through an exhaustive interaction of a knowledge engineer with expert(s) and creating a knowledge base that could be examined only through the inference engines based on exhaustive or optimal/suboptimal search strategies. Furthermore, any update in the knowledge base would require going back to the knowledge engineer and the expert which in some cases may lead to a major restructure of the system. Unfortunately, the structure of expert systems based on such concepts has now become a commercial standard and a majority of acclaimed expert systems currently available have blindly followed such standards.

In fact, knowledge is an integrated concept which is acquired through the extensive use of six human senses. The five senses of vision, smell, hearing, touch and taste usually help in carrying out the everyday chores. The sixth sense is the human perception and intuition (deep knowledge) which an individual acquires through his experience spanning over his/her lifetime. There are disciplines such as signal processing, computer vision, statistical decision theory and pattern recognition that use a sub-/super-set of these senses implicitly or explicitly, and have techniques available which are rich in abstracting and formalizing domain-specific knowledge concepts and can be used to partially simulate, if not to replace, the human perception.

For example, pattern recognition (PR) techniques have evolved from the human processes of vision, recognition and perception. One of the theories considers pattern recognition as a paradigm-oriented inductive process [WATA-84] that has also been one of the approaches used in training expert systems. This theory suggests that the selection of appropriate PR tools may reduce the time required by the knowledge acquisition process. The use of PR techniques, however, cannot be generalized for acquiring knowledge pertaining to all application areas. They are more useful than other methods in some application areas.

One of the suitable areas, for example, is the problem domain of random signal processing which has applications in material testing, quality assurance and evaluation, medical diagnostic systems, chemometrics, spectroscopy, etc. In these applications, the domain-specific knowledge and the decision parameters used by a human operator or expert can be broken down to very low level primitives. A majority of these knowledge primitives can be obtained automatically using feature extraction methods used in PR and signal processing fields.

However, some of the knowledge components such as intuition, judgement, etc., cannot be directly represented using PR or signal processing methods. There, we can borrow some concepts from statistical decision theory. Human judgement and intuition is primarily based on experience and observations. Knowledge primitives extracted using signal processing and PR techniques, on processing through analytical procedures, would provide some empirical results which can be validated by using decision theory methods. This approach thus provides analytical and empirical means to simulate human judgement. This wholesome perspective of knowledge was then used to design an integrated system for knowledge acquisition, representation, and organization system, hereafter referred to as the KARO subsystem.

## **2.6 The Design of IRS System**

The Intelligent Recognition System (IRS) outlined in Section 1.8 was a formidable task, however, we carefully identified the major components with three objectives in front of us: 1) components constituting the system should be implemented as realistically as possible, 2) conceptually achieve the overall functionality of the original design, 3) consider the components not implemented as "black boxes" at present and that they may be added on later without any restructure of the system.

Our original efforts were concentrated towards the development of the entire system. Acquisition of problem-dependent a priori and heuristic knowledge for four diverse areas of applications was a formidable task, particularly, in situations where we were dealing with commercially sensitive and proprietary applications such as EEG problem and the CEL data (19 class) problem. In addition, the availability of analytically oriented expert in each field of our interest was a

next to impossible task, let alone the transfer of the heuristic knowledge into procedural knowledge. Hence we decided to rely on analytical knowledge and the knowledge derived therefrom.

The architecture developed here consists of only the components that could be automated using analytical, empirical and procedural knowledge and algorithms. However, the design is structured in such a form that expert knowledge and other components dropped at present could be incorporated at a later stage as a black box.

In developing this architecture we basically kept the same structure and the same functionality of the system as described in Section 1.8 with the exception that knowledge will comprise mainly of analytical and empirical knowledge. In addition, we eliminated the expert/user interface, since it is mainly an exhaustive programming exercise, and called the system as intelligent recognition system instead of a knowledge based system.

#### **2.6.1 The Knowledge Acquisition, Representation and Organization (KARO) Subsystem**

The first major component of the recognition system is the Knowledge Acquisition, Representation and Organization (KARO) subsystem. The objective behind the design of this subsystem was to acquire a larger set of knowledge primitives and concepts so that an integrated knowledge base could be developed. The KARO subsystem is a composite of three independent phases, namely, Fact Gathering, Knowledge Base, and Knowledge Formalization and Organization (see Fig. 2.4). The fact gathering phase includes the acquisition of the input data (waveform signals), data preprocessing and the measurements of physical

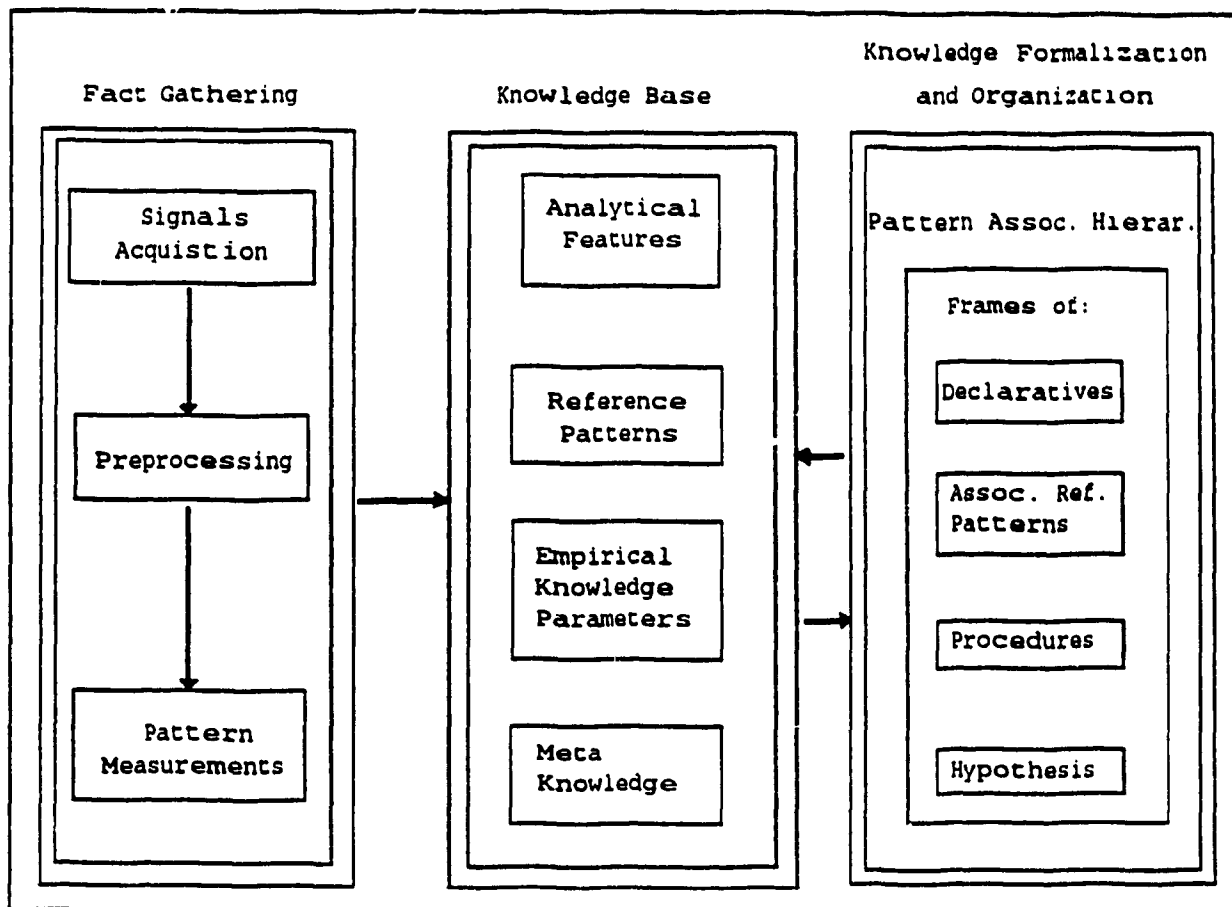


Fig. 2.4: The Knowledge Acquisition, Representation, and Organization (KARO) Subsystem

observations from waveform patterns (feature extraction). The features thus extracted are organized into a knowledge base.

The Knowledge Base is a knowledge storage and houses three types of knowledge: analytical, empirical, and meta-knowledge about the problem-domain. Analytic features are a large subset of pattern measurements performed during the fact gathering phase. Empirical knowledge is derived from the analytical observations and meta knowledge is obtained through a combination of empirical knowledge and statistical inference. Meta-knowledge, in fact, partially simulates expert's judgement.

### **2.6.2 Inference Engine**

The structure of the inference engine was kept the same as discussed in Section 1.8, except that it was trained using supervised learning only. It will still operate in two modes of operation, i.e., executive and consultant. In the consultant mode of operation it will still allow the user to select an algorithm of his/her choice, however, he/she will not be able to train this mode of operation using unsupervised learning.

### **2.7 Signal Conditioning and Treatment**

The model presented in equation 2.3.1 was considered as a composite of several independent terms. Hypothetically by evaluating the six input components one can minimize the effect of a majority of noise contributing parameters, but in practice it cannot be justified as cost effective and a small gain in signal quality may not worth the time and efforts. In addition, the interaction of the factors influencing the components in equation 2.3.1 is not possible to determine exactly. However, using software based conditioning and treatment of the waveforms, the noise factor  $W(a)$  (see equation 2.3.2) can be significantly reduced. In addition, the effect of other parameters, in reality, can be identified if more information is extracted from the physical observations and the parameters listed in Tables 2.1 through 2.5.

The NDT data used in this research was collected using Acousto-ultrasonic (AU) method. The amount of information in the ultrasonic (UT) waveform is not known precisely. However, information theory tells us that the greater the rate of information transmission, the greater is the required bandwidth. Thus a guiding principle in the design of UT or AU-based NDT experiments is to use broadband transducers and

amplifiers. The use of broadband transducers and instruments assures that the system will not limit the information contents of the signals. There is, however, a corresponding increase in the signal noise level due to broader bandwidth. Therefore, additional steps must be taken to determine that signals do, in fact, contain sufficient information on the defect(s) to permit full exploitation.

Defect detection under simultaneous occurrence of interfering effects, discussed in previous sections present a considerable problem in NDT. If a comprehensive approach is to be used to relate signal characteristics to reflector properties, it would be necessary to consider the characteristics of the defect as a function of signal properties. Therefore, before a satisfactory application of a test method it is always necessary to determine the relationship between different occurring indications by means of pilot experiments, i.e., between the magnetic as well as electrical and the mechanical properties of the test objects. It has been suggested that reference samples of known properties have to be available for exact calibration considering the test parameters [MATT-88].

Even after the above stated calibration it is not guaranteed that the signals received are noise free. Cross correlation analysis seems to be promising for testing, because this method compares a selected reference signal with each signal occurring during testing and is giving a measure of the similarity. Additional treatment measures suggested are as follows:

1. Deconvolution: to remove the transducer characteristics from the observed signal.
2. Spatial Averaging: to reduce the spatial resolution and the effect of grain scattering.
3. Stationary (i.e., temporal) Averaging: to remove noise

mainly from amplifier and other random events and to improve signal-to-noise ratio.

4. Calibration for Maximum Defect Response: by jogging the probe in both axial and circumferential positions determine the maximum defect response and repeat the process on all visually identifiable defects [ORR-79]. The associated position coordinates of the transducer were then noted and the same should be used for data collection.

The conditioning and treatment on NDT data was performed by the staff at the Tektrend Int., Montreal. The preprocessing performed on PNA data is reported in [SIDD-91a].

## **2.8 Mapping and Parameterization of Waveforms**

From the previous discussion it became clear that the time waveform alone is not sufficient for analysis. For flexible and reliable machine processing, and analysis additional information is required. In the field of signal processing it is known that from preprocessed time waveforms, a number of other domains (mapping spaces) can be generated to provide a more illustrative representation of the available information. Siddiqui et al. suggested a pattern measurement system in [SIDD-90a] and this is reproduced in Fig. 2.5. The important feature of the system is the transformation switch whose function is to transform a waveform into other information domains and this can be done by using a number of suitable transformation techniques available in the field of signal processing [BRAC-86]. One such approach is described in the following section.

### **2.8.1 Mapping Space**

Although there are a number of transformation techniques available in the field of signal processing and information theory, the Fourier transformation has been used extensively in waveform analysis [BRAC-86].

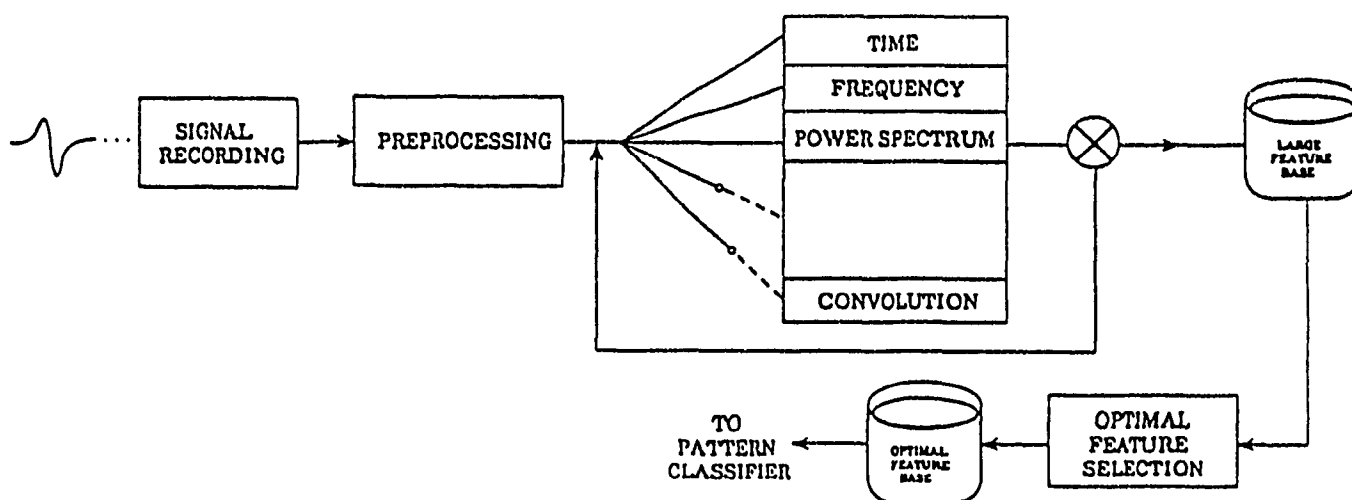


Fig. 2.5: Pattern Measurement System [SIDD-90a]

The time varying signals, their transformations and the functions derived therefrom such as a spectrum, correlation function or cepstrum, can be processed further to extract the information contents. A formal discussion on waveform transformation now follows.

Formally, we defined a signal as: "a sequence of discrete real and/or complex numbers and is a time function,  $x(t)$ . The value of the function at any time  $t_i$ ,  $x(t_i)$ , is a random variable."

The variable  $t$  is chosen since the signals that are considered here are time-dependent signals. We assume that we have a source which generates the function  $x(t)$ , which is denoted as

a sample function. The source generates  $N$  sample functions which together are known as an ensemble. At any time,  $t_1$ , we observed the values of all sample functions, to get many "results of experiments." For example, consider the NDT signal taken by means of a surface transducer located at a certain location on a piece of material. We want to investigate the properties of the source material through the NDT signals.

Thus a data sequence consisting of  $N$  samples of signal  $x(t)$  is given by:

$$\begin{aligned} \text{samples of } x(t) &= [ x_k ] & \dots 2.8.1 \\ &= [ x_0, x_1, \dots, x_{N-1} ] \end{aligned}$$

where  $k$  is a time index which ranges from 0 to  $N-1$ . The discrete Fourier transform (DFT) of  $[ x_k ]$  consists of  $(N/2 + 1)$  complex samples (assume that  $N$  is even) given by

$$\begin{aligned} [ X_m ] &= \text{DFT} [ x_m ] & \dots 2.8.2 \\ &= [ X_0, X_1, \dots, X_{N/2} ] \end{aligned}$$

where  $[ X_m ]$  is the DFT of  $[ x_k ]$  and that the index  $m$  designates the frequency of each component  $X_m$ .  $X_m$  can also be represented in polar coordinates as:

$$X_m = | X_m | \exp (j \theta_m) \quad \dots 2.8.3$$

where  $| X_m |$  is the amplitude of  $X_m$ , it is equal to

$$| X_m | = [ R^2(x) + I^2(x) ]^{1/2} \quad \dots 2.8.4$$

where  $R(x)$  and  $I(x)$  are the real and imaginary components of the transform. The square of the spectrum  $| X_m |$  is commonly referred to as its power and is denoted as,

$$\begin{aligned} P(x) &= | X_m |^2 \\ &= R^2(x) + I^2(x) & \dots 2.8.5 \end{aligned}$$

The relationship implemented by the transform between  $[x_k]$  and  $[X_m]$  can be expressed as:

$$X_m = \sum_{k=0}^{N-1} x_k \exp(-j(2\pi m k/N)) \quad \dots 2.8.6$$

for  $m = 0, 1, \dots, N/2$

In this formula  $X_m$  is an exponential function and it is complex sinusoidal and periodic. These characteristics will be more clearly represented by separating the real and imaginary parts,

$$X_m = \sum_{k=0}^{N-1} x_k \cos(2\pi m k/N) - j \sum_{k=0}^{N-1} x_k \sin(2\pi m k/N)$$

for  $m = 0, 1, \dots, N/2$

... 2.8.7

The equations 2.8.2 through 2.8.7 were used to derive a number of information domains wherein the analytical features in a problem domain at hand can be measured. The information domains that this study includes are described below:

- Time waveform: The original time waveform, given by equation 2.8.1 (raw time versus amplitude signals),
- Frequency waveform: Real components of the complex exponential in the DFT, equation 2.8.6 (Fourier transform of the time waveform),
- Phase spectrum: The Fourier transform also produces a value of phase for each particular frequency in the spectrum of signal which is useful in determining the ratio of stored energy to that dissipated in the system. Phase spectrum of  $[x_k]$  is obtained by plotting  $\theta_m$  against  $m$  (equation 2.8.3),
- Power Spectrum: The square of the spectrum given in equation 2.8.5, which is the plot of the power against each frequency component of the transform,
- Auto Correlation: This domain is useful in determining whether a signal is periodic or cyclic. The time

domain signal given by equation 2.8.1 is compared with itself at different positions (time) and the similarity between signal segments is determined,

- Cepstrum: Using a Fourier transform of the logarithm of the power spectrum given by equation 2.8.5),
- Log Power Spectrum: Taking the logarithm of the power spectrum,
- Convolution: Taking the inverse Fourier transform of the product of Fourier transform of two sample signals from a pattern class.

### 2.8.2 Parameter Extraction

It is difficult to measure the pulse shape descriptors directly from the above waveforms or spectra. Alternately, an envelope is constructed from which the pulse information is extracted. The literature [HAYD-88, SEDG-88] provides several standard signal envelope extraction algorithms to facilitate these operations and the feature extraction process. One such algorithm is outlined below:

1. A convex shape with finite arc length is used to construct a rough convex hull of the given signal profile.
2. Smoothing is then performed to obtain the desired signal envelope.
3. A set of typical features listed in Table 2.6 were then extracted from the envelope. Figure 2.6 shows their geometrical interpretation.

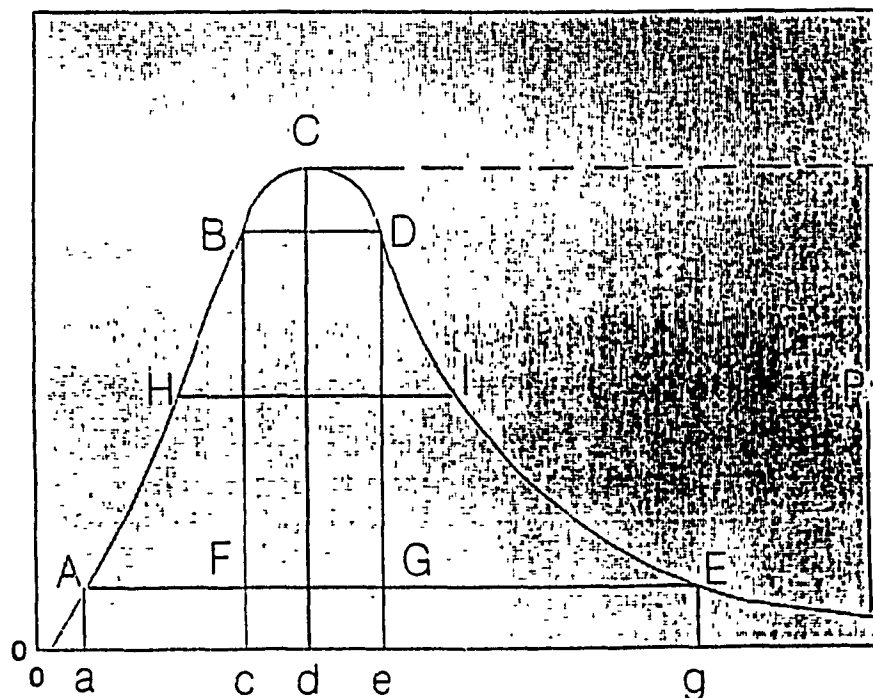
The feature extraction process essentially measures a number of statistical, waveform, geometrical, absolute and shape features in a number of selected domains from the list described above. These features, generically, are listed in Table 2.6. The choice of a transformation domain is again a problem-dependent activity. For different types of data different domains and features were used. The set of

procedures that were used to measure these features are described in Appendix A.

Table - 2.6

### Analytical knowledge features used

Statistical	Waveform	Geometrical	Absolute	Shape
mean, standard deviation, higher order moments, maxima, minima	impulse sum in different data windows	peak location, rise time, fall time, rise slope, fall slope, peak width	skewness, kurtosis, no. peaks, full pulse, half pulse	amplitude, area, weighted area, energy



Rise Time	= AF	Pulse Width	= AE	Fall Slope	= DG/GZ
Rise Slope	= BF/AF	Peak Width	= BD	Pulse Amplitude	= p
Pulse Location	= d	Fall Time	= GZ	Half Max. Width	= HT

### Pulse Shape Factors

Fig. 2.6: Geometrical Interpretation of Envelope and Features Derived Therefrom

## **Chapter 3**

### **Analytical Features and Pattern Association Hierarchy**

#### **3.1. Introduction**

Analytical features constitute a major subset of pattern measurements and they may be large enough to prohibit exhaustive analysis. To process them with good performance (recognition) a hierarchy of naturally associated pattern classes was developed. The fact gathering phase and the techniques to develop a pattern association hierarchy are described in this chapter.

#### **3.2 Fact Gathering Phase**

This phase includes three components, namely, signal acquisition, preprocessing, and pattern measurements. Signal acquisition and preprocessing are not among the mainstream of the subjects we studied in this thesis. Both of these steps were performed by the institutions who have provided their respective data sets. Tektrend International, Inc. of Montreal supplied the data on NDT-signals, EEG signals, and cell data in the form of feature vectors; the Lockheed-ESC, located in Las Vegas, furnished the digitized data on polynuclear aromatic compounds (petroleum oils). These data sets will be referred to as NDT-data, EEG-data, CEL-data, and PNA-data in the following chapters.

Brief descriptions of instrumentation and experimental conditions underlying data collection for each problem domain are presented in Appendix B.

### 3.2.1 The Pattern Data

The algorithms we developed were tested on problems from four different areas; classification of material defects non-destructively (NDT-data), the classification of electroencephalogram signals (EEG-data), classification of polynuclear aromatic compounds (PNA-data), and classification of body cells (CEL-data). The characteristics of the latter three data are described in Appendix B, whereas the characteristics of the NDT-data are described below.

NDT data were collected by applying the ultrasonic signals to mild steel bars of measurements 0.5 inch thick, 1.0 inch wide, and approximately 2 feet long, wherein slots of different depths and lengths were artificially machined to simulate varying degrees of wall erosion. A total of nine flaws of different lengths were introduced into the bars. In addition, to acquire signals representative of no flaw condition, a bar without flaw was also tested. The dimensions of each slot machined into the bar and their corresponding flaws are shown in Table 3.1. A micro-computer controlled acousto-ultrasonic data acquisition system ARIUS [LACA-85, MATT-89] was then used to acquire, digitize, process and store the signals. A total of 400 data files were created, 40 for each of the nine flaw types and 40 for the flawless bar. Each data file consisted of 2048 data points. Four sample waveforms representing four typical pattern classes are shown in Figures 3.1a through 3.1d.

### 3.2.2 Pattern Measurement Problems

A central problem in using PR techniques is that of extracting from the pattern the information (features) which is most relevant for classification. If effective features have been obtained, then, the pattern classification problem becomes one

of partitioning the feature space into regions, one region for each class. Selection of properties that contain the most discriminatory information is important because the cost of decision making is considered directly related to the number of features used in the decision rules. Thus for large applications when the complexity of the problem increases, it becomes especially important to develop methods for efficient design of feature selection and classification algorithms.

Selection of features strongly affects the design of a classifier. That is, if the features show significant differences from one class to another, the classifier can be designed more easily with better performance. Therefore, the selection of features remains a key issue in PR.

Table 3.1

Sizes of Defect Areas and Their Identification

	length	76mm (3")	152mm (6")	228mm (9")
depth				
0.25mm (0.01")	smsh (A)	mesh (D)	lash (G)	
1.52mm (0.06")	smme (B)	meme (E)	lame (H)	
3.18mm (0.125")	smde (C)	mede (F)	lade (I)	
	no (J)			

Legend:

length => la: large (9"), me: medium (6"),  
sm: small (3")

depth => de: deep (.125"), me: medium (.06"),  
sh: shallow (.01")

no: no flaw

Example: meme: a class of defect of length 152mm (6")  
at depth 1.52 mm (0.06")

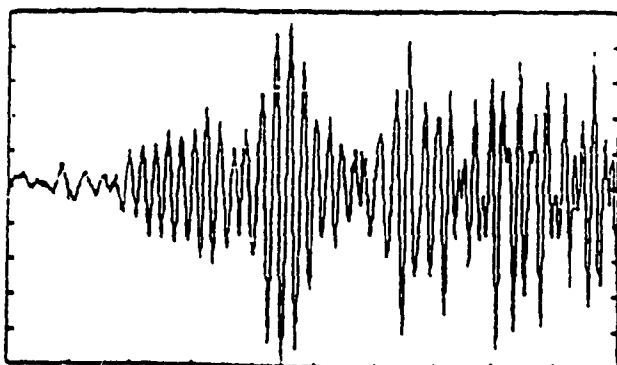


Fig. 3.1a: A typical waveform from a flawless bar (class J)

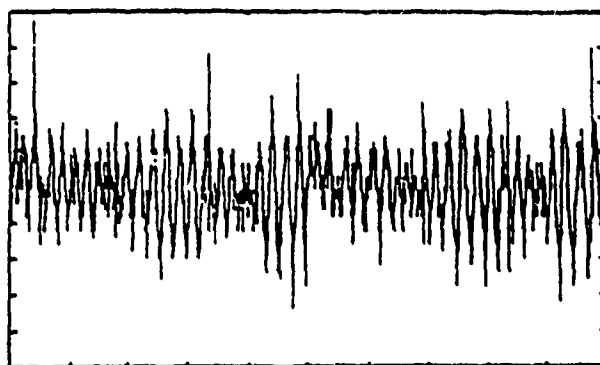


Fig. 3.1 b: A typical waveform representing a smsh pattern (class A)

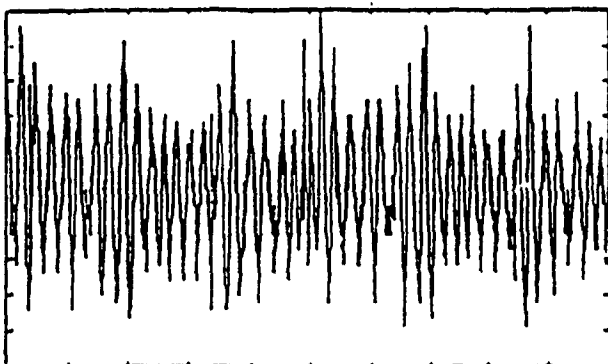


Fig. 3.1c: A typical waveform representing a meme pattern (class E)

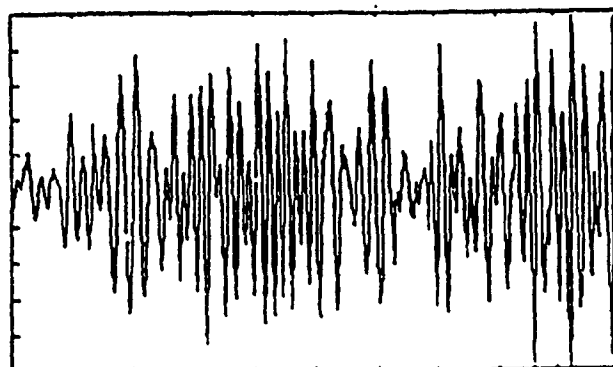


Fig. 3.1 d: A typical waveform representing a lade pattern (class I)

Legend:

Horizontal Scale: 12.8  $\mu$ s/div.

Vertical Scale: 5.14 units/div.

Data Width : 2048 points

Fig. 3.1: A few typical samples from NDT signals.

The more complex the pattern we are dealing with, the more difficult it is to decide what the important measurements are. The approach we adopted to get around this difficulty is to collect whatever specific knowledge about the problem has been suggested in the literature and by the practicing experts [HAYD-87, MATT-88]. In addition, we included all those measurements that, in our opinion, could possibly provide additional valuable information.

An increase in the number of measurements that resulted from this approach brings about an increasingly complex classifier structure. Also the larger the feature set (compared to number of classes) the greater the possibility that a number of irrelevant and redundant features may have been selected. The presence of such redundancies in the input data detrimentally affects the reliability of the classifier.

To minimize these problems, several measures for feature dimensionality reduction and optimization were employed. These measures are described in Chapter 4. The classifier design complexity is reduced by organizing the pattern classes using a pattern association hierarchy, a concept introduced in Section 3.3. The PAH concept is also used to resolve the information redundancy and explosion problems (see Chapter 4).

#### **3.2.2.1 Analytical Feature Extraction**

Considering the pattern measurement issues discussed above, a set of features, which are referred to as analytical features were extracted from an array of waveforms in a class of problems, such as NDT signal classification.

Based on the problem domain a set of information domains given in equations 2.8.2 through 2.8.7 were used to measure a number of analytical features discussed in Section 2.8.2. The choice

of a transformation domain is a problem dependent activity. For different types of data different domains and features were used. The information domains that were selected for NDT-problems include, time waveform, phase spectrum, power spectrum, auto correlation, and cepstrum [HAYD-88].

The feature extraction process, essentially measures a number of statistical, waveform, geometrical, absolute and shape features in a number of selected domains from the list described in Section 2.8.2. The set of procedures that were used to measure these features are described in Appendix A. The procedures adopted for the measurement of the features from NDT signals are described in [HAYD-88]. The list of features provided by Tektrend for the NDT data is presented in Table 3.2.

The scheme we adopted conceivably captures a large number of features among which only a few may be needed. The few which will be most suitable for classification, were identified using feature selection algorithms described in Chapter 4. A number of empirical features were estimated using the analytical features. The empirical features, in turn, were used in deriving the components of meta knowledge (see Chapter 4).

#### **3.2.2.2. Homogenizing the Analytical Features**

Each analytical pattern measurement varies both in unit and the range of magnitude from pattern to pattern. However, the result of analysis (or classification) should be independent of these variations. Rather than trying to develop an analysis algorithm which tolerates these variations, it seems reasonable to eliminate them by proper normalization prior to analysis. Thus it is expected that analysis will become easier if parameter variations are eliminated in advance.